Universidad de Valladolid

Escuela de Doctorado Universidad de Valladolid

PROGRAMA DE DOCTORADO EN INGENIERÍA
TERMODINÁMICA DE FLUIDOS

TESIS DOCTORAL:

Valorization of Black Liquor using Hydrothermal Treatment

Presentada por **Emre Demirkaya** para optar al grado
de Doctor por la Universidad de Valladolid

Dirigida por:
Dr. María José Cocero Alonso
Dr. Danilo Cantero Sposetti

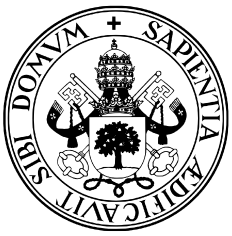

Universidad de Valladolid

PressTech

The presented thesis has been realized in the research group PressTech at the University of Valladolid, Spain. The authors would like to express their gratitude to the Ministerio de Ciencia, Innovación y Universidades, the Agencia Estatal de Investigación, and the European Regional Development Fund of the EU (FEDER) for their financial support under projects CTQ2016-79777-R and PID2019-105975GB-100. Additional support was provided by the Junta de Castilla y León - Consejería de Educación and FEDER through project CLU-2019-04 - BIOECOUVA Unidad de Excelencia de la Universidad de Valladolid. The research fellowship from the University of Valladolid awarded to Emre Demirkaya is gratefully acknowledged. Special thanks to Ence Energía y Celulosas for supplying the black liquor necessary for this research. A part of this thesis was created in collaboration with Universidad de Huelva, Pro2TecS Group in Chemical Product and Process Technology Centre. PressTech Group and personally Emre Demirkaya are grateful for their contributions, guidance and support during this collaboration.

TABLE OF CONTENTS

TABLE OF CONTENTS

LIST OF TABLES

Introduction

Chapter I

Chapter II

Chapter III

Annex I

Annex II

LIST OF FIGURES

Introduction

Chapter I

Chapter II

Chapter III

Annex I

Annex II

ABSTRACT

Valorization of Black Liquor

using Hydrothermal Treatment

Historically, society has relied heavily on fossil fuels for energy, but their role has evolved over time. After a boom during the Industrial Revolution and the years that followed, concerns arose about the potential depletion of these resources. However, the oil shale revolution reinforced fossil fuels as a dominant energy source. Despite this resurgence, there is a growing consensus about the environmental impact of fossil fuel consumption, particularly greenhouse gas emissions and global warming. This realization has led to increased interest in alternative energy sources such as solar, wind, biomass, and hydro. While each can produce heat and electricity and reduce net carbon emissions, biomass stands out for its ability to provide carbon precursors essential for the synthesis of chemicals, fuels, and materials. In this regard, black liquor, a by-product produced in significant quantities in pulp mills and biorefineries, is emerging as a promising candidate for these purposes.

The main objective of this thesis is valorization of black liquor using hydrothermal processing technology (HTL). It is aimed to create an end-user material (bio-lubricant) and test different conditions to monitor the effects of HTL in this research.

The first chapter of the research was about the supercritical water depolymerization of black liquor, refining and comprehensive analysis of products including biopolyols. In this study, polyols presence in depolymerized black liquor (DBL) revealed and proposed a fast and scalable approach to increase the yield of this fraction. Hydrothermal treatment (HTL) of black liquor (385°C, 26 MPa) was performed in a custom designed supercritical water (SCW) pilot-plant with rapid reaction times of around 0.4 s. As an improvement, a higher concentration of black liquor (20 wt% total solids) was used as a raw material in this work.

A simple downstream processing method was investigated to minimize the cost and time for industrial purposes. Direct oven drying, freeze drying, spray drying, and a comprehensive fractionation method were examined. Spray drying and freeze drying were superior to oven drying in terms of the extracted bio-oil yield. Spray drying was further characterized in this study as it is easier to scale-up compared to freeze drying. The fractionation method gave the highest bio-oil yields compared to the other processes. Ash-free, total bio-oil yield was found to be ~77 wt%. In this method, the sample was first acidified instead of drying the sample directly, and the phase separation was performed using centrifugation. After the liquid (DS) fraction was separated from the solids (SS), the SS fraction was washed three times with pH 2 water, using a 1:1 ratio

of water to solids. The liquid from these washes was combined with the DS fraction. Ethyl acetate extraction of both DS and SS fraction was followed, and four distinct fractions were obtained. these were; ethyl acetate-soluble in dissolved solids (DS-EA – light oil), water-soluble in dissolved solids (DS-W – aqueous residue), ethyl acetate-soluble in suspended solids (SS-EA – heavy oil), insoluble suspended solids (SS-Insol. – insolubles). In addition to the contribution of the detailed fractionation methods, this study highlights continuous operation (>1 hour), and short reaction times (~0.4 s) of raw black liquor in SCW to produce biopolyols and aromatic bio-oil.

The second chapter of this research aimed to valorize black liquor through supercritical water treatment, opening up a new line of research for the production of semi-solid bio-lubricants. To achieve this, original black liquor subjected to supercritical water depolymerization, and downstream processing, and three different fractions (spray-drying, oven-drying, and ethyl acetate extraction) were obtained. These fractions subsequently added to epoxy-modified vegetable oils to create sustainable lubricant formulations. Their rheological and tribological properties were then evaluated. Produced bio-lubricants exhibited notable physical stability, desirable appearance, characteristic shear-thinning and viscoelastic behaviors, and adequate tribological performance, making them potential eco-friendly semi-solid lubricants. Moreover, all lignin samples used for dispersions in epoxidized castor oil demonstrated similar shear-thinning behavior, comparable to conventional lithium soap-thickened greases modified with polymers. In addition to that, retaining the inorganic content (ash content) within the depolymerized black liquor fraction enhanced the thickening effect of the bio-lubricants, synergistically influenced by the molecular weight and polydispersity of the samples. These lignin-thickened formulations significantly reduce wear in contact elements compared to epoxidized castor oil alone, with the ECO_EA (bio-oil mixed with epoxidized castor oil formulation system) system, characterized by lower viscosity, providing the highest wear protection. These highlights the feasibility of depolymerization to valorize black liquor, with the resulting lignin fractions improving the lubricity of castor oil-based formulations.

In the last chapter of this work, black liquor and kraft lignin were depolymerized using supercritical water, where no additional catalyst was used for black liquor, but NaOH served as the basic catalyst for kraft lignin. This study represented the first rapid reaction screening of black liquor and precipitated kraft lignin, providing a comprehensive characterization of all fractions. The experiments were carried out at TRL4 in a

continuous pilot plant with fast reaction times, at temperatures of 380°C and 390°C and a pressure of 26 MPa. Reaction times of 0.5, 1 and 1.5 seconds were investigated for both temperatures and feedstocks. The bio-oil fraction was separated by the fractionation method and its aromatic content was analyzed by detailed characterization techniques.

This study showed that longer reaction times and higher temperatures during supercritical water (SCW) treatment of black liquor (BL) and kraft lignin (KL) significantly increased phenolic compound concentrations, resulting in lower pH and reduced total solids content. SCW treatment reduced the SSI fraction of BL from 24.96 wt% to only 1.25 wt% at 390°C, while the SSI fraction of KL decreased from 37.57 wt% to 5 wt% under similar conditions. The rapid depolymerization of BL indicated its high susceptibility to solubilization, making it a prime candidate for organic degradation processes. BL's ethyl acetate extracted dissolved solids (DSEA) fraction (aromatic monomer rich oil) initially contained 9.32 wt% whereas KL started with only 5.74 wt%. BL achieved maximum DSEA yields of 21 wt% at 380°C and 24.64 wt% at 390°C compared to KL's peak yields of 13.36 wt% and 16.82 wt% respectively. Overall, the SCW process achieved maximum total oil yields of 79.45 wt% for BL and 68.54 wt% for KL at 390°C.

INTRODUCTION

Valorization of Black Liquor

using Hydrothermal Treatment

1. CONCEPTUAL GROUNDWORK & FUNDAMENTALS

Throughout history, society heavily relied on fossil fuels for energy [1–3]; however, their role was evolved over time. After the boom during the industrial revolution and subsequent years, there was concern about the possible depletion of these resources. However, following the advances of the oil shale revolution, fossil fuels once again strengthened their position as an energy resource. Yet, there's growing consensus about the environmental implications of fossil fuel consumption, particularly in terms of greenhouse gas emissions and global warming. This heightened awareness fostered increased interest in alternative energy sources. These prominent renewable possibilities include solar, wind, biomass, and hydropower. Carbon capture and storage or carbon utilization are still in their early stages. Involvement in alternative and renewable energy options has been leading to more subsidies and grants available for new ventures. While each can be used to generate heat and electricity or used to decrease net carbon flux to the atmosphere; biomass uniquely serves as a carbon precursor essential for the synthesis of chemicals, fuels and materials [4,5]. As a biomass, lignocellulosic materials, which include non-edible parts of forestry and agricultural crops and residues, are particularly promising due to their abundance when compared to other biomass sources like sewage, animal residues, and municipal solid wastes.

Lignocellulose consists of predominant biopolymers, namely: cellulose, hemicellulose, and lignin, besides traces of pectin and triglycerides. Its intricate structural matrix poses challenges to (bio)chemical conversions. Currently, no universally accepted method exists to fully process lignocellulosic materials. Today’s biorefineries are highly capable of driving a fractionation strategy to decrease the complexity of biomass, which allows a tailored downstream of targeted products. For this purpose, carbohydrate fractionation is being prioritized by these traditional biorefineries to produce paper/pulp or bioethanol. Due to the carbohydrate-first biorefineries objectives, the lignin fraction is often relegated to the status of a low-value by-product or being used as an energy source for heating or electricity generation [6,7]. Nevertheless, there's an ongoing endeavor to innovate and produce materials derived from lignin that are both economically viable and sustainable. Recent advancements suggest the potential of utilizing lignin as a raw material to synthesize chemicals, demonstrating promising outcomes like the fabrication of adhesives, absorbents, and polymeric composites. In this context, the

strategic upgrading of lignin into targeted chemicals is gaining significant attention lately [8–13].

Converting lignin into valuable chemicals and materials can be achieved by three key aspects: (i) the fractionation of lignocellulose, (ii) the depolymerization of lignin, and (iii) the refinement or upgrading to the intended chemicals. These three pathways have been a focal point of lignin research in recent decades [14,15]. Although making a comparison and classification are quite complex and exhausting, a brief overview that fits the objective of this work will be delineated in this report.

1.1 Understanding Lignocellulosic Biomass: A Brief Overview

Lignocellulose is the most common source of biomass as it is the primary structural component of plants. [16,17]. Predominantly composed of cellulose, hemicellulose and lignin, with smaller amounts of other elements such as pectin, proteins, terpenes, waxes, triglycerides and ash [18,19]. Together, these components contribute to the diverse nature of lignocellulosic feedstocks, which can be found in both woody (hardwood and softwood) and herbaceous (switchgrass, corn stover, miscanthus) biomass [20]. The resistance of lignocelluloses to degradation is primarily due to the strong covalent and non-covalent bonds between cellulose, hemicellulose and lignin. A simple schematic illustration of the lignocellulose matrix is given in Figure 1.

The cellulose fraction consists of glucose units linked by β-1,4 glycosidic linkages. The polymerization degree of cellulose chains can reach 10,000 units. A combination of hydrogen bonding, van der Waals forces and hydrophobic forces contribute to the rigid, semi-crystalline macrostructure of this polymer chain [21–24]. Due to these robust interactions, cellulose is insoluble in water and conventional solvents. While these properties are essential for the chemical stability and mechanical strength of plants, they also result in low conversion rates to fuels (such as bioethanol and other alcohols) and chemicals (e.g., levulinic acid, sorbitol) [21].

Hemicellulose, on the other hand, has an amorphous structure that makes it more soluble and more prone to chemical attack. It is composed of a variety of pentose (e.g., xylose, arabinose) and hexose (e.g., glucose, mannose, galactose) units [25,26]. The xylose, glucose and mannose units in these branched carbohydrate polymers are predominantly linked by β-1,4 glycosidic linkages. The presence of galactose, arabinose, acetyl fragments and uronic acids on the chain are responsible for amorphous structure

and being open to chemical attack. Its degree of polymerization, which is lower than that of cellulose, ranges from 50 to 300 units [27]. Apart from cellulose and hemicellulose, holocellulose is often referred to as the total carbohydrate fraction and includes small amounts of other carbohydrate biopolymers (e.g., pectin). It also has a significant effect on biomass recalcitrance [28].

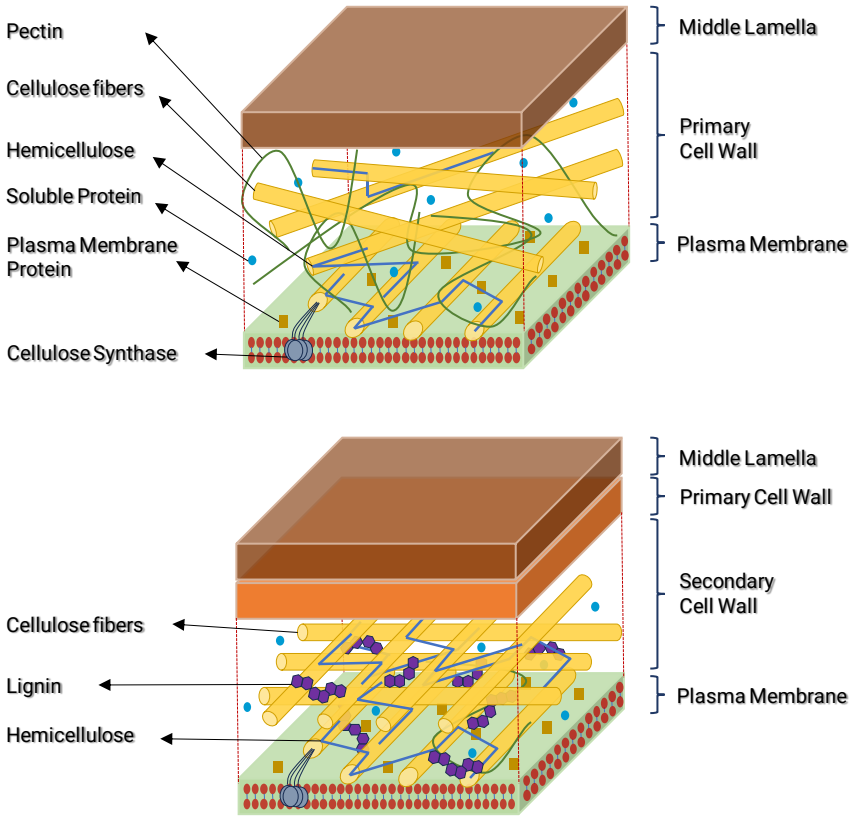

Figure 1. Illustration of lignocellulosic matrix in plant cell wall structure. Inspired and recreated from the work of Loix et al., 2017 [29].

Lignin, as described in the literature, is a non-crystalline aromatic structure that is irregularly formed by radical polymerization reactions of monolignols within the plant cell wall [30,31]. Achyuthan et al (2010) expresses the nature of lignin as supramolecular self-assembled chaos [32]. Lignin provides rigidity and resistance against microbial attacks in plant cell walls and supports complex and recalcitrance nature of biomass. The process of lignin formation is complex, involving not only biochemical and physiological mechanisms, but also non-biological, spontaneous chemical reactions that regulate its formation. Biosynthesis of the lignin basic units, trio of monolignols, are responsible for starting lignin synthesis, mainly but not solely. The process of lignin synthesis contains a few steps: 1) formation of monolignols, 2) monolignols transportation to lignifying sites, 3) enzymatic transformation of monolignols into

radical monomers, 4) non-enzymatic interactions of these monomers into enlarging lignin polymer [33]. Although this description categorizes lignin synthesis in a simple way, several aspects of even these fundamental stages are still on debate.

Although a detailed discussion of the lignin synthesis pathway is beyond the scope of this work, giving a simple explanation will be suitable here. Genealogical tree of lignin traces back from the completely developed lignin is being associated with a plant cell wall's heteropolysaccharides. Formation of phenylalanine and tyrosine are being generated from carbohydrates, namely erythrose 4-phosphate over shikimate pathway [34,35]. An illustration of this mechanism can be found in Figure 2 together with phenylpropanoid mechanism, which lead to monolignols formation. Readers that are interested in detailed shikimate pathway can find detailed information in the study of Arcuri et al. [36].

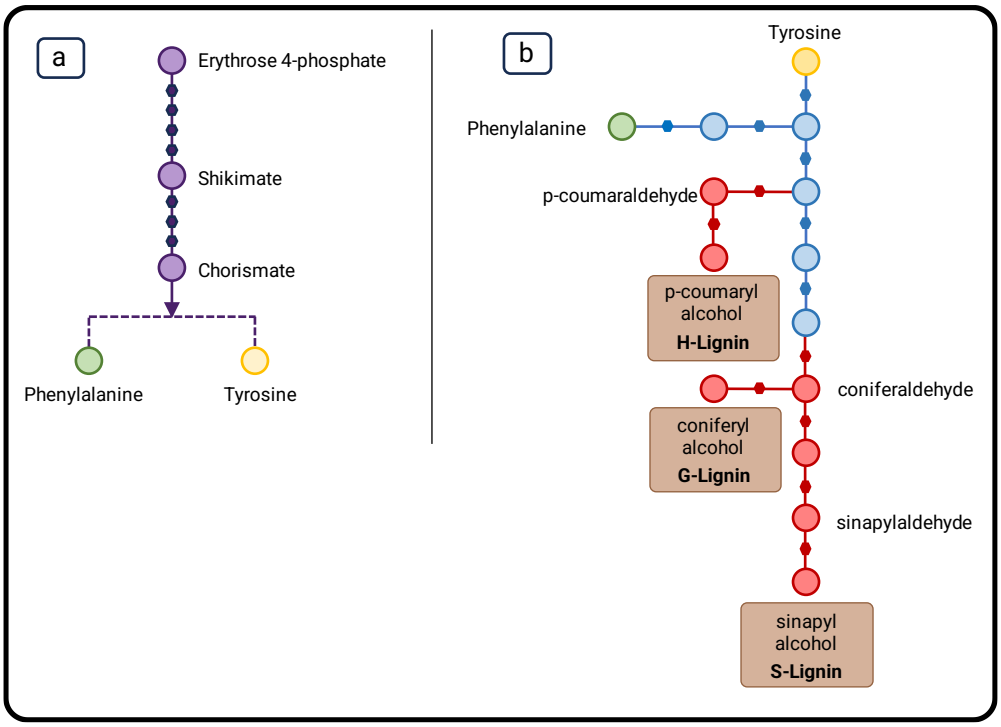

Figure 2. Biological synthesis pathway of monolignols (a) simplified illustration of shikimate pathway for the biosynthesis of phenylalanine and tyrosine – hexagonal structures show enzymatic activities participated, (b) simplified illustration of monolignol biosynthesis mechanism following shikimate mechanism – hexagonal structures correspond to enzymes. Phenylpropanoid pathway is shown in blue and monolignols biosynthesis in red. Illustrations are inspired and recreated from the work of Achyuthan et al. [32].

These two amino acids, which are the precursors of hydroxycinnamyl alcohols (monolignols), later transform into the three main monolignols by a few enzymatically catalyzed reactions, which are considered as the basic building blocks of lignin: p-coumaryl alcohol, coniferyl alcohol and sinapyl alcohol [31]. Each monolignol has different methoxy groups on their phenolic units, and according to these differences three monolignols phenolic units are commonly described as p-hydroxyphenyl (H), quaiacyl (G), and syringyl (S), respectively.

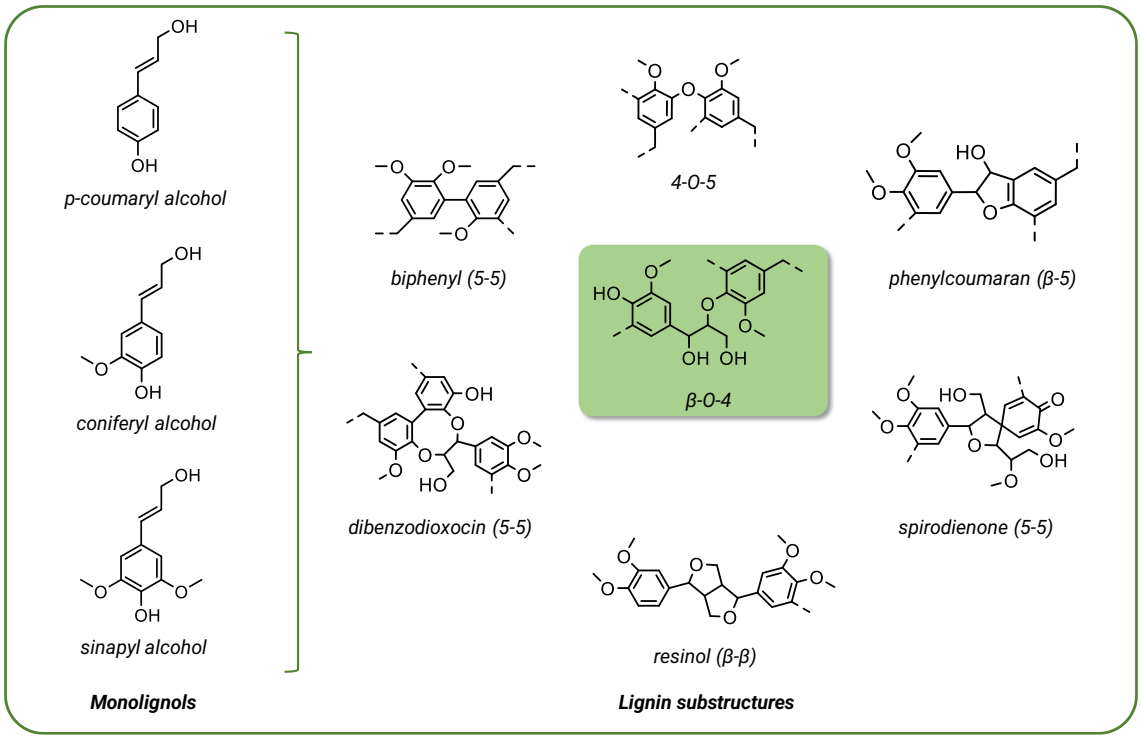

Figure 3. Following phenylpropanoid pathway and forming of the monolignols, radical polymerization leads to different type ether-carbon and carbon-carbon interunit linkages. These substructures exist in native lignin at different occurrence percentages. Fractionation and depolymerization results in cleaving these bonds. Illustrations are inspired and recreated from the work of Schutyser et al. [6].

The composition of these phenolic units and the linkages between them vary considerably between different plant species. For example, hardwood lignin (found in poplar, eucalyptus, birch, etc.) contains both G and S units, whereas softwood lignin (found in spruce, pine, etc.) contains only G units. Conversely, herbaceous biomass contains all three units, but predominantly G units, with an H content typically below 5%. Besides these primary building blocks, lignin contains significant further phenolic compounds, including ferulates and others [37]. Following the biosynthesis of monolignols in plant cells, they migrate to the cell wall and initiate the lignification

process. This sequence of radical polymerization reactions is initiated by two enzymes - laccase and peroxidase - which generate phenoxy radicals by oxidizing phenolic hydroxyl groups [30]. Polymerization continues as the generated radicals combine, resulting in a variety of inter-unit linkages formed randomly by different monolignol phenoxy radicals. The most prevalent of these linkages is the β-O-4 ether motif, which makes up 50-80% of the lignin structure and is therefore predominant [7]. Considering both α-O-4 and β-O-4 ether linkages, it is evident that these are the most easily cleaved and, consequently, the main targets of lignin depolymerization. β-aryl ether substructure's bond dissociation energy is between 54-80 kcal/mol, while BDE for α-O-4 subgroup is in the range of 50-63 kcal/mol. In addition to ether linkages originated from carbohydrate polymers, lignin contains a large number of carbon-carbon linkages between units, including 4-O-5 linkages in phenylcoumaran, 5-5 linkages in biphenyl and dibenzodioxocin, β-β linkages in resinol, and β-1 linkages in spirodienone [38]. BDE of β linkages is between 68-81 kcal/mol, while this value is between 65-69 kcal/mol for β-1 linkages, 78-83 kcal/mol for 4-O-5 bonds, and 115-118 kcal/mol for 5-5 linkages. The bond dissociation energies and the occurrence of the linkages of lignin substructures can be found in Figure 4. H, G and S units contain different amounts of ortho-methoxy groups: H units lack ortho-methoxy groups, while G and S units contain one and two ortho-methoxy groups, respectively [39]. Analysis of these chemical interactions shows that ortho-methoxy groups are not involved in the development of 5-5 and β-5 bonds. Consequently, hardwoods have a lower proportion of C-C bonds than softwood lignin. These structural differences significantly affect the delignification of biomass and lignin depolymerization processes by generating different species during these reactions [40].

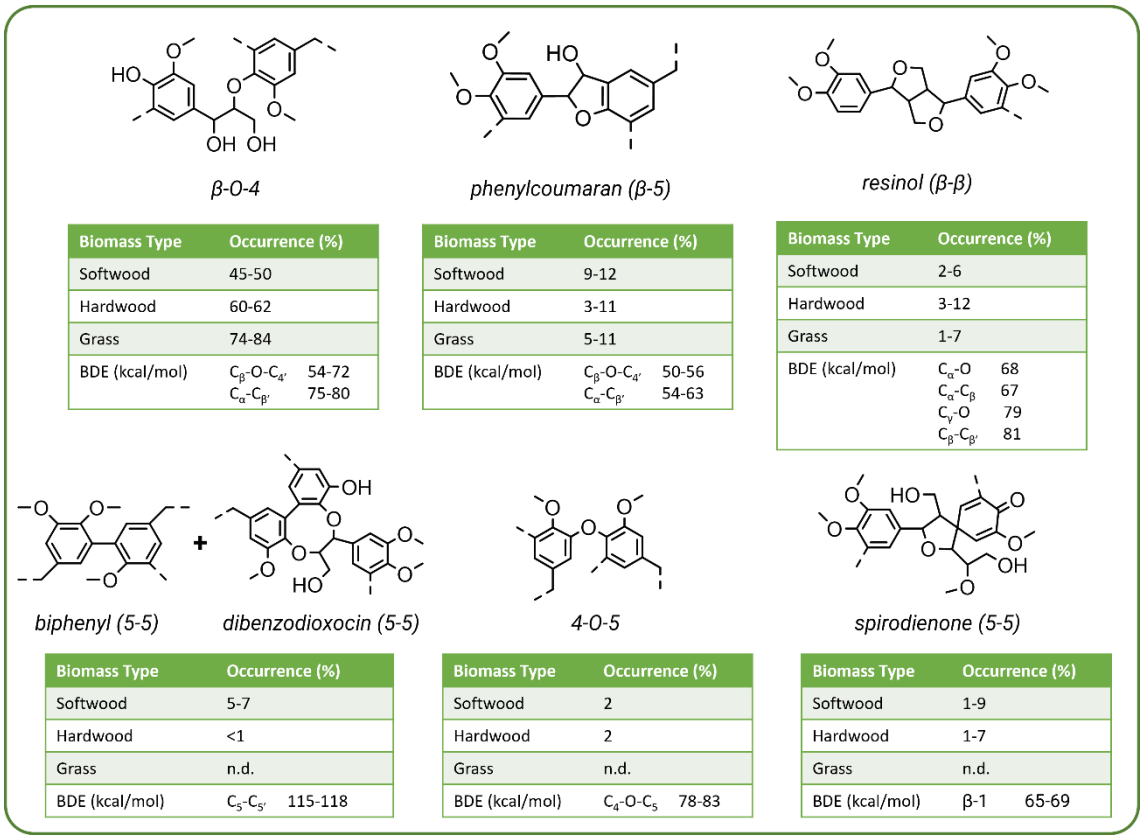

Biomass Type	Occurrence (%)
Softwood	45-50
Hardwood	60-62
Grass	74-84
BDE (kcal/mol)	C_β-O-$C_{4'}$ 54-72 C_α-$C_{\beta'}$ 75-80

Biomass Type	Occurrence (%)
Softwood	9-12
Hardwood	3-11
Grass	5-11
BDE (kcal/mol)	C_β-O-$C_{4'}$ 50-56 C_α-$C_{\beta'}$ 54-63

Biomass Type	Occurrence (%)
Softwood	2-6
Hardwood	3-12
Grass	1-7
BDE (kcal/mol)	C_α-O 68 C_α-C_β 67 C_γ-O 79 C_β-$C_{\beta'}$ 81

Biomass Type	Occurrence (%)
Softwood	5-7
Hardwood	<1
Grass	n.d.
BDE (kcal/mol)	C_5-$C_{5'}$ 115-118

Biomass Type	Occurrence (%)
Softwood	2
Hardwood	2
Grass	n.d.
BDE (kcal/mol)	C_4-O-C_5 78-83

Biomass Type	Occurrence (%)
Softwood	1-9
Hardwood	1-7
Grass	n.d.
BDE (kcal/mol)	β-1 65-69

Figure 4. Types of ether-carbon and carbon-carbon interunit linkages of lignin substructures. These motifs linkages are the primary targets for effective depolymerization strategies. These substructures form in native lignin at different occurrence percentages. Illustrations are inspired and recreated from the work of Rinaldi et al. [7].

The molecular weight (M_w) distribution analysis of native lignin is challenging due to the potential modification of the molecule during the isolation and fractionation processes. Tolbert et al (2014) indicated that the average M_w of almost-native lignin ranges from 2500 to 10000 g/mol [41]. Typically, hemicellulose and lignin are assessed together as they form complexes. Native lignin and hemicellulose are linked together to form an amorphous matrix that reinforces the semicrystalline cellulose fibers, which are known as lignin-carbohydrate complexes (LCCs) [42]. Biomass samples can exhibit distinct variability, even between samples of the same species, due to differences in tissue, cell type and cell wall content, which affect monolignol distribution as well as lignin structure and chemistry. Nevertheless, it is possible to broadly categorize the lignin content of different biomass types. Softwood biomass typically contains the highest lignin content (21-29 wt.%), followed by hardwood biomass (18-25 wt.%) and herbaceous biomass (15-24 wt.%) [43].

1.2. The concept of lignin to valuable products

In order to break down the complex, heterogeneous and recalcitrant structure of lignin, biorefineries typically perform fractionation as a primary step. Conventional fractionation methods, mainly used in the pulp and paper industry, facilitate the recovery of lignin as a solid by-product. This results in a form of lignin different from native lignin, known as isolated lignin, which is characterized by unique structural and chemical properties due to the different techniques used [44]. Examples of isolated lignin include kraft lignin, soda lignin, lignosulfonates, and organosolv lignin, collectively referred to commercially as technical/engineered lignin [45].

Reducing reliance on fossil fuel-derived chemicals is paramount, necessitating the development of a universal approach to lignin valorization, particularly for the synthesis of lignin-derived chemicals. There are three primary pathways to build a successful lignin valorization chain to produce lignin-based fuels and chemicals which are most often considered by the experts: (i) separate and sequential processes of fractionation, depolymerization and upgrading; (ii) combined fractionation and depolymerization followed by upgrading; and (iii) fractionation followed by simultaneous depolymerization and upgrading [46]. Each pathway, as documented in the literature, has distinct advantages and limitations.

Particular attention will be given to base-catalyzed fractionation and kraft pulping due to their global dominance. As the objectives of this thesis are to find a simple way to depolymerize using continuous rapid hydrothermal treatment, refine the depolymerized product, and exploring an application for the prospective products, the rationale behind of this focus will be discussed in more detail in the following chapters.

1.3. Grasping the lignin chemistry during fractionation

The strategy of fractionation is typically employed to mitigate the complex and recalcitrant nature of lignin and to facilitate the production of tailored downstream products. During the thrive of the traditional pulp industry in the 19th and 20th centuries, conventional fractionation processes primarily aimed at isolating and purifying cellulose [4]. This significance on the carbohydrate fraction continued with the emergence of the bioethanol industry. In both strategies, lignin was considered as an underappreciated side stream product, where the separation of the carbohydrates from the lignin was the subject of severe process conditions, resulting in permanent changes to the lignin

structure. As a result, lignin side stream started to be treated as a by-product and utilized in the process cycle in kraft recovery boilers for heat and power generation via incineration [47]. In this section, traditional fractionation methods are described and summarized, with a close look on the structure of lignin, especially the β-O-4 ether linkage.

1.3.1. Base-Catalyzed Fractionation

1.3.1.1. Application and Mechanism

In industrial applications, alkaline media are quite commonly used to extract lignin fractions from biomass, especially lignocellulosic materials. The pulp and paper industry uses various alkaline fractionation techniques to obtain commercially important technical lignin variants, namely kraft, sulfite and soda lignin [48]. Lignin, characterized by its medium-polarity structure, is insoluble in water. However, when exposed to alkaline conditions, its solubility undergoes a significant increase. Under these alkaline conditions, phenolic and benzylic hydroxyl (-OH) groups are deprotonated, leading to the formation of ionic intermediates with significantly increased solubility unlike the native lignin [49].

A key aspect of this process is the cleavage of lignin-carbohydrate linkages, particularly β-O-4 linkages, resulting in the solubilization of the resulting fragments. This alkaline medium also allows depolymerization and/or repolymerization of lignin. The mechanism of the base-catalyzed reactions can be found in the paper of Van den Bosch et al. [39]. The cleavage of β-O-4 bonds within non-phenolic units results in the formation of phenolate ions and epoxide compounds slowly. Epoxide formation contributes to the repolymerization reactions within the medium, which is not the desired outcome in terms of lignin-first biorefineries.

Conversely, the formation of phenolate ions leads to the formation of quinone methide intermediates. These intermediates provide favorable leaving groups such as hydroxyl (-OH) and alkoxy (-OR). In particular, quinone methide is a key intermediate that determines the final composition of the resulting lignin product, a property that is influenced by the alkalinity of the media. Furthermore, due to its susceptibility to nucleophilic attack, quinone methide plays an important role in creating new carbon-carbon (C-C) bonds by triggering repolymerization reactions with the nucleophiles

derived from lignin. In addition, quinone methide is a precursor in the formation of an alkali-stable enol-ether structure [49].

The specific reactions involving the quinone methide intermediate have a significant impact on the end product, and this influence varies depending on the fractionation method employed. While kraft pulping will be discussed in detail, the sulfite and soda pulping techniques will be briefly discussed in the following section.

1.3.1.2. Kraft Pulping

Nowadays, the kraft pulping process is dominating the industry, showing over 90% of the global market share from chemical pulping process. NaOH and Na_2S assisted aqueous solution is used to fractionate lignocellulosic biomass at temperatures between 160°C and 170°C. This technique produces a cellulose-enriched solid pulp as well as a liquid product stream. This liquid product stream, known as black liquor, consists of a composite of lignin and hemicellulose components [39].

Due to the dominance of kraft pulping process, the largest isolated (technical) lignin stream is being produced via this technology. Nevertheless, only a small portion is used to produce isolated kraft lignin commercially. This is due to the utilization of black liquor for heat and electricity generation for the recovery boiler unit of the pulping process. Besides, NaOH and Na_2S recovery and regeneration inside the process cycle in terms of process economics is being crucial.

Strong nucleophilic HS^- ions readily attack the quinone methide intermediates, initiating the cleavage of β-O-4 bonds and facilitating the formation of thiol groups through the involvement of sulfur. The alkaline environment within this process promotes a diverse network culminating in repolymerization reactions. Consequently, in the isolated structure of Kraft lignin, a minimal amount of β-O-4 ether linkages remain intact, besides the presence of low concentration of sulfur (a catalyst inhibitor) [39]. This final structure renders the lignin water-insoluble and significantly more recalcitrant than its native lignin version. When considered together, these characteristics are challenging for the conversion of cellulose-based biorefinery produced isolated kraft lignin into valuable chemicals and fuels.

The odor problems associated with the Kraft cooking process arise from the interaction between intermediates resulting from the cleavage of methyl-aryl ether bonds and sulfur-containing species such as HS^- and CH_3S^-. These interactions lead to the formation of

dimethyl sulfide and methanethiol, compounds responsible for the undesired odors that observed throughout the Kraft pulping process [50].

The pulping process produces many free phenolic groups with some carboxylic and aliphatic -OH groups. Additionally, softwood kraft lignin has a higher average molecular weight than its hardwood equivalent. This difference is due to the reduced C-C bond content characteristic of hardwood lignin (S-type). Consequently, owing to the nature of hardwood lignin, it may show less condensation reactions compared to softwood lignin [39].

1.3.1.3. Black Liquor

Black liquor, a consequential side stream product, includes modified lignin following the separation of cellulosic pulp from digested wood chips through the use of specific solvents/salts, followed by a series of washing steps in traditional cellulose-first chemical pulping processes [51]. The choice of solvents/salts for lignin removal may vary, as long as the primary objective remains to dissolve lignin to facilitate cellulosic pulp production. Whether the process is carried out in an alkaline, acidic or organic solvent medium, the remaining stream is called black liquor. The pH of kraft black liquor is typically in the range of 12-13, and the dissolved solids amount (DS) will vary depending on the stage of the black liquor (weak liquor/strong liquor) [52].

After the digestion of wood chips with NaOH and Na_2S, the pulp stream is separated from the liquor fraction. This specific liquor fraction just after the pulp stream separation is called weak black liquor and contains approximately 15-20 wt.% DS. The next step is to feed this stream to evaporators to increase the lignin concentration, with achievable levels up to 85 wt.% DS [53]. Lignin amount at this stage accounts for approximately 30-45 wt.% of the dry matter content of the black liquor, while inorganic components and aliphatic carboxylic acids together account for approximately 30 wt.%. Major inorganic cations are Na^+ and K^+, while the major inorganic anions are HS^-, CO_3^{2-}, Cl^-, SO_4^{2-}, SO_3^{2-} and $S_2O_3^{2-}$ [54].

The highly alkaline nature of the medium results in almost complete dissolution of organic constituents within the black liquor. Elevated salt concentrations within this highly alkaline medium lead to the dissociation of inorganic salts into ionic species. The result is a complex environment characterized by the coexistence of electrolytes and macromolecules in the presence of inorganic ions and organic materials under highly alkaline conditions. The lignin fragments present in the black liquor consist of mainly

phenolic functional groups incorporated into macromolecular structures. Under alkaline environment, these macromolecules undergo ionization, resulting in the formation of charged groups. As highlighted earlier, the specific nature of each tree contributes to the variability of black liquor composition, thereby imparting a unique quality to the pulping conditions in each mill in different regions. It is also worth noting that even within a single mill, black liquor and lignin characteristics can vary over time. This intricate interaction between lignin macromolecules and electrolytes results in a pronounced thermodynamic complexity [52,54,55].

1.3.1.4. Sulfite Pulping

Until the 1950s, sulfite pulping was the most used process, before the rise of Kraft pulping. Today, the sulfite process has a reduced market share of less than 10%. The pH of the process can be adjusted according to the requirements within a range of 1 to 13 using various cations derived from sulfite or bisulfite salts. Similar to the kraft pulping process, the sulfite pulping process produces quinone methide, which is susceptible to nucleophilic attack by the (bi)sulfite anion. This susceptibility results in the cleavage of the β-O-4 ether configuration. Interestingly, the pH-dependent nature of the process is not a barrier to nucleophilic attack.

A notable outcome of this process is the formation of lignosulfonates, which significantly increase the solubility in water. This increased solubility can positively enable their implementation to different applications such as dispersants and adhesives [6]. However, the sulfite pulping process has a higher sulfur content than the kraft pulping process. Nevertheless, having higher sulfur content compared to kraft pulping process, and having good solubility in water makes its isolation a little bit harder for separation. However, lignosulfonates are the most important commercial source of lignin [39].

1.3.1.5. Soda Pulping

This process bears notable similarity to the kraft pulping process, where the only difference is the use of an NaOH solution instead of Na_2S. In this operation, nucleophilic attacks are orchestrated by OH^- ions, although having relatively weak potency. As a result, these less powerful nucleophilic attacks lead to a reduced efficiency in cleaving ether bonds, thereby inducing quinone methide to participate in repolymerization reactions. This technique finds its primary application in the fractionation of herbaceous

feedstocks, that is driven by their more accessible structural composition and reduced lignin content. A key feature of this process is its sulfur-free nature, which is a significant advantage. However, similar to the previous two methods, this approach also contributes to the strengthening of the recalcitrant lignin structure. This is achieved by the reduction of β-aryl ether bonds and depolymerized fractions participation in repolymerization reactions [39,42].

1.3.2. Lignin Isolation from Black Liquor

Several methods are still relevant today for the separation and purification of lignin from black liquor. The selection criteria for these processes include the need to produce large quantities with high purity, while being simple to operate and economically viable.

The oldest of these techniques is the acidification of black liquor to precipitate lignin. This approach dates back to 1872 when CO_2 injection into hot black liquor was patented [55]. This was followed by another patent that combines acidification and high temperature filtration in 1910. Acidification that followed by high temperature filtration was improving the filtration process [55]. Alen and colleagues further contributed to the field by investigating CO_2-based lignin precipitation. They found that the carbonation time was shortened, and higher yield was observed by increasing the CO_2 pressure [55].

Comparative studies conducted by Uloth and Wearing highlighted three major techniques that are still valid nowadays: i) sulfuric acid/chlorine dioxide precipitation, ii) CO_2-induced precipitation, and iii) ultrafiltration. It's clear that ultrafiltration has higher capital and operating costs compared to acidification. In addition, their research showed that acidification allows for a greater degree of lignin precipitation [55]. Öhman and coworkers investigated the precipitation, filtration and washing steps and found that temperature and pH have a notable effect on lignin yield. In particular, their study showed that CO_2 and strong acid treatments yielded equivalent amounts of lignin [56].

Wallmö et al. extended these findings by identifying increased filtration resistance in hardwood black liquor with increased hemicellulose concentrations. In addition, the parameter of ionic strength was found to be a critical determinant of lignin precipitation [57]. Research by Villar and co-workers shed light on the influence of alcohol-calcium solutions, noting their tendency for significant lignin precipitation along with favorable filtration characteristics [58].

Some researchers explored ultrafiltration of black liquor as a means of lignin separation. Although technically feasible, this method requires significant capital investment, operating costs and besides the cost of the membrane maintenance [55,59].

1.3.3. Kraft Lignin Precipitation Mechanism

Kraft lignin molecules can be described as macromolecular entities that form a polyelectrolyte system in an aqueous environment like black liquor. The abundant availability of phenolics on the surface of the molecule can be considered as the role of the weak acid groups in the alkaline medium of black liquor. Under these conditions, large number of phenolic groups dissociate, resulting in the charging of kraft lignin and becomes dissolved in the surrounding medium. A simplified model of the dissolved state of a kraft lignin macromolecule in black liquor, as proposed by Rezanowich and Goring, and Zhu et al. [55,60,61], can be found as illustrated in Figure 5.

The proposed configuration of the kraft lignin microgel model contain interconnected polyaromatic chains forming a network that is crosslinked at its core, which is charge-free. The negatively charged weak acid groups, namely phenolic groups, are uniformly distributed either on the surface of the network or very close to the surface. The kraft lignin macromolecule is encircled by a multi-layer of cations, mainly sodium and potassium ions. The spatial distribution of these ions demonstrates the characteristics of a Boltzmann distribution [61]. It is important to recognize that this model serves as a simplified, illustrative representation of Kraft lignin macromolecules in black liquor, primarily for quantitative theoretical modelling efforts. In practice, the real-world manifestation of this representative model is likely to be irregular in nature.

Briefly, due to the phenolic groups' dissociation, kraft lignin macromolecules in black liquor become negatively charged in alkaline medium and solubilized. Electrostatic repulsive forces play a key role in causing dissolved lignin macromolecules to repel each other. This phenomenon is at the heart of the stability and solubility of lignin under alkaline conditions. However, when the solution is subjected to acidification, the concentration of hydrogen ions in the

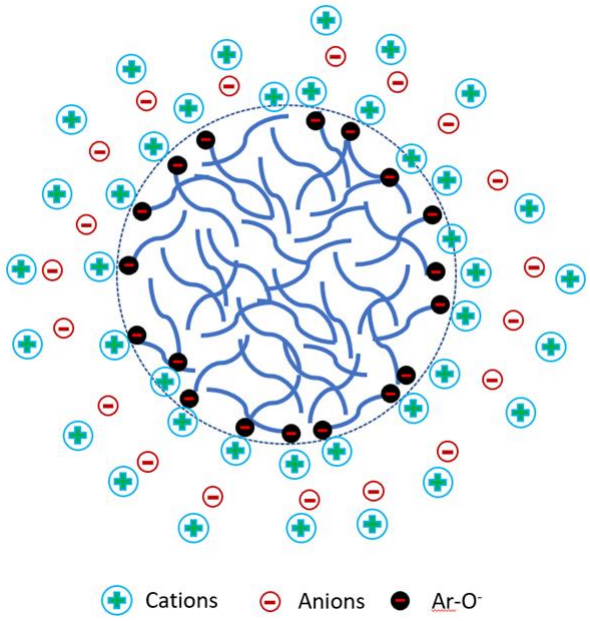

Figure 5. Simplified illustration of a kraft lignin macromolecule in an electrolyte solution. Dissociated phenolic groups shown as Ar-O^-. Illustration inspired by the work of Rezanovich et al. [61].

protonation of the negatively charged phenolic groups. This process ultimately reaches equilibrium and charges become neutralized in each microgel-like kraft lignin macromolecule. As the dominance of repulsive forces diminishes, attractive forces between the molecules increase. This shift towards attractive interactions results in the aggregation of lignin macromolecules, and ultimately lignin precipitates in the solution.

1.4. Isolated Lignin and Black Liquor Depolymerization

Depolymerization of isolated lignin is an area of research that received more attention than methods targeting native lignin, resulting in a considerable number of studies. This section organizes the body of research into four main categories: (i) depolymerization catalyzed by bases and acids, (ii) solvolytic and thermal depolymerization, (iii) reductive depolymerization, and (iv) oxidative depolymerization. The literature within a given category can be further divided into subcategories, each defined by a particular depolymerization technique. However, there is not a strong line that separates these techniques from each other since the combinations of these techniques are carried out frequently. Although hydrothermal liquefaction can be categorized as a subgroup of any depolymerization technique given above, due to the focus of the thesis, it was explained in more detail after oxidative depolymerization technique separately.

1.4.1. Base and Acid Catalyzed Depolymerization

1.4.1.1. Base-catalyzed depolymerization (BCD)

Lignin typically studied at temperatures between 240-330°C using soluble bases, mainly sodium hydroxide (NaOH) [62–67], or alternatively solid bases [68,69]. The experiments are generally conducted by using water or aqueous organic solvent mediums. Maximum yields that were observed do not exceed 20 wt%, and monomer yields are usually under 10 wt%. Although the main products are methoxyphenols at temperatures below 300°C [64,65], the selectivity shifts towards alkyl-catechols, such as methyl- and ethyl-catechol over 300°C [62,64,66]. In a comparative study by Lin et al., between base catalyzed lignin depolymerization and fast pyrolysis showed that BCD produces a narrower range of products, with catechol and methyl catechol as the dominant outputs. In contrast, fast pyrolysis produces a large variety of products, including both substituted and unsubstituted methoxyphenols. A study examined the conversion of hardwood organosolv lignin in water-NaOH mixture at 300°C, and obtained 15 wt% monomer yield in less than 5 min of remarkably short residence time, after which repolymerization reactions caused a steep drop of the yield [65].

The solvent used significantly affects both the yield and the structure of the product. Long et al. demonstrated that the use of MgO as a catalyst in the conversion of pine lignin at 250°C using solvents, such as ethanol/water mixture or methanol, ethanol and THF. It resulted in significantly higher monomer yields (up to 13 wt%) compared to the use of water as a solvent (2 wt%) [70]. A comprehensive study by Chaudhary et al. evaluated different type of solid bases using softwood alkali lignin at 250°C by using ethanol/water mixture and reported 18 wt% monomer yield as the highest using the basic zeolite Na-X [69].

1.4.1.2. Acid catalyzed depolymerization (ACD)

In this technique, lignin is usually worked at over 250°C of moderate-high temperatures. However, some processes often use temperatures in the range of 140-180°C. Acid catalyzed depolymerization of model lignin compounds showed that β-aryl ether linkages can be dissociated at temperatures of 85°C. Different type of soluble Lewis [71–75] and Brønsted acids [70,76–78], and solid Brønsted acids [78–81] was used in these processes, usually in aqueous mediums, organic solvents or solvent mixtures.

Wide range of the monomer yields was reported, where the minimum was 2 wt% and the maximum was around 60 wt%.

In extensive lignin conversion studies using different kind of solid and soluble Brønsted acids, Deepa and Dhepe discovered a rich distribution of products [78,80]. The main compounds were methoxyphenol derivatives such as vanillin, guaiacyl acetone and homovanillic acid. No products were obtained when pure water was the reaction medium, which can be attributed to poor solubility of softwood alkali lignin [80]. Conversely, employing methanol/water mixture at 250°C, depolymerization in mineral acid medium such as H_2SO_4 and HCl gave ~40 wt% and ~30 wt% monomer yield, respectively [78]. In another study, Ma et al. obtained 11 wt% monomer yields by acid catalyzed depolymerization of softwood alkali lignin using H_2O and H_3PO_4 at 260 °C, where the major observed monomer was guaiacol [70].

Another research on lignin conversion using metal salts at an elevated temperature of 400°C conducted by Hensen et al. [74]. They observed low monomer yields and increased char formation when water was used as the solvent. However, the use of ethanol reduced char formation and increased monomer yields. Specifically, when wheat straw lignin was used with $Cu(OAc)_2$ they produced 13 wt% monomers in ethanol, and 6 wt% in water. Researchers claim that $Cu(OAc)_2$ proved to be the most effective catalyst in their study. Phenols and catechols were predominant products in water-based reactions, whereas in ethanol-based reactions phenols and guaiacols were the prevailing ones. Although, a range of products, including aliphatics, acids, ketones, and deoxygenated aromatics were observed, it worths to mention here that these compounds are not considered for the monomer yield calculations due to their potential partial or complete derivation from the ethanol solvent. In particular, the use of ethanol as a solvent introduces complications due to its partial conversion under certain reaction conditions.

Formic acid, often used as a hydrogen donor in lignin conversion studies. However, it is occasionally used in the absence of a redox catalyst, which shifted it to perform primarily as a Brønsted acid catalyst in the reaction medium. [79,82,83]. Formic acid is usually shown to generate hydrogen without a catalyst at high temperatures, whereas a redox catalyst is often required to release hydrogen from donors such as methanol or ethanol. Consequently, lignin conversion in formic acid medium is not only an acid-catalyzed process, but also exhibits a reductive reaction process characteristic. Monomer yields from such reactions were documented to vary widely, ranging from 3 wt% for wheat

straw soda lignin conversion at 360°C in organic solvent [83] to 33 wt% softwood kraft lignin conversion at 246°C in water [82].

1.4.2. Solvolytic and Thermal Depolymerization

1.4.2.1. Solvolytic depolymerization

The process of solvolytic lignin depolymerization includes conversion of lignin by solving and applying heat. A variety of solvents including water [66,68,70,74,82,84], organic compounds [63,68,70,74,85–87], and mixtures of them were used [79,80,84,88]. Hydrogen donating solvents such as short chain alcohols and tetralin are also used often [89]. The operating temperatures of solvolytic depolymerization are usually between 250°C and 450°C. The range of monomeric products derived from lignin solvolysis is extensive and the resulting product distribution is being affected by the type of solvent and the reaction temperature. Despite the wide range of products, selectivity is generally limited, although more selective solvolytic methods were reported in the literature [82,85,86,89]. Predominant aromatic monomers are methoxyphenols with various substitutions, which can be oxygenated (aldehyde, carboxylic acid), saturated and unsaturated moieties. Unsubstituted or alkyl-substituted products are being dominant at temperatures above 300°C, whereas unsaturated and oxygenated substitutions are primarily formed at temperatures below 300°C [84,88]. Besides, greater amount of unsubstituted and alkyl-substituted compounds were observed by using solvolysis in water or water/organic solvents compared to pure organic solvents [84]. In addition, being exposed to high temperature in water medium during lignin solvolysis results in the conversion of methoxyphenols (e.g. guaiacol) to catechol, phenol and cresols [90–92]. When hydrogen donating solvents such as isopropanol or tetralin are used, the primary product predominantly consists of methoxyphenols with alkyl moieties [89].

Catalytic techniques are superior to solvolytic depolymerization to achieve higher monomer yields in most of the studies. It is obvious that monomer yields from solvolytic depolymerization are less favorable than those achieved by catalytic methods, such as acidic, basic or reductive processes. In general, solvolysis of lignin led to monomer yields of less than 10 wt% [6]. However, some studies reported better results. Onwudili and coworkers found 22 wt% monomer yield at 265°C identifying guaiacol as the major product [82]. Jiang et al. used solubilized lignin fraction in depolymerization studies in THF at 300°C [85]. As a result, they reported 24 wt% monomer yield where syringol, ethyl-phenol and ethyl-guaiacol are the predominant products. Solvolytic conversion of

softwood kraft lignin using water was performed by Sasaki and colleagues [90]. They achieved an impressive monomer yield of 37 wt% at 350°C, observing catechol as the predominant product.

1.4.2.2. Fast pyrolysis

Fast pyrolysis is a process characterized by the thermal decomposition of biomass in an inert atmosphere. This decomposition is achieved by rapidly heating the biomass to a temperature range of 450-600°C in an oxygen-deficient medium [93]. As a result of this process, pyrolysis vapors are produced and instantly condensed to produce bio-oil, while other products such as char and gases are produced. The optimum reaction temperature varies between 400°C and 800°C during fast pyrolysis of lignin. Yet, maximum liquid and monomer yields are achieved up to 600°C. In literature, fast pyrolysis of lignin is mostly performed at microscale, in the range of 0.5-1 mg by using micropyrolyzer [94–98]. However, there are also some studies carried out at intermediate scales of 0.2-0.5 g [99,100] and multigram scales approaching >30 g [101–105]. Generally, reported monomer yields do not exceed 20 wt%, and only very few researchers achieved more than 20 wt% monomer yield. To highlight a few prominent studies, Ma et al. reached 27 wt% monomer yield at 650°C [106], whereas Zheng and colleagues obtained 30 wt% at 700°C using softwood alkali lignin [98]. Zhao et al. also observed similar monomer yields of 34-37 wt% using rice husk lignin at 600°C via fast pyrolysis, while the yields using softwood alkali lignins were not exceeding 6-7 wt% under identical conditions [100]. During fast pyrolysis, production of bio-oil is attributed to the rapid condensation of the pyrolysis vapors released. However, most of these research studies are executed by using fast pyrolysis in a micropyrolyzer. The studies that use micropyrolyzer mainly perform direct GC analysis of the vapors, often bypassing the condensation phase [94]. Patwardhan et al. conducted fast pyrolysis experiments of lignin with and without condensation of the vapors to examine the effect of condensation on product distribution . Their observations underlined that the condensation process leads to considerable amount of repolymerization of the reactive aromatic compounds, which in turn limits the monomer yield. Another highlight from their work was the influence of acetic acid. Acetic acid is one of the main products of lignin fast pyrolysis, and Patwardhan et al. found acetic acid facilitates this repolymerization. These results were supported by Zhou et al. by investigating fast pyrolysis of agriculture originated organosolv lignin with and without condensation. They found that FP without

condensation monomer yields 12 wt%, while FP with condensation yields only 6 wt% [102].

Fast pyrolysis processes, like solvolysis processes, result in the synthesis of a wide range of monomeric products. These are mainly methoxyphenols (both substituted and unsubstituted), phenols and catechols. Again, similar to solvolysis product distribution, the main substituents are unsaturated (mainly vinyl), saturated (alkyl) and, to a lesser extent, oxygen including groups such as aldehyde, ketone and carboxylic acid [94,101,107]. The report of Faix et al. demonstrated that the product composition of fast pyrolysis is more complex compared to mild hydroprocessing [96]. Du et al. demonstrated similar result of FP product composition complexity compared to base-catalyzed depolymerization [67]. This underlines the non-selective nature of fast pyrolysis. In the work of Shen et al. unsaturated and oxygenated substituted molecules are obtained at below 650°C. Conversely, at temperatures above 650°C, the product mix is dominated by alkyl-substituted and unsubstituted molecules [108]. Besides, the selectivity shifts towards catechols to phenols from methoxyphenols at elevated temperatures. Various native and isolated lignin pyrolysis are performed by Evans et al. [109]. Main native lignin products were discovered to be sinapyl and coniferyl alcohol. It is important to note that milled wood lignin pyrolysis product composition is similar to native lignin. Conversely, kraft lignin and organosolv lignin pyrolysis yield smaller components which are generally simple substituted or unsubstituted methoxyphenols. The presence of these groups confirms the degraded characteristic of isolated lignins once more.

Lignin FP studies mainly focused on microscale in batch reactors, and the transition to larger continuous scale processes proved to be challenging. An international study on fast pyrolysis of lignin was conducted for high and low purity of lignin [107]. A key finding was not being able to pyrolyze pure lignin effectively in bubbling fluidized bed reactors. Having characteristics of agglomeration tendency and low melting temperature of lignin causes clogging in the pipes or disrupting the reactor bed fluidization. Moreover, lignin with high carbohydrate content performed more effective pyrolysis than pure lignin, that led to the researchers agree on the necessity of new reactor designs for continuous lignin fast pyrolysis. A research study conducted by Zhou et al. showed that lignin pretreatment with calcium hydroxide allows operator to perform continuous pyrolysis of lignin by preventing its melting and agglomeration [102]. Trinh et al. on the other hand

proposed an alternative reactor design that effectively eliminates the feeder clogging issues, although they did encounter problems with the cooling nozzle clogging [104].

1.4.2.3. Catalytic Fast Pyrolysis (CFP)

This depolymerization technique is performed by using a catalyst in fast pyrolysis process. Mirroring the trends observed in lignin fast pyrolysis, most of the research on lignin CFP is carried out using batch micropyrolyzer by using 0.5 to 2 mg of lignin. In situ lignin CFP is often employed with an increased catalyst:lignin ratio, which varies between 2-20 [110–113]. However, ex situ variants of the technique can be implemented in micropyrolyzer, either by using quartz wool to maintain separation between lignin and catalyst within the pyrolysis tube or by incorporating another small furnace to facilitate pyrolysis and catalytic conversion at different temperatures [98,114]. Most of the lignin CFP studies demonstrate a tendency to produce more deoxygenated aromatic molecules. Chemicals like benzene, toluene, xylene and naphthalene can be given as an example. It is also likely to obtain methoxyphenol formation usually. Short chain alkanes and olefins production are also reported in several studies [112,114,115]. However, although a few studies reported higher yields, monomer yields are generally less than 20 wt%. As these compounds can be generated using both carbohydrates and lignin, monomer yields should be calculated carefully due to the dominant presence of deoxygenated aromatics. [100,106,110].

1.4.3. Reductive Depolymerization

Reductive depolymerization involves the decomposition or hydrocracking of lignin using redox catalysts and a reduction agent, such as hydrogen. Hydrogen can be supplied as either gaseous hydrogen or by the presence of hydrogen-donating agents. Usually, the solvent acts as hydrogen donating species, although lignin can also serve this purpose. The use of gaseous hydrogen for this process is called "hydroprocessing". Conversely, if the hydrogen is derived from the solvent or from the lignin itself, the process is called "liquid phase reforming" [6]. A distinctive feature of reductive depolymerization is its dual functionality: not only does it facilitate the depolymerization of lignin, but it also promotes deoxygenation, by the help of hydrogen, through a mechanism known as hydrodeoxygenation. The deoxygenation degree depends on the catalyst used and the process conditions. Hydroprocessing can be further examined under mild, harsh and bifunctional hydroprocessing sections.

1.4.3.1. Mild hydroprocessing

Mild hydroprocessing is performed under comparatively moderate conditions (predominantly ≤300°C) and yields a spectrum of p-substituted methoxyphenols [96,116–120]. Compared to harsh hydroprocessing, mild conditions help to keep the methoxy group products. Mild conditions are generally formed by using a liquid phase and a catalyst. Liquid phase is generally water, organic solvent or mixture of solvents, and the catalyst is usually a base or noble metal catalyst. The main chemical groups attached to these methoxyphenols are alkyl groups and propanol. Faix et al. demonstrated the monomeric product obtained from the mild processing has a reduced complexity compared to that of fast pyrolysis by obtaining similar monomer yields [96]. Usually, monomer yields do not surpass 20 wt% although a few documented much higher.

1.4.3.2. Harsh hydroprocessing

Harsh Hydroprocessing is characterized by the treatment of lignin at elevated temperatures (>320°C) and moderate hydrogen pressure (>35 bar), generally in the absence of solvents [121–123]. Hence a direct interaction occurs between the solid catalyst and the substrate. Although conventional NiMo and CoMo are primarily used as catalysts in this process, there are several studies where different types of noble and base metal catalysts are employed. Exposing to high temperature led to removal of methoxy groups, producing short chained and long chained alkylated phenols or phenol. Besides, mono- and polycyclic deoxygenated aromatics, alkanes, and catechols are reported. The majority of the studies emphasized low selectivity and a wide range of product composition. Monomer yields do not exceed 20 wt% generally, but several studies claimed higher monomer yields. Kloekhorst and coworkers achieved more than 20 wt% of monomer yields by using hardwood organosolv lignin with Ru/C or Pd/C at 400°C in the absence of solvent [123]. Kumar et al. obtained 26 wt% monomer yield by using sulfided NiMo/MgO-La_2O_3 at 350°C without any solvent, and 35 wt% monomer yield by using sulfided NiW/C at 320°C in methanol [122,124].

1.4.3.3. Bifunctional hydroprocessing

In bifunctional hydroprocessing the conversion of lignin to cycloalkanes takes place by using a bifunctional catalyst including acid and metal sites together. In this process, the acid sites are responsible for conducting hydrolysis (depending on the presence of

water) and dehydration reactions, while hydrogenation and hydrogenolysis reactions are selectively enabled by the metal sites [125–127]. This dual-function mechanism promotes both the depolymerization of lignin and the extensive HDO of phenolic molecules, narrowing down the oxygenated molecules presence towards a limited group of alkanes. Ni- and Ru-based catalysts showed their superiority for the production of selective cycloalkanes from lignin. Reaction media can be alkanes, water/organic solvents mixture or water alone. The obtained products include a wide variety of cycloalkanes from C_6 to C_{18} compounds derived from both monomeric and dimeric lignin structures [125–127].

1.4.4. Oxidative Depolymerization

In contrast to reductive strategies, oxidative lignin depolymerization employs the principle of lignin conversion in the context of an oxidant by increasing the oxygen content. Prominent oxidants, such as hydrogen peroxide and dioxygen are in use. Regarding analytical experiments copper oxide and nitrobenzene are usually chosen [128]. The mechanism of oxidative depolymerization discussed elsewhere more in detail. For more information, interested readers are referred to these papers [129,130]. To summarize the conclusion of these studies, oxidative pathway follows either the cleavage of side chains to produce phenolic units and retains aromaticity or disrupting the aromaticity by the aromatic rings cleavage to produce aliphatic carboxylic acids. Most of the studies of oxidative lignin depolymerization primarily aims to phenolic compounds production, whereas only a few studies focus on aliphatic carboxylic acids production. Production of phenolic compounds are mostly conducted by using air or oxygen in alkaline media, while it is possible to find several studies that use acidic media or ionic liquids [6].

Alkaline lignin oxidation gained significant attention in industry and academia because of the selective production of aromatic monomer vanillin by performing lignin oxidation in alkaline medium. Vanillin from lignin production in commercial ways dates to 1936 by using sulfite pulping liquor. In 1981 it is known that 60% of vanillin market were being supplied by lignin oxidation [131]. Later, decreasing sulfite pulping production, and increasing the convenience of synthetic vanillin production using fossil-based resources affected vanillin market from lignin negatively. Today, only 15% of the market is being supplied by vanillin from lignin oxidation [131,132]. Borregaard holds the title of only producer of lignin derived vanillin by oxidation [131,132].

Sodium hydroxide and/or potassium hydroxide are generally preferred as oxidation medium. Oxidation of alkaline lignin is significantly investigated by the presence of oxygen in concentrated NaOH or KOH medium [131–137]. Use of high pH conditions enables ionization of phenolic hydroxyl groups in lignin, and decelerating degradation of the aromatic aldehydes. Besides, it is also published that high pH medium is essential to deprotonate specific reaction intermediates and enabling hydroxyl groups nucleophilic addition reactions [132,138]. Air, pure oxygen or oxygen with nitrogen are generally used for lignin oxidation studies. The reaction conditions were between 120-190 °C, and 2-14 bar. An extensive study of lignin oxidation to produce vanillin was performed to investigate the temperature, pressure, oxygen and NaOH influence on the product yield [132–134]. In conclusion, researchers demonstrated that increasing oxygen pressure and temperature decreases the reaction time to obtain maximum vanillin yield. Moreover, higher reaction temperatures were favoring to increase maximum vanillin yield opposite to increasing oxygen pressure.

Acidic lignin oxidation to produce phenolic compounds is mostly investigated by using pure oxygen or air. The primary solvents for these reactions were inorganic acids, and pure or concentrated acetic acid. A series of work conducted by von Rohr et al. for lignin oxidation in diluted inorganic acid medium, and it was shown that using co-solvent in acidic solutions increases the monomer presence significantly [139–142]. They used methanol as co-solvent to prevent repolymerization interactions [139]. Spruce and pine kraft lignin oxidation in acidic conditions showed a selective formation of vanillin and methyl vanillate. Researchers claimed that they were able to reach 9 wt% and 7 wt% of these two compounds yield by using spruce and pine kraft lignin, respectively [139,140]. When the oxidation process was catalyzed by H_2SO_4, in the presence of metal salts, particularly $CuSO_4$ and $CoCl_2$, a slight increment was observed for the vanillin and methyl vanillate generation [141]. Further experiments performed in continuous setups highlighted the importance of elevated temperatures and short reaction times necessity to obtain optimal yields of monomer, comparable to the alkaline lignin oxidation processes [142].

1.5. Hydrothermal Liquefaction: Thesis Spotlight

Hydrothermal liquefaction (HTL) process can be simply explained like the quickened version of biomass transformation to the crude oil over millions of years deep underground [143]. The HTL process enables user to obtain an oil like liquid product (bio-oil) or biocrude. Pyrolysis also results with bio-oil production, although the bio-oil

produced by pyrolysis has distinct characteristics compared to HTL bio-oils. Since HTL bio-oil has lower oxygen content, it leads to higher heating value compared to pyrolysis, and making HTL bio-oil long lasting. Although this generalization is usually valid, reaction conditions and input material type and concentration play a greater role in the characteristics of bio-oil [143,144].

Under hydrothermal liquefaction category, supercritical water is a state of water where its temperature and pressure are above their critical values: T_c (critical temperature) and P_c (critical pressure). The behavior of a fluid at supercritical state is a combination of a liquid and gas at the same time. These properties give unique abilities to the fluid [145]. For instance, high diffusivity and low viscosity properties above SCW conditions, makes the penetration of water into the macromolecular structure of lignocellulosic material. Besides, having low dielectric constant serves as a non-polar organic solvent behavior and helps to improve the organic components solubility. When the fluid is close to its critical point, small changes in the temperature and/or pressure leads to major changes in its density, dielectric constant and diffusion properties [145]. The ability to change the thermodynamic properties makes the fluid a very tunable medium to improve heat and mass transfer, promote faster reaction kinetics and facilitate the scalability of the process. Supercritical water depolymerization of lignin produces water soluble and insoluble products, besides char and volatile component production [145,146]. It is also possible to carry out lignin depolymerization below critical point of water. That leads to obtaining different reaction mechanisms or product profile according to the chosen conditions. Nevertheless, the reaction media differs between sub- and supercritical water. Subcritical regions favor the ionic reactions, whereas supercritical regions favor the radical reactions [145].

There are a few roles of water during hydrothermal processes which are acting as a solvent, reactant, catalyst, and reaction medium [143]. By different types of mechanism, in both sub- and supercritical conditions, the properties of water can boost the degradation and dissolution of biomasses. It is known that degradation of lignin occurs by different reaction mechanisms like hydrolysis, alkylation, and/or repolymerization [90,147]. The end product after the process is separated usually by centrifuge, which allows solid, liquid, and oil phases separation. After separation of solids and non-oil liquid fraction (water soluble organics), these fractions oily fractions can further be separated by using a suitable organic solvent according to the process conducted. In the end, water soluble organics fraction, which mainly consists of small alcohols, and/or

organic acids, is forming another fraction [148]. Contrarily, less-polar (or non-polar) bio-oil fraction can comprise a large variety of different molecular weight including organic compounds, which can be aromatic monomers, dimers, oligomers, and long chain aliphatic compounds. The common characteristics of bio-oils are having lower oxygen content and higher heating value compared to the raw material used in the process [148].

The complexity of the liquefaction processes includes both sequential and parallel reactions such as hydrolysis (depolymerization) and repolymerization. These result in a wide distribution of product profile that leads to significant analytical challenges. To the best of our knowledge, a complete reaction pathway describing lignin degradation under sub- and supercritical water conditions is still lacking [90]. As a result, studies involving lignin degradation mechanism that exists in the literature are often an oversimplification of the any actual reactions [91,149–151]. Understanding these mechanisms by considering additives (e.g., co-solvents) and catalysts, which play a crucial role in selectivity, is critical to improve bio-oil yield and quality. Grasping these mechanisms is specifically important by taking into account the behavior of by-products such as gas products and char, which are significantly related to bio-oil production [152].

Leading factors that have strong influence on HTL products are temperature, pressure, residence time, catalysts, solvents and raw materials. Research studies mainly depend on playing and modifying these parameters to increase the bio-oil yield. Some of the key articles observations from hydrothermal liquefaction studies on both black liquor and isolated lignin (lignin from black liquor) can be found as summarized in Table 1 [88,90,153–163]. Since it is highly backed up by some countries, LignoBoost lignin constitutes a large fraction among these investigations. This approach is being applied to many traditional kraft pulping processes nowadays with small differences in each mill, which follows acidification, filtration and washing steps. Contrarily, some commercial companies apply membrane filtration, acid precipitation and water removal steps preferably [143].

Some of the major findings that were extracted from key research articles on black liquor or black liquor derived lignin were summarized in Table 2. Even though there are differences in terms of the maximum bio-oil yield expressions of the studies given in Table 2, and not comparable between each other, they are indicating the bio-oil yield according to their own expression in each study. Our previous group member's study highlighted 72.6 wt.% and 91.5 wt.% total bio-oil yield using Sigma Kraft lignin and commercial kraft black liquor extracted lignin, respectively [164]. The optimum reaction

time was 0.3 seconds, at 386°C and 26 MPa. Yong and Matsumura observed that lignin is being completely dissolved even at rapid reaction times of 0.5 seconds [91,151]. They worked on different supercritical water conditions, and maximum bio-oil yield was observed as 21 wt.% at 390°C. They claimed that even at 0.5 seconds repolymerization reactions can take place.

Table 1. Raw material and the reactor types used in the hydrothermal liquefaction studies.

Material	**Reactor**	**C**	**H**	**O**	**S**	**Ash**	**Ref**
Black Liquor	Batch	61.8	6.1	23.0	2.29	-	[156]
Kraft Lignin	Batch	-	-	-	-	-	[88]
LignoBoost Lignin	Continuous, Fixed Bed	65.6	5.7	26	1.85	0.8	[158]
Alkaline	Batch	49	4.4	46.6[a]	0	-	[160]
Black Liquor	Batch	33.7	3.9	38.4	4.3	50.1	[155]
LignoBoost Lignin	Continuous, Fixed Bed	65.6	5.7	26	1.8	0.8	[165]
Black Liquor	Batch	30.5	3.2	66.7[a]	0	-	[159]
Kraft Lignin	Continuous, Plug flow	49.1	4.6	42.1	4.1	-	[164]

[a] the value is sum of sulfur and oxygen, plug flow is used for without heterogeneous catalyst processes, fixed bed is used for with heterogeneous catalyst processes.

Another study using Sigma kraft lignin was performed by Lee et al [88]. They reached max yield of 62 wt.% after 5 min of reaction time at 350°C. Nguyen and coworkers' investigation on LignoBoost lignin at 310°C and 25 MPa between 10-13 min of residence time concluded with 87.7 wt% bio-oil yield [158]. Solantausta et al. studied the hydrothermal liquefaction of commercial softwood kraft black liquor and reached 70 wt.% bio-oil yield at 350°C in 45 min [155]. There are two experiments conducted over 1h and more (2h). Orebom et al. pointed out the yield of 78 wt.% using black liquor at 380°C, 34 MPa and 1 hour [156], while Cheng et al reported 90 wt.% yield using Sigma alkali lignin at 320°C, in 1:1 (v:v) water:ethanol mixture and employing 5 MPa initial H_2 pressure [160]. The latest also gives an example of solvothermal hydrogenation process.

Table 2. Maximum bio-oil yields vs corresponding process conditions. Each process should be evaluated considering corresponding conditions.

Material	Reactor	Max_Yield	Conditions	Time	Ref.
Kraft Lignin	Continuous, Plug Flow	91.5 wt%	386°C, 26 MPa, with NaOH	0.3 sec	[164]
Sigma Kraft Lignin	Continuous, Plug Flow	72.6 wt%	386°C, 26 MPa, with NaOH	0.3 sec	[164]
Sigma Kraft Lignin	Continuous, Plug Flow	21 wt%	390°C	5 sec	[91,151]
Sigma Kraft Lignin	Batch	62 wt%	350°C	5 min	[88]
LignoBoost Lignin	Continuous, Fixed Bed	87.7 wt%	310°C, 25 MPa, ZrO2 catalyst	10-13 min	[158]
Black Liquor	Batch	70 wt%	350°C	45 min	[155]
Black Liquor	Batch	78 wt%	340-350°C, 34-41 MPa	1 h	[156]
Alkali Lignin	Batch	90 wt%	320°C, EtOH:H2O 1:1 (v:v), 5 MPa H2	2 h	[160]

The main outcomes of these studies demonstrate that increasing carbon and hydrogen, and the decreasing oxygen weight are generally encountered by increased temperature that leads to higher heating values of the bio-oil [143]. Besides increased yields of cresol, phenol and alkyl- substituted phenol, temperature rising also results in decreased yields of guaiacol. In addition, phenol and cresol yields increase at higher pressures by using constant temperature due to favored hydrolysis. On the other hand, gas yield increment and tar/char formation decrement are observed when the process pressure is decreased, or temperature increased [143]. Regarding the optimal production of specific chemicals, such as phenol or catechol, requires a balance between the residence time and temperature. Although higher temperatures increase the yield of bio-oil, it is essential to reduce the residence time significantly to prevent gasification and char formation. Higher reaction rates help to intensify processes, yet they can also reduce the selectivity at longer reaction times, which can lead to degradation of the hydrolysis products. This degradation results in forming higher molecular weight products that hinders extracting products and intermediates efficiently from biomass. It is therefore essential to gain a deeper understanding of hydrothermal liquefaction processes. This

will allow us to fully exploit the potential of subcritical and supercritical water depolymerization and improve process selectivity [143].

The initial concentration of lignin is also closely related to bio-oil yield and char formation. Higher concentrations of lignin as raw material led to decreasing bio-oil yield and increasing char formation. It can also be said that the char formation is almost directly proportional to the elevated lignin concentration [143]. One another thing to note here, some studies support keeping the initial lignin concentration at 5 wt.%, which is important to generate higher yields of bio-oil, and lower yields of char. The role of the alkali salts is generally found in catalyzing demethoxylation and decarboxylation reactions, whereas higher NaOH concentrations increased the heavy oil yields by decreasing suspended solids [143].

1.6. Lignin Based Applications

Due to its special properties, lignin attracted more attention from academics and industrial players to be used as an additive in a range of polymers, including synthetic and bio-based polymers such as poly(vinyl alcohol) and polypropylene, polystyrene, polyethylene and polyamide [166]. Lignin is a flexible component that can be used to create new biomaterials because it can dramatically transform or improve the properties of these materials. Improvements in lubricant, flame retardancy, plasticizer, antioxidant, stiffening agent, color additive, and thermal and UV stability are some of these advances [167]. These properties enabled the use of lignin in a wide range of industries, including bioplastics, thermosets, rubber composites, thermoplastics, carbon fibers, aerogels, and foams [166].

The ability of lignin to improve ***resistance to photodegradation*** without affecting processability was proved in polyethylene and polystyrene matrices with additions of up to 20% [168]. Its role as a UV absorber in PVC films, increasing resistance to UV light, further highlights its value in materials exposed to sunlight, with potential applications in automotive parts, acrylic glass and lenses [169]. The effectiveness of lignin in providing UV protection was found to vary with the solvent used to extract it, suggesting that its performance as an antioxidant is dependent on the extraction method and the content of phenolic hydroxyl groups [170,171].

Another area where the addition of lignin was shown a promise is ***thermal resistance***, which is often a limiting factor in traditional polymers and composites. Recent studies

showed that the addition of lignin at concentrations up to 10% can significantly increase the thermal resistance of materials such as natural rubber and polypropylene blends, thereby improving their long-term thermo-oxidative stability [172,173]. Due to the widespread interest in the potential of lignin to improve thermal properties, some reviews were carried out evaluating lignin modification processes and the thermal response of the resulting products. Interested readers can have the benefits of the review article cited here [10].

The ability of lignin to improve the mechanical properties of various materials as a ***reinforcing filler*** was also extensively investigated. The studies showed that lignin presence improves tensile strength, storage modulus and reduces dissipative loss in natural rubber [174]. Studies using lignin as a compatibilizer in composites such as coconut fiber and polypropylene blends was reported improved flexural properties [175]. Lignin was showed to be effective in improving mechanical properties such as tensile strength, modulus of elasticity ductility, and impact strength in polypropylene/chitosan composites [176]. The role of lignin as a reinforcing agent in bioplastics and its reinforcement properties in the rubber industry have been the subject of comprehensive reviews, which were summarized the most recent advances in these areas [177,178].

Flame retardancy is another important property that lignin can contribute to the biomaterials it is used in. Some studies in the literature showed that lignin and its derivatives can improve the combustion time and char yield of polypropylene matrices, minimize heat release and mass loss rates, and maintain mechanical properties [179]. The flame-retardant properties of lignin were also investigated in polylactic acid-based biopolymers and polybutylene succinate, with significant increases in heat release rates and total heat release, making these materials more suitable for a wider range of applications[180,181].

One of the most common uses of lignin is as a ***plasticizer***, which was used in a variety of forms, including lignosulphonates for concrete and chemical modifications such as alkylation to improve the plasticity of polymers such as PVC. These modifications enable lignin to act effectively as a plasticizer, with studies demonstrating its usefulness in different molecular weight fractions, particularly the lower ones, to improve material flexibility and processability [10,182]. In addition, innovative lignin valorization techniques, such as alkaline oxidation (LigniOx), were developed with the aim of using it as a plasticizer. This was recognized by the European Commission as one of the most

innovative bio-based products [183]. Advanced modifications was also aimed at producing super-plasticizers to compete with traditional naphthalene plasticizers [184].

In addition to its role as a plasticizer, the presence of hydroxyl groups in lignin enables the formation of hydrogen bonds, which contribute to ***reduced wear and friction*** when added to base oils. Research highlighted the exceptional ***tribological*** and ***anti-corrosive*** properties of lignin, particularly in bio-based lubricants formulated with lignin and ionic liquids for use on aluminum and iron surfaces. Comparisons of lignins from different sources and extraction processes were stressed the importance of hydrogen bonding and molecular weight in determining thermal and lubricating efficacy, with significant wear reductions reported [185,186]. Lignin-based green ***lubricants*** also demonstrated superior performance over commercial lubricants in specific applications, such as diamond-like carbon-steel contact [187]. In addition, lignin-enriched residues from sugar cane bioethanol production were blended with castor oil to explore the tuning of rheological and lubricant properties, demonstrating the versatility of lignin in the production of both liquid and semi-solid lubricants, including greases [188,189].

The application of lignin extends to ***coloring and pigmentation***, where its inherent dark brown color after separation from cellulose and hemicellulose were used in leather dyeing and in the encapsulation of blue pigments for improved solubilization and stabilization, making them suitable for industrial applications [190,191]. In addition, the antioxidant properties of lignin, attributed to its aromatic structure, were exploited in the production of biomaterials for cosmetics, healthcare, agricultural products and pharmaceuticals. The antioxidant capacity of lignin varies with its origin and extraction method, allowing for tunable properties in applications. Some studies investigated the antioxidant properties of lignin fractions, relating them to solvent solubility, molecular weight and phenolic hydroxyl group content, and found that these factors exert a significant influence on antioxidant activity [192–194].

On an industrial scale, lignin is used as a dispersion, binder, chelating agent and as an alternative to phenolic powder resins in products such as brake pads and molds in automotive industry, and oriented strand boards, polyurethane foams, and epoxy resins. Companies such as Bioconsult GmbH and Nippon Paper developed and marketed lignin-based systems and biomaterials for a variety of applications, including the control of microbial growth in industrial wastewater and the creation of biomaterials with specific functional properties [195]. TECNARO and Prisma Renewable Composites extended the

use of lignin to elastomers, thermoplastics, and carbon fibers, demonstrating its promise as a replacement for traditional materials such as improved mechanical and UV resistance properties of ABS material [196].

Lignin, as a natural polymer by itself or its derivatives, showed great promise in the development of ***polyurethanes*** (PUs) due to its inherent properties and chemical versatility. The utility of this polymer in PU formation is largely attributed to the hydroxyl groups present in its structure, making lignin an attractive ***biopolyol substitute***. Both aromatic and aliphatic hydroxyl groups in lignin are capable of reacting with diisocyanates, which are key components in PU synthesis. However, the reactivity of these groups can sometimes be limited by steric hindrance, which is influenced by the network ordering and self-association of lignin [197,198]. Several modification strategies were used to improve the compatibility of lignin with PU production. For example, demethylation is the process of replacing methyl groups in lignin with hydrogen, thereby increasing the availability of hydroxyl groups. Hydroxyalkylation is another way of introducing primary and secondary alcohols into the lignin structure, increasing its hydroxyl content [197]. Phenolation, which aims to increase the hydroxyl content, and the introduction of amine groups through lignin amination and nitration were also investigated due to the affinity of diisocyanates for amine groups [197,199]. Yet, the high molecular weight and structural complexity of lignin can cause viscosity and reactivity problems, necessitating techniques such as depolymerization to reduce molecular weight and improve processing properties.

Lignin-based PUs have several advantages, including high fire resistance, cross-linking density, UV stability, biodegradability, insulation, compressive strength, antioxidant capacity, thermal stability and reinforcing capabilities [9,197,200]. These properties, together with the widespread availability and low cost of lignin, make it ideal for foam applications where it can be used as a polyol or filler. While lignin concentrations above 30 wt% can increase stiffness and brittleness, flexible chains such as castor oil, butanediol and polypropylene oxide can help to compensate [197]. The performance of lignin-based PUs varies widely depending on the lignin extraction method, biomass source and other parameters, resulting in materials with different properties [201,202].

Despite certain limitations, lignin foams were proved to be comparable, if not superior, to petroleum foams, demonstrating the potential of lignin to replace non-renewable resources in PU applications [9,197]. In addition to foams, lignin was also used in

elastomers, coatings and other specialty applications, demonstrating the versatility of lignin. Griffini et al. used unmodified lignin to produce films with excellent formability, adhesion, tensile and hydrophobic properties [203]. Coatings based on lignin-PU provided anti-oxidation, gas impermeability, and UV resistance, among other benefits [204]. Xie et al. generated PUs with high lignin content and excellent thermal and mechanical properties, which were further enhanced by the incorporation of Ag nanoparticles for antibacterial activities [205]. Fuqiang and Xiangjiao produced UV-cured lignin PUs with improved hydrophobicity, while Hu et al. mixed lignin, carbon nanotubes and Fe_3O_4 nanoparticles to produce PUs with good electromagnetic shielding properties [206,207]. The incorporation of lignin into these polymer matrices not only improves weathering performance, but also helps to create materials with specialized functions [197]. In addition to its use in PUs, lignin utilization was explored as a component in composites for various applications, including tent fabrics, potentiometric chemical sensors, chromatographic and chemoselective membranes, and even as an ink for stereolithography 3D-printing [208,209]. This wide range of applications highlights the potential of lignin as a sustainable and versatile material for advanced materials science and engineering.

Recent research studies also focused on exploring the potential of lignin as a lubricant additive, particularly in developing polyurethane (PU)-based ***lubricant*** systems. The versatility and sustainability of lignin as a bio-based material is highlighted by its diverse role in lubricant formulations. One of the most notable advances was the successful development of lignin-based PUs by Ma et al., in which lignin was used as an emulsifier for the ionic liquid lubricant [BMIm]PF_6 [210]. The resulting products exhibited remarkably low coefficients of friction and wear scars, as well as excellent thermal stability, highlighting the effectiveness of lignin in improving lubrication while maintaining the integrity of the material under thermal stress.

Further investigations examined lignin-based PU formulations acting as gelling agents in castor oil media, paving the way for their promising lubricant applications. Initial studies evaluated various diisocyanates. HDI (hexamethylene diisocyanate) was identified as the superior crosslinker due to its ability to impart rheological properties similar to those of commercial lithium soap-based greases [211]. In a more environmentally friendly approach, subsequent research presented a one-step process for the production of lignin-thickened greases without the need for solvents or catalysts. By carefully controlling the production conditions (such as temperature and stirring

speed), effective formulations were obtained not only with HDI but also with toluene diisocyanate (TDI). This demonstrated the adaptability of the process to different diisocyanates at room temperature and relatively low stirring speeds [212]. Additionally, the innovations were further enriched by patents on lignin-based greases incorporating a polyurea-polyurethane thickener [213], alongside other patented lubricants using lignin as a dispersant and polyurethane as a polymeric binder [214], underlining the ongoing development and commercial potential of lignin-based lubricant solutions.

The use of ***biomass-derived polyols*** was proved to be useful in the production of a wide range of bio-based chemicals, as described in recent research [215,216]. These materials are used as alternatives to petroleum-derived chemicals in a variety of applications including coatings, lubricants, emulsions and bioplastics [217–219]. In the lubricant industry, several studies focused on the substitution of mineral or synthetic oils with vegetable oils or their derivatives over the past decades, as environmental concerns drive the replacement of non-renewable raw materials with renewable resources [220,221]. However, the addition of additives or the application of chemical modifications may be required to improve the lubricating performance when using vegetable oils as lubricants [222]. This is critical when oil structuring is required to produce semi-solid lubricants. For example, sustainable lubricant formulations were prepared by using vegetable oils and biopolymers as a source of polyols and by facilitating the chemical cross-linking between the functional sites of the polyols [223,224]. Among the various cross-linking techniques, the use of epoxides, which can readily react with molecules containing active hydrogen atoms via nucleophilic attack, was proposed previously. For the preparation of environmentally friendly lubricant formulations, two different epoxidation techniques gave satisfactory results. The first involves the epoxidation of lignocellulosic hydroxyl groups with a di- or trifunctional epoxide followed by a reaction with castor oil [189], whereas the second involves the epoxidation of vegetable oil glycerol double bonds followed by a reaction with lignocellulosic hydroxyl groups [188]. However, the rheological properties were different in both cases, although well-structured cross-linked networks were produced. Hence, the dispersion of an epoxy-modified lignocellulosic material in castor oil leads to the formation of highly structured systems, which typically exhibit a solid-state gel reaction [189]. In contrast, by epoxidation of castor oil and subsequent dispersion of lignocellulosic materials, a wider range of rheological properties from Newtonian to non-Newtonian viscoelastic fluids can be obtained, mainly by adjusting the degree of epoxidation [188].

1.7. PressTech Group Contributions

As a PressTech group, we previously contributed to the lignin and black liquor studies. A short summary of these investigations is given below. The differences of this thesis between the previous studies are the use of black liquor as raw material for a detailed mass balance of the experiments, screening studies of black liquor at different conditions and the production of semi-solid bio-lubricant starting from raw black liquor.

In the first chapter of Abad-Fernandez's thesis, the identification of optimal operating conditions for the depolymerization of Kraft lignin using subcritical and supercritical water, with the utilization of continuous sudden-expansion microreactors was the main objective [164]. The research was examined the decomposition of Kraft lignin at four different temperatures—two subcritical (300 and 370°C) and two supercritical (386 and 400°C)—and reaction times below 0.5 seconds to understand how these variables affect the breakdown into phenolic compounds. The experiments were employed commercial Kraft lignin with a molecular weight of approximately 10 kDa. The main low-molecular-weight phenolic compounds in the liquid product fractions were quantified using gas chromatography-mass spectrometry (GC-MS), while the solid residues were analyzed by Fourier transform infrared spectroscopy (FTIR) [164,225].

The results indicated that the optimal conditions for the highest yield of aromatic oils and monomers were at 386°C and 0.17s. Under these conditions, the process achieved an aromatic oil yield of 44.6% and a total monomer yield of 9.9%, effectively suppressing the formation of solid residues. The few solids that did form were primarily repolymerized products, which tended to occur more frequently at higher temperatures and longer reaction times. The first chapter of her study indicates that precise control of temperature and time is crucial for maximizing the yield of valuable low-molecular-weight components from Kraft lignin and minimizing unwanted repolymerization [164].

The second chapter of Abad-Fernandez's thesis was focused to enhance the depolymerization process of lignin using supercritical water in conjunction with the addition of NaOH as a catalyst, with the objective of optimizing the yield of monomeric aromatic compounds derived from Kraft lignin. The process was operated under alkaline conditions at 386°C with reaction times capped at 0.3 seconds, achieving a light oil yield of 60% with notable selectivity (20 wt%) for key phenolic monomers like guaiacol, creosol, vanillin, and acetovanillone. Furthermore, her method effectively suppresses char formation, keeping it to a minimal 4 wt% [164,226].

The depolymerization process commenced with a rapid dehydration phase, followed by the cleavage of C-O and C-C bonds. This resulted in the formation of high yields of low-molecular-weight fragments. However, extending the reaction times promoted the reformation of these fragments into char, which highlights the critical need to maintain short reaction durations for optimal results. The technology has been demonstrated to be highly effective in the treatment of industrial black liquors, with yields exceeding 50 wt% in light oil. The main monomers, including guaiacol, syringol, and syringaldehyde, have been observed to surpass the performance of traditional processes utilizing isolated lignin [164].

These findings served to reinforce the technological advances achieved by employing a Sudden Expansion Micro Reactor, which allows for precise control over reaction time and conditions in order to maximize yields and minimize undesirable by-products. This innovative approach has led to the patenting of the "ULTRA-FAST LIGNIN DEPOLYMERIZATION PROCESS" (European Patent Office, Application number 17382892.2 – 1109), which represents a significant step forward in the valorization of lignin into high-value products [164].

In the third chapter of Abad-Fernandez's thesis, the potential of ultra-fast base-catalyzed supercritical water (SCW) technology for the valorization of various lignin sources derived from hardwoods, softwoods, and crop residues were examined. The SCW process, was conducted at 386°C and 260 bar with a 0.3 second reaction time, was designed to produce high-value, low-molecular-weight compounds from lignins processed via kraft, organosolv, enzymatic, and hydrolysis methods [164,227].

Significant findings include the highest phenolic yield from commercial Kraft lignin was derived from softwood at 9.4 wt%, which surpassed yields from hardwood and crop residue lignins, the latter of which exhibited yields below 1.0 wt%. Notably, this technology was assumed to be capable of efficiently processing black liquors directly from the pulp and paper industry, achieving phenolic yields up to 9.2 wt% without the necessity for prior lignin isolation [164].

The depolymerization of different lignins exhibited variable behaviors, influencing yields and selectivity. Notably, two hardwood lignins processed through Kraft and Organosolv methods showed similar properties and depolymerization patterns, achieving high total bio-oil yields up to 92 wt% and aromatic monomer selectivity up to 16 wt%. The

organosolv lignin was also demonstrated high yields in bio-oils with substantial phenolic monomer content [164].

Her study confirmed that the SCW process induces lignin dehydration without altering its aromatic structure post-polymerization. This can be controlled by short reaction times, which minimizes char formation. This methodology suggests a promising route for incorporating bio-oil production into kraft processes without additional catalysts. She claimed that this approach represented a significant advancement in the utilization of SCW technology for the efficient conversion of lignin to valuable products in a biorefinery setting, thereby enhancing the potential for the economic valorization of lignin [164].

In another thesis from our group, ***the first chapter*** of Adamovic's thesis examined the valorization of defatted grape seeds, a high-lignin-content biomass, through hydrolysis using supercritical water (SCW) at conditions of 380°C and 260 bar, with reaction times ranging from 0.18 second to 1 second. The primary objective was to assess the feasibility of utilizing these grape seeds for sugar recovery and to analyze the structural changes in the lignin during hydrolysis, with a particular focus on both the sugar yield in the liquid phase and the characterization of the solid phase enriched in polyaromatic compounds [228,229].

Her study found that the presence of 36 wt% lignin in the biomass significantly impedes mass transfer, acting as a major barrier during the hydrolysis process. Despite this challenge, a sugar recovery yield of 61 wt% was achieved in the liquid phase within 0.27 second. However, after the longest reaction time of 1 second, 10 wt% of carbohydrates still remained in the solid phase, highlighting the inefficiency caused by the high lignin content [228].

Further analysis of the solid phase included the characterization of milled wood lignin and a dioxane extract of the residue. The dioxane extraction, which utilized an 80% solution, produced a complex mixture that included lignin with chemically linked carbohydrates, residual lipophilic extractives, and flavonoids. The 2D-NMR analysis of the extract indicated subtle cleavages in β-O-4 linkages and other lignin moieties, such as β-β' (resinol) and β-5 (phenylcoumaran), suggesting minimal structural alterations to the lignin [228].

Adamovic's study demonstrated that supercritical water hydrolysis can effectively valorize high-lignin biomass, such as defatted grape seeds, producing significant yields

of sugars and preserving the integrity of lignin structures for potential further applications. The minimal alterations in lignin structure and the significant recovery of sugars demonstrate the potential for further utilization of this byproduct in value-added applications. However, the efficiency of the process is still limited by the inherent properties of the lignin-rich biomass [228].

In Adamovic's second chapter, repolymerization of sulfonated kraft lignin (SKL) in supercritical water (SCW) was examined, which is a significant challenge in the enhancement of monomer recovery from lignin depolymerization. The research focused on the interactions between monomeric compounds released during lignin hydrolysis and lignin fragments, assessing their propensity to form higher molecular weight molecules through repolymerization reactions. In order to gain insight into the repolymerization dynamics of SKL in the SCW environment, a number of specific monomers were studied alongside Indulin Kraft lignin, including vanillin, vanillic acid, vanillyl alcohol, and acetovanillone [228,230].

The key findings of this study include the formation of diarylmethane structures within the 2D-HSQC spectra of the solid residue post-SCW treatment. This indicates that monomers and lignin fragments, particularly those with free phenolic β-O-4 structures, actively contribute to the formation of complex repolymerization structures. The chemical structure of kraft lignin before and after the SCW process remained remarkably similar, suggesting that repolymerization predominantly occurs through cross-linking polymerization within the low molecular weight fractions [228].

Her study observed an increase in the yield of solid fractions when SKL was processed with lignin model compounds (MC) in SCW compared to processing SKL alone. This indicates that MC plays a significant role in solid formation, highlighting the complex dynamics of repolymerization under SCW conditions. In order to improve the recovery of monomers and reduce repolymerization, it was recommended that the light oil fraction enriched in monomers should be separated from the reaction mixture as soon as it is produced [228].

The research findings emphasized the necessity of developing effective methods to inhibit unwanted repolymerization reactions, thereby increasing the recovery of aromatic compounds from lignin. By delving deeper into the mechanisms behind these reactions, it is possible to enhance the efficiency and effectiveness of lignin valorization in an industrial perspective [228].

1.7.1. Considering the unconsidered: Energetic approach at a glance

The energetic approach of biomass hydrolysis in supercritical water was studied by Cantero et al [231]. In this study, a comparative thermodynamic analysis of integrating biomass hydrolysis in supercritical water with power generation via gas turbines was examined. The goal was to produce sugars from biomass through energetically efficient processes having the benefits of a cogeneration cycle and a flash distillation unit. However, the logic behind the background work can be applied to any biomass for the specific pilot plant that works in supercritical water conditions continuously.

It is mentioned that the integration of biomass hydrolysis in supercritical water with power generation by gas turbines with steam injection is a promising alternative to produce sugars from biomass. As the examples were given for the case of cellulose, which was a trend topic at that time, and the main interest of the author, cellulose hydrolysis can be achieved selectively with 98% efficiency and low energy demand when linked to a gas turbine with steam injection, resulting in sugars concentration in the products of 40% [231].

To briefly summarize, the supercritical water hydrolysis pilot plant involves several stages: pressurization of cellulose and water up to the reactor pressure using a positive displacement pump, rapid heating of the biomass stream by mixing it with supercritical water to avoid uncontrolled reactions, almost instantaneous hydrolysis reactions in the reactor with residence times critical for product selectivity, and rapid cooling of the hydrolysis products by sudden decompression to stop the reactions. The use of supercritical water necessitates high pressures and temperatures, and cogeneration, defined as the simultaneous production of various forms of energy from one power source, is highlighted as an efficient solution. This process often involves gas turbines, which offer several advantages including higher overall yields, better flexibility, and higher efficiency compared to other methods [231].

In this work, three options for integrating the hydrolysis process with energy production were analyzed: hydrolysis combined with a gas turbine and vapor injection, hydrolysis combined with a gas turbine without steam injection, and hydrolysis using a biomass burner. The first option involves using a gas turbine with steam injection, where the turbine compresses the necessary airflow in two stages without intercooling, increasing the temperature and thereby generating more work during expansion. The second option is similar but without steam injection. The third option replaces the gas turbine with a

biomass burner. The results show that the setup with gas turbine and steam injection consumes 73 tons of air per hour, 1.23 tons of natural gas per hour, and 13.68 tons of water per hour, producing 554 kg of sugars per hour and 8.9 tons of steam per hour, with the gas turbine producing 5.12 MW of work. The gas turbine without steam injection consumes slightly less natural gas and water (1.1 tons/h, and 12.6 tons/h, respectively), but produces less sugar and less steam, with a lower work output of 4 MW. The biomass burner setup uses biomass instead of natural gas, requiring more biomass due to its lower heating value, producing less sugars and no work output from a turbine. An experimental evaluation using a pilot plant developed by the research group was conducted to validate the simulation results, particularly focusing on the flash temperature and the composition of the vapor phase. The experimental temperatures closely matched the simulated ones, and the concentration of sugars in the vapor phase was negligible (0.0034 w/w), indicating successful separation. These comparative analyses between three different process scenarios showed that the integration of biomass hydrolysis in supercritical water with gas turbines using steam injection is the most efficient and promising method for producing sugars from biomass, highlighted for its high selectivity and low energy demand, with the added benefit of enhancing the yield of the gas turbine when steam from the hydrolysis process is injected [231].

Overall, this approach gives an outlook for the researchers who are interested in learning more about the feasibility and/or scalability of this work. As was mentioned before, it is possible to apply this approach to black liquor and kraft lignin depolymerization using supercritical water.

1.7.2. Observations on the challenges and improvements related to lignin

In Abad-Fernandez's pioneering study of lignin conversion, some critical challenges are found out. One of them is the low biomass concentration of 3% in the biomass tank. This limitation is a significant bottleneck for a scale-up, limiting the amount of aromatic monomer rich oil produced, and increasing water consumption, raising sustainability concerns. To address these issues, in the next step it is necessary to enhance the biomass concentration, which would increase process efficiency and significantly reduce environmental impact by reducing water consumption.

In the literature it is found out the lack of blank tests. Including these experiments is essential to make accurate comparisons between the feedstocks and the final products, which would bias the results. Making these comparisons is crucial to validate the

efficiency of the biomass conversion process, ensuring that any observed differences are truly due to the process and not external factors.

In the case of black liquor, for example, since it is a by-product of the pulp mills, the presence of degradation compounds from the pulping process affects the yield of the products and the mass balance. Therefore, a consistent mass balance was essential to verify the difference between raw materials and products, and to provide unbiased results.

The downstream processing of depolymerized lignin usually involves complex methods in the literature, which affects the feasibility of the separation negatively for industrial purposes. Therefore, it is necessary to investigate the simple downstream processing options to reduce both time and cost which are key elements of process scalability. This pragmatic approach aims to ensure a seamless transition from laboratory success to industrial viability, ensuring widespread adoption without prohibitive costs or inefficiencies.

In order to simplify downstream processing and achieve a consistent mass balance, it is necessary to take a close look at the acidification process. For this reason, the behavior of the pH versus acid amount added should be examined more in detail.

REFERENCES

[1] A.J. Ragauskas, C.K. Williams, B.H. Davison, G. Britovsek, J. Cairney, C.A. Eckert, W.J.. Frederick Jr, J.P. Hallett, D.J. Leak, C.L. Liotta, J.R. Mielenz, R. Murphy, R. Templer, T. Tschaplinski, W.J. Frederick, J.P. Hallett, D.J. Leak, C.L. Liotta, J.R. Mielenz, R. Murphy, R. Templer, T. Tschaplinski, The path forward for biofuels and biomaterials, Science (80-.). 311 (2006) 484–489. https://doi.org/10.1126/science.1114736.

[2] M.I. Hoffert, K. Caldeira, G. Benford, D.R. Criswell, C. Green, H. Herzog, A.K. Jain, H.S. Kheshgi, K.S. Lackner, J.S. Lewis, H.D. Lightfoot, W. Manheimer, J.C. Mankins, M.E. Mauel, L.J. Perkins, M.E. Schlesinger, T. Volk, T.M.L. Wigley, Engineering: Advanced technology paths to global climate stability: Energy for a greenhouse planet, Science (80-.). 298 (2002) 981–987. https://doi.org/10.1126/science.1072357.

[3] K. McCormick, N. Kautto, The Bioeconomy in Europe: An Overview, Sustain. 5 (2013) 2589–2608. https://doi.org/10.3390/su5062589.

[4] B. Kamm, P.R.. Gruber, M. Kamm, eds., Biorefineries-Industrial Processes and Products: Status Quo and Future Directions, 2006.

[5] C.E. Wyman, B.E. Dale, V. Balan, M.T. Holtzapple, Aqueous Pretreatment of Plant Biomass for Biological and Chemical Conversion to Fuels and Chemicals 34 SBE Update : Biofuels Meet the Authors The Need for Biofuels Producing Biofuels via the Thermochemical Platform Producing Biofuels via the Sugar Platfor, (2013) 33–65.

[6] W. Schutyser, T. Renders, S. Van Den Bosch, S.F. Koelewijn, G.T. Beckham, B.F. Sels, Chemicals from lignin: An interplay of lignocellulose fractionation, depolymerisation, and upgrading, Chem. Soc. Rev. 47 (2018) 852–908. https://doi.org/10.1039/c7cs00566k.

[7] R. Rinaldi, R. Jastrzebski, M.T. Clough, J. Ralph, M. Kennema, P.C.A.A. Bruijnincx, B.M. Weckhuysen, Paving the Way for Lignin Valorisation: Recent Advances in Bioengineering, Biorefining and Catalysis, Angew. Chemie - Int. Ed. 55 (2016) 8164–8215. https://doi.org/10.1002/anie.201510351.

[8] A.J. Ragauskas, G.T. Beckham, M.J. Biddy, R. Chandra, F. Chen, M.F. Davis, B.H. Davison, R.A. Dixon, P. Gilna, M. Keller, P. Langan, A.K. Naskar, J.N. Saddler, T.J. Tschaplinski, G.A. Tuskan, C.E. Wyman, Lignin valorization: Improving lignin processing in the biorefinery, Science (80-.). 344 (2014). https://doi.org/10.1126/science.1246843.

[9] B.M. Upton, A.M. Kasko, Strategies for the conversion of lignin to high-value polymeric materials: Review and perspective, Chem. Rev. 116 (2016) 2275–2306. https://doi.org/10.1021/acs.chemrev.5b00345.

[10] S. Sen, S. Patil, D.S. Argyropoulos, Thermal properties of lignin in copolymers, blends, and composites: a review, Green Chem. 17 (2015) 4862–4887. https://doi.org/10.1039/c5gc01066g.

[11] W.J. Liu, H. Jiang, H.Q. Yu, Thermochemical conversion of lignin to functional materials: a review and future directions, Green Chem. 17 (2015) 4888–4907. https://doi.org/10.1039/c5gc01054c.

[12] D. Esposito, M. Antonietti, Redefining biorefinery: the search for unconventional building blocks for materials, Chem. Soc. Rev. 44 (2015) 5821–5835. https://doi.org/10.1039/c4cs00368c.

[13] H. Chung, N.R. Washburn, Chemistry of lignin-based, 1 (2012) 137–160.

[14] C. Li, X. Zhao, A. Wang, G.W. Huber, T. Zhang, Catalytic Transformation of Lignin for the Production of Chemicals and Fuels, Chem. Rev. 115 (2015) 11559–11624. https://doi.org/10.1021/acs.chemrev.5b00155.

[15] J. Zakzeski, P.C.A. Bruijnincx, A.L. Jongerius, B.M. Weckhuysen, The catalytic valorization of lignin for the production of renewable chemicals, Chem. Rev. 110 (2010) 3552–3599. https://doi.org/10.1021/cr900354u.

[16] G.W. Huber, S. Iborra, A. Corma, Synthesis of transportation fuels from biomass: Chemistry, catalysts, and engineering, Chem. Rev. 106 (2006) 4044–4098. https://doi.org/10.1021/cr068360d.

[17] W.V.. Dashek, G.S. Miglani, eds., Plant Cells and Their Organelles, John Wiley & Sons, Ltd., 2017.

[18] P. Kumar, D.M. Barrett, M.J. Delwiche, P. Stroeve, Methods for pretreatment of lignocellulosic biomass for efficient hydrolysis and biofuel production, Ind. Eng. Chem. Res. 48 (2009) 3713–3729. https://doi.org/10.1021/ie801542g.

[19] J. Zakzeski, A.L. Jongerius, P.C.A. Bruijnincx, B.M. Weckhuysen, Catalytic lignin valorization process for the production of aromatic chemicals and hydrogen, ChemSusChem. 5 (2012) 1602–1609. https://doi.org/10.1002/cssc.201100699.

[20] J. Kudakasseril Kurian, G. Raveendran Nair, A. Hussain, G.S. Vijaya Raghavan, Feedstocks, logistics and pre-treatment processes for sustainable lignocellulosic biorefineries: A comprehensive review, Renew. Sustain. Energy Rev. 25 (2013) 205–219. https://doi.org/10.1016/j.rser.2013.04.019.

[21] D. Klemm, B. Heublein, H.P. Fink, A. Bohn, Cellulose: Fascinating biopolymer and sustainable raw material, Angew. Chemie - Int. Ed. 44 (2005) 3358–3393. https://doi.org/10.1002/anie.200460587.

[22] H. Chen, Biotechnology of Lignocellulose, 2014. https://doi.org/10.1007/978-94-007-6898-7.

[23] R. Orlando J., Cellulose Chemistry and Properties: Fibers, Nanocelluloses and Advanced Materials, 2016.

[24] P. Harmsen, W.J.J.. Huijgen, L. Bermudez, R. Bakker, Literature review of physical and chemical pretreatment processes for lignocellulosic biomass, Wageningen UR Food & Biobased Research, 2010.

[25] F.M. Gírio, C. Fonseca, F. Carvalheiro, L.C. Duarte, S. Marques, R. Bogel-Łukasik, Hemicelluloses for fuel ethanol: A review, Bioresour. Technol. 101 (2010) 4775–4800. https://doi.org/10.1016/j.biortech.2010.01.088.

[26] J. Puls, Chemistry and biochemistry of hemicelluloses: Relationshio between hemicellulose structure and enzymes required for hydrolysis, Structure. 120 (1997) 183–196.

[27] Y. Pu, D. Zhang, P.M. Singh, A.J. Ragauskas, The new forestry biofuels sector, Biofuels, Bioprod. Biorefining. 2 (2008) 58–73. https://doi.org/10.1002/bbb.48.

[28] M.B.G. Latarullo, E.Q.P. Tavares, G.P. Maldonado, D.C.C. Leite, M.S. Buckeridge, Pectins, endopolygalacturonases, and bioenergy, Front. Plant Sci. 7 (2016) 1–7. https://doi.org/10.3389/fpls.2016.01401.

[29] C. Loix, M. Huybrechts, J. Vangronsveld, M. Gielen, E. Keunen, A. Cuypers, Reciprocal interactions between cadmium-induced cell wall responses and oxidative stress in plants, Front. Plant Sci. 8 (2017) 1–19. https://doi.org/10.3389/fpls.2017.01867.

[30] W. Boerjan, J. Ralph, M. Baucher, Lignin Biosynthesis, Annu. Rev. Plant Biol. 54 (2003) 519–546. https://doi.org/10.1146/annurev.arplant.54.031902.134938.

[31] R. Vanholme, B. Demedts, K. Morreel, J. Ralph, W. Boerjan, Lignin biosynthesis and structure, Plant Physiol. 153 (2010) 895–905. https://doi.org/10.1104/pp.110.155119.

[32] K.E. Achyuthan, A.M. Achyuthan, P.D. Adams, S.M. Dirk, J.C. Harper, B.A. Simmons, A.K. Singh, Supramolecular self-assembled chaos: Polyphenolic lignin’s barrier to cost-effective lignocellulosic biofuels, Molecules. 15 (2010) 8641–8688. https://doi.org/10.3390/molecules15118641.

[33] R. Hatfield, W. Vermerris, Lignin formation in plants - The dilemma of linkage specificity, Plant Physiol. 126 (2001) 1351–1357. https://doi.org/https://doi.org/10.1104/pp.126.4.1351.

[34] A. Ros Barceló, L. V. Gómez Ros, C. Gabaldón, M. López-Serrano, F. Pomar, J.S. Carrión, M.A. Pedreño, Basic peroxidases: The gateway for lignin evolution, Phytochem. Rev. 3 (2004) 61–78. https://doi.org/10.1023/B:PHYT.0000047803.49815.1a.

[35] S.D. Mansfield, Solutions for dissolution-engineering cell walls for deconstruction, Curr. Opin. Biotechnol. 20 (2009) 286–294. https://doi.org/10.1016/j.copbio.2009.05.001.

[36] H.A. Arcuri, G.F.D. Zafalon, E.A. Marucci, C.E. Bonalumi, N.J.F. da Silveira, J.M. Machado, W.F. de Azevedo, M.S. Palma, SKPDB: A structural database of shikimate pathway enzymes, BMC Bioinformatics. 11 (2010). https://doi.org/10.1186/1471-2105-11-12.

[37] R. Vanholme, K. Morreel, C. Darrah, P. Oyarce, J.H. Grabber, J. Ralph, W. Boerjan, Metabolic engineering of novel lignin in biomass crops, New Phytol. 196 (2012) 978–1000. https://doi.org/10.1111/j.1469-8137.2012.04337.x.

[38] Y. Mottiar, R. Vanholme, W. Boerjan, J. Ralph, S.D. Mansfield, Designer lignins: Harnessing the plasticity of lignification, Curr. Opin. Biotechnol. 37 (2016) 190–200. https://doi.org/10.1016/j.copbio.2015.10.009.

[39] S. Van Den Bosch, S.F. Koelewijn, T. Renders, G. Van den Bossche, T. Vangeel, W. Schutyser, B.F. Sels, Catalytic Strategies Towards Lignin - Derived Chemicals, Springer International Publishing, 2018. https://doi.org/10.1007/s41061-018-0214-3.

[40] D.D. Laskar, B. Yang, H. Wang, J. Lee, Pathways for biomass-derived lignin to hydrocarbon fuels, Biofuels, Bioprod. Biorefining. 7 (2013) 602–626. https://doi.org/10.1002/bbb.1422.

[41] A. Tolbert, H. Akinosho, R. Khunsupat, A.K. Naskar, A.J. Ragauskas, Characterization and analysis of the molecular weight of lignin for biorefining studies, Biofuels, Bioprod. Biorefining. 8 (2014) 836–856. https://doi.org/10.1002/bbb.1500.

[42] S.P.S. Chundawat, G.T. Beckham, M.E. Himmel, B.E. Dale, Deconstruction of lignocellulosic biomass to fuels and chemicals, Annu. Rev. Chem. Biomol. Eng. 2 (2011) 121–145. https://doi.org/10.1146/annurev-chembioeng-061010-114205.

[43] H. Wang, J. Male, Y. Wang, Recent advances in hydrotreating of pyrolysis bio-oil and its oxygen-containing model compounds, ACS Catal. 3 (2013) 1047–1070. https://doi.org/10.1021/cs400069z.

[44] T. Aro, P. Fatehi, Production and Application of Lignosulfonates and Sulfonated Lignin, ChemSusChem. 10 (2017) 1861–1877. https://doi.org/10.1002/cssc.201700082.

[45] S. Constant, H.L.J. Wienk, A.E. Frissen, P. De Peinder, R. Boelens, D.S. Van Es, R.J.H. Grisel, B.M. Weckhuysen, W.J.J. Huijgen, R.J.A. Gosselink, P.C.A. Bruijnincx, New insights into the structure and composition of technical lignins: A comparative characterisation study, Green Chem. 18 (2016) 2651–2665. https://doi.org/10.1039/c5gc03043a.

[46] M. V. Galkin, J.S.M. Samec, Lignin Valorization through Catalytic Lignocellulose Fractionation: A Fundamental Platform for the Future Biorefinery, ChemSusChem. 9 (2016) 1544–1558. https://doi.org/10.1002/cssc.201600237.

[47] R.J.A. Gosselink, E. De Jong, B. Guran, A. Abächerli, Co-ordination network for lignin - Standardisation, production and applications adapted to market requirements (EUROLIGNIN), Ind. Crops Prod. 20 (2004) 121–129. https://doi.org/10.1016/j.indcrop.2004.04.015.

[48] J.H. Lora, Lignin: A Platform for Renewable Aromatic Polymeric Materials, in: P.C.K. Lau (Ed.), Qual. Living Through Chemurg. Green Chem., Springer, 2016. https://doi.org/10.1007/978-3-662-53704-6.

[49] J. Gierer, Chemistry of delignification - Part 1: General concept and reactions during pulping, Wood Sci. Technol. 19 (1985) 289–312. https://doi.org/10.1007/BF00350807.

[50] G. Gellerstedt, E. Sjöholm, I. Brodin, The Wood-Based Biorefinery : A Source of Carbon Fiber ? Average Swedish Mill 2000, Open Agric. J. 3 (2010) 119–124.

[51] P. Bajpai, Biermann's Handbook of Pulp and Paper: Raw Material and Pulp Making, 3rd ed., Elsevier, 2018. https://doi.org/10.1016/C2017-0-00530-X.

[52] T.N. Adams, W.J. Frederick, T.M. Grace, M. Hupa, K. Lisa, A.K. Jones, H. Tran, Black Liquor Properties, in: H. Tran (Ed.), Kraft Recover. Boil., TAPPI Press, Atlanta, GA, 1997: p. 380.

[53] C.L. Verrill, Evaporation principles and black liquor properties, TAPPI Kraft Recover. Course 2007. (n.d.).

[54] K.. Niemelä, R. Alén, Characterization of pulping liquors, in: S. Eero, R. Alén (Eds.), Anal. Methods Wood Chem. Pulping, Papermak., 1st ed., Springer, 1999: pp. 193–232. https://doi.org/10.1007/978-3-662-03898-7.

[55] W. Zhu, Precipitation of Kraft Lignin Yield and Equilibrium, Chalmers University, 2015. http://publications.lib.chalmers.se/records/fulltext/216246/216246.pdf.

[56] Ö. Fredrik, H. Theliander, Filtration properties of lignin precipitated from black liquor, Tappi J. 6 (2007) 3–9. https://doi.org/10.32964/tj6.7.3.

[57] H. Wallmo, H. Theliander, A.S. Jönsson, O. Wallberg, K. Lindgren, The influence of hemicelluloses during the precipitation of lignin in kraft black liquor, Nord. Pulp Pap. Res. J. 24 (2009) 165–171. https://doi.org/10.3183/npprj-2009-24-02-p165-171.

[58] J.C. Villar, A. Caperos, Precipitation of Kraft Black Liquors by Alcohol-Calcium Solutions, Sep. Sci. Technol. 31 (1996) 1721–1739.

[59] A. Toledano, A. García, I. Mondragon, J. Labidi, Lignin separation and fractionation by ultrafiltration, Sep. Purif. Technol. 71 (2010) 38–43. https://doi.org/10.1016/j.seppur.2009.10.024.

[60] D.A.I. Goring, The physical chemistry of lignin, Pure Appl. Chem. 5 (1962) 233–310. https://doi.org/10.1351/pac196205010233.

[61] A. Rezanowich, D.A.I. Goring, Polyelectrolyte expansion of a lignin sulfonate microgel, J. Colloid Sci. 15 (1960) 452–471. https://doi.org/10.1016/0095-8522(60)90049-0.

[62] R. Katahira, A. Mittal, K. McKinney, X. Chen, M.P. Tucker, D.K. Johnson, G.T. Beckham, Base-Catalyzed Depolymerization of Biorefinery Lignins, ACS Sustain. Chem. Eng. 4 (2016) 1474–1486. https://doi.org/10.1021/acssuschemeng.5b01451.

[63] J. Long, Y. Xu, T. Wang, Z. Yuan, R. Shu, Q. Zhang, L. Ma, Efficient base-catalyzed decomposition and in situ hydrogenolysis process for lignin depolymerization and char elimination, Appl. Energy. 141 (2015) 70–79. https://doi.org/10.1016/j.apenergy.2014.12.025.

[64] J.M. Lavoie, W. Baré, M. Bilodeau, Depolymerization of steam-treated lignin for the production of green chemicals, Bioresour. Technol. 102 (2011) 4917–4920. https://doi.org/10.1016/j.biortech.2011.01.010.

[65] V.M. Roberts, V. Stein, T. Reiner, A. Lemonidou, X. Li, J.A. Lercher, Towards quantitative catalytic lignin depolymerization, Chem. - A Eur. J. 17 (2011) 5939–5948. https://doi.org/10.1002/chem.201002438.

[66] A. Toledano, L. Serrano, J. Labidi, Organosolv lignin depolymerization with different base catalysts, J. Chem. Technol. Biotechnol. 87 (2012) 1593–1599. https://doi.org/10.1002/jctb.3799.

[67] L. Du, Z. Wang, S. Li, W. Song, W. Lin, A comparison of monomeric phenols produced from lignin by fast pyrolysis and hydrothermal conversions, Int. J. Chem. React. Eng. 11 (2013) 135–145. https://doi.org/10.1515/ijcre-2012-0085.

[68] J.S. Kruger, N.S. Cleveland, S. Zhang, R. Katahira, B.A. Black, G.M. Chupka, T. Lammens, P.G. Hamilton, M.J. Biddy, G.T. Beckham, Lignin Depolymerization with Nitrate-Intercalated Hydrotalcite Catalysts, ACS Catal. 6 (2016) 1316–1328. https://doi.org/10.1021/acscatal.5b02062.

[69] R. Chaudhary, P.L. Dhepe, Solid base catalyzed depolymerization of lignin into low molecular weight products, Green Chem. 19 (2017) 778–788. https://doi.org/10.1039/c6gc02701f.

[70] J. Long, Q. Zhang, T. Wang, X. Zhang, Y. Xu, L. Ma, An efficient and economical process for lignin depolymerization in biomass-derived solvent tetrahydrofuran,

Bioresour. Technol. 154 (2014) 10–17. https://doi.org/10.1016/j.biortech.2013.12.020.

[71] C.S. Lancefield, I. Panovic, P.J. Deuss, K. Barta, N.J. Westwood, Pre-treatment of lignocellulosic feedstocks using biorenewable alcohols: Towards complete biomass valorisation, Green Chem. 19 (2017) 202–214. https://doi.org/10.1039/c6gc02739c.

[72] P.J. Deuss, C.W. Lahive, C.S. Lancefield, N.J. Westwood, P.C.J. Kamer, K. Barta, J.G. de Vries, Metal Triflates for the Production of Aromatics from Lignin, ChemSusChem. 9 (2016) 2974–2981. https://doi.org/10.1002/cssc.201600831.

[73] R. Jastrzebski, S. Constant, C.S. Lancefield, N.J. Westwood, B.M. Weckhuysen, P.C.A. Bruijnincx, Tandem catalytic depolymerization of lignin by water-tolerant Lewis acids and rhodium complexes, ChemSusChem. 9 (2016) 2074–2079. https://doi.org/10.1002/cssc.201600683.

[74] B. Güvenatam, E.H.J. Heeres, E.A. Pidko, E.J.M. Hensen, Lewis-acid catalyzed depolymerization of Protobind lignin in supercritical water and ethanol, Catal. Today. 259 (2016) 460–466. https://doi.org/10.1016/j.cattod.2015.03.041.

[75] B. Güvenatam, E.H.J. Heeres, E.A. Pidko, E.J.M. Hensen, Lewis acid-catalyzed depolymerization of soda lignin in supercritical ethanol/water mixtures, Catal. Today. 269 (2016) 9–20. https://doi.org/10.1016/j.cattod.2015.08.039.

[76] P.J. Deuss, M. Scott, F. Tran, N.J. Westwood, J.G. De Vries, K. Barta, Aromatic Monomers by in Situ Conversion of Reactive Intermediates in the Acid-Catalyzed Depolymerization of Lignin, J. Am. Chem. Soc. 137 (2015) 7456–7467. https://doi.org/10.1021/jacs.5b03693.

[77] C.W. Lahive, P.J. Deuss, C.S. Lancefield, Z. Sun, D.B. Cordes, C.M. Young, F. Tran, A.M.Z. Slawin, J.G. De Vries, P.C.J. Kamer, N.J. Westwood, K. Barta, Advanced Model Compounds for Understanding Acid-Catalyzed Lignin Depolymerization: Identification of Renewable Aromatics and a Lignin-Derived Solvent, J. Am. Chem. Soc. 138 (2016) 8900–8911. https://doi.org/10.1021/jacs.6b04144.

[78] A.K. Deepa, P.L. Dhepe, Solid acid catalyzed depolymerization of lignin into value added aromatic monomers, RSC Adv. 4 (2014) 12625–12629. https://doi.org/10.1039/c3ra47818a.

[79] R.J.A. Gosselink, W. Teunissen, J.E.G. van Dam, E. de Jong, G. Gellerstedt, E.L. Scott, J.P.M. Sanders, Lignin depolymerisation in supercritical carbon dioxide/acetone/water fluid for the production of aromatic chemicals, Bioresour. Technol. 106 (2012) 173–177. https://doi.org/10.1016/j.biortech.2011.11.121.

[80] A.K. Deepa, P.L. Dhepe, Lignin Depolymerization into Aromatic Monomers over Solid Acid Catalysts, ACS Catal. 5 (2015) 365–379. https://doi.org/10.1021/cs501371q.

[81] T. Yoshikawa, S. Shinohara, T. Yagi, N. Ryumon, Y. Nakasaka, T. Tago, T. Masuda, Production of phenols from lignin-derived slurry liquid using iron oxide catalyst, Appl. Catal. B Environ. 146 (2014) 289–297. https://doi.org/10.1016/j.apcatb.2013.03.010.

[82] J.A. Onwudili, P.T. Williams, Catalytic depolymerization of alkali lignin in subcritical water: Influence of formic acid and Pd/C catalyst on the yields of liquid monomeric aromatic products, Green Chem. 16 (2014) 4740–4748. https://doi.org/10.1039/c4gc00854e.

[83] D. Forchheim, J.R. Gasson, U. Hornung, A. Kruse, T. Barth, Modeling the lignin degradation kinetics in a ethanol/formic acid solvolysis approach. part 2. validation and transfer to variable conditions, Ind. Eng. Chem. Res. 51 (2012) 15053–15063. https://doi.org/10.1021/ie3026407.

[84] Y. Ye, J. Fan, J. Chang, Effect of reaction conditions on hydrothermal degradation of cornstalk lignin, J. Anal. Appl. Pyrolysis. 94 (2012) 190–195. https://doi.org/10.1016/j.jaap.2011.12.005.

[85] Z. Jiang, T. He, J. Li, C. Hu, Selective conversion of lignin in corncob residue to monophenols with high yield and selectivity, Green Chem. 16 (2014) 4257–4265. https://doi.org/10.1039/c4gc00620h.

[86] L. Hu, Y. Luo, B. Cai, J. Li, D. Tong, C. Hu, The degradation of the lignin in Phyllostachys heterocycla cv. pubescens in an ethanol solvothermal system, Green Chem. 16 (2014) 3107–3116. https://doi.org/10.1039/c3gc42489h.

[87] X. Erdocia, R. Prado, J. Fernández-Rodríguez, J. Labidi, Depolymerization of Different Organosolv Lignins in Supercritical Methanol, Ethanol, and Acetone to Produce Phenolic Monomers, ACS Sustain. Chem. Eng. 4 (2016) 1373–1380. https://doi.org/10.1021/acssuschemeng.5b01377.

[88] H. shik Lee, J. Jae, J.M. Ha, D.J. Suh, Hydro- and solvothermolysis of kraft lignin for maximizing production of monomeric aromatic chemicals, Bioresour. Technol. 203 (2016) 142–149. https://doi.org/10.1016/j.biortech.2015.12.022.

[89] K.H. Kim, R.C. Brown, M. Kieffer, X. Bai, Hydrogen-donor-assisted solvent liquefaction of lignin to short-chain alkylphenols using a micro reactor/gas chromatography system, Energy and Fuels. 28 (2014) 6429–6437. https://doi.org/10.1021/ef501678w.

[90] Wahyudiono, M. Sasaki, M. Goto, Recovery of phenolic compounds through the decomposition of lignin in near and supercritical water, Chem. Eng. Process. Process Intensif. 47 (2008) 1609–1619. https://doi.org/10.1016/j.cep.2007.09.001.

[91] T.L.K. Yong, M. Yukihiko, Kinetic analysis of guaiacol conversion in sub- and supercritical water, Ind. Eng. Chem. Res. 52 (2013) 9048–9059.

https://doi.org/10.1021/ie4009748.

[92] H. Pińkowska, P. Wolak, A. Złocińska, Hydrothermal decomposition of alkali lignin in sub- and supercritical water, Chem. Eng. J. 187 (2012) 410–414. https://doi.org/10.1016/j.cej.2012.01.092.

[93] C. Liu, H. Wang, A.M. Karim, J. Sun, Y. Wang, Catalytic fast pyrolysis of lignocellulosic biomass, Chem. Soc. Rev. 43 (2014) 7594–7623. https://doi.org/10.1039/c3cs60414d.

[94] P.R. Patwardhan, R.C. Brown, B.H. Shanks, Product distribution from the fast pyrolysis of hemicellulose, ChemSusChem. 4 (2011) 636–643. https://doi.org/10.1002/cssc.201000425.

[95] J.Q. Bond, A.A. Upadhye, H. Olcay, G.A. Tompsett, J. Jae, R. Xing, D.M. Alonso, D. Wang, T. Zhang, R. Kumar, A. Foster, S.M. Sen, C.T. Maravelias, R. Malina, S.R.H. Barrett, R. Lobo, C.E. Wyman, J.A. Dumesic, G.W. Huber, Production of renewable jet fuel range alkanes and commodity chemicals from integrated catalytic processing of biomass, Energy Environ. Sci. 7 (2014) 1500–1523. https://doi.org/10.1039/c3ee43846e.

[96] O. Faix, D. Meier, Pyrolytic and hydrogenolytic degradation studies on lignocellulosics, pulps and lignins, Holz Als Roh- Und Werkst. 47 (1989) 67–72. https://doi.org/10.1007/BF02628617.

[97] V.B.F. Custodis, C. Bährle, F. Vogel, J.A. Van Bokhoven, Phenols and aromatics from fast pyrolysis of variously prepared lignins from hard- and softwoods, J. Anal. Appl. Pyrolysis. 115 (2015) 214–223. https://doi.org/10.1016/j.jaap.2015.07.018.

[98] Y. Zheng, D. Chen, X. Zhu, Aromatic hydrocarbon production by the online catalytic cracking of lignin fast pyrolysis vapors using Mo2N/γ-Al2O3, J. Anal. Appl. Pyrolysis. 104 (2013) 514–520. https://doi.org/10.1016/j.jaap.2013.05.018.

[99] R. Lou, S. Wu, G. Lyu, Quantified monophenols in the bio-oil derived from lignin fast pyrolysis, J. Anal. Appl. Pyrolysis. 111 (2015) 27–32. https://doi.org/10.1016/j.jaap.2014.12.022.

[100] Y. Zhao, L. Deng, B. Liao, Y. Fu, Q.X. Guo, Aromatics production via catalytic pyrolysis of pyrolytic lignins from bio-oil, Energy and Fuels. 24 (2010) 5735–5740. https://doi.org/10.1021/ef100896q.

[101] P.J. De Wild, W.J.J. Huijgen, H.J. Heeres, Pyrolysis of wheat straw-derived organosolv lignin, J. Anal. Appl. Pyrolysis. 93 (2012) 95–103. https://doi.org/10.1016/j.jaap.2011.10.002.

[102] S. Zhou, R.C. Brown, X. Bai, The use of calcium hydroxide pretreatment to

overcome agglomeration of technical lignin during fast pyrolysis, Green Chem. 17 (2015) 4748–4759. https://doi.org/10.1039/c5gc01611h.

[103] S. Farag, D. Fu, P.G. Jessop, J. Chaouki, Detailed compositional analysis and structural investigation of a bio-oil from microwave pyrolysis of kraft lignin, J. Anal. Appl. Pyrolysis. 109 (2014) 249–257. https://doi.org/10.1016/j.jaap.2014.06.005.

[104] T.N. Trinh, P.A. Jensen, Z. Sárossy, K. Dam-Johansen, N.O. Knudsen, H.R. Sørensen, H. Egsgaard, Fast pyrolysis of lignin using a pyrolysis centrifuge reactor, Energy and Fuels. 27 (2013) 3802–3810. https://doi.org/10.1021/ef400527k.

[105] S. Farag, B.P. Mudraboyina, P.G. Jessop, J. Chaouki, Impact of the heating mechanism on the yield and composition of bio-oil from pyrolysis of kraft lignin, Biomass and Bioenergy. 95 (2016) 344–353. https://doi.org/10.1016/j.biombioe.2016.07.005.

[106] Z. Ma, E. Troussard, J.A. Van Bokhoven, Controlling the selectivity to chemicals from lignin via catalytic fast pyrolysis, Appl. Catal. A Gen. 423–424 (2012) 130–136. https://doi.org/10.1016/j.apcata.2012.02.027.

[107] D.J. Nowakowski, A. V. Bridgwater, D.C. Elliott, D. Meier, P. de Wild, Lignin fast pyrolysis: Results from an international collaboration, J. Anal. Appl. Pyrolysis. 88 (2010) 53–72. https://doi.org/10.1016/j.jaap.2010.02.009.

[108] D.K. Shen, S. Gu, K.H. Luo, S.R. Wang, M.X. Fang, The pyrolytic degradation of wood-derived lignin from pulping process, Bioresour. Technol. 101 (2010) 6136–6146. https://doi.org/10.1016/j.biortech.2010.02.078.

[109] R.J. Evans, T.A. Milne, M.N. Soltys, Direct mass-spectrometric studies of the pyrolysis of carbonaceous fuels. III. Primary pyrolysis of lignin, J. Anal. Appl. Pyrolysis. 9 (1986) 207–236. https://doi.org/10.1016/0165-2370(86)80012-2.

[110] M. Zhang, F.L.P. Resende, A. Moutsoglou, Catalytic fast pyrolysis of aspen lignin via Py-GC/MS, Fuel. 116 (2014) 358–369. https://doi.org/10.1016/j.fuel.2013.07.128.

[111] Y. Yu, X. Li, L. Su, Y. Zhang, Y. Wang, H. Zhang, The role of shape selectivity in catalytic fast pyrolysis of lignin with zeolite catalysts, Appl. Catal. A Gen. 447–448 (2012) 115–123. https://doi.org/10.1016/j.apcata.2012.09.012.

[112] K. Wang, K.H. Kim, R.C. Brown, Catalytic pyrolysis of individual components of lignocellulosic biomass, Green Chem. 16 (2014) 727–735. https://doi.org/10.1039/c3gc41288a.

[113] M. Zhang, A. Moutsoglou, Catalytic fast pyrolysis of prairie cordgrass lignin and quantification of products by pyrolysis-gas chromatography-mass spectrometry,

Energy and Fuels. 28 (2014) 1066–1073. https://doi.org/10.1021/ef401795z.

[114] Y. Xue, S. Zhou, X. Bai, Role of Hydrogen Transfer during Catalytic Copyrolysis of Lignin and Tetralin over HZSM-5 and HY Zeolite Catalysts, ACS Sustain. Chem. Eng. 4 (2016) 4237–4250. https://doi.org/10.1021/acssuschemeng.6b00733.

[115] G. Zhou, P.A. Jensen, D.M. Le, N.O. Knudsen, A.D. Jensen, Direct upgrading of fast pyrolysis lignin vapor over the HZSM-5 catalyst, Green Chem. 18 (2016) 1965–1975. https://doi.org/10.1039/c5gc01976a.

[116] J.Y. Kim, J. Park, U.J. Kim, J.W. Choi, Conversion of Lignin to Phenol-Rich Oil Fraction under Supercritical Alcohols in the Presence of Metal Catalysts, Energy and Fuels. 29 (2015) 5154–5163. https://doi.org/10.1021/acs.energyfuels.5b01055.

[117] X. Wang, R. Rinaldi, Solvent effects on the hydrogenolysis of diphenyl ether with raney nickel and their implications for the conversion of lignin, ChemSusChem. 5 (2012) 1455–1466. https://doi.org/10.1002/cssc.201200040.

[118] V. Molinari, G. Clavel, M. Graglia, M. Antonietti, D. Esposito, Mild Continuous Hydrogenolysis of Kraft Lignin over Titanium Nitride-Nickel Catalyst, ACS Catal. 6 (2016) 1663–1670. https://doi.org/10.1021/acscatal.5b01926.

[119] J.Y. Kim, J. Park, H. Hwang, J.K. Kim, I.K. Song, J.W. Choi, Catalytic depolymerization of lignin macromolecule to alkylated phenols over various metal catalysts in supercritical tert-butanol, J. Anal. Appl. Pyrolysis. 113 (2015) 99–106. https://doi.org/10.1016/j.jaap.2014.11.011.

[120] A. McVeigh, F.P. Bouxin, M.C. Jarvis, S.D. Jackson, Catalytic depolymerisation of isolated lignin to fine chemicals: Part 2-process optimisation, Catal. Sci. Technol. 6 (2016) 4142–4150. https://doi.org/10.1039/c5cy01896j.

[121] A. Kloekhorst, H.J. Heeres, Catalytic hydrotreatment of Alcell lignin fractions using a Ru/C catalyst, Catal. Sci. Technol. 6 (2016) 7053–7067. https://doi.org/10.1039/c6cy00523c.

[122] A. Narani, R.K. Chowdari, C. Cannilla, G. Bonura, F. Frusteri, H.J. Heeres, K. Barta, Efficient catalytic hydrotreatment of Kraft lignin to alkylphenolics using supported NiW and NiMo catalysts in supercritical methanol, Green Chem. 17 (2015) 5046–5057. https://doi.org/10.1039/c5gc01643f.

[123] A. Kloekhorst, H.J. Heeres, Catalytic Hydrotreatment of Alcell Lignin Using Supported Ru, Pd, and Cu Catalysts, ACS Sustain. Chem. Eng. 3 (2015) 1905–1914. https://doi.org/10.1021/acssuschemeng.5b00041.

[124] C.R. Kumar, N. Anand, A. Kloekhorst, C. Cannilla, G. Bonura, F. Frusteri, K. Barta, H.J. Heeres, Solvent free depolymerization of Kraft lignin to alkyl-phenolics using supported NiMo and CoMo catalysts, Green Chem. 17 (2015) 4921–4930.

https://doi.org/10.1039/c5gc01641j.

[125] J. Kong, M. He, J.A. Lercher, C. Zhao, Direct production of naphthenes and paraffins from lignin, Chem. Commun. 51 (2015) 17580–17583. https://doi.org/10.1039/c5cc06828b.

[126] H. Wang, H. Ruan, M. Feng, Y. Qin, H. Job, L. Luo, C. Wang, M.H. Engelhard, E. Kuhn, X. Chen, M.P. Tucker, B. Yang, One-Pot Process for Hydrodeoxygenation of Lignin to Alkanes Using Ru-Based Bimetallic and Bifunctional Catalysts Supported on Zeolite Y, ChemSusChem. 10 (2017) 1846–1856. https://doi.org/10.1002/cssc.201700160.

[127] S. Kasakov, H. Shi, D.M. Camaioni, C. Zhao, E. Baráth, A. Jentys, J.A. Lercher, Reductive deconstruction of organosolv lignin catalyzed by zeolite supported nickel nanoparticles, Green Chem. 17 (2015) 5079–5090. https://doi.org/10.1039/c5gc02160j.

[128] C. Lapierre, Determining Lignin Structure by Chemical Degradations, 2016. https://doi.org/10.1201/EBK1574444865-6.

[129] R.E. Key, J.J. Bozell, Progress toward Lignin Valorization via Selective Catalytic Technologies and the Tailoring of Biosynthetic Pathways, ACS Sustain. Chem. Eng. 4 (2016) 5123–5135. https://doi.org/10.1021/acssuschemeng.6b01319.

[130] G. Chatel, R.D. Rogers, Review: Oxidation of lignin using ionic liquids-an innovative strategy to produce renewable chemicals, ACS Sustain. Chem. Eng. 2 (2014) 322–339. https://doi.org/10.1021/sc4004086.

[131] M. Fache, B. Boutevin, S. Caillol, Vanillin Production from Lignin and Its Use as a Renewable Chemical, ACS Sustain. Chem. Eng. 4 (2016) 35–46. https://doi.org/10.1021/acssuschemeng.5b01344.

[132] P.C.. Rodrigues Pinto, E.A.. Borges da Silva, A.E. Rodrigues, Lignin as Source of Fine Chemicals: Vanillin and Syringaldehyde, in: R.S. Baskar, Chinnappan; Baskar, Shikha; Dhillon (Ed.), Biomass Convers. Interface Biotechnol. Chem. Mater. Sci., Springer Berlin Heidelberg, 2012: pp. 381–420. https://doi.org/10.1007/978-3-642-28418-2.

[133] P. Sridhar, J.D. Araujo, A.E. Rodrigues, Modeling of vanillin production in a structured bubble column reactor, Catal. Today. 105 (2005) 574–581. https://doi.org/10.1016/j.cattod.2005.06.044.

[134] J.D.P. Araújo, C.A. Grande, A.E. Rodrigues, Vanillin production from lignin oxidation in a batch reactor, Chem. Eng. Res. Des. 88 (2010) 1024–1032. https://doi.org/10.1016/j.cherd.2010.01.021.

[135] X. Ouyang, T. Ruan, X. Qiu, Effect of solvent on hydrothermal oxidation depolymerization of lignin for the production of monophenolic compounds, Fuel

Process. Technol. 144 (2016) 181–185. https://doi.org/10.1016/j.fuproc.2015.12.019.

[136] A. Azarpira, J. Ralph, F. Lu, Catalytic Alkaline Oxidation of Lignin and its Model Compounds: A Pathway to Aromatic Biochemicals, Bioenergy Res. 7 (2014) 78–86. https://doi.org/10.1007/s12155-013-9348-x.

[137] A.W. Pacek, P. Ding, M. Garrett, G. Sheldrake, A.W. Nienow, Catalytic conversion of sodium lignosulfonate to vanillin: Engineering aspects. part 1. effects of processing conditions on vanillin yield and selectivity, Ind. Eng. Chem. Res. 52 (2013) 8361–8372. https://doi.org/10.1021/ie4007744.

[138] V.E. Tarabanko, D. V Petukhov, Study of mechanism and improvement of the process of oxidative cleavage of lignins into the aromatic aldehydes, Chem. Sustain. Dev. 11 (2003) 655–667.

[139] T. Voitl, P.R. Von Rohr, Oxidation of lignin using aqueous polyoxometalates in the presence of alcohols, ChemSusChem. 1 (2008) 763–769. https://doi.org/10.1002/cssc.200800050.

[140] T. Voitl, M. V. Nagel, P.R. Von Rohr, Analysis of products from the oxidation of technical lignins by oxygen and H3PMo12O40 in water and aqueous methanol by size-exclusion chromatography, Holzforschung. 64 (2010) 13–19. https://doi.org/10.1515/HF.2010.006.

[141] H. Werhan, J.M. Mir, T. Voitl, P.R. Von Rohr, Acidic oxidation of kraft lignin into aromatic monomers catalyzed by transition metal salts, Holzforschung. 65 (2011) 703–709. https://doi.org/10.1515/HF.2011.071.

[142] H. Werhan, N. Assmann, P.R. Von Rohr, Lignin oxidation studies in a continuous two-phase flow microreactorHolger microreactor, Chem. Eng. Process. Process Intensif. 73 (2013) 29–37. https://doi.org/10.1016/j.cep.2013.06.015.

[143] J. Lappalainen, D. Baudouin, U. Hornung, J. Schuler, K. Melin, S. Bjelić, F. Vogel, J. Konttinen, T. Joronen, Sub- And supercritical water liquefaction of kraft lignin and black liquor derived lignin, Energies. 13 (2020) 3309. https://doi.org/10.3390/en13133309.

[144] P. Basu, Biomass Gasification, Pyrolysis and Torrefaction: Practical Design and Theory, 2013. https://doi.org/10.1016/C2011-0-07564-6.

[145] M.J. Cocero, Á. Cabeza, N. Abad, T. Adamovic, L. Vaquerizo, C.M. Martínez, M.V. Pazo-Cepeda, Understanding biomass fractionation in subcritical & supercritical water, J. Supercrit. Fluids. 133 (2018) 550–565. https://doi.org/10.1016/j.supflu.2017.08.012.

[146] X. Wang, J.H. Zhou, H.M. Li, G.W. Sun, Depolymerization of lignin with supercritical fluids: A review, Adv. Mater. Res. 821–822 (2013) 1126–1134.

https://doi.org/10.4028/www.scientific.net/AMR.821-822.1126.

[147] J. Schuler, U. Hornung, N. Dahmen, J. Sauer, Lignin from bark as a resource for aromatics production by hydrothermal liquefaction, GCB Bioenergy. 11 (2019) 218–229. https://doi.org/10.1111/gcbb.12562.

[148] A. Kruse, N. Dahmen, Water - A magic solvent for biomass conversion, J. Supercrit. Fluids. 96 (2015) 36–45. https://doi.org/10.1016/j.supflu.2014.09.038.

[149] D. Forchheim, Optimisation of the reaction parameters in a batch reactor and a CSTR for the recovery of phenol from hydrothermal biomass liquefaction, (2013).

[150] D. Forchheim, U. Hornung, A. Kruse, T. Sutter, Kinetic Modelling of Hydrothermal Lignin Depolymerisation, Waste and Biomass Valorization. 5 (2014) 985–994. https://doi.org/10.1007/s12649-014-9307-6.

[151] T.L.K. Yong, Y. Matsumura, Reaction kinetics of the lignin conversion in supercritical water, Ind. Eng. Chem. Res. 51 (2012) 11975–11988. https://doi.org/10.1021/ie300921d.

[152] K.Q. Tran, Fast hydrothermal liquefaction for production of chemicals and biofuels from wet biomass – The need to develop a plug-flow reactor, Bioresour. Technol. 213 (2016) 327–332. https://doi.org/10.1016/j.biortech.2016.04.002.

[153] T. Belkheiri, S.I. Andersson, C. Mattsson, L. Olausson, H. Theliander, L. Vamling, Hydrothermal liquefaction of kraft lignin in sub-critical water: the influence of the sodium and potassium fraction, Biomass Convers. Biorefinery. 8 (2018) 585–595. https://doi.org/10.1007/s13399-018-0307-9.

[154] T. Belkheiri, C. Mattsson, S.I. Andersson, L. Olausson, L.E. Åmand, H. Theliander, L. Vamling, Effect of pH on Kraft Lignin Depolymerisation in Subcritical Water, Energy and Fuels. 30 (2016) 4916–4924. https://doi.org/10.1021/acs.energyfuels.6b00462.

[155] Y. Solantausta, C. Anacker, U. Armbruster, D. Meier, J. Appelt, A. Martin, J.O. Strüven, P. Eidam, C. Mirodatos, Y. Schuurman, F. Chapon, A. Oasmaa, A. Välimäki, K. Melin, V. Passikallio, Liquid fuels from lignin by hydrothermal liquefaction and deoxygenation (LIGNOHTL), 1 (2018) 1–11. https://forestvalue.org/wp-content/uploads/2018/07/wwnet_jc4_final_reporting_lignoHTL.pdf.

[156] A. Orebom, J.J. Verendel, J.S.M. Samec, High Yields of Bio Oils from Hydrothermal Processing of Thin Black Liquor without the Use of Catalysts or Capping Agents, ACS Omega. 3 (2018) 6757–6763. https://doi.org/10.1021/acsomega.8b00854.

[157] M. Maschietti, T.D.H. Nguyen, T. Belkeiri, L.-E. Åmand, H. Theliander, L. Vamling, L. Olausson, S.-I. Andersson, Catalytic hydrothermal conversion of LignoBoost Kraft lignin for the production of biooil and aromatic chemicals, Int. Chem. Recover. Conf. (2014).

[158] T.D.H. Nguyen, M. Maschietti, L.E. Åmand, L. Vamling, L. Olausson, S.I. Andersson, H. Theliander, The effect of temperature on the catalytic conversion of Kraft lignin using near-critical water, Bioresour. Technol. 170 (2014) 196–203. https://doi.org/10.1016/j.biortech.2014.06.051.

[159] M. Sugano, H. Takagi, K. Hirano, K. Mashimo, Hydrothermal liquefaction of plantation biomass with two kinds of wastewater from paper industry, J. Mater. Sci. 43 (2008) 2476–2486. https://doi.org/10.1007/s10853-007-2106-8.

[160] S. Cheng, C. Wilks, Z. Yuan, M. Leitch, C. Xu, Hydrothermal degradation of alkali lignin to bio-phenolic compounds in sub/supercritical ethanol and water-ethanol co-solvent, Polym. Degrad. Stab. 97 (2012) 839–848. https://doi.org/10.1016/j.polymdegradstab.2012.03.044.

[161] T. Belkheiri, L. Vamling, T.D.H. Nguyen, M. Maschietti, L. Olausson, S.I. Andersson, L.E. Åmand, H. Theliander, Kraft lignin depolymerization in near-critical water: Effect of changing co-solvent, Cellul. Chem. Technol. 48 (2014) 813–818.

[162] K.R. Arturi, M. Strandgaard, R.P. Nielsen, E.G. Søgaard, M. Maschietti, Hydrothermal liquefaction of lignin in near-critical water in a new batch reactor: Influence of phenol and temperature, J. Supercrit. Fluids. 123 (2017) 28–39. https://doi.org/10.1016/j.supflu.2016.12.015.

[163] T. Belkheiri, S.I. Andersson, C. Mattsson, L. Olausson, H. Theliander, L. Vamling, Hydrothermal Liquefaction of Kraft Lignin in Subcritical Water: Influence of Phenol as Capping Agent, Energy and Fuels. 32 (2018) 5923–5932. https://doi.org/10.1021/acs.energyfuels.8b00068.

[164] N. Abad-Fernández, PhD Thesis: Lignin depolymerization by supercritical water ultrafast reactions, Universidad de Valladolid, 2019.

[165] T.D.H. Nguyen, M. Maschietti, T. Belkheiri, L.E. Åmand, H. Theliander, L. Vamling, L. Olausson, S.I. Andersson, Catalytic depolymerisation and conversion of Kraft lignin into liquid products using near-critical water, J. Supercrit. Fluids. 86 (2014) 67–75. https://doi.org/10.1016/j.supflu.2013.11.022.

[166] O. Faruk, S. Mohini, LIGNIN IN POLYMER COMPOSITES, 2015.

[167] O. Gordobil, New Products From Lignin, Universidad del Pais Vasco, 2018.

[168] R. Pucciariello, V. Villani, C. Bonini, M. D'Auria, T. Vetere, Physical properties of straw lignin-based polymer blends, Polymer (Guildf). 45 (2004) 4159–4169.

https://doi.org/10.1016/j.polymer.2004.03.098.

[169] W. Yang, M. Rallini, D.Y. Wang, D. Gao, F. Dominici, L. Torre, J.M. Kenny, D. Puglia, Role of lignin nanoparticles in UV resistance, thermal and mechanical performance of PMMA nanocomposites prepared by a combined free-radical graft polymerization/masterbatch procedure, Compos. Part A Appl. Sci. Manuf. 107 (2018) 61–69. https://doi.org/10.1016/j.compositesa.2017.12.030.

[170] S.B. Mishra, A.K. Mishra, N.K. Kaushik, M.A. Khan, Study of performance properties of lignin-based polyblends with polyvinyl chloride, J. Mater. Process. Technol. 183 (2007) 273–276. https://doi.org/10.1016/j.jmatprotec.2006.10.016.

[171] Y. Sheng, Z. Ma, X. Wang, Y. Han, Ethanol organosolv lignin from different agricultural residues: Toward basic structural units and antioxidant activity, Food Chem. 376 (2022) 131895. https://doi.org/10.1016/j.foodchem.2021.131895.

[172] A. Gregorová, B. Košíková, R. Moravčík, Stabilization effect of lignin in natural rubber, Polym. Degrad. Stab. 91 (2006) 229–233. https://doi.org/10.1016/j.polymdegradstab.2005.05.009.

[173] M. Canetti, F. Bertini, A. De Chirico, G. Audisio, Thermal degradation behaviour of isotactic polypropylene blended with lignin, Polym. Degrad. Stab. 91 (2006) 494–498. https://doi.org/10.1016/j.polymdegradstab.2005.01.052.

[174] Y. Ikeda, T. Phakkeeree, P. Junkong, H. Yokohama, P. Phinyocheep, R. Kitano, A. Kato, Reinforcing biofiller “lignin” for high performance green natural rubber nanocomposites, RSC Adv. 7 (2017) 5222–5231. https://doi.org/10.1039/c6ra26359c.

[175] H.D. Rozman, K.W. Tan, R.N. Kumar, A. Abubakar, Z.A. Mohd. Ishak, H. Ismail, Effect of lignin as a compatibilizer on the physical properties of coconut fiber-polypropylene composites, Eur. Polym. J. 36 (2000) 1483–1494. https://doi.org/10.1016/S0014-3057(99)00200-1.

[176] F.A. Tanjung, S. Husseinsyah, K. Hussin, Chitosan-filled polypropylene composites: The effect of filler loading and organosolv lignin on mechanical, morphological and thermal properties, Fibers Polym. 15 (2014) 800–808. https://doi.org/10.1007/s12221-014-0800-0.

[177] N.A. Mohamad Aini, N. Othman, M.H. Hussin, K. Sahakaro, N. Hayeemasae, Lignin as Alternative Reinforcing Filler in the Rubber Industry: A Review, Front. Mater. 6 (2020). https://doi.org/10.3389/fmats.2019.00329.

[178] J. Yang, Y.C. Ching, C.H. Chuah, Applications of lignocellulosic fibers and lignin in bioplastics: A review, Polymers (Basel). 11 (2019) 1–26. https://doi.org/10.3390/polym11050751.

[179] A. De Chirico, M. Armanini, P. Chini, G. Cioccolo, F. Provasoli, G. Audisio, Flame retardants for polypropylene based on lignin, Polym. Degrad. Stab. 79 (2003) 139–145. https://doi.org/10.1016/S0141-3910(02)00266-5.

[180] S. Chen, S. Lin, Y. Hu, M. Ma, Y. Shi, J. Liu, F. Zhu, X. Wang, A lignin-based flame retardant for improving fire behavior and biodegradation performance of polybutylene succinate, Polym. Adv. Technol. 29 (2018) 3142–3150. https://doi.org/10.1002/pat.4436.

[181] B. Chollet, J.M. Lopez-Cuesta, F. Laoutid, L. Ferry, Lignin nanoparticles as a promising way for enhancing lignin flame retardant effect in polylactide, Materials (Basel). 12 (2019). https://doi.org/10.3390/ma12132132.

[182] X. Yue, F. Chen, X. Zhou, G. He, Preparation and characterization of poly (vinyl chloride) polyblends with fractionated lignin, Int. J. Polym. Mater. Polym. Biomater. 61 (2012) 214–228. https://doi.org/10.1080/00914037.2011.574659.

[183] D.-G. for R. and I. European Commission, Detailed Case Studies on the Top 20 Innovative Bio-Based Products, Luxembourg, 2019. https://doi.org/http://doi.org/10.2777/85805.

[184] G. Yu, B. Li, H. Wang, C. Liu, X. Mu, Preparation of concrete superplasticizer by oxidation- sulfomethylation of sodium lignosulfonate, BioResources. 8 (2013) 1055–1063. https://doi.org/10.15376/biores.8.1.1055-1063.

[185] L. Mu, Y. Shi, X. Guo, T. Ji, L. Chen, R. Yuan, L. Brisbin, H. Wang, J. Zhu, Non-corrosive green lubricants: strengthened lignin-[choline][amino acid] ionic liquids interaction via reciprocal hydrogen bonding, RSC Adv. 5 (2015) 66067–66072. https://doi.org/10.1039/c5ra11093a.

[186] L. Mu, J. Wu, L. Matsakas, M. Chen, U. Rova, P. Christakopoulos, J. Zhu, Y. Shi, Two important factors of selecting lignin as efficient lubricating additives in poly (ethylene glycol): Hydrogen bond and molecular weight, Int. J. Biol. Macromol. 129 (2019) 564–570. https://doi.org/10.1016/j.ijbiomac.2019.01.175.

[187] J. Hua, Y. Shi, Non-corrosive Green Lubricant With Dissolved Lignin in Ionic Liquids Behave as Ideal Lubricants for Steel-DLC Applications, Front. Chem. 7 (2019) 1–8. https://doi.org/10.3389/fchem.2019.00857.

[188] E. Cortés-Triviño, C. Valencia, J.M. Franco, Thickening Castor Oil with a Lignin-Enriched Fraction from Sugarcane Bagasse Waste via Epoxidation: A Rheological and Hydrodynamic Approach, ACS Sustain. Chem. Eng. 9 (2021) 10503–10512. https://doi.org/10.1021/acssuschemeng.1c02166.

[189] E.C. Triviño, C. Valencia, M.A. Delgado, J.M. Franco, Modification of Alkali Lignin with Poly(Ethylene Glycol) Diglycidyl Ether to Be Used as a Thickener in Bio-Lubricant Formulations, Polymers (Basel). 10 (2018) 670. https://doi.org/10.3390/polym10060670.

[190] P. Araújo, A. Costa, I. Fernandes, N. Mateus, V. de Freitas, B. Sarmento, J. Oliveira, Stabilization of bluish pyranoanthocyanin pigments in aqueous systems using lignin nanoparticles, Dye. Pigment. 166 (2019) 367–374. https://doi.org/10.1016/j.dyepig.2019.03.020.

[191] P. Balasubramanian, S. Ramalingam, M.A. Javid, J.R. Rao, Lignin Based Colorant: Modified Black Liquor for Leather Surface Coating Application, J. Am. Leather Chem. Assoc. 113 (2018) 311–317.

[192] Z. Mahmood, M. Yameen, M. Jahangeer, M. Riaz, A. Ghaffar, I. Javid, Lignin as Natural Antioxidant Capacity, Lignin - Trends Appl. (2018). https://doi.org/10.5772/intechopen.73284.

[193] B. Jiang, Y. Zhang, L. Gu, W. Wu, H. Zhao, Y. Jin, Structural elucidation and antioxidant activity of lignin isolated from rice straw and alkali-oxygen black liquor, Int. J. Biol. Macromol. 116 (2018) 513–519. https://doi.org/10.1016/j.ijbiomac.2018.05.063.

[194] M.F. Li, S.N. Sun, F. Xu, R.C. Sun, Sequential solvent fractionation of heterogeneous bamboo organosolv lignin for value-added application, Sep. Purif. Technol. 101 (2012) 18–25. https://doi.org/10.1016/j.seppur.2012.09.013.

[195] Nippon Paper, Lignin products, (n.d.). https://www.nipponpapergroup.com/english/products/chemical/lignin_products/index.html.

[196] J.H. Lora, W.G. Glasser, Recent industrial applications of lignin: A sustainable alternative to nonrenewable materials, J. Polym. Environ. 10 (2002) 39–48. https://doi.org/10.1023/A:1021070006895.

[197] M. Alinejad, S. Nikafshar, A. Gondaliya, S. Bagheri, N. Chen, S.K. Singh, D.B. Hodge, M. Nejad, Lignin-Based Polyurethanes: Opportunities for Bio-Based Foams, Elastomers, Coatings and Adhesives, Polymers (Basel). 11 (2019) 1202.

[198] A. Gandini, M.N.. Belgacem, Z.-X. Guo, S. Montanari, LIGNINS AS MACROMONOMERS FOR POLYESTERS AND POLYURETHANES, in: T.Q. Hu (Ed.), Chem. Modif. Prop. Usage Lignin, Springer, Vancouver, 2002: pp. 57–80. https://doi.org/10.1007/978-1-4615-0643-0_10.

[199] S. Nikafshar, Z.. Fang, M. Nejad, Development of a Novel Curing Accelerator-Blowing Agent for Formulating Epoxy Rigid Foam Containing Aminated-Lignin, Ind. Eng. Chem. Res. 59 (2020) 15146–15154. https://doi.org/10.1021/acs.iecr.0c02738.

[200] J.E.Q. Quinsaat, E. Feghali, D.J. Van De Pas, R. Vendamme, K.M. Torr, Preparation of Mechanically Robust Bio-Based Polyurethane Foams Using Depolymerized Native Lignin, ACS Appl. Polym. Mater. 3 (2021) 5845–5856.

https://doi.org/10.1021/acsapm.1c01081.

[201] P. Ortiz-Serna, M. Carsí, M. Culebras, M.N. Collins, M.J. Sanchis, Exploring the role of lignin structure in molecular dynamics of lignin/bio-derived thermoplastic elastomer polyurethane blends, Int. J. Biol. Macromol. 158 (2020) 1369–1379. https://doi.org/10.1016/j.ijbiomac.2020.04.261.

[202] J.A. Pinto, I.P. Fernandes, V.D. Pinto, E. Gomes, C.F. Oliveira, P.C.R. Pinto, L.M.R. Mesquita, P.A.G. Piloto, A.E. Rodrigues, M.F. Barreiro, Valorization of lignin side-streams into polyols and rigid polyurethane foams—a contribution to the pulp and paper industry biorefinery, Energies. 14 (2021) 1–15. https://doi.org/10.3390/en14133825.

[203] G. Griffini, V. Passoni, R. Suriano, M. Levi, S. Turri, Polyurethane coatings based on chemically unmodified fractionated lignin, ACS Sustain. Chem. Eng. 3 (2015) 1145–1154. https://doi.org/10.1021/acssuschemeng.5b00073.

[204] S.I. Seyed Shahabadi, J. Kong, X. Lu, Aqueous-Only, Green Route to Self-Healable, UV-Resistant, and Electrically Conductive Polyurethane/Graphene/Lignin Nanocomposite Coatings, ACS Sustain. Chem. Eng. 5 (2017) 3148–3157. https://doi.org/10.1021/acssuschemeng.6b02941.

[205] H. Xie, H. Zhang, X. Liu, S. Tian, Y. Liu, S. Fu, Ag immobilized lignin-based PU coating: A promising candidate to promote the mechanical properties, thermal stability, and antibacterial property of paper packaging, Int. J. Biol. Macromol. 189 (2021) 690–697. https://doi.org/10.1016/j.ijbiomac.2021.08.184.

[206] C. Fuqiang, W. Xiangjiao, Water-based UV-curable polyurethane based on wheat straw lignin obtained by ethanol extraction, Adv. Mater. Res. 295–297 (2011) 278–281. https://doi.org/10.4028/www.scientific.net/AMR.295-297.278.

[207] W. Hu, J. Zhang, B. Liu, C. Zhang, Q. Zhao, Z. Sun, H. Cao, G. Zhu, Synergism between lignin, functionalized carbon nanotubes and Fe3O4 nanoparticles for electromagnetic shielding effectiveness of tough lignin-based polyurethane, Compos. Commun. 24 (2021) 100616. https://doi.org/10.1016/j.coco.2020.100616.

[208] M.S. Karunarathna, R.C. Smith, Valorization of lignin as a sustainable component of structural materials and composites: Advances from 2011 to 2019, Sustain. 12 (2020). https://doi.org/10.3390/su12020734.

[209] S.S.L. Gonçalves, A. Rudnitskaya, A.J.M. Sales, L.M.C. Costa, D. V. Evtuguin, Nanocomposite polymeric materials based on eucalyptus lignoboost® kraft lignin for liquid sensing applications, Materials (Basel). 13 (2020). https://doi.org/10.3390/ma13071637.

[210] Y. Ma, Z. Li, H. Wang, H. Li, Synthesis and optimization of polyurethane microcapsules containing [BMIm]PF6 ionic liquid lubricant, J. Colloid Interface

Sci. 534 (2019) 469–479. https://doi.org/10.1016/j.jcis.2018.09.059.

[211] A.M. Borrero-López, C. Valencia, J.M. Franco, Rheology of lignin-based chemical oleogels prepared using diisocyanate crosslinkers: Effect of the diisocyanate and curing kinetics, Eur. Polym. J. 89 (2017) 311–323. https://doi.org/10.1016/j.eurpolymj.2017.02.020.

[212] A.M. Borrero-López, C. Valencia, J.M. Franco, Green and facile procedure for the preparation of liquid and gel-like polyurethanes based on castor oil and lignin: Effect of processing conditions on the rheological properties, J. Clean. Prod. 277 (2020). https://doi.org/10.1016/j.jclepro.2020.123367.

[213] T. Litters, F. Hahn, T. Goerz, H.J. Erkel, PROCESS FOR THE PREPARATION OF POLYUREA -THICKENED LIGNIN DERIVATIVE -BASED LUBRICATING GREASES, SUCH LUBRICANT GREASES AND USE THEREOF, US 10,604,721 B2, 2020.

[214] A. Perez, K.A.. Vaught, G.P. Hansen, LOW VOLATILE ORGANIC CONTENT LUBRICANT, US 7,524,797 B1, 2009.

[215] D.S. Bajwa, G. Pourhashem, A.H. Ullah, S.G. Bajwa, A concise review of current lignin production, applications, products and their environment impact, Ind. Crops Prod. 139 (2019) 111526. https://doi.org/10.1016/j.indcrop.2019.111526.

[216] F.H. Isikgor, C.R. Becer, Lignocellulosic biomass: a sustainable platform for the production of bio-based chemicals and polymers, Polym. Chem. 6 (2015) 4497–4559. https://doi.org/10.1039/c5py00263j.

[217] P. Figueiredo, K. Lintinen, J.T. Hirvonen, M.A. Kostiainen, H.A. Santos, Properties and chemical modifications of lignin: Towards lignin-based nanomaterials for biomedical applications, Prog. Mater. Sci. 93 (2018) 233–269. https://doi.org/10.1016/j.pmatsci.2017.12.001.

[218] M.A. Delgado, E. Cortés-Triviño, C. Valencia, J.M. Franco, Tribological study of epoxide-functionalized alkali lignin-based gel-like biogreases, Tribol. Int. 146 (2020). https://doi.org/10.1016/j.triboint.2020.106231.

[219] A. Tenorio-Alfonso, M.C. Sánchez, J.M. Franco, Impact of the processing method on the properties of castor oil/cellulose acetate polyurethane adhesives for bonding wood, Int. J. Adhes. Adhes. 116 (2022). https://doi.org/10.1016/j.ijadhadh.2022.103153.

[220] P. Nagendramma, P. Kumar, Eco-friendly multipurpose lubricating greases from vegetable residual oils, Lubricants. 3 (2015) 628–636. https://doi.org/10.3390/lubricants3040628.

[221] T.M. Panchal, A. Patel, D.D. Chauhan, M. Thomas, J. V. Patel, A methodological review on bio-lubricants from vegetable oil based resources, Renew. Sustain. Energy Rev. 70 (2017) 65–70. https://doi.org/10.1016/j.rser.2016.11.105.

[222] H. Jahromi, S. Adhikari, P. Roy, M. Shelley, E. Hassani, T.S. Oh, Synthesis of Novel Biolubricants from Waste Cooking Oil and Cyclic Oxygenates through an Integrated Catalytic Process, ACS Sustain. Chem. Eng. 9 (2021) 13424–13437. https://doi.org/10.1021/acssuschemeng.1c03523.

[223] C. Fajardo, A. Blánquez, G. Domínguez, A.M. Borrero-López, C. Valencia, M. Hernández, M.E. Arias, J. Rodríguez, Assessment of sustainability of bio treated lignocellulose-based oleogels, Polymers (Basel). 13 (2021) 1–12. https://doi.org/10.3390/polym13020267.

[224] R. Gallego, J.F. Arteaga, C. Valencia, M.J. Díaz, J.M. Franco, Gel-Like Dispersions of HMDI-Cross-Linked Lignocellulosic Materials in Castor Oil: Toward Completely Renewable Lubricating Grease Formulations, ACS Sustain. Chem. Eng. 3 (2015) 2130–2141. https://doi.org/10.1021/acssuschemeng.5b00389.

[225] N. Abad-Fernández, E. Pérez, M.J. Cocero, Aromatics from lignin through ultrafast reactions in water, Green Chem. 21 (2019) 1351–1360. https://doi.org/10.1039/c8gc03989e.

[226] N. Abad-Fernández, E. Pérez, Á. Martín, M.J. Cocero, Kraft lignin depolymerisation in sub- and supercritical water using ultrafast continuous reactors. Optimization and reaction kinetics, J. Supercrit. Fluids. 165 (2020). https://doi.org/10.1016/j.supflu.2020.104940.

[227] E. Pérez, N. Abad-Fernández, T. Lourençon, M. Balakshin, H. Sixta, M.J. Cocero, Base-catalysed depolymerization of lignins in supercritical water: Influence of lignin nature and valorisation of pulping and biorefinery by-products, Biomass and Bioenergy. 163 (2022). https://doi.org/10.1016/j.biombioe.2022.106536.

[228] T. Adamovic, PhD Thesis: Lignin valorization using supercritical water technology, University of Valladolid, 2021.

[229] T. Adamovic, D. Tarasov, E. Demirkaya, M. Balakshin, M.J. Cocero, A feasibility study on green biorefinery of high lignin content agro-food industry waste through supercritical water treatment, J. Clean. Prod. 323 (2021). https://doi.org/10.1016/j.jclepro.2021.129110.

[230] T. Adamovic, X. Zhu, E. Perez, M. Balakshin, M.J. Cocero, Understanding sulfonated kraft lignin re-polymerization by ultrafast reactions in supercritical water, J. Supercrit. Fluids. 191 (2022). https://doi.org/10.1016/j.supflu.2022.105768.

[231] D.A. Cantero, L. Vaquerizo, F. Mato, M.D. Bermejo, M.J. Cocero, Energetic approach of biomass hydrolysis in supercritical water, Bioresour. Technol. 179 (2015) 136–143. https://doi.org/10.1016/j.biortech.2014.12.006.

GOALS & CONTENTS

Valorization of Black Liquor

using Hydrothermal Treatment

The pulp and paper industry generates significant quantities of black liquor, a by-product rich in lignin and inorganic chemicals used in the pulping process. This by-product represents both a challenge and an opportunity for industry. As discussed in the first section, the current practice for dealing with black liquor is mainly to concentrate and burn it in a recovery boiler. As a result of developments in lignin over the last decade, its importance has been better understood and black liquor acid hydrolysis has increased to produce more lignin. However, this step may be unnecessary compared to direct use of black liquor, which can provide many benefits if it is directly valorized.

Therefore, the main objective of this thesis was that:

Valorization of black liquor by hydrothermal treatment using continuous ultrafast reactions and production of end-user materials.

To achieve this objective, the challenges mentioned in section 1.7.1., and the best results based on lignin from the previous thesis of our group from Nerea Abad-Fernandez, PhD Thesis: Lignin depolymerization by supercritical water ultrafast reactions, Universidad de Valladolid, 2019 was followed [1].

To explain more broadly, the main goal of this study was to depolymerize black liquor through a green process that enables to work with ultrafast reaction times to prevent or manage the side reactions, thereby achieving a high yield and selectivity of desired aromatic monomers, oligomers, or polyols including fractions. To accomplish this, a continuous hydrothermal processing with sudden-expansion micro-reactors was carried out in this study.

To meet the main goal of this dissertation, the work was planned into three chapters. Although our will was to produce more biomaterials using depolymerized black liquor fractions, a few challenges led us to redirect the third chapter objectives. These challenges were the necessity of the improvement of the mass balance and examining a detailed characterization of the products obtained from continuous black liquor. Details of the challenges can be grasped in each chapter.

Therefore, the final structure of the subgoals were constituted as follows:

1. Depolymerization and characterization of black liquor using continuous hydrothermal treatment.

Subgoals:

- Understanding the effect of higher concentration of black liquor (20wt%. total solids) and longer operation hours on the product yields.
- Studying different downstream processes and their effect on product yields.
- Examining the effect of pH on the product fractions and the aromatic monomer yields.
- Characterization of the products to be further used in applications.

2. Product development: Bio-lubricant production using selected depolymerized black liquor products.

- Further characterization of the most suitable black liquor depolymerization fractions for bio-lubricant production.
- Producing consumer ready lubricants by creating new formulations using epoxidized vegetable oil.
- Investigating the characteristics of the produced bio-lubricant formulations and comparing them with commercial ones.

3. Process development: Continuous black liquor and kraft lignin fractionation by supercritical water technology

Subgoals:

- Studying the effect of different operation variables of temperature, residence time and raw material.
- Focusing on the comprehensive characterization of all fractions from the same raw material with this technology.
- Employing a consistent and comparable mass balance of the process.

[1] N. Abad-Fernández, PhD Thesis: Lignin depolymerization by supercritical water ultrafast reactions, Universidad de Valladolid, 2019.

SYNOPSIS

Valorization of Black Liquor

using Hydrothermal Treatment

The background of this dissertation is based on Abad-Fernandez's thesis, which was the Lignin depolymerization by supercritical water ultrafast reactions.

In Abad-Fernandez's pioneering study of lignin conversion, some critical challenges are found out. One of them is the low biomass concentration of 3% in the biomass tank. This limitation is a significant bottleneck for a scale-up, limiting the amount of aromatic monomer rich oil produced, and increasing water consumption, raising sustainability concerns. To address these issues, in the next step it was necessary to enhance the biomass concentration, which would increase process efficiency and significantly reduce environmental impact by reducing water consumption.

In literature, it can be seen that the most efficient lignin concentration was 5% as raw material in batch processing. Higher concentrations of lignin as a starting material resulted in either lower yield of the bio-oil or produced more char. However, under supercritical conditions, in a continuous process and fast reaction time higher concentration of lignin/black liquor was not evaluated before. One of the reasons was technical limitations depending on the scale of the lab equipment (pumps).

Using the TRL5 pilot plant, the first question was can we pump higher concentrations of black liquor to increase process efficiency and reduce water consumption? The work we conducted in chapter 1 answers yes to this question.

The next question that we asked was "Higher concentrations of black liquor (20 wt% total solids) and longer operation hours will decrease the total bio-oil and aromatic monomers yield?". We still observed very high yields (77wt% total bio-oil yield), but not as much as it was claimed in our previous group member's study. However, to make the supercritical water depolymerization process feasible for industry, higher concentration of black liquor as the raw material was still essential to continue. Therefore, we decided to work with 20 wt% total solids including black liquor for chapter 1.

The downstream processing of depolymerized lignin usually involves complex methods in literature, which affects the feasibility of the separation negatively for industrial purposes. Therefore, it was necessary to investigate the simple downstream processing options to reduce both time and cost which are key elements of process scalability. This pragmatic approach aims to ensure a seamless transition from laboratory success to industrial viability, ensuring widespread adoption without prohibitive costs or inefficiencies. For this reason, another question that we wanted to answer was "Is it

possible to find a simple downstream processing method for the depolymerized black liquor products?". This question was answered in chapter 1.

Including blank tests was essential to make accurate comparisons between the feedstocks and the final products, which would bias the results. Making these comparisons is crucial to validate the efficiency of the biomass conversion process, ensuring that any observed differences are truly due to the process and not external factors. Therefore, blank tests were included in this study, starting from chapter 1. Also, in the case of black liquor, for example, since it is a by-product of the pulp mills, the presence of degradation compounds from the pulping process affects the yield of the products and the mass balance. Thus, a consistent mass balance was essential to verify the difference between raw materials and products, and to provide unbiased results. In the first two chapters, the mass balance of the process was only focused on the downstream process as it was crucial to find a consistency for the produced fractions yields. In chapter 3, this mass balance was improved.

In order to simplify downstream processing and achieve a consistent mass balance, as a first step, it is necessary to take a close look at the acidification process. For this reason, the behavior of the pH versus acid amount added should be examined more in detail in chapter 1.

Chapter 1 of this study includes a transition section for the work of chapter 2. Until section 3.4, the focus was given on the refining methods, in other words downstream processing. Simple downstream processing scenarios, pH behavior of the raw material and the product during the acidification, total bio-oil and aromatic monomer yields after depolymerization were covered here. By section 3.4, four selected samples (that will be used in chapter 2) characterization results were given. Details such as why these samples were selected can be found in chapter 1.

After the conclusion of the first chapter, the next step was to address the question: "Is it possible to produce consumer-ready lubricants using these selected samples?" Chapter 2 answers yes to this question. The four samples initially tested in Chapter 1 were produced in larger quantities for the work in Chapter 2 and were characterized in more detail to assess their suitability for bio-lubricant production. For this reason, molecular weight, OH content, elemental analysis, and GC-MS were used as characterization techniques. As the scope of this chapter is the development of a new product using (non)depolymerized black liquor products, the majority of the chapter was constructed

to answer basic screening questions. The answers that were sought during this chapter are outlined below:

- Different drying methods and extraction processes were examined to understand their impact on the properties of lignin fractions. The effects of spray drying, oven drying, and ethyl acetate extraction on the composition and properties of lignin fractions, including ash content and molecular weight distribution, were investigated.
- The rheological properties of lignin dispersions in epoxidized castor oil (ECO) were analyzed. Parameters such as apparent viscosity, shear-thinning behavior, and viscoelastic properties were studied through steady-state viscous flow tests and small-amplitude oscillatory shear tests.
- The tribological performance of lignin-based bio-lubricants was evaluated, focusing on the friction coefficients and wear scar areas of the lignin dispersions in comparison to neat epoxidized castor oil. The potential of these formulations as semi-solid bio-lubricants was discussed.
- The hydroxyl group content and functionality of lignin fractions were assessed to determine their suitability for bio-lubricant applications. The total hydroxyl group content (both aliphatic and aromatic) of the lignin samples was evaluated and correlated with their potential use in producing bio-lubricants. These values were compared to those required for industrial polyols and lubricants.
- The effects of ash content and molecular weight on the flow properties of lignin dispersions were analyzed. The importance of these parameters in achieving the desired rheological characteristics in the resulting bio-lubricants was highlighted.
- These points were addressed through a series of experimental procedures and analytical techniques, providing insights into the potential of depolymerized black liquor products for sustainable lubricant formulations.

The outcomes of first two chapters directed us to reconsider examining the effect of temperature and residence time on both black liquor and kraft lignin. The light oil yield compared to the literature was obtained lower than what was expected. Therefore, the main goal for this chapter, if possible, was to optimize the process, and to find a clear global trend that gives the highest light oil yield. In this case, the most valuable monomers produced could have been separated, and the rest of the oligomers and the

heavy oil could have been used for different applications. Another essential point was to employ the new mass balance approach to the design of experiment points that we created to see the real effect of the process.

In this chapter, several key questions related to the depolymerization of black liquor (BL) and kraft lignin (KL) using supercritical water were addressed. The study began with understanding the effects of supercritical water treatment on the depolymerization process for both BL and KL. A study was conducted to ascertain the impact of varying temperatures (380°C and 390°C) and reaction times (0.5s, 1s and 1.5s) on the decomposition of these complex materials.

The influence of temperatures and reaction times on the yields of different fractions, specifically DSW (aqueous residue), DSEA (light oil), SSI (char), and SSEA (heavy oil), obtained from BL and KL was also examined. This investigation was crucial for determining the optimal conditions for maximizing yield and understanding the characteristics of the resulting fractions under various conditions.

Detailed calculations of the carbon and mass balance of the depolymerized products were provided. How the insoluble material converted to soluble material through the supercritical water process was demonstrated, offering insights into the efficiency and effectiveness of the conversion.

Characterizing the specific compositions of the fractions obtained after supercritical water treatment was another focal point of this study. Various techniques, such as FTIR, GC-MS, GPC, and elemental analysis, were used to thoroughly examine the resulting products, providing a comprehensive understanding of their properties.

The potential applications and benefits of using supercritical water depolymerization for BL and KL were also discussed. The feasibility and efficiency of this method for industrial applications were highlighted, emphasizing the use of intrinsic pulping chemicals as catalysts and the ability to process raw materials directly without prior drying or separation.

Furthermore, the depolymerization mechanisms between BL and KL under similar conditions were compared. This comparison shed light on the differences in their responsiveness to supercritical water treatment, providing valuable insights for optimizing the process for different types of lignin.

Delving into these key points has guided our understanding of the efficiency, effectiveness, and potential industrial applications of supercritical water depolymerization of BL and KL.

CHAPTER I

Supercritical Water Depolymerization of Black Liquor, Refining and Comprehensive Analysis of Products Including Biopolyols

Abstract

Black liquor (BL) has valuable lignin and its derived compounds, which can be used for many purposes, such as polyol synthesis. Herein, we reveal polyols presence in depolymerized black liquor (DBL) and propose a fast and scalable approach to increase the yield of this fraction. Hydrothermal treatment (HTL) of black liquor (385°C, 26 MPa) was performed in a custom designed supercritical water (SCW) pilot-plant with rapid reaction times of around 0.4 s. Ash-free, total ethyl acetate extracted bio-oil yield was found 77% w/w. In addition to the contribution of the detailed fractionation methods, this study highlights continuous operation (>1 hour), and short reaction times (~0.4 s) of raw black liquor in SCW to produce biopolyols and aromatic bio-oil.

1. Introduction

Approximately, 170 MT of black liquor is produced annually from pulp & paper industry on a dry basis [1,2], whereas the lignin production is estimated to be between 50-70 MT worldwide [3]. Unfortunately, only around 2% of this lignin is utilized as high-value chemicals. The remaining lignin is usually burned as low-value fuel to balance the economics of the plant by creating thermal energy. [4]. The undervalued black liquor can be utilized as a feedstock that would enable industrial application for bio-oil production in a biorefinery. This would provide plenty of benefits; (i) the raw material (black liquor) is already present within the pulp and paper facility, which eliminates transportation costs and emissions [1], (ii) the byproducts like cellulose, hemicellulose, mono-, di-, and oligomeric lignin fragments can be used for various purposes such as functionalized materials production [3,5], (iii) pulping chemicals can serve as potential catalysts [2,6], (iv) diversifying pulp mill economics with another product reduces their sensitivity to pulp prices [1], and (v) the capital and operational costs of the new hydrothermal treatment (HTL) unit will be compensated by high temperature steam production and the recovery of pulping chemicals, providing a more feasible approach [1].

Over the last decade, kraft lignin has gained significant importance among researchers for its potential to replace fossil fuel-derived aromatic compounds [4,7–9]. Lignin is a distinctly complex 3D heteropolymer that confers mechanical rigidity to plants through the incorporation of phenylpropanoid units that include methoxy groups, such as syringyl (S-unit), guaiacyl (G-unit), and p-hydroxyphenyl (H-unit) units. It is composed of an abundance of C-O-C (4-O-5, α-O-4, β-O-4) and C-C (5-5, β-β, β-1, β-5) bonds and is intricately linked to cellulose and hemicellulose, rendering its conversion complex. Therefore, the fractionation of lignocellulosic biomass by using various pretreatment methods is essential [10–13]. Predominantly, these methods operate through the cleavage of C-O-C (β-O-4) linkages due to their lower bond dissociation energy (BDE) (between 218 - 314 kJ/mol), compared to the relatively stronger C-C bonds of greater BDE (~384 kJ/mol). This cleavage results in recondensation reactions that modify the structure of lignin, producing what is known as technical lignin [10–13]. Depolymerization of both isolated and native lignin have been extensively researched and it was found that native lignin depolymerization gives around seven times greater monomer yields [4,13]. The existing literature on this topic can be categorized into four main groups: (i) reductive [14–17], (ii) oxidative [18,19], (iii) base- and acid-catalyzed [20–23], and (iv) solvolytic and thermal depolymerization [24,25]. All approaches have

specific advantages and disadvantages, which are already discussed in some papers [4,26]. The most promising technology is the reductive catalytic depolymerization and its derivative technologies due to reaching almost complete theoretical monomer yield of lignin used [4,26]. Yet, their common characteristics of long reaction times, the requirement for organic solvents, and low flow rates are major hurdles to overcome to facilitate industrial scale-up [16]. Although for native lignin applications it is favorable and profitable, these technologies do not offer an advantageous solution to the black liquor and lignin produced by traditional biorefineries. Additionally, except SCW gasification studies [27], there are only few research focused on black liquor liquefaction studies in the literature [2,6].

In our laboratory, a custom-designed continuous pilot plant was developed to carry out rapid reactions (<1 sec) using supercritical water mediums. The plant possesses unique properties for hydrothermal processes such as instantaneous heating and cooling [28,29]. This efficient thermal management helps to prevent biomass degradation and char-like formations. The device that is used for this study allows a more precise and accurate control of the reaction time, avoiding repolymerization reactions according to the desired conditions [28]. Supercritical water was selected as the medium since it is environmentally friendly, low-cost, abundant, and does not cause contamination [30]. Taking advantage of the enhanced mass transfer and reaction kinetics in supercritical medium allows to intensify the process and work at rapid reaction times [31].

In this study, black liquor obtained from a commercial pulp & paper company is used without any pretreatment in a supercritical water (SCW) depolymerization process. The reaction conditions used in this study were 385°C, 260 bar, and 0.4 s. The product was subjected to different refining methods for optimization purposes to separate the bio-oil fraction and determine the aromatics and biopolyols present in this fraction. Several characterization techniques were used to understand the product characteristics and the potential use of these novel fractions. This approach presents a good opportunity because it uses the intrinsic pulping chemicals as catalysts, there is no need for drying or separating lignin, skips logistics by directly using black liquor, and benefits from the degradation compounds from lignin in black liquor.

2. Materials and methods

2.1. Materials

Black Liquor was provided by Ence Energía & Celulosa (Pontevedra, Spain). Chemicals used in analysis; ethyl acetate (99%), acetone (99%), sulfuric acid (72% & 96%), sodium hydroxide pellets (98%) were purchased from PanReac. N,O-Bis(trimethylsilyl)trifluoro-acetamide (BSTFA – 99%) and pyridine (99%) were purchased from Merck. The standards used for the gas chromatography calibration were all purchased from Sigma-Aldrich: guaiacol (≥99%), syringol (98%), vanillin (99%), acetosyringone (97%), acetovanillone (98%), and syringaldehyde (97%). Milli-Q grade water was used in the analyses.

2.2. Depolymerization Process

A detailed description of the pilot plant used in this study can be found in previous work by our research group [29], and a simplified block flow diagram (BFD) of the pilot plant is presented in Figure 1. The black liquor (BL) slurry is pumped directly to the reactor at room temperature. As soon as the BL slurry mixes with the supercritical water at the reactor entrance, the BL is instantaneously heated to the desired temperature. The hydrothermal treatment starts at that moment. The plant operates with different reaction times (<1 s to 1 minute) by changing the reactor dimensions. A notable feature of the plant is the Sudden Expansion Micro Reactor (SEMR), which is rapidly decompressed at the outlet by a letdown valve. The sudden depressurization through a control valve, based on the Joule-Thomson effect, allows an instantaneous cooling from supercritical water conditions to approximately 150 ± 10°C, while the pressure drops to ~5 ± 2 bar. These conditions are sufficiently low to ensure that degradation reactions are instantaneously halted or minimized. Furthermore, a subsequent heat exchanger is employed to further reduce the temperature of the products to ambient levels [29]. The desired reaction times are achieved by adjusting the reactor length, inner diameter, or flow rates of the streams.

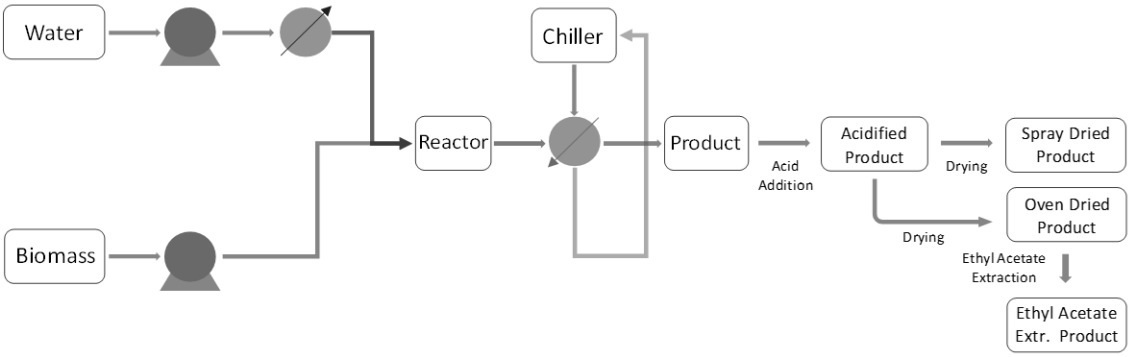

Figure 1. Simplified block flow diagram of the TRL5 supercritical water depolymerization pilot plant and post-processing steps.

Black liquor was subjected to hydrothermal treatment in supercritical water at 385 ± 1°C and 260 ± 5 bar. Experiments were conducted in triplicates, each with a steady state operation time of 1 hour. The reaction time inside the reactor ranged between 0.36 s and 0.40 s. The flow rates for the SCW and biomass were set at 15.0 kg/h and 7.5 kg/h, respectively. The BL stream was diluted with water to achieve a slurry concentration of 20% w/w total solids (TS) due to the high solids content in black liquor.

2.3. Solids analysis and downstream processing

The products obtained from the hydrothermal processing were analyzed gravimetrically to conduct a mass balance. First, a dissolved solids analysis (DS) was applied to both raw black liquor (BL) and depolymerized black liquor (DBL) obtained after the process. The DS analysis is a gravimetric technique that allows the determination of water-soluble material in a liquid sample. These results allowed us to evaluate the effect of the hydrothermal process on the amount of the water-soluble fraction [32]. The samples (DBL and BL) were acidified to different pH levels by adjusting sulfuric acid amounts. After acidification, the samples were centrifuged, and the dissolved solids (DS) and suspended solids (SS) fractions were separated. The suspended solids fraction was further washed with pH 2 water to completely remove the DS from the SS phase. The final material was dried in an oven at 105ºC, and dry matter weights for both DS and SS were logged against the measured pH values. This technique was used to understand the amount of suspended solids (SS), dissolved solids, and total solids (TS) generated at different values of pH. This solids analysis method is given in Figure S1.

A comparison between different refining methods was performed using two different approaches. A simplified scheme of these separation methods can be found in Figure

S2. In procedure A, after acidification of the BL or DBL to different pH levels, the sample was subjected to direct drying (Oven Drying or Freeze Drying). Subsequently, an ethyl acetate extraction was applied to the dried material, which was then separated by centrifugation. The ethyl acetate-extracted fraction was labeled as EtAc Extracted, whereas the water-extracted fraction was labeled as Water Extracted, and the remaining sample was called Insoluble. Oven Drying was performed at 105°C, while freeze drying was conducted at -55°C and 20 mbar.

In procedure B (*fractionation method*), a fractionation procedure was conducted for detailed separation. Once acidification was completed, instead of using a direct drying method, phase separation was performed by centrifugation. After decanting the DS from the SS, the SS fraction was washed three more times with pH 2 water, and the liquid part was combined with the DS. The ratio of pH 2 water to solids was 1:1. Ethyl acetate extraction was then performed on both fractions, resulting in four different fractions being obtained. At the end of this process, four different fractions were collected: Ethyl Acetate-Soluble in Dissolved Solids (DS-EA), Water-Soluble in Dissolved Solids (DS-W), Ethyl Acetate-Soluble in Suspended Solids (SS-EA), and Insoluble Suspended Solids (SS-Insol.). The organic solvent was removed using a rotary evaporator for the DS-EA fraction. The water bath was set to 50°C, and evaporation was carried out under a vacuum pressure of 350 mbar. After evaporation, the material was further dried in an oven at 50°C. Characterization of other materials (SS-EA, DS-W, SS-Insol.) was beyond the scope of this study.

2.4. Depolymerized black liquor performance evaluation

After the fundamental solids analysis, four different types of samples, along with one blank sample, were designated for further in-depth characterization to evaluate the process performance. These are named as follows: Black Liquor (BL) as the raw material (blank sample), Depolymerized BL (DBL) as the product from the pilot plant, Oven Dried product (OD), Spray Dried product (SD), and Ethyl Acetate soluble (EA) product. Oven Dried and Spray Dried products were obtained by following acidification of DBL and direct drying (oven or spray drying) steps. Product OD was ball milled after drying. Ball milling of the OD product was performed using a Retsch PM 100 for 4 hours. Since freeze-drying extraction results were not promising at lower pH compared to the *fractionation method*, and spray drying process is much faster than freeze-drying, spray drying is included in this part of the research. As the SD particles were uniform, with an

average particle size of 10 microns, no further grinding operation was necessary. The spray drying inlet air temperature was set to 160°C, and the product exit temperature was 85°C, while the flow rate was 1.5 kg/h. OD and SD samples were selected to check the effects of particle size and temperature on the chemical composition of the materials. The ethyl acetate-extracted product was produced by subsequent ethyl acetate extraction applied to the OD product. The ethyl acetate-extracted fraction from DBL essentially consists of lignin depolymerized products of black liquor, including monomers and oligomers (containing biopolyols), plus possible repolymerization of oligomers and monomers produced after the depolymerization of black liquor in SCW. A simplified BFD including the post-processing steps to obtain the designated products for further characterization can be found in Figure 1. A study that focuses specifically on the repolymerization reactions carried out by our previous group member can be found in the literature [33].

The characterization techniques applied to the samples are described below:

The chemical composition of these five samples was determined using the Laboratory Analytical Procedure (LAP) from the National Renewable Energy Laboratory (NREL). Moisture content, acid-soluble and insoluble lignin, carbohydrates, and ash content were determined using methods from NREL [32,34–36]. Acid Soluble Lignin amount was determined for the raw material and the product profiles by using UV-Vis Spectroscopy. The absorbance was recorded at 205 nm, and absorptivity coefficient used was 110 L g^{-1} cm^{-1} [35].

Elemental Analysis of the materials was carried out using a Leco CS-225 Elemental C-S Analyzer to determine the hydrogen, carbon, nitrogen, and sulfur content. The balance of the remaining parts was considered as oxygen and inorganics.

Fourier Transform Infrared (FTIR) characterization of the materials was performed using a Bruker Tensor 27 equipped with a universal attenuated total reflectance accessory with internal diamond crystal lens. The operating range was between 4000 to 400 cm^{-1}, and each spectrum was a mean of 64 single scans.

Thermogravimetric Analysis was conducted using a Mettler Toledo TGA/SDTA RSI Analyzer. Approximately 5 mg of the sample was heated at a rate of 10°C/min under a nitrogen atmosphere with a flow of 50 mL/min. The temperature started at 30°C and

increased to 900°C. The temperature was held constant at 900°C under a nitrogen flow for 10 minutes with the same flow rate.

DS-EA fraction precipitated at different pH levels analyzed and quantified by using an Agilent 7820 GC gas chromatograph with a quadrupole mass spectrometer detector (5978A-Agilent Tech., USA). As the monomer-focused method all the samples were prepared by dissolving them in acetone prior to analysis. The separation was done with a low bleed, non-polar capillary Agilent HP-5ms column, 30m x 0.25mm x 0.25µm. Helium was used as a carrier gas, and the injection was in splitless mode. The temperature program of the oven started at 32°C and held for 10 min; then it was raised to 52°C by an increment rate of 2°C/min, kept for 2 min; then to 65°C at 2°C/min with 2 min holding time was followed; then increased to 93°C by 4°C/min rate, which held for 2 min; followed by a raise to 230°C at 2°C/min and kept for 3 min; lastly to 300°C at a rate of 15°C/min and kept for 3 min. Solvent delay program was set to 4 minutes to keep acetone away from sending to MS detector. The compounds identification was done by both validating from NIST library by comparing m/z values and the retention times. This method was used to identify the monomers and is a modified version of a previous study performed by our group [37]. Biopolyols and oligomers of the depolymerized black liquor DS-EA fraction were analyzed using a derivatization method which will be called oligomer-focused method. 10 mg/mL lignin oil (LO) solution was prepared in acetone, and a 10:1:2 (v:v:v) mixture (LO:Pyridine:BSTFA) was heated for 20 minutes at 45°C before injection to GC-MS. N,O-Bis(trimethylsilyl)trifluoroacetamide with 1% trimethylchlorosilane (BSTFA) was used as the silylating agent. The oven was started at 150°C and increased at a rate of 4°C/min until 300°C and held for 18 min. TMS-derivatized oligomers were determined using a 2.5:1 split ratio, and a solvent delay of 15 minutes, to avoid detector overload with an excess of monomers.

Gel Permeation Chromatography (GPC) was performed to check the molecular weight distribution of the selected samples qualitatively. Samples were prepared for GPC by using their dried versions at the end of each process. The samples were dissolved in 1% w/v LiBr in DMSO, and the concentrations were set for 1 mg/mL. Phenomenex Phenogel 5µ 10^3 Å GPC column with a size of 350 x 7.8 mm was used for the analysis. The column temperature was set to 35ºC, DMSO was the carrier solvent at a flow rate of 0.8 mL/min. The eluents were analyzed using a UV-DAD detector at a wavelength of 254 nm.

Sugar and derivative analyses were performed using high-performance liquid chromatography (HPLC). The column used during the analyses was a Shodex SH-1011 column, with sulfuric acid (0.01 N) as the mobile phase at a flow rate of 0.8 mL/min. A Waters 2414 RI Detector was used for component detection. The NREL Protocol for carbohydrate determination was followed for HPLC analysis.

3. Results and Discussion

3.1. Refining methods

Different methods were tested to find an easy and quick separation method to make a product ready for industrial use or processing. The primary objective was to minimize time and cost to create an efficient method.

BL and DBL were refined according to the procedures A and B described above. The ethyl acetate-extracted fractions from both procedures are compared in Figure 2. Both procedures show that the highest yield of ethyl acetate fraction is obtained at pH 2. Also, it was observed that the yield increases as the pH drops. Remarkable differences were observed for the ethyl acetate-extracted fractions between procedure A (drying) and procedure B (not drying). Using the oven drying method, the maximum ethyl acetate-extracted fraction yields was 25% for BL and 37% for DBL. However, the oven drying method yielded less than 5% ethyl-acetate extract at pH values higher than 2.5. This was observed for both BL and DBL. A similar behavior was observed for the freeze-drying method above pH 4 for BL and pH 3.5 for DBL. The *fractionation method* showed higher extraction performance compared to the oven and freeze-drying methods at lower pH values. The oven drying method seems to “encapsulate” smaller fractions of lignin that would be soluble in EA. Additionally, the freeze-dried samples were easier to extract than the oven-dried ones. This is likely related to better particle formation and less agglomeration during the freeze-drying method. Black Liquor ethyl acetate-extracted bio-oil yield was found to be 25% for oven drying, 41% for freeze-drying, and 38% for the *fractionation method*, whereas for depolymerized black liquor, the yields were 37% for oven drying, 44% for freeze-drying, and 40% for the *fractionation method*. Experimental error of these results was less than 6%. These results show that the drying of the samples as they come from the reactor will not affect the availability of the bio-oil fraction (extracted with ethyl-acetate). However, it was seen that the drying technique could affect that bio-oil availability. The combination of oven drying and milling yielded less bio-oil than the samples produced from freeze drying. Industry could expect

depolymerized black liquor products as dried samples, but drying should be done in a way to prevent macro agglomeration of the material.

Interestingly, the material created emulsions at high pH values, >6.5 for BL, and >5 for DBL. The presence of emulsions made the separation of suspended and dissolved solids less efficient, resulting in lower bio-oil yields. Although the freeze-drying method and the *fractionation method* had similar extraction yields at pH 2, the *fractionation method* was chosen for detailed aromatic component analysis since it outperformed the freeze-drying method at lower pH levels. For example, the extracted fraction from BL by freeze drying is 1%, whereas by the *fractionation method* is ~22% at pH 5. A similar behavior can be observed for DBL, where using freeze drying yields a 2% extraction fraction, while the *fractionation method* yields 25% at pH 5.

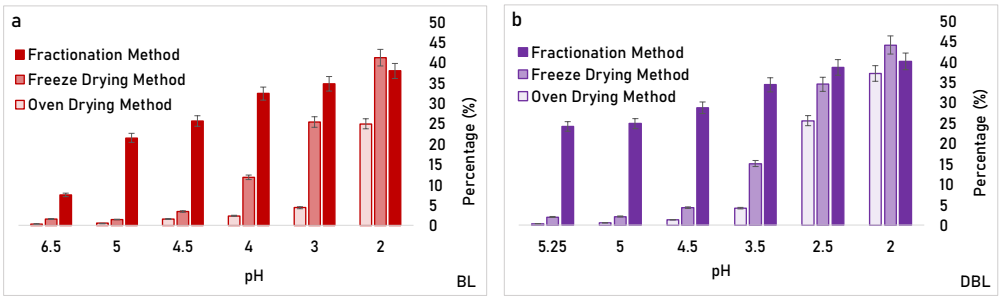

Figure 2. Yield comparison of ethyl acetate extracted fraction for different separation methods at different pH values; (a) BL and (b) DBL.

3.2. Effect of pH on solids yield

The solids yield of BL and DBL after acid precipitation are presented in Figure 3. The graph 3-a shows the amount of acid (% - g of acid per g dried material) added to the product versus the resulting pH after acid addiction. On the other hand, graph 3-b shows the amount of soluble material (% Dissolved Solids) at different acid additions for both BL and DBL. As depicted in Figures 3a and 3b, the pH evolution of BL and DBL differs, indicating that the consumption of -OH groups before and after the reaction in SCW varies. The evolution of the DS amount with acid addition shows an intriguing difference between BL and DBL. The discussion can be divided into three distinct regions: between 0-20% w/w (region 1); 20-50% w/w (region 2); and 50-65% w/w (region 3) acid addition.

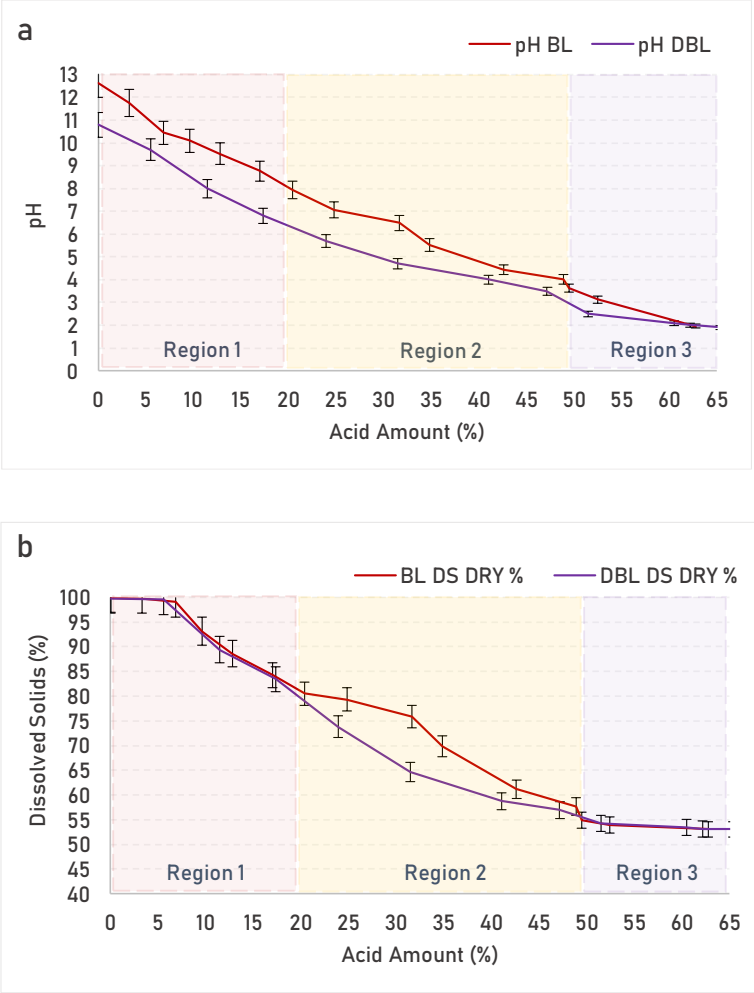

Figure 3. Effect of pH and acid added during acidification on dissolved & suspended solids; (a) BL and (b) DBL.

In region 1, the DS decreased gradually for both BL and DBL, with no significant difference between them. In region 2, a distinct gap between DBL and BL is observed up to 50% acid addition, which continues until pH ~4. This gap indicates that the DBL requires less acid than BL to precipitate the lignin. Although the overall DS% has a declining trend, the BL acidification experiments showed a slower drop of pH in the region of 20% to 30%. Precipitation of suspended solids for BL (down to pH 9) and DBL (down to pH 7) was very low due to the low acidity of the medium, which is insufficient to precipitate weakly acidic groups (typically molecules that contain phenols/phenolic groups). Lignin was charged and soluble in the medium. Simply, at this point lignin can be envisioned as an amorphous macromolecule formed by crosslinked microgel coil-like structures [38–40]. The cations used in the kraft pulping processes (Na^+, K^+, etc.) surround the lignin macromolecules, which are negatively charged by phenolic groups.

This effect makes lignin soluble in an alkaline medium [41]. As the medium acidifies and hydrogen ion concentration increases, weakly acidic phenolic groups become protonated. There is a point where repulsive and attractive forces reach equilibrium. Thus, the second region represents a transition where repulsive forces become less dominant and attractive forces predominate. In this region, self-aggregation of the lignin molecules was observed for both BL and DBL [41,42]. This aggregation occurs when the pH is close to the acidic strength of phenolic groups (pKa). At the end of this transition region, a substantial amount of lignin molecules precipitates.

The amount of precipitated solids decreased significantly beyond 50% w/w of acid (region 3), and the precipitation became nearly constant between pH 2 – 4. Figure 3 additionally shows that DBL had a lower initial pH (10.8) than BL (12.6). This is likely due to an increased number of phenolic groups made during the hydrothermal process, causing a decrease in the pH level of the product. A similar observation is reported by Orebom [6]. Ultimately, despite slight differences in formation, both BL and DBL have nearly the same percentage of DS (~53%) and SS (~47%) around pH 2.

The *fractionation method* (from procedure B) samples of both BL and DBL are evaluated in Figures 4a-d. The samples were divided into: Insoluble Suspended Solids (SS-Insol.), Suspended Solids in Ethyl Acetate (SS-EA), Dissolved Solids in Ethyl Acetate (DS-EA), and Dissolved Solids in Water (DS-W). Additionally, SS, DS, and TS are depicted in Figures 4e-f. These yields were obtained without removing the inorganics amount from the calculations in a dry basis compared to the total solids. Details of the calculations can be found in Annex 1. The main observations can be summarized as follows:

- The EA insoluble fraction from the suspended solids was consistently higher for BL than DBL. It is noteworthy that BL yielded an insoluble fraction of about 17% regardless of the pH. In contrast, DBL was significantly affected by pH, with the insoluble fraction increasing from 11% to 16% as the pH dropped from 5 to 2. This effect could be related to the presence of smaller lignin fractions in DBL compared to the original BL. These oligomers might be more stable in dissolution or microemulsion due to their smaller molecular size.

- The EA soluble fraction of the suspended solids was similar for DBL and BL. In both cases, the soluble fraction increased when the pH was reduced to 2, reaching a maximum.

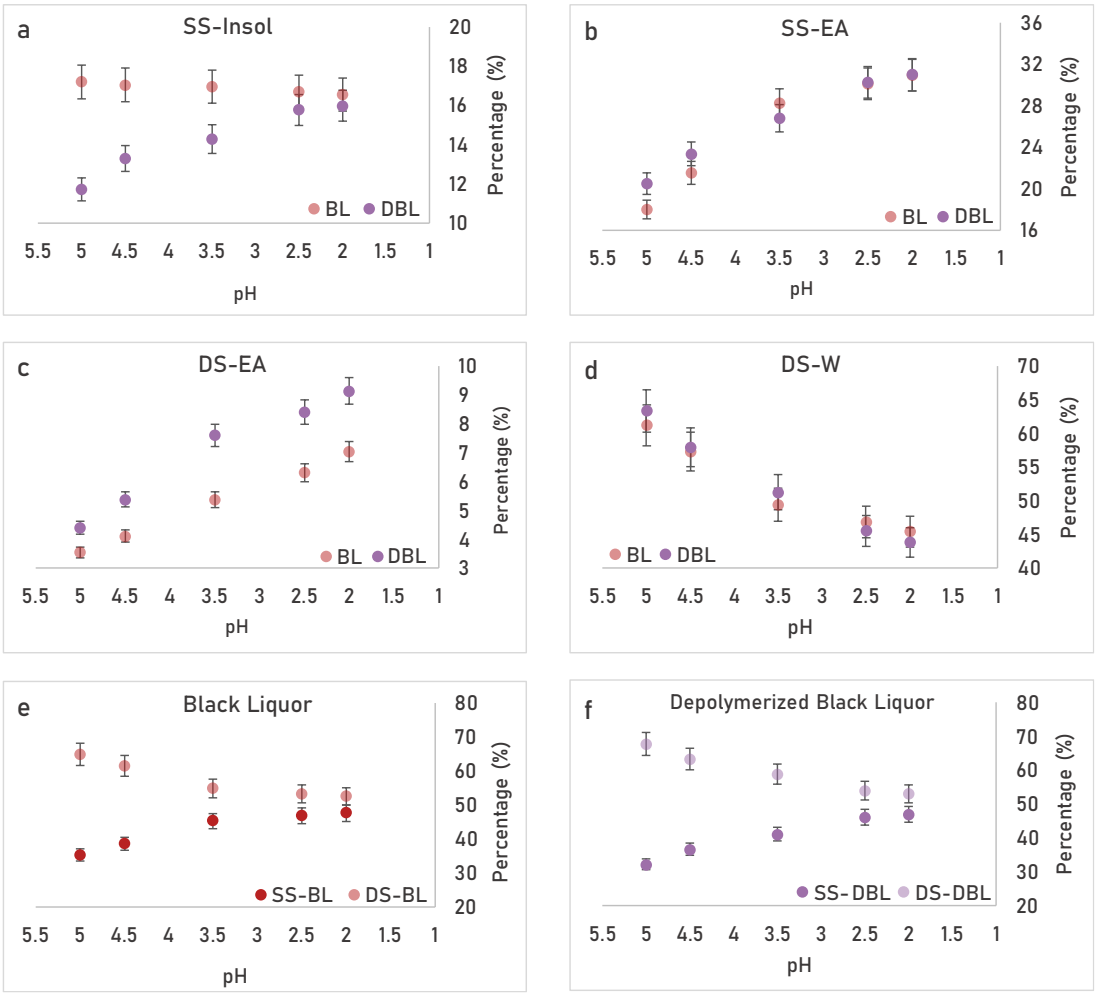

Figure 4. Comparison of black liquor (BL) and depolymerized black liquor (DBL); (a) insoluble suspended solids, (b) suspended solids in ethyl acetate, (c) dissolved solids in ethyl acetate, (d) dissolved solids in water, (e) suspended (SS) & dissolved solids (DS) of black liquor, (f) suspended (SS) & dissolved solids (DS) of depolymerized black liquor. Percentages are given on a dry basis.

- The EA soluble fraction in the DS was increased by the hydrothermal treatment. The DS fraction of the DBL contained about 9% EA soluble compounds, while the BL samples had 7%, which is about a 30% increase compared to the BL (Figure 4c). The total ethyl acetate-soluble fraction yield was found to be 40% (9% DS-EA + 31% SS-EA) on a dry basis, including ash. Conversely, when the ash content is removed from the calculations, the total ethyl acetate-extracted fraction yield was found to be 77% (17% DS-EA + 60% SS-EA) on a dry basis.

- The EA insoluble fraction in DS (water-soluble) represents the largest fraction since it includes the inorganics from the kraft pulping process. Both DBL and BL exhibited similar results, with pH reduction prompting a decrease in water-soluble material. In this case, the reduction of pH promotes the reduction of water-soluble material. Separating this fraction is crucial for plant economics, as it enables the recycling of inorganics back into the kraft pulping process cycle.

Figures 4e and 4f demonstrate that the total solids amount has negligible changes between pH 4 and 2 for both BL and DBL. However, SS and DS did vary with the change in pH. A pH of 2 was determined to be an appropriate level for performing the *fractionation method* since the goal was to recover a greater amount of DS-EA fraction to search for biopolyols in DBL.

3.3. Bio-oil composition

The monomers in the EA fractions were determined by using GC-MS. Comparison of these aromatic monomers at different pH levels can be seen in Figure 5a-f. Guaiacol (G), Syringol (S), Vanillin (V), Acetovanillone (AVA), Syringaldehyde (SA), and Acetosyringone (ASY) were the main monomers observed in GC-MS analysis. A previous study conducted by our team members, which used lower concentrations of black liquor, monitored the same main aromatic monomers as found in this study, except creosol [43]. According to Figure 5, generally, the concentration of the monomers decreased as the pH of the samples lowered. However, Figure 4c demonstrates that DS-EA percentage increases by decreasing pH. This observation indicates that the drop of pH promotes the precipitation of dimers, trimers, and oligomers which are still linked to the metal cations in the DS fraction.

The main difference between DBL and BL was observed in the syringol yields. The syringol concentration in the EA-soluble fraction of DS increased approximately fourfold after hydrothermal treatment. The percentage of monomers in the DS-EA fraction was higher for both DBL and BL at pH 5 than at pH 2. Total quantified aromatic monomer yield, based on the DS-EA fraction, was found to be 8% w/w for DBL and 7% w/w for BL at pH 2, while it was 22% w/w for DBL and 13% w/w for BL at pH 5. The remaining DS-EA fraction consists of higher molecular weight compounds such as dimers, trimers, oligomers and biopolyols.

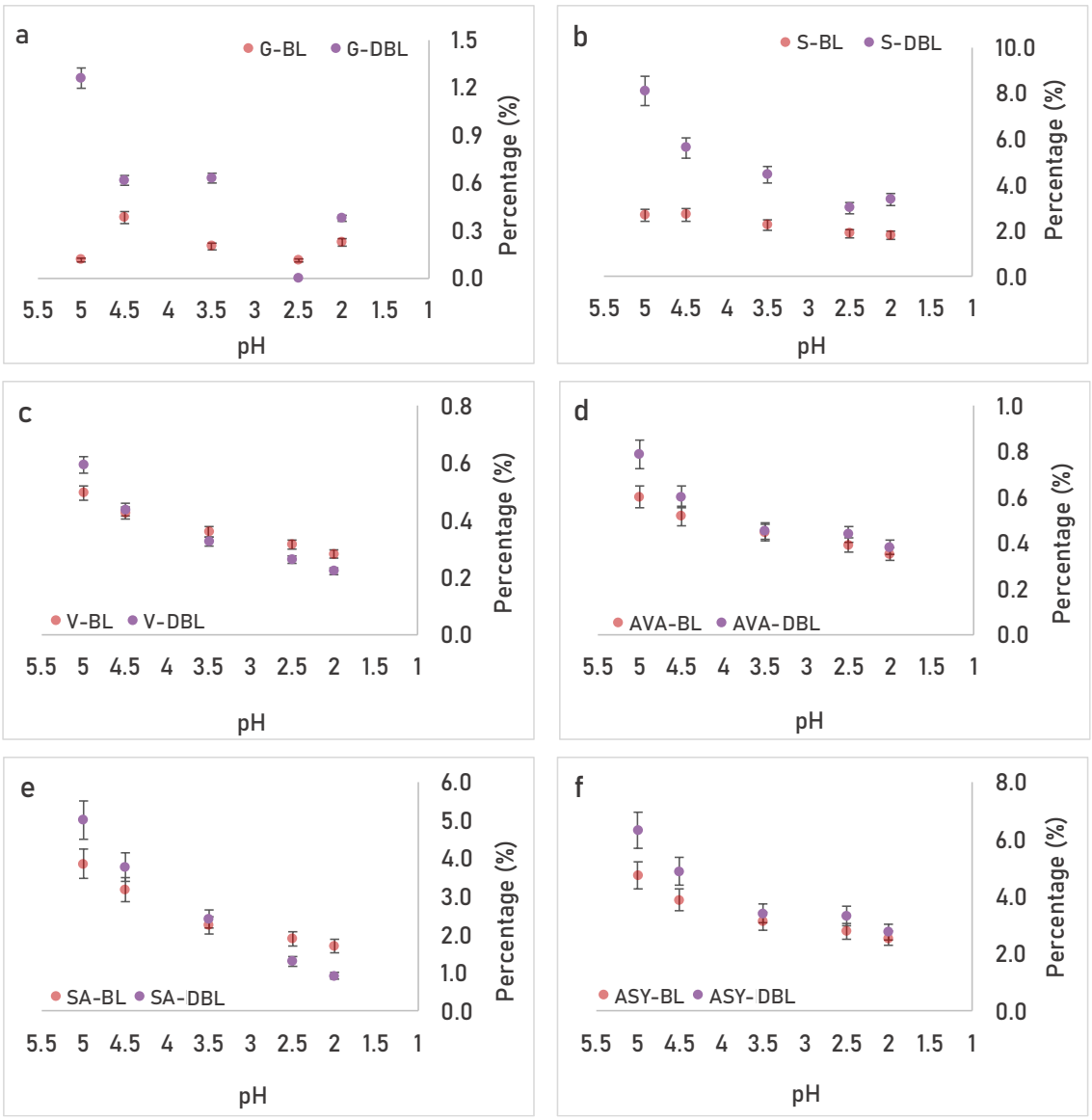

Figure 5. Distribution of main aromatic monomers percentage; (a) guaiacol, (b) syringol, (c) vanillin, (d) acetovanillone, (e) syringaldehyde, (f) acetosyringone in DS-EA fraction at different pH values that were analyzed by GC-MS.

The differences in the molecules identified by the monomer-focused GC-MS method between black liquor and the depolymerized black liquor DS-EA fraction are shown in Figure 6. As the dominant raw material of the black liquor used in this study was eucalyptus wood, and eucalyptus is a hardwood, the presence of both guaiacyl (G) and syringyl (S) derived monomers was expected in the GC-MS analysis. Mutual monomers present in both BL & DBL were 2,4-di-tert-butylphenol, 5-tert-butylpyrogallol, 3,4,5-trimethoxyphenol, and 4-ethylguaiacol. Mesitylene, homosyringic acid, vanillic acid, and syringic acid, which were detected in BL were not present in DBL. On the other hand, several low molecular weight aromatics formed after the supercritical water

depolymerization of BL can also be seen in Figure 6. Using the monomer-focused GC-MS method, three different biopolyols (5-tert-butylpyrogallol, 4-methylcatechol, and 3-methoxycatechol) were detected.

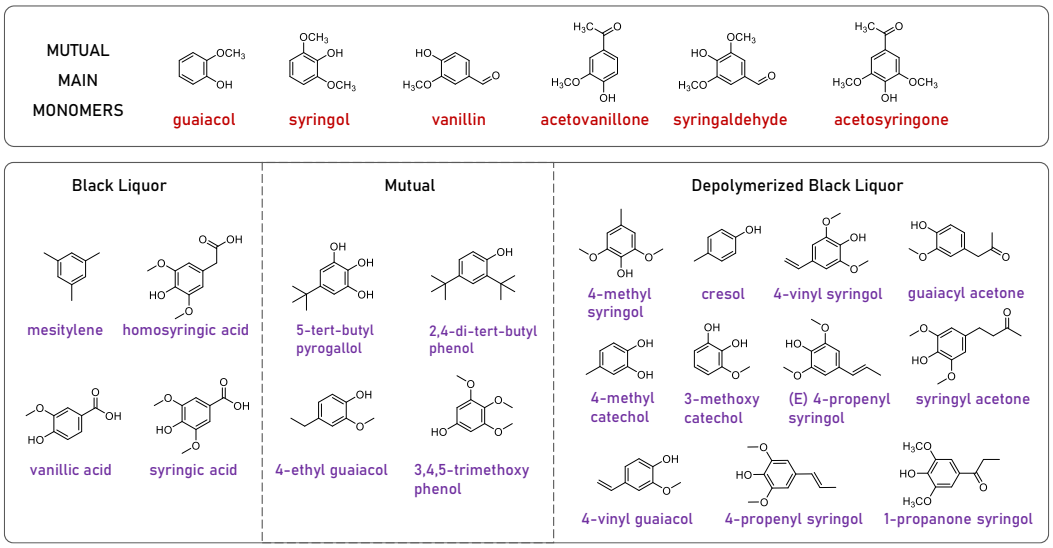

Figure 6. Difference between black liquor & depolymerized black liquor samples DS-EA fraction identified products by monomer focused GC-MS method.

The main biopolyols identified after the supercritical water depolymerization of black liquor are shown in Figure 7. A detailed table of the components identified using the oligomer-focused GC-MS method can be found in Table S1. The identified biopolyols can be categorized into three groups: aromatic polyols, sugar polyols and long-chain fatty acid-derived polyols. Stilbene, D-glucopyranosiduronic acid, and Prostaglandin F2α were found as derivatized versions in DS-EA fraction. For simplicity, in Figure 7, their backbone (non-derivatized forms) was only given. Interested readers can find the full names of these molecules in Table S1 in Appendix A.

The presence of biopolyols allows us to utilize the DS-EA fraction produced by performing supercritical water depolymerization for various purposes, such as lubricant or polyurethane production [5,44,45]. Therefore, the next step considered was to conduct a more thorough chemical characterization of five different samples for comparison purposes.

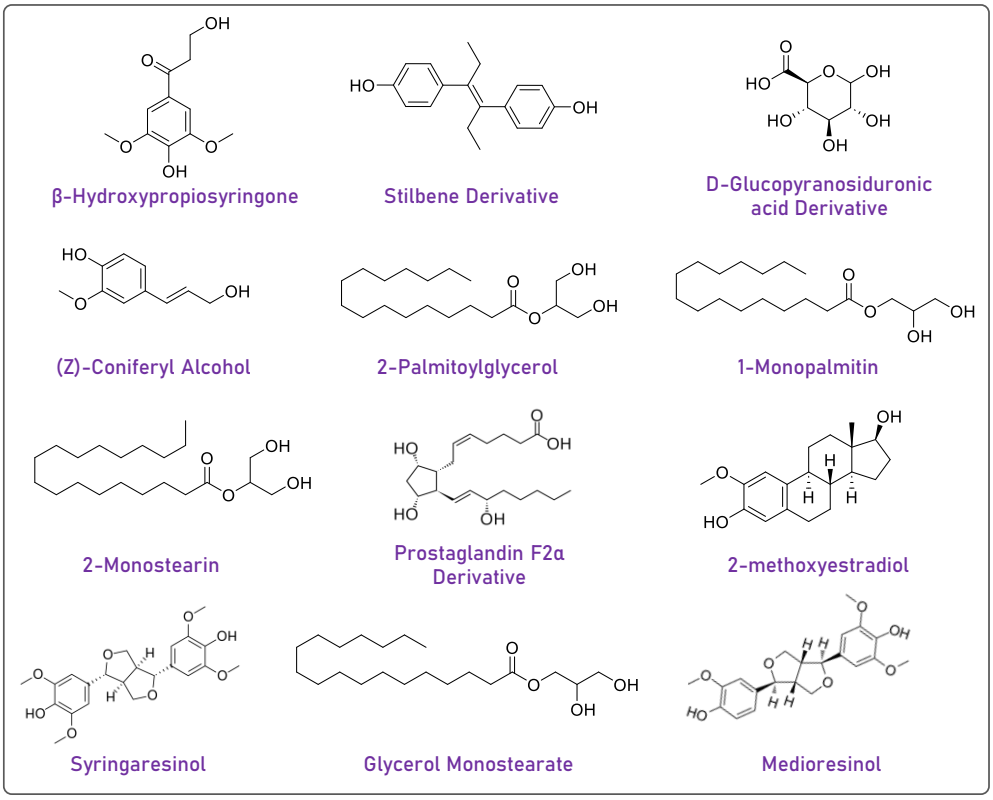

Figure 7. Identification of depolymerized black liquor DS-EA fraction products by oligomer focused GC-MS method (identified biopolyols).

3.4. Characterization of the selected samples

The samples were subjected to chemical composition analysis using NREL Protocols, and the results were summarized in Table 1. The carbohydrate content was found negligible as less than 1% w/w. The ash content of black liquor is quite high, as was presumed, due to the kraft pulping process. After depolymerization in supercritical conditions, the ash content of DBL was observed to be the same as that of BL, suggesting that inorganics did not get stuck in the system. As expected, the ash content of SD and OD were increased due to the sulfuric acid addition during precipitation step. However, the increment of the ash content for OD and SD were only around 25%, which is much lower than the acid amount added for precipitation. This might have been due to gas formation during precipitation [46]. Therefore, some part of the lignin or lignin-derived compounds could have been recovered from the inorganics and contributed to the total lignin calculations, which can explain the slight increment of total lignin in SD and OD products.

Table 1. Chemical Composition Percentages of the Samples (Dry Basis)

	Klason Lignin	Soluble Lignin	Total Lignin	Ash	Carbs
Black Liquor (BL)	20.5 ± 1.4	11.8 ± 1.2	32.2 ± 1.4	48.9 ± 0.9	<1
Depoylm. BL (DBL)	18.5 ± 2.2	8.0 ± 0.8	26.4 ± 2.9	48.5 ± 1.1	<1
Spray Dried (SD)	19.7 ± 2.4	10.4 ± 0.4	30.1 ± 2.7	60.7 ± 0.8	<1
Oven Dried (OD)	24.3 ± 1.6	6.3 ± 0.6	30.7 ± 1.1	59.8 ± 0.6	<1
EA Extracted (EA)	47.8 ± 2.1	18.9 ± 2.1	66.7 ± 2.1	2.0 ± 0.2	<1

Table 1 shows the difference in total lignin percentages between before the reaction (BL) and after the reaction (DBL) were different (32% w/w vs 26% w/w). The configuration of the pilot plant does not allow checking the gases formed during the reaction. However, it is known that during supercritical water depolymerization of lignin, some gases are being formed. The difference between BL and DBL in terms of total lignin percentages could have been due to gas formation during the process. Another possibility that caused this decrease could be gas formation during precipitation by strong acid. Modification in the structure of the lignin and lignin-derived materials after depolymerization in SCW may have made the compounds in the DBL more prone to gas evolution during precipitation. It is also widely known in industry and literature that extreme gas evolution occurs during precipitation, including CO_2 and H_2S [47]. Yet, this argument should be verified in-depth using other characterization techniques. The total lignin in the EA product was found to be the highest since the aromatic depolymerized fraction was extracted from the complex matrix into the ethyl acetate fraction and became almost completely free of ash.

Elemental analysis results of the selected products are given in Table 2. CHNS elements were analyzed by elemental analyzer, inorganics were determined via ash analysis, and oxygen was estimated as the balance. The maximum error percentage was less than 3% w/w. According to these results, the products can be grouped into three categories. In the first group, the H:C ratio decreased from 1.55 in BL to 1.29 in DBL, indicating that dehydration reactions took place during hydrothermal treatment, which is common for the supercritical water depolymerization of lignin [37]. This suggests that more aromaticity and/or the presence of double bonds in DBL are expected. However, when examining the H:C and O:C ratios together, it appears that demethylation occurred overall. Van Krevelen diagram of elemental analysis results can be found in Figure S7. Another important point is the difference of the components identified by GC-MS in Figure 6 between BL and DBL. The carboxylic group-containing components present in

raw BL disappeared in DBL samples, indicating that decarboxylation occurs during the process. A study by a previous group member also supports the existence of decarboxylation reactions during supercritical water experiments [33]. Nevertheless, the increase in methoxy groups in DBL samples, alongside elemental and GC-MS analysis results, indicates that various types of reactions occur simultaneously. The second group includes SD and OD, and these products have H:C ratios of 1.04 and 1.01, respectively. The last group contains the EA product, which has the lowest H:C ratio of 1.00. The difference between DBL and the second group is only in the acidification and drying of the materials, suggesting that CO_2 was likely released during the drying process. The varying ash content in the products resulted in broad higher heating value (HHV) calculations. The lack of ash content gives an advantage to the EA product, showing an HHV value of 22.2 MJ/kg.

Table 2. Elemental Analysis of Samples (Dry Basis)

	AVERAGES									
	N	**C**	**H**	**S**	**O + Inorg.**	**Inorg.**	**HHV (MJ/kg)**	**LHV (MJ/kg)**	**H:C**	**O:C**
BL	1.51	33.36	4.34	0.00	60.79	48.9	14.47	13.50	1.55	0.27
DBL	1.69	33.02	3.56	0.49	61.25	48.5	13.40	12.61	1.29	0.29
SD	1.59	23.79	2.07	0.28	72.27	60.7	8.27	7.81	1.04	0.36
OD	1.54	24.41	2.08	1.96	70.01	59.8	8.83	8.36	1.01	0.31
EA	1.50	57.56	4.85	0.00	36.09	2	22.22	21.13	1.00	0.44

The chemical structures of black liquor, and the products were examined by attenuated total reflection FTIR spectroscopy which can be found in Figure 8. Figure 8a and 8b are the spectra obtained by this technique. Total wavenumber range analysis is given in Figure 8a, whereas a close-up view of fingerprint range analysis can be found in Figure 8b. The broad band formed by EA-extracted product at 3400 cm^{-1} belongs to the phenolic and/or alcoholic units O-H stretching. Regarding the bands at 2930 and 2840 cm^{-1}, aliphatic groups C-H bonds vibration can be assigned to these bands (-CH_2 groups for 2930 cm^{-1}, and -CH_3 groups for 2840 cm^{-1}). Black liquor 3400 cm^{-1} and 2940 cm^{-1} absorption bands were vaguely recognizable, although the intensity of the bands was very low because of high inorganic content. The fingerprint region of these products started around 1900 cm^{-1}. The stretching of C=O bonds at 1730 cm^{-1} was originated from lignin, and as it can be seen in Figure 8b, it is visible for all three products except black liquor. The aromatic skeletal vibrations of lignin can be found between 1700 and 1400 cm^{-1} (Figure 8b - dotted area). The signals observed at 1600 and 1510 cm^{-1} were due to

the C-C aromatic skeletal vibrations, while the bands at 1460 and 1420 cm^{-1} were formed by the $-CH_2$ and $-CH_3$ groups' C-H deformation, and C-H aromatic ring vibrations, respectively. The bands between 1700 and 1200 cm^{-1} found the highest in ethyl acetate extracted product compared to the other products, that supports the increased aromaticity of the ethyl acetate extracted fraction of the DBL.

The nature of the feedstock brings along some small differences for the bands that can be observed in FTIR in terms of being softwood or hardwood. Since the starting material was eucalyptus, as it was mentioned before, signals that correspond to both syringyl (S units) and guaiacyl units (G units) can be seen in Figure 8b clearer. The bands at 1270 and 815 cm^{-1} are the typical signals that were well known in the literature which correspond to G units [5]. Considering the S units absorption signals, the bands at 1330 cm^{-1} that were formed from C=O stretching, also a small shoulder of C=O stretching in syringyl units was assigned to 1240 cm^{-1}, and at 1110 cm^{-1} was due to aromatic C-H in plane deformation of S units. Additionally, the small shoulder around 1030 cm^{-1} could be attributed to aromatic ring deformation which is usually more intense for G units compared to S units.

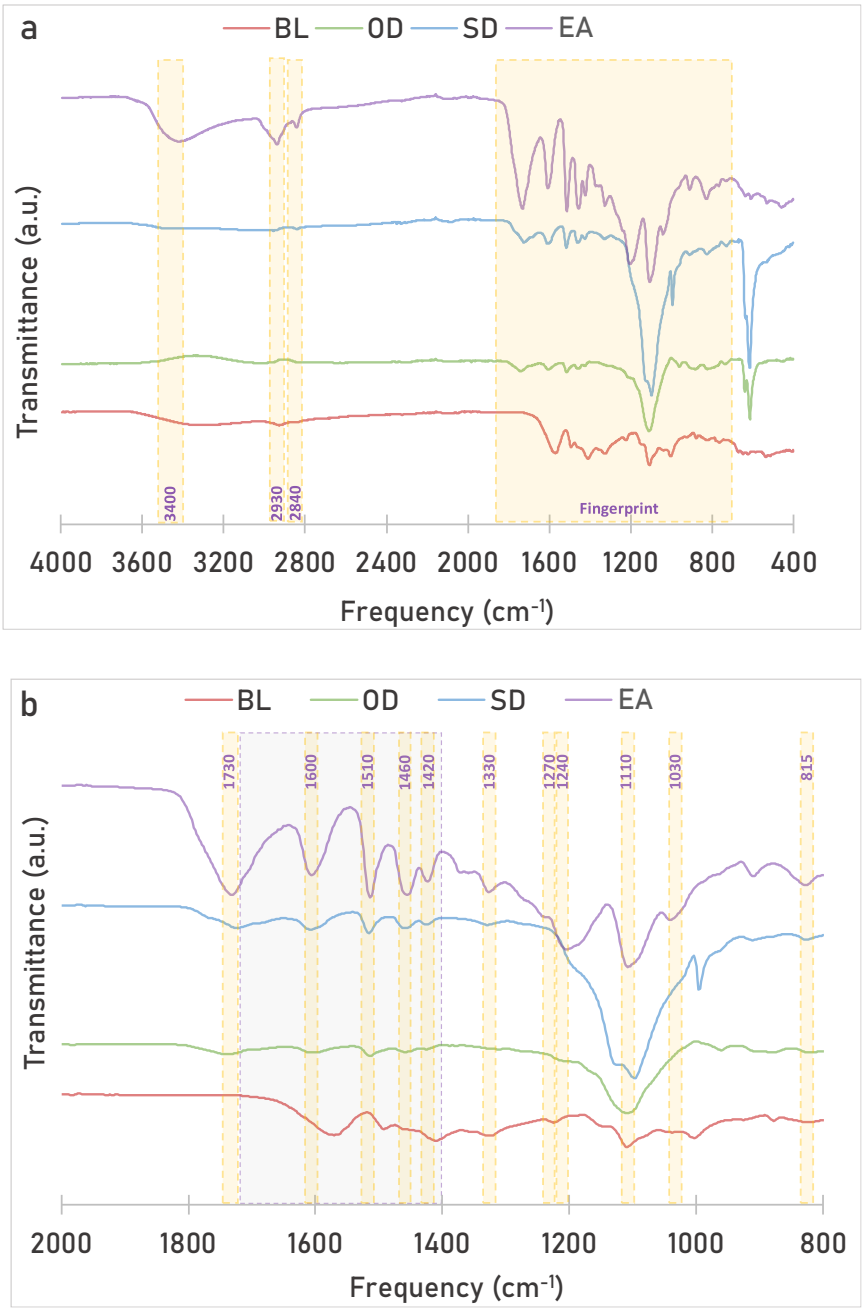

Figure 8. FTIR Spectra; (a) full spectrum, (b) fingerprint region in detail

Thermogravimetric analysis (TGA) was performed to study the stability and degradation behavior of the selected products (Figure 9). As with the elemental analysis, TGA/DTG results can also be divided into three groups. Although the samples were dried before analysis, the BL and DBL samples showed some moisture content up to 100°C. For the other products, the moisture content was less than 1%. The degradation of lignin-derived monomeric compounds generally occurs between 120-265°C, in addition to carbohydrate degradation [48,49]. Regarding high boiling point monomeric components,

the last degradation zone for lignin was accepted as between 300-500°C [50]. BL and DBL started to degrade at around 190°C, and only one peak was observed up to 300°C. Nevertheless, while OD exhibited similar behavior between 120-300°C, SD degradation started around 120°C. This supports that SD has a greater amount of lower molecular weight components compared to OD. This could also explain why SD had a higher acid-soluble lignin (ASL) content in its chemical composition according to Table 1. Apart from that, the EA product had the highest degradation among the other products between 120-500°C, where lignin degradation ends. Figure 9 demonstrates that the degradation profiles of BL, DBL, OD, and SD are quite similar between 300-500°C. However, their profiles changed above 575°C, the region that is accepted as the end of total carbon removal. Above 575°C, the BL and DBL samples exhibited volatilization at higher temperatures compared to SD and OD. Since BL and DBL were not acidified, large amounts of lignin remained bonded to inorganics as phenolates/carboxylates of sodium or potassium. SD and OD were acidified before their drying processes; however, lignin volatilization did not increase. Nevertheless, they showed a lower volatilization temperature for the degradation of inorganic-metal bonded materials compared to BL and DBL. The inorganic-metal bonded materials' degradation occurred between 675-775°C for SD and OD. However, for BL and DBL, this range was between 750-900°C. According to studies on the thermal degradation of black liquor, carbon compounds do not completely consume up to 575°C. These studies showed that intermediate alkaline compounds still exist at 900°C. These components can be present as –[CO_2M], –[COM], and –[CM], where M represents sodium (Na), potassium (K), or sulfur (S). During the degradation of these intermediates, CO forms [50]. Hence, it can be said that acidification appears to aid in releasing CO and CO_2 gases from the solution. Moreover, from Figure 9, it can be understood that carboxylates/phenolates of alkaline metals are still present in SD and OD products.

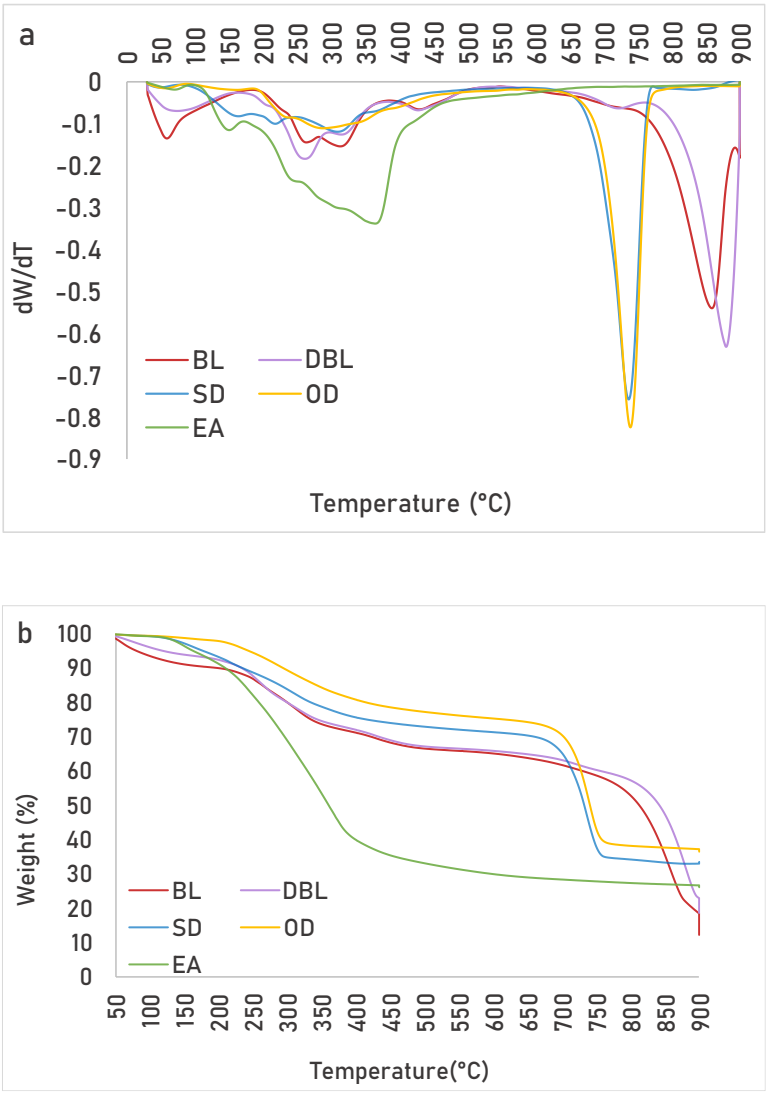

Figure 9. DTG (a) & TGA (b) diagrams of the samples

Another important point to note is the degradation peak shift of DBL compared to BL at temperatures over 750°C. The DBL DTG peak shifted around 50°C compared to BL. This could result from repolymerization reactions during the process. The shift in the DTG diagram may indicate the formation of high molecular weight components bonding with metals present in the mixture. After degradation completed at 900°C, the products were subjected to this temperature for an additional 10 minutes. The BL and DBL products continued to lose weight at this temperature, while other products showed no significant difference. Having alkaline metal-carbon structures still present in the matrix should be the reason for this behavior.

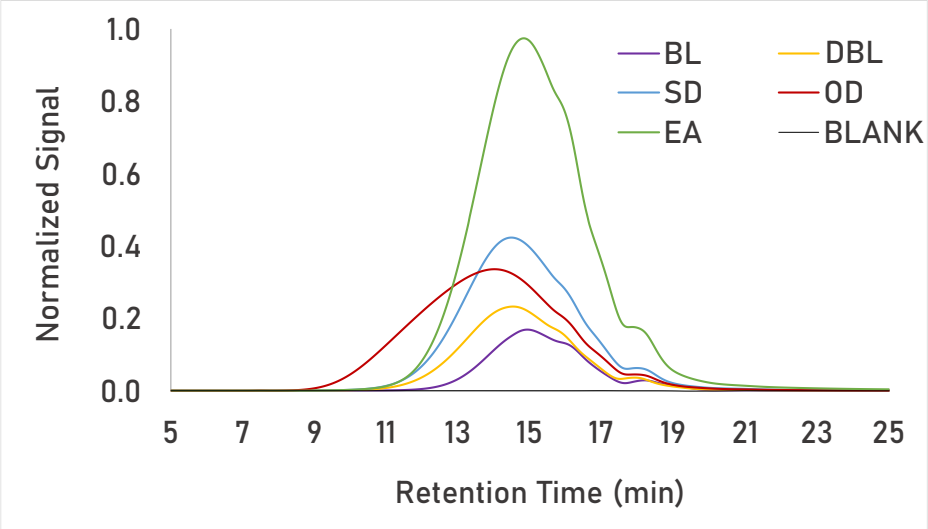

Figure 10. GPC chromatograms of the samples

The Gel Permeation Chromatography results graph is presented in Figure 10. The DBL shifted slightly to a lower residence time compared to black liquor, indicating a greater number of high-molecular-weight components in DBL compared to BL. Among all, the OD sample was the first to show a peak. SD, compared to OD, had a narrower peak, and its highest peak point occurred later than OD, suggesting that SD contains a greater amount of low molecular weight components. According to Gordobil, the drying process and its severity can affect the final lignin product observed. In that study, the difference between 25°C and 55°C drying temperatures of kraft lignin resulted in increased hygroscopicity in the 25°C dried product, and lighter-colored lignin particles were mentioned [51]. Hygroscopicity could be related to the difference in acid-soluble lignin (ASL) amounts between SD and OD, since SD had a lower drying temperature (85°C) compared to OD (105°C). The EA product showed the highest peak abundance compared to other products, as expected, due to having low ash content.

4. Conclusions

It is possible to dry the SCW depolymerized black liquor without losing bio-oil yield. However, the drying technique affects the yields. Spray drying gave better bio-oil yields than the combination of oven drying and milling. The *fractionation method* was better than the drying methods when separating monomers at high pH. Biopolyol included in the DS-EA fraction yield was found 30% w/w more in DBL. Ash-free total ethyl acetate extracted bio-oil yield found as 77% w/w. Polyols existence in bio-oil enables the production of functionalized materials such as lubricants or polyurethanes by using this

fraction directly. This study shows continuous and fast HTL of BL could be a noteworthy option to upgrade traditional pulp & paper refineries in the future.

REFERENCES

[1] K. Maniatis, Black Liquor Gasification, 2007. https://www.ieabioenergy.com/wp-content/uploads/2013/10/Black-Liquor-Gasification-summary-and-conclusions3.pdf.

[2] J. Lappalainen, D. Baudouin, U. Hornung, J. Schuler, K. Melin, S. Bjelić, F. Vogel, J. Konttinen, T. Joronen, Sub- And supercritical water liquefaction of kraft lignin and black liquor derived lignin, Energies. 13 (2020) 3309. https://doi.org/10.3390/en13133309.

[3] F.R. Vieira, S. Magina, D. V. Evtuguin, A. Barros-Timmons, Lignin as a Renewable Building Block for Sustainable Polyurethanes, Materials (Basel). 15 (2022) 6182.

[4] S. Van Den Bosch, S.F. Koelewijn, T. Renders, G. Van den Bossche, T. Vangeel, W. Schutyser, B.F. Sels, Catalytic Strategies Towards Lignin - Derived Chemicals, Springer International Publishing, 2018. https://doi.org/10.1007/s41061-018-0214-3.

[5] F. Hernandez-Ramos, M.G. Alriols, T. Calvo-Correas, J. Labidi, E. Xabier, Renewable Biopolyols from Residual Aqueous Phase Resulting after Lignin Precipitation, ACS Sustain. Chem. Eng. 9 (2021) 3608–3615. https://doi.org/10.1021/acssuschemeng.0c09357.

[6] A. Orebom, J.J. Verendel, J.S.M. Samec, High Yields of Bio Oils from Hydrothermal Processing of Thin Black Liquor without the Use of Catalysts or Capping Agents, ACS Omega. 3 (2018) 6757–6763. https://doi.org/10.1021/acsomega.8b00854.

[7] Z. Sun, B. Fridrich, A. De Santi, S. Elangovan, K. Barta, Bright Side of Lignin Depolymerization: Toward New Platform Chemicals, Chem. Rev. 118 (2018) 614–678. https://doi.org/10.1021/acs.chemrev.7b00588.

[8] B.M. Upton, A.M. Kasko, Strategies for the conversion of lignin to high-value polymeric materials: Review and perspective, Chem. Rev. 116 (2016) 2275–2306. https://doi.org/10.1021/acs.chemrev.5b00345.

[9] H. Wang, Y. Pu, A. Ragauskas, B. Yang, From lignin to valuable products–strategies, challenges, and prospects, Bioresour. Technol. 271 (2019) 449–461.

https://doi.org/10.1016/j.biortech.2018.09.072.

[10] M. V. Galkin, J.S.M. Samec, Lignin Valorization through Catalytic Lignocellulose Fractionation: A Fundamental Platform for the Future Biorefinery, ChemSusChem. 9 (2016) 1544–1558. https://doi.org/10.1002/cssc.201600237.

[11] J. He, C. Zhao, D. Mei, J.A. Lercher, Mechanisms of selective cleavage of C-O bonds in di-aryl ethers in aqueous phase, J. Catal. 309 (2014) 280–290. https://doi.org/10.1016/j.jcat.2013.09.012.

[12] A.R. Mankar, A. Modak, K.K. Pant, Recent Advances in the Valorization of Lignin: A Key Focus on Pretreatment, Characterization, and Catalytic Depolymerization Strategies for Future Biorefineries, Adv. Sustain. Syst. 6 (2022) 1–25. https://doi.org/10.1002/adsu.202100299.

[13] L. Shuai, J. Sitison, S. Sadula, J. Ding, M.C. Thies, B. Saha, Selective C-C Bond Cleavage of Methylene-Linked Lignin Models and Kraft Lignin, ACS Catal. 8 (2018) 6507–6512. https://doi.org/10.1021/acscatal.8b00200.

[14] P.J. Deuss, M. Scott, F. Tran, N.J. Westwood, J.G. De Vries, K. Barta, Aromatic Monomers by in Situ Conversion of Reactive Intermediates in the Acid-Catalyzed Depolymerization of Lignin, J. Am. Chem. Soc. 137 (2015) 7456–7467. https://doi.org/10.1021/jacs.5b03693.

[15] T. Renders, W. Schutyser, S. Van Den Bosch, S.F. Koelewijn, T. Vangeel, C.M. Courtin, B.F. Sels, Influence of Acidic (H3PO4) and Alkaline (NaOH) Additives on the Catalytic Reductive Fractionation of Lignocellulose, ACS Catal. 6 (2016) 2055–2066. https://doi.org/10.1021/acscatal.5b02906.

[16] L. Shuai, M.T. Amiri, Y.M. Questell-Santiago, F. Heroguel, Y. Li, H. Kim, R. Meilan, C. Chapple, J. Ralph, J.S. Luterbacher, Formaldehyde stabilization facilitates lignin monomer production during biomass depolymerization, Science (80-.). 354 (2016) 329–334.

[17] H. Wang, H. Ruan, M. Feng, Y. Qin, H. Job, L. Luo, C. Wang, M.H. Engelhard, E. Kuhn, X. Chen, M.P. Tucker, B. Yang, One-Pot Process for Hydrodeoxygenation of Lignin to Alkanes Using Ru-Based Bimetallic and Bifunctional Catalysts Supported on Zeolite Y, ChemSusChem. 10 (2017) 1846–1856.

https://doi.org/10.1002/cssc.201700160.

[18] M. Fache, B. Boutevin, S. Caillol, Vanillin Production from Lignin and Its Use as a Renewable Chemical, ACS Sustain. Chem. Eng. 4 (2016) 35–46. https://doi.org/10.1021/acssuschemeng.5b01344.

[19] T. Voitl, P.R. Von Rohr, Oxidation of lignin using aqueous polyoxometalates in the presence of alcohols, ChemSusChem. 1 (2008) 763–769. https://doi.org/10.1002/cssc.200800050.

[20] A.K. Deepa, P.L. Dhepe, Lignin Depolymerization into Aromatic Monomers over Solid Acid Catalysts, ACS Catal. 5 (2015) 365–379. https://doi.org/10.1021/cs501371q.

[21] X. Erdocia, R. Prado, M.Á. Corcuera, J. Labidi, Base catalyzed depolymerization of lignin: Influence of organosolv lignin nature, Biomass and Bioenergy. 66 (2014) 379–386. https://doi.org/10.1016/j.biombioe.2014.03.021.

[22] P.J. Deuss, C.S. Lancefield, A. Narani, J.G. De Vries, N.J. Westwood, K. Barta, Phenolic acetals from lignins of varying compositions: Via iron(iii) triflate catalysed depolymerisation, Green Chem. 19 (2017) 2774–2782. https://doi.org/10.1039/c7gc00195a.

[23] T. Yokoyama, Revisiting the mechanism of β-O-4 bond cleavage during acidolysis of lignin. Part 6: A review, J. Wood Chem. Technol. 35 (2014) 27–42. https://doi.org/10.1080/02773813.2014.881375.

[24] X. Huang, T.I. Korányi, M.D. Boot, E.J.M. Hensen, Catalytic depolymerization of lignin in supercritical ethanol, ChemSusChem. 7 (2014) 2276–2288. https://doi.org/10.1002/cssc.201402094.

[25] J.Y. Kim, J. Park, U.J. Kim, J.W. Choi, Conversion of Lignin to Phenol-Rich Oil Fraction under Supercritical Alcohols in the Presence of Metal Catalysts, Energy and Fuels. 29 (2015) 5154–5163. https://doi.org/10.1021/acs.energyfuels.5b01055.

[26] W. Schutyser, T. Renders, S. Van Den Bosch, S.F. Koelewijn, G.T. Beckham, B.F. Sels, Chemicals from lignin: An interplay of lignocellulose fractionation, depolymerisation, and upgrading, Chem. Soc. Rev. 47 (2018) 852–908.

https://doi.org/10.1039/c7cs00566k.

[27] C. Cao, L. Xu, Y. He, L. Guo, H. Jin, Z. Huo, High-Efficiency Gasification of Wheat Straw Black Liquor in Supercritical Water at High Temperatures for Hydrogen Production, Energy and Fuels. 31 (2017) 3970–3978. https://doi.org/10.1021/acs.energyfuels.6b03002.

[28] D.A. Cantero, M.D. Bermejo, M.J. Cocero, Reaction engineering for process intensification of supercritical water biomass refining, J. Supercrit. Fluids. 96 (2015) 21–35. https://doi.org/10.1016/j.supflu.2014.07.003.

[29] C.M. Martínez, T. Adamovic, D.A. Cantero, M.J. Cocero, Scaling up the production of sugars from agricultural biomass by ultrafast hydrolysis in supercritical water, J. Supercrit. Fluids. 143 (2019) 242–250. https://doi.org/10.1016/j.supflu.2018.08.017.

[30] E.G. Mission, M.J. Cocero, Accessing suberin from cork via ultrafast supercritical hydrolysis, Green Chem. 24 (2022) 8393–8405. https://doi.org/10.1039/d2gc02498e.

[31] T. Adamovic, D. Tarasov, E. Demirkaya, M. Balakshin, M.J. Cocero, A feasibility study on green biorefinery of high lignin content agro-food industry waste through supercritical water treatment, J. Clean. Prod. 323 (2021). https://doi.org/10.1016/j.jclepro.2021.129110.

[32] A. Sluiter, B. Hames, D. Hyman, C. Payne, R. Ruiz, C. Scarlata, J. Sluiter, D. Templeton, J.W. Nrel, Determination of total solids in biomass and total dissolved solids in liquid process samples, 2008.

[33] T. Adamovic, X. Zhu, E. Perez, M. Balakshin, M.J. Cocero, Understanding sulfonated kraft lignin re-polymerization by ultrafast reactions in supercritical water, J. Supercrit. Fluids. 191 (2022). https://doi.org/10.1016/j.supflu.2022.105768.

[34] B. Hames, R. Ruiz, C. Scarlata, a Sluiter, J. Sluiter, D. Templeton, Preparation of Samples for Compositional Analysis Laboratory Analytical Procedure (LAP). Tech. Rep. NREL/TP-510-42620., Natl. Renew. Energy Lab. (2008) 1–9.

[35] A. Sluiter, B. Hames, R. Ruiz, C. Scarlata, J. Sluiter, D. Templeton, Determination

of Sugars , Byproducts , and Degradation Products in Liquid Fraction Process Samples Laboratory Analytical Procedure (LAP) Issue Date : 12 / 08 / 2006 Determination of Sugars , Byproducts , and Degradation Products in Liquid Fraction Proce, (2008).

[36] A. Sluiter, B. Hames, R. Ruiz, C. Scarlata, J. Sluiter, D. Templeton, Determination of ash in biomass. NREL Laboratory Analytical Procedure (LAP), Natl. Renew. Energy Lab. (2008) 18. http://www.nrel.gov/docs/gen/fy08/42622.pdf.

[37] N. Abad-Fernández, E. Pérez, M.J. Cocero, Aromatics from lignin through ultrafast reactions in water, Green Chem. 21 (2019) 1351–1360. https://doi.org/10.1039/c8gc03989e.

[38] D.A.I. Goring, The physical chemistry of lignin, Pure Appl. Chem. 5 (1962) 233–310. https://doi.org/10.1351/pac196205010233.

[39] T. Lindströmn, The colloidal behaviour of kraft lignin - Part I.: Association and gelation of kraft lignin in aqueous solutions, Colloid Polym. Sci. 257 (1979) 277–285. https://doi.org/10.1007/BF01382370.

[40] A. Rezanowich, D.A.I. Goring, Polyelectrolyte expansion of a lignin sulfonate microgel, J. Colloid Sci. 15 (1960) 452–471. https://doi.org/10.1016/0095-8522(60)90049-0.

[41] M. Norgren, B. Lindström, Dissociation of phenolic groups in kraft lignin at elevated temperatures, Holzforschung. 54 (2000) 519–527. https://doi.org/10.1515/HF.2000.088.

[42] M. Norgren, H. Edlund, L. Wågberg, B. Lindström, G. Annergren, Aggregation of kraft lignin derivatives under conditions relevant to the process, part I: phase behaviour, Colloids Surfaces A Physicochem. Eng. Asp. 194 (2001) 85–96. https://doi.org/10.1016/S0927-7757(01)00753-1.

[43] E. Pérez, N. Abad-Fernández, T. Lourençon, M. Balakshin, H. Sixta, M.J. Cocero, Base-catalysed depolymerization of lignins in supercritical water: Influence of lignin nature and valorisation of pulping and biorefinery by-products, Biomass and Bioenergy. 163 (2022). https://doi.org/10.1016/j.biombioe.2022.106536.

[44] A.M. Borrero-López, F.J. Santiago-Medina, C. Valencia, M.E. Eugenio, R. Martin-

Sampedro, J.M. Franco, Valorization of kraft lignin as thickener in castor oil for lubricant applications, J. Renew. Mater. 6 (2018) 347–361. https://doi.org/10.7569/JRM.2017.634160.

[45] Y. Li, X. Luo, S. Hu, Bio-based Polyols and Polyurethanes, SPRINGER BRIEFS IN MOLECULAR SCIENCE, 2015.

[46] E. Pérez, C.O. Tuck, Quantitative analysis of products from lignin depolymerisation in high- temperature water, Eur. Polym. J. 99 (2018) 38–48. https://doi.org/10.1016/j.eurpolymj.2017.11.053.

[47] M. Kienberger, S. Maitz, T. Pichler, P. Demmelmayer, Systematic review on isolation processes for technical lignin, Processes. 9 (2021). https://doi.org/10.3390/pr9050804.

[48] C. Girometta, D. Dondi, R.M. Baiguera, F. Bracco, D.S. Branciforti, S. Buratti, S. Lazzaroni, E. Savino, Characterization of mycelia from wood-decay species by TGA and IR spectroscopy, Cellulose. 27 (2020) 6133–6148. https://doi.org/10.1007/s10570-020-03208-4.

[49] M.M. Jensen, D.T. Djajadi, C. Torri, H.B. Rasmussen, R.B. Madsen, E. Venturini, I. Vassura, J. Becker, B.B. Iversen, A.S. Meyer, H. Jørgensen, D. Fabbri, M. Glasius, Hydrothermal Liquefaction of Enzymatic Hydrolysis Lignin: Biomass Pretreatment Severity Affects Lignin Valorization, ACS Sustain. Chem. Eng. 6 (2018) 5940–5949. https://doi.org/10.1021/acssuschemeng.7b04338.

[50] G. Gea, M.B. Murillo, J. Arauzo, Thermal degradation of alkaline black liquor from straw. Thermogravimetric study, Ind. Eng. Chem. Res. 41 (2002) 4714–4721. https://doi.org/10.1021/ie020283z.

[51] O. Gordobil, R. Herrera, F. Poohphajai, J. Sandak, A. Sandak, Impact of drying process on kraft lignin: Lignin-water interaction mechanism study by 2D NIR correlation spectroscopy, J. Mater. Res. Technol. 12 (2021) 159–169. https://doi.org/10.1016/j.jmrt.2021.02.080.

CHAPTER II

Product development:

Bio-lubricant production

using selected depolymerized

black liquor products

Abstract

According to the International Energy Agency, the paper and pulp industry reportedly produces about 170 million tons of black liquor annually. However, it is worth noting the scarcity of studies focusing on the direct utilization of black liquor. Consequently, the development of techniques to revalorize black liquor has become a significant challenge in the research field. Furthermore, the lubricant industry has been incorporating vegetable oils and their derivatives to synthesize eco-friendly lubricants and is demanding effective environmentally friendly thickeners to formulate semi-solid lubricants from them. In this framework, this study aims to revalorize weak black liquor through supercritical water hydrolysis, opening up a new line of research for the production of semi-solid bio-lubricants. To achieve this, original black liquor subjected to supercritical water depolymerization, and downstream processing, and four different fractions (spray-drying, oven-drying, and ethyl acetate extraction) were obtained. These fractions subsequently added to epoxy-modified vegetable oils to create sustainable lubricant formulations. Their rheological and tribological properties were then evaluated. The results indicate that the formulated castor oil-based biolubricants not only exhibited suitable stability and appearance but also demonstrated noteworthy rheological and tribological performances. This highlights the feasibility of depolymerization to valorize black liquor, with the resulting lignin fractions improving the lubricity of castor oil-based formulations.

1. Introduction

The pulp & paper industry is the dominant supplier of lignin and is unlikely to be overtaken by modern lignin-based biorefineries and start-ups in the near future. Kraft pulping process sustains its predominant position among other pulping processes by producing more than 90% of all chemical pulps [1]. According to the International Energy Agency (IEA), the paper and pulp industry produces around 170 million tons of black liquor (dry basis) annually, while this number is between 50-70 million tons for lignin [2]. This material is mostly burnt in energy recovery boilers or used for kraft lignin production. Great and centralized availability of black liquor brings an opportunity to find cost-effective valorization techniques to generate valuable bio-based products.

Despite the vast number of studies on lignin depolymerization and its applications, there are only few studies that directly use black liquor [1]. Considering lignin as an aromatic biopolymer in black liquor can lead to remarkable advancements in both literature and industry. The lignin fraction from black liquor is a promising aromatic feedstock to make different types of materials, such as lubricant or polyurethane. [3–5]. Some studies also covered the use of lignin or modified lignin from hardwood or softwood and obtained a polyol-rich fraction that can be used to create different types of materials [6,7]. The lignin used in these studies is generally a solid made from acidification of black liquor [8], modified lignin [9], or depolymerized [10,11]. One approach to generate polyols from black liquor is the continuous hydrothermal depolymerization. This technology offers several advantages like the use of inexpensive and safe solvents, and the direct treatment of black liquor [12–14]. Hence, a custom-designed continuous hydrothermal depolymerization pilot plant was developed in the PressTech Group to carry out rapid reactions (<1 sec) [15]. The device allows precise control of the reaction time that prevents side reactions that could lead to repolymerization. Supercritical water was selected as reacting medium since it is abundant, low-cost, and environmentally friendly [16]. A rapid depolymerization of lignin is a result of the combination of multiple factors, such as unique set of properties for supercritical water, a process design with instantaneous heating and cooling, and enhanced reaction kinetics and mass transfer [17].

The use of polyols derived from biomass has proven advantages in the production of biobased compounds [18,19]. These materials are alternatives to petroleum-derived substances in different applications like: coatings, lubricants, emulsions, or bioplastics,

among others [20–23]. A growing application is the substitution of mineral or synthetic oils with vegetable oils or their derivatives for lubricants production [24,25]. However, the use of vegetable oils as lubricating oils may need the inclusion of additives or the implementation of chemical modifications to enhance the lubricating performance [26]. This is crucial when oil structuring is required to obtain semi-solid lubricants. For instance, sustainable lubricant formulations were previously developed by promoting the chemical crosslinking of vegetable oils and biopolymers (as a source of polyols) [27,28]. The use of epoxides that react with active hydrogen atom-containing compounds via nucleophilic attack is a promising strategy. Two different approaches concerning epoxidation have showcased suitable outcomes for synthesizing ecofriendly lubricant compositions. The first one includes the epoxidation of hydroxyl groups found in lignocellulose with di- or tri-functional epoxides, followed by the reaction with castor oil [4]. The second one entails the epoxidation of the double bonds of vegetable oil glycerides and subsequent reaction with lignocellulose hydroxyl groups [29]. The rheological properties of both materials are different despite achieving well-structured crosslinked networks in both scenarios. Thus, the dispersion of epoxy-modified lignocellulosic material into castor oil, leads to the formation of highly structured systems that generally exhibit gel-like responses [4]. On the contrary, a wider range of rheological properties ranging from Newtonian to non-Newtonian viscoelastic liquids can be achieved by epoxidizing castor oil and subsequent dispersion of lignocellulosic materials, basically by controlling the epoxidation degree [29].

This study focuses on achieving sustainable lubricant formulations by adding depolymerized fractions of black liquor (as a biopolyol) to epoxidized vegetable oil. To the best of our knowledge, this is the first time that black liquor depolymerization, fractionation, and upgrading is employed to produce semi-solid bio-lubricants. The present work demonstrates a new pathway to produce consumer-ready products, besides investigating the influence of the black liquor depolymerization treatment on the rheological and tribological properties of resulting bio-lubricants.

2. Materials and methods

2.1. Materials

Black Liquor was procured from ENCE wood pulping factory (Pontevedra, Spain). Refined castor oil was supplied by Import-quimia, S.L. (Guipuzkoa, Spain). The main physico-chemical properties of castor oil and its fatty acid composition can be found in

Annex II. The reagents used for the epoxidation reaction of castor oil were hydrogen peroxide (30% w/w), glacial acetic acid (99.7% w/w), and phosphoric acid (≥85% w/w). The reagents and solvents were purchased at Merck Sigma-Aldrich (Darmstadt, Germany) and used without further modification.

2.2. Supercritical Water Hydrolysis Unit

Black liquor was treated with supercritical water in continuous reactors at very short reaction times [30]. The device allows the operator to pump the feedstock suspended in water without any preheating, which prevents side reactions during the heating stage. Briefly, water is pumped through an in-line heater that increase the fluid temperature up to supercritical conditions. The hot water stream is then mixed with the cold feedstock in a T-junction, which is the beginning of the reactor. The reaction starts as soon as these two streams are mixed. The reactor is made of stainless-steel tube (SS 316) and works as plug-flow type. The pressure of the reactor is controlled by using a needle valve manually actuated by the operator. The pressure drop in the system is around 250 bar before and after the valve. That sudden depressurization promotes the production of vapor, which provides instantaneous cooling of the product stream. The temperature and pressure suddenly decrease from supercritical water conditions to about 150 ± 10 °C, and 5 ± 2 bar at the reactor outlet. This temperature is low enough to prevent lignin side reactions. After that, the product stream is cooled down to room temperature by a chiller. The hydrothermal treatment of black liquor was done at 385 ± 1 °C and 260 ± 5 bar, whereas the reaction times were between 0.36 and 0.40s. The system was operated continuously for 60 minutes to generate the samples. The black liquor slurry concentration in the was 20 wt.% of total solids. The slurry and supercritical water (SCW) flows were set to 7.5 kg/h and 15 kg/h, respectively.

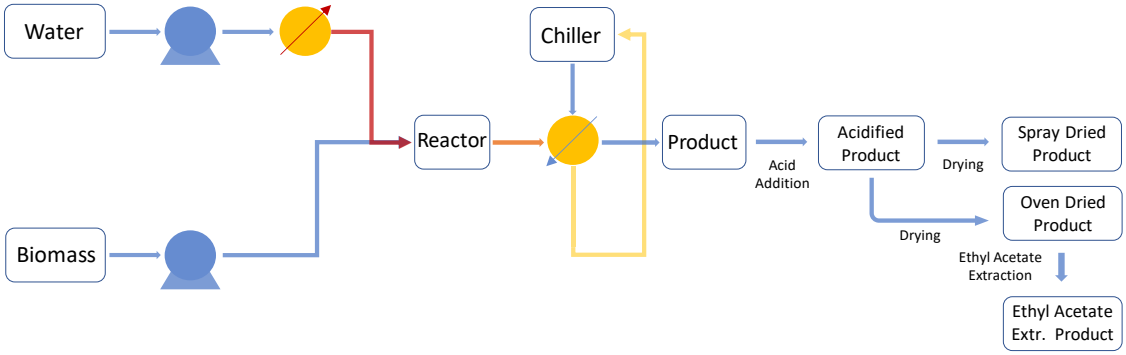

Figure 1. Supercritical water depolymerization unit and downstream separation basic flow diagram.

2.3. Refining of Hydrothermal Products

Four black liquor samples were created to assess their potential as oil structuring agents for lubricant applications. The Black Liquor (BL) sample was obtained directly from a traditional pulp and paper mill and it was used in this research as feedstock for hydrothermal treatment. The Spray Dried (SD) sample was obtained from drying the acidified (pH=2) hydrolyzed black liquor (HBL) from the SCW hydrolysis. This fraction was spray dried without further treatment. Spray drying was carried out using a mobile minor spray dryer with rotary atomizer supplied by Gea Niro. The acidified HBL sample was pumped using a peristaltic pump (Watson-Marlow 520) with a flow rate of 1.5 kg/h. The inlet air temperature was 160°C and the product outlet temperature was approximately 85-90°C. The pressure supply of compressed air to the dryer nozzle was 6 bar [31]. The Oven Dried (OD) sample was obtained similarly to the SD but changing the drying method. The oven drying was carried out at 100 °C and the fraction was then ball milled to reduce particle size. The Ethyl Acetate Extracted (EA) sample was obtained by subjecting the OD sample to extraction with ethyl acetate. After extraction, the ethyl acetate was evaporated, and the EA sample was ground. The reasons for selecting these products were to check the effects of inorganic matter and drying methods on the bio-lubricant properties.

2.4. Castor Oil Epoxidation

The characteristics of the castor oil that was used in this study can be found in Tables S1 and S2. The refined castor oil was chemically modified according to the procedure outlined in a previous study [29]. In brief, castor oil was initially brought into contact with glacial acetic and phosphoric acid in a round-bottom flask fitted with a thermometer, a reflux condenser, and a dropping funnel. Upon heating the reagents mixture to 70 ºC, a

specific amount of H2O2 was dropwise added, maintaining the molar ratio of C=C/acetic acid/H2O2 of 1/0.77/24.4 (see mass proportions in Table 1). The epoxidation reaction was run for 4 hours under agitation (700 rpm). After completion of the reaction procedure, the resulting solid product was filtered, washed with distilled water, and dried in a vacuum oven at 60 ºC overnight.

Table 1. Mass proportions of reagents used in the castor oil epoxidation reaction.

Epoxidized Castor Oil	Castor Oil (g)	CH_3COOH (g)	H_3PO_4 (g)	H_2O_2 (g)	Epoxy index (mol/kg) *
ECO	80.0	12.0	0.8	48.0	2.0

*Epoxy index determination as described elsewhere [29].

2.5. Dispersion of Black Liquor Samples in Epoxidized Castor Oil

Lignin dispersions in the epoxidized castor oil (ECO) were prepared according to the following two-step procedure. The black liquor and derived fractions were dispersed into ECO maintaining a 20:80 lignin fraction:ECO weight ratio (see codes applied in Table 2). The materials were mixed using a controlled-rotational speed mixing device (RW 20, Ika, Germany) fitted with an anchor impeller (60-70 rpm) for 24 hours at room conditions to promote the chemical interaction between the lignocellulosic fraction and ECO. Afterwards, the ensuing intermediate product was left for curing in a second stage for 2 h in a convection oven under static conditions and subsequently homogenized with the aid of an Ultra-Turrax turbine (Ika T-25, Germany) at a rate of 10000 rpm for 60 s. Resulting gel-like dispersions were stored at room temperatures and further characterized, at least, one month after preparation to ensure complete sample curing.

Table 2. Proportions used in lignin-structured epoxidized castor oil formulations.

Bio-lubricant nomenclature	ECO content (wt. %)	Lignin fraction	Content of lignin fraction (wt. %)
ECO_BL	80	BL	20
ECO_SD	80	SD	20
ECO_OD	80	OD	20
ECO_EA	80	EA	20

2.6. Analytical Techniques

Compositional characterization

The content of carbohydrates, acid soluble and insoluble lignin, moisture, and ash were determined using the National Renewable Energy Laboratory (NREL) Laboratory Analytical Procedure (LAP) [32–35]. The carbohydrates and their derivatives were analyzed by high pressure liquid chromatography (HPLC). A Shodex SH-1011 column was used with 0.01 N sulfuric acid as the mobile phase. The flow rate was 0.8 mL·min-1 and the column temperature was 60 °C. A Waters 2414 refractive index detector was used component detection. Samples for carbohydrate analysis were prepared according to the NREL protocol.

Characterization of Bioaromatics and Biopolyols

A fractionation method was applied to characterize low molecular weight compounds, such as aromatic monomers, biopolyols, and oligomers (mainly dimers and trimers) for BL and HBL. Sulfuric acid was added to HBL sample to lower the pH to 2 and precipitate larger lignin molecules. That material was centrifuged, and two fractions were obtained: dissolved solids (DS), and suspended solids (SS). The suspended solids fraction was further washed with pH 2 water to ensure that all DS was extracted from SS. The DS and SS fractions were then extracted separately with ethyl acetate. The ethyl acetate was recovered by evaporation in rotavapor. The ethyl acetate-extracted fractions were labelled as DS-EA and SS-EA. GC-MS characterization was applied to the DS-EA fraction to identify aromatic components.

Gas chromatography analyses were performed using an Agilent 7820 GC-MS with quadrupole mass spectrometer detector. A low bleed, non-polar capillary HP-5MS (Agilent, USA) column, 30 m x 0.250 mm x 0.25 µm was used for the analyses. Helium was used as the carrier gas. Biopolyol including monomers and oligomers were analyzed by using a derivatization method. Briefly, 10 mg·mL-1 lignin oil (LO) was dissolved in acetone, and then 10:1:2 (v:v:v) of the LO:pyridine:BSTFA mixture was heated at 45°C for 20 min before injection, using BSTFA (N,O-Bis(trimethylsilyl)trifluoroacetamide with 1% trimethylchlorosilane) as the silylating agent. The oven was started at 150°C, and increased at a rate of 4 °C·min-1 until 300°C, and held for 18 min. Trimethylsilyl (TMS) derivatized monomers determination was carried out with a 10:1 split ratio, solvent delay of 4 min and an oven start temperature of 80°C, while the determination of TMS-

derivatized oligomers was carried out with a 2.5:1 split ratio and a solvent delay of 15 min to avoid overloading the detectors with the monomers.

Elemental analysis

Elemental analysis of the black liquor and its depolymerized products was performed using a Leco CS-225 instrument. Carbon, hydrogen, nitrogen and sulfur contents were determined by this analysis. The ash analysis was also used in calculations to estimate the amount of oxygen by difference.

Hydroxyl groups analysis

The aliphatic hydroxyl groups were analyzed according to ASTM D4274 technique [36]. According to the literature, method B of this standard was followed. Each sample was subjected to a phthalation process in a pyridine:phthalic anhydride medium. The mixture was heated to 98 ± 2 ºC. After heating, a specific amount of pyridine was added, and the mixture was back-titrated with 1 N NaOH solution. Due to the dark color of the samples, the change in potential was read and recorded using a pH meter. In accordance with the test method, the OH number was determined as mg KOH/g sample and converted to mmol OH/g sample.

Phenolic hydroxyl groups were analyzed by the Folin-Ciocalteu method. For this analysis, the samples were dissolved in 0.01N NaOH medium. The method used to determine the phenolic content is a UV-Vis spectrophotometric method in which the absorbance at 765 nm is recorded by means of the blue color developed by the samples after incubation with the reagents for 2 hours at room temperature. The concentrations are calculated from a phenol calibration line.

Molecular weight distribution

Four samples were prepared for gel permeation chromatography to check the molecular weight distribution of the products. The samples were dried overnight in an oven at 50ºC to remove moisture prior to preparation. THF was used to dissolve the dried samples at 1 mg/mL concentrations. A Phenomenex Phenogel 5 µm GPC column with the dimensions of 300 x 7.8 mm was used for the analysis. A Hewlett Packard 1100 series autosampler injected 25 µL injection volumes from each sample. The column temperature was kept constant at 26 ºC. THF was used as the carrier solvent at a flow rate of 1 mL·min-1. UV diode array detector at a wavelength of 220 nm with a reference wavelength of 360 nm and a slit width of 4 nm was used to analyze the samples. A

calibration curve was established between molecular weight and the residence time using PSS low molecular polystyrene ReadyCal set M(p) 266-66000. The UV response and residence time data were correlated with the calibration curve, and used to calculate Mw, Mn, and Mz.

Rheological characterization

Dispersions of black liquor and derived fractions in ECO were subjected to rheological characterization at 25ºC in a controlled-stress Rheoscope (Thermo Haake, Germany) rheometer. Grooved 20 mm-diameter parallel plates geometry (1 mm gap) was selected to prevent wall slip phenomena. Steady-state viscous flow tests were carried out in the shear rate range from 0.01 up to 100 s-1. In addition, small-amplitude oscillatory shear (SAOS) tests were also conducted in the frequency range from 0.03-100 rad·s-1 within the linear viscoelastic region, previously determined in stress sweep experiments performed at 1 Hz. All rheological results are reported as the average of at least two replicates.

Tribological characterization

Aiming to test the different dispersions of black liquor fractions in ECO as potential bio-lubricants, tribological experiments were carried out at 25 ºC using a tribological cell coupled to a Physica MCR 501 controlled-stress rheometer (Anton Paar, Graz, Austria) fitted with a ball-on-three-plates friction pair. As detailed elsewhere [37], this experimental arrangement comprises a lower geometry holding three 45°-inclined steel plates (1.4301 AISI 304) and an upper measuring tool coupled with a 12.7 mm diameter polished bearing ball (1.4401 grade 100 AISI 316). The ball was fixed to the upper geometry to prevent likely rolling and slides in the tribological contact. This configuration enabled the evaluation of the friction coefficient (μ), defined as the ratio between the applied normal force (FN) and monitored friction force (FF). All the samples were submitted to sliding speed sweep tests from 0-1000 rpm by applying 20 N normal force to obtain their characteristic Stribeck diagrams. Afterward, transient friction measurements were conducted at 20 N for approximately 10 min, at a given rotational speed within the mixed friction lubrication region, which were determined from the Stribeck curves. Each tribological measurement was replicated at least six times on fresh samples. After performing the transient friction tests, at constant rotational speed, the area of the ensuing wear tracks located on the plates were examined by using an

Olympus System Microscope BX52 (Japan) coupled with a Digital Camera C5050Z (4x and 10x magnification objectives). Reported areas are an average of three replicates.

3. Results and discussion

3.1. Extraction and characterization of lignin fractions

The chemical compositions of the black liquor and hydrolyzed black liquor can be seen in Table 3. The ash content of the black liquor is 49 wt.% on a dry basis. According to the procedures that were described in section 2.3, OD and SD samples include the acid added during the precipitation. For this reason, the ash contents of OD and SD are higher than BL. On the contrary, EA sample had a low amount of ash (viz. 2.3 wt.%), and a higher total lignin content since it is the fraction that was extracted by ethyl acetate. The carbohydrate content of the samples was less than 1% by weight in all cases.

Table 3. Composition in weight percentage (%) of the different lignin fractions.

Designation	Acid Insoluble Lignin	Acid Soluble Lignin	Total Lignin	Ash	Carbs.
BL	21.0	12.3	33.3	49.0	<1
SD	18.3	9.8	28.1	60.7	<1
OD	23.5	6.2	29.7	59.8	<1
EA	50.9	18.8	69.7	2.3	<1

The results of the elemental analysis can be found in Table S3. The atomic ratios of hydrogen to carbon, and oxygen to carbon were calculated and presented in a Van Krevelen diagram in Figure 2. Black liquor shows a higher H:C ratio compared to the hydrolyzed products of SCW. The difference between BL and HBL products indicates that demethylation occurred during the SCW hydrolysis and subsequent refining processes. Although there is a decrease in the H:C ratio, which normally indicates the presence of dehydration reactions [14], the increase in the O:C ratio suggests demethylation overall. SD has a higher O:C ratio than OD, and EA has the highest O:C ratio. This is an indication of increased aromaticity after the SCW process of BL. Gaseous products were possibly formed during the acidification of HBL. CO_2, H_2S, and methanethiol are known to occur during the acidification of black liquor [38]. It is therefore probable that these gases played a role in the decrease of the H:C ratio and an increase in the O:C ratio.

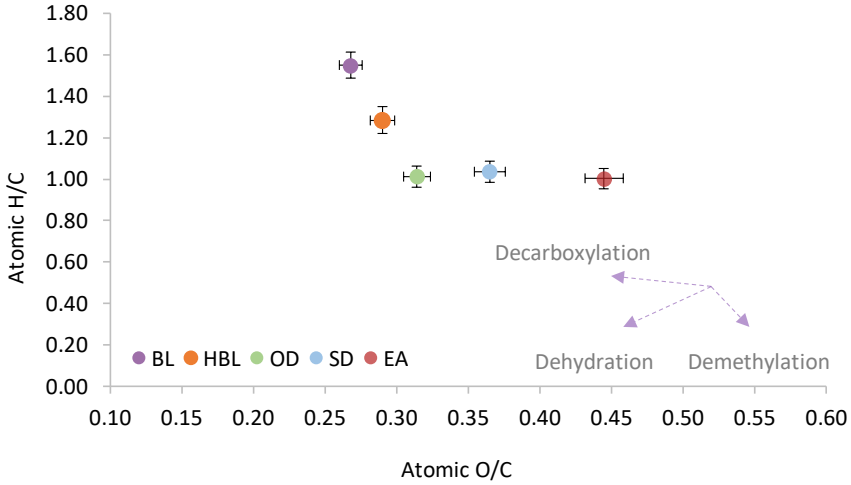

Figure 2. Van Krevelen diagram of the raw material and the depolymerized products.

The chemical composition of biopolyols including monomers and oligomers was determined using GC-MS. The chromatograms are shown in Figure 3 and Figure 4. The chromatograms were observed by applying two different methods. Figure 3 shows the monomer focused GC-MS method results, while Figure 4 demonstrates the output of the oligomer focused GC-MS method as it was mentioned in section 2.6. In Figure 3, the compounds detected up to the first 15 min of the residence time (RT) were mainly responsible for the carbohydrate-derived compounds (Region 1). Compared to the HBL sample, BL has larger intensity and area, which means that simple carbohydrate-derived compounds were consumed during SCW treatment. This indicates that decarboxylation occurs during the process. A recent study also emphasizes the presence of decarboxylation reactions during rapid SCW process [30]. On the other hand, monomeric compounds of lignin can be seen between the residence times of 15-40 min (Region 2) (Figure 3). In comparison to the BL sample, HBL sample has much higher intensity and area. This region includes mutual identified monomers for both BL and HBL samples such as, guaiacol, catechol, syringol, vanillin, acetovanillone, syringaldehyde, and acetosyringone. These monomeric compounds were also observed in other studies [13,14,39]. The total area of peaks in this region was found 75% higher than BL. GC-MS analysis showed that this region includes aldehyde and ketone groups like the structures of ArOH, ArOR, ArCHO, ArCOR, and particularly the presence of methoxy and hydroxyl groups. The aromatic monomers and some of the main peaks are summarized in Table 4. Increased abundance of these substructures in HBL products after depolymerization process proves the raise of the methoxy and hydroxyl group compounds. The molecular weight of this region was found to be in the range ~120-300 Da. It is possible that some

of these compounds were formed by the compounds detected after 40 min of the residence time.

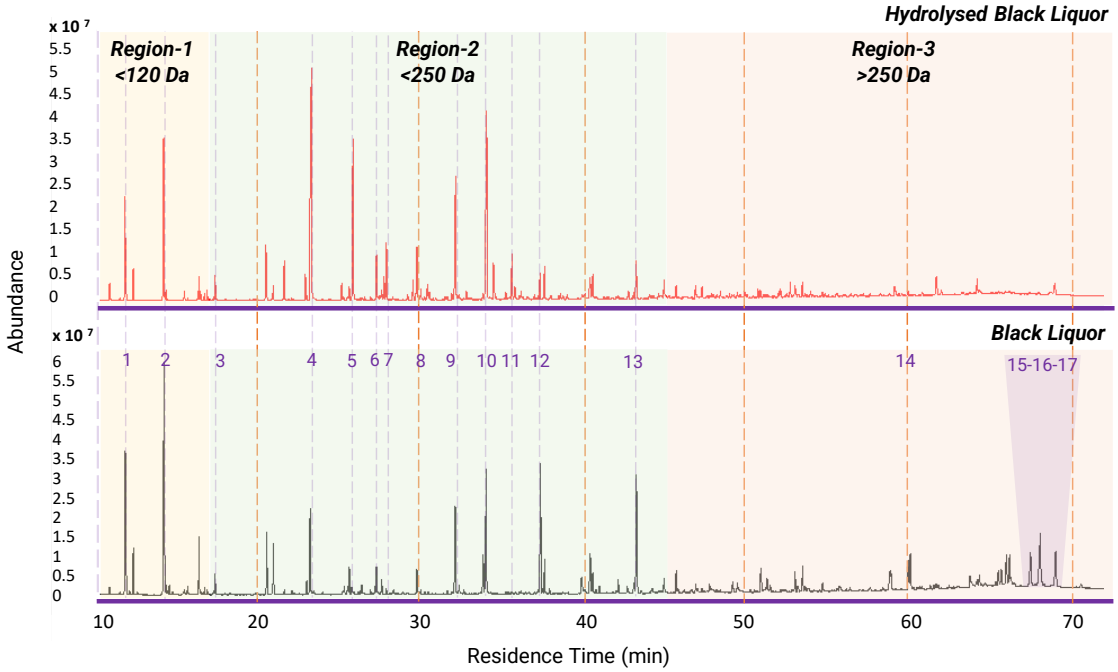

Figure 3. GC-MS chromatograms of Dissolved Solids Ethyl Acetate extracted fraction by using a derivatization method. Obtained by using monomer focused method.

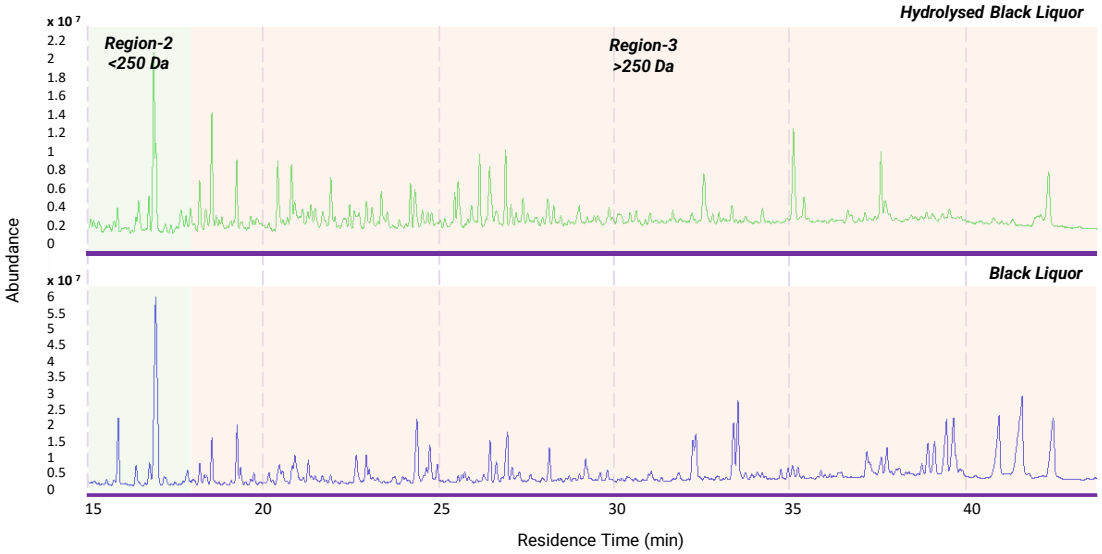

Figure 4. GC-MS chromatograms of Dissolved Solids Ethyl Acetate extracted fraction by using a derivatization method. Obtained by using oligomer focused method.

It was difficult to identify the exact composition of the compounds after 40 min of residence time. However, as the resolution was very low in monomer focused method,

this region better examined using oligomer focused method bypassing the detector overload with the monomers. Figure 4 chromatograms consisted of polyphenols, stilbenoids, terpenes, flavonoids, hydroxy naphtoquinones, resinols, and plant hormones (phytoestrogen, phytoandrogen, phytosterol, etc.) were existed which can be generalized as oligomers and have typical molecular weight of more than 250-350 Da. Although, some of the familiar structures that consists within the lignin, such as resinol (β- β), phenylcoumaran (β-5), dibenzodioxocin (5-5) and spirodienone (β -1) were tracked, exact compositions require deeper analysis like NMR [40]. The total area calculated for HBL sample in this region was about 3.5 times less than the BL sample, which states the existence of the depolymerization reactions took place. To summarize, GC-MS analysis demonstrated the occurrence of decarboxylation, increment of methoxy and hydroxyl groups, and depolymerization reactions. However, even though these happened in a smaller scale, in the big picture elemental analysis verifies the demethylation took place. The major compounds (mainly >1% of total area) identified using GC-MS were summarized in Tables S5 and S6.

Table 4. Some of the major structures identified and corresponding area percentages in black liquor and hydrolyzed black liquor using monomer focused GC-MS method – peaks can be found in Figure 3.

Region	*Peak #*	*Avg. Retention Time (min)*	*Compound Name*	*Area % in BL*	*Area % In HBL*
Region_1	*1*	*12.05*	*lactic acid*	*6.47*	*3.30*
	2	*14.45*	*2-hydroxybutyric acid*	*13.87*	*6.08*
Region_2	*3*	*17.55*	*guaiacol*	*0.82*	*0.98*
	4	*20.72*	*catechol*	*2.40*	*2.61*
	5	*23.36*	*syringol*	*3.70*	*16.00*
	6	*27.43*	*vanillin*	*1.31*	*1.86*
	7	*29.91*	*acetovanillone*	*1.24*	*2.38*
	8	*32.25*	*syringaldehyde*	*4.11*	*6.03*
	9	*33.95*	*vanillic acid*	*2.09*	*0.31*
	10	*34.15*	*acetosyringone*	*6.72*	*10.28*
	11	*35.71*	*homovanillic acid*	*n.d.*	*1.68*
	12	*37.47*	*syringic acid*	*6.09*	*0.96*
	13	*43.33*	*gallic acid*	*6.55*	*2.03*
Region_3	*14*	*60.10*	*tocopherol (β-carotene) derivative*	*1.82*	*n.d.*
	15	*67.46*	*medioresinol*	*2.58*	*n.d.*
	16	*68.06*	*phytosterol derivative*	*4.47*	*n.d.*
	17	*69.01*	*syringaresinol*	*2.84*	*0.37*

Due to the presence of polyphenols and high Mw biopolyols which are not possible to identify by GC-MS, gel permeation chromatography and hydroxyl groups determination were carried out to have a better understanding the characteristics of these molecules. The molecular weight distribution of the biopolyol containing samples was analyzed to determine the number average molecular weight (Mn), weight average molecular weight (Mw), z-average molecular weight (Mz) and polydispersity index (PDI). The corresponding values can be seen in Table 5.

Table 5. Peak maxima (min), Mn (g/mol), Mw (g/mol), Mz (g/mol), and PDI values of the black liquor and its depolymerized products.

Sample	Peak Maxima (min)	M_n (g/mol)	M_w (g/mol)	M_z (g/mol)	PDI
BL	10.690	1461	2002	2547	1.371
SD	11.227	1004	1485	1997	1.478
OD	11.181	1069	1598	2162	1.495
EA	11.129	1207	1522	2262	1.261

The BL had the highest average molecular weight (2002 g/mol), and this value is in the range of the kraft lignin Mw in different types of black liquor according to the previous reports [41–43]. The observed peak height sequence was SD > OD > EA > BL. In contrast, the average molecular weight sequence was BL < OD < EA < SD. Although sample EA was expected to have the lowest molecular weight (1522 g/mol), sample SD had a slightly lower molecular weight (1485 g/mol). TGA data of these samples were given in Figure S3 and Table S4. Thermogravimetric analysis (TGA) data indicated that sample EA underwent the most significant degradation of the samples in the temperature range of 120-550°C, where lignin degradation usually ends [44]. This would normally represent a lower molecular weight for sample EA. The EA sample exhibited three times greater intensity at the higher molecular weight peak compared to the other samples (Figure 5). This behavior can be explained by the fact that sample EA was obtained following the ethyl acetate extraction of sample OD, resulting in the transfer of the entire organic fraction from sample OD to sample EA, culminating in an approximate molecular weight of 1522 g/mol for sample EA. Sample SD, subjected to milder spray drying conditions, should theoretically contain a slightly higher amount of low molecular weight short chain aromatic compounds, resulting in an average molecular weight of 1485 g/mol. As

expected, the molecular weight of sample OD was slightly higher at 1598 g/mol compared to the other two samples.

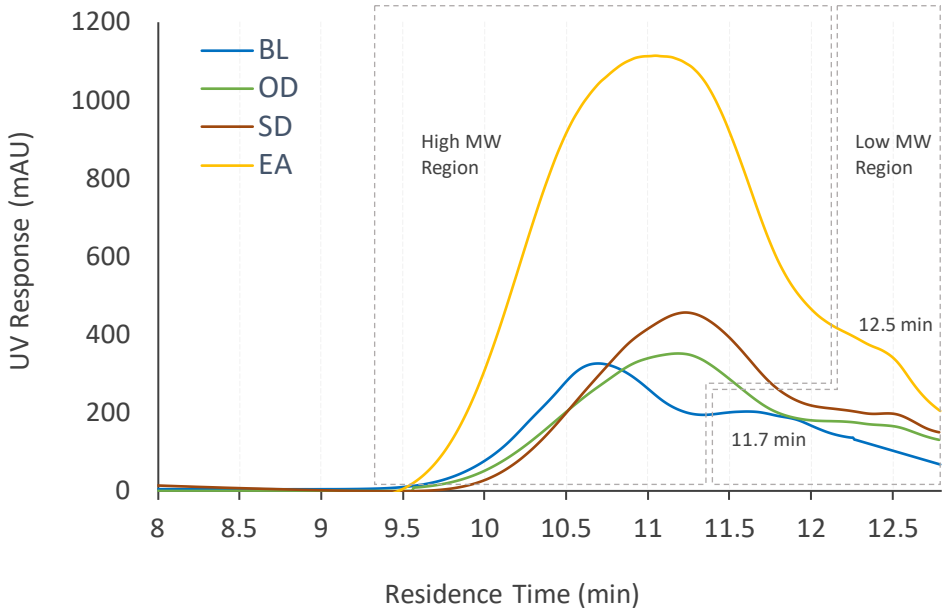

Figure 5. Molecular weight distribution of black liquor and its depolymerized products.

As it can be seen in Table 5, the polydispersity index values of all samples were similar. Sample EA had the lowest PDI at 1.261, while sample OD had the highest at 1.495. The PDI for sample BL was recorded as 1.371, reflecting a smaller difference between its high and low molecular weight regions compared to samples OD and SD. The low molecular weight region for sample BL produced a signal at 11.7 minutes (~937 g/mol) with an intensity about half of the main peak. On the other hand, the samples SD and OD had a much lower intensity at low molecular weight region (~432 g/mol) than their respective main peaks. Overall, the PDI values suggest a homogeneous molecular weight distribution, close to that of industrial polyethers and polyesters, which typically have PDIs of 1.05 and 1.3 respectively [45]. The molecular weights corresponding to the retention times of the signals at 937 g/mol (at 11.7 minutes) and 432 g/mol (at 12.5 minutes) imply that, in this region, samples SD and OD consist mainly of dimers and trimers, whereas sample BL consists mainly of trimers and larger oligomers. In summary, the molecular weights of all samples are in the range of 150-6500 g/mol, suitable for lubricant or polyurethane production [46]. Another notable point is the decrease in molecular weight of the depolymerized samples compared to BL. The GPC results support the previous discussion about oligomers depolymerization observed with the GC-MS results.

As it can be seen in Table 6, the content of aliphatic hydroxyl groups was quantified, and the following order was obtained SD > EA > OD > BL. Conversely, the aromatic hydroxyl group content was found to be in the order EA > OD > SD ≈ BL. These results differ significantly from those reported in the literature where biopolyols have been produced by liquefaction of lignin. For example, Briones et al. used agro-industrial residues and polyhydric alcohols, obtaining a range of ~7.04-10.45 mmol OH/g across different feedstocks [47]. Similarly, da Silva et al. used polyhydric alcohols and organic acids with kraft lignin and reported ~11.76 mmol OH/g [48].

Table 6. Aliphatic and Aromatic Hydroxyl Groups and Functionality of the black liquor and its depolymerized products.

	mmol OH/g	mmol OH/g	mmol OH/g
Sample	Aliphatic OH groups	Aromatic OH groups	Total OH groups
BL	0.00	1.08	1.08
SD	4.83	1.08	5.91
OD	0.93	1.56	2.49
EA	1.59	2.36	3.95

To the best of our knowledge, there is a void of hydrothermal treatment studies where biopolyol fractions have been obtained directly from the processing of alkali black liquor, which restricts direct comparison with the existing literature. The closest parallel is the study by Hernandez-Ramos et al. where they extracted biopolyols from organosolv black liquor using ultrasonication [6]. Though their monomer fraction lacked certain biopolyols, they isolated dimers, trimers, and oligomers rich in hydroxyl groups fractions from eucalyptus black liquor (~10.46 mmol OH/g) and pine organosolv black liquor (~11.02 mmol OH/g). To compare, the hydroxyl group content observed in this study is lower than that reported in the literature. However, it is important to note that the samples BL, OD and SD contain significant amounts of inorganic matter which contribute to the observed reduction in hydroxyl numbers.

The ASTM D4274 method is the most effective for samples with a higher proportion of aliphatic hydroxyl groups. Due to the significant aromatic components detected by GC-MS analysis, the total phenol content was also evaluated to estimate the amount of aromatic hydroxyl groups. According to the data presented in Table 6, the total hydroxyl

group content is in decreasing order SD > EA > OD > BL. These figures help to clarify the presence of increased number of OH reactive groups in each sample compared to sample BL. Even though the analysis of aromatic hydroxyl groups does not provide a direct measure of the abundance of OH reactive groups, it does provide a close approximation. Hence, by correlating molecular weight analysis with hydroxyl group data, we infer that all samples underwent rapid depolymerization under supercritical water conditions, fragmenting into smaller, more reactive components.

3.2. Dispersions of black liquor and derived fractions in ECO

As detailed in the experimental section, upon epoxidation, castor oil was structured by dispersing 20% w/w of the different lignin-rich fractions studied. In general terms, all lignin-structured ECO formulations exhibited long-term physical stability and showed a homogeneous appearance, which has been previously related to the chemical interaction between the epoxidized oil and lignin [29]. The viscous flow curves of the resulting dispersions are shown in Figure 6 in comparison with the lignin-free ECO sample. All lignin dispersions in ECO showed a shear-thinning behavior where the apparent viscosity decreased with the shear rate until reaching a high-shear rate-limiting viscosity. This rheological behavior has been previously found in traditional lithium soap-thickened lubricating greases modified with polymers [50], and can be suitably described by the Sisko model [51]:

$$\eta = \eta_{\infty} + K \cdot \dot{\gamma}^{n-1}$$

where η is the apparent viscosity, η∞ the high-shear rate-limiting viscosity, and K and n are the consistency and flow indexes, respectively. The lignin-free ECO sample also showed a shear-thinning flow characteristics in the whole shear rate range studied, although the tendency to reach a high-shear rate-limiting viscosity, η∞, was not observed in this case. Table 7 collects the values of the fitting parameters.

In principle, the highest viscosity modification should be expected when adding the most lignin-enriched fraction, i.e. EA, or those with a higher amount of available –OH groups, i.e. EA and SD (see Table 6), due to the more extensive chemical crosslinking that occurs between lignin hydroxyl groups and the generated epoxy rings in ECO. However, in the light of experimental data shown in Figure 6, ash content may exert an important effect on the ensuing flow properties acting as fillers. Therefore, the dispersion of BL, OD and SD fractions, whose ash content ranges from 49.0 to 60.7% (see Table 3), into ECO

yielded bio-lubricants with higher apparent viscosity values. Additionally, the lower average molecular weight in OD, SD and EA products as a consequence of SCW hydrolysis compared to BL (see Table 5), gave rise to ECO_BL having the higher viscosity, with a K value more than 30-fold higher than that of ECO.

Table 7. Sisko model fitting parameters for the dispersions of lignin fractions in epoxidized castor oil.

System	*K* (Pa·s^n)	*n*	η_∞ (Pa·s)	R^2
ECO (lignin-free)	46.5	0.692	-	0.996
ECO_BL	1502.4	0.020	22.0	0.977
ECO_SD	912.2	0.075	30.4	0.998
ECO_OD	490.9	0.047	31.0	0.993
ECO_EA	63.7	0.285	18.0	0.995

On the other hand, ECO_OD and ECO_SD lignin dispersions exhibited higher values of the high shear rate-limiting viscosity values (η∞), while extremely low values of the flow index were obtained in the three more structured samples, which were also typically found in traditional lubricating greases [52,53] and it is indicative of their characteristic yielding behavior [54].

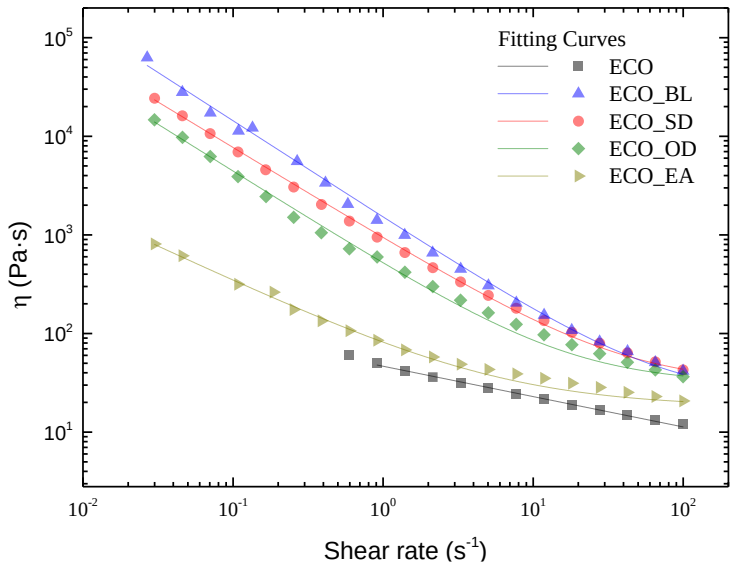

Figure 6. Evolution of the apparent viscosity with shear rate for the dispersions of lignin fractions in epoxidized castor oil.

As stated in previous lines, there must be a synergistic thickening effect of different variables such as the ash content, the molecular weight (Mw), the PDI and the total amount of available hydroxyl groups. These parameters would contribute differently to the enhancement of the apparent viscosity with respect to ECO in this order: ECO_BL > ECO_SD > ECO_OD (Figure 6), depending on the composition of the different residual lignin fractions, To better understand the effect of these different individual parameters on the viscous flow behavior of lignin dispersions, an analysis based on the correlation between the normalized values of the consistency index and a power function of these variables (also normalized respecting the maximum values) was made, and the predicted K values were plotted against the experimental K values, as shown in Figure S5. According to the obtained regression coefficient, R2= 0.992, a proper correlation among the experimental and predicted K values was achieved (see Figure S5), with different weights of each variable reflected in the exponents of the power series. As reflected by the power exponents, all these variables exert a positive influence over the K values, except for the PDI, which showed an inverse relationship (see Table S8), being PDI and the molecular weight the most influencing parameters and the amount of available hydroxyl groups the least influential.

The viscoelastic properties of the dispersions of black liquor and derived hydrolyzed fractions in ECO were also investigated through SAOS experiments performed inside the linear viscoelastic regime, and the corresponding mechanical spectra are shown in Figure 7. As can be seen from the evolution of both the storage (G') and loss (G'') moduli with frequency (Figure 7a), ECO and the ECO_EA lignin dispersion exhibited a predominant viscous response over an extended frequency range. Moreover, similarly to what was found in the viscous flow measurements, the values of both viscoelastic functions for the ECO_EA sample are only slightly higher than those obtained for ECO. Similar liquid-like rheological response was previously found when dispersing lignocellulosic sugarcane bagasse waste in epoxidized vegetable oil [29]. This behavior was attributed to a high level of compatibilization due to the extensive crosslinking achieved. On the contrary, much higher values of the SAOS functions were obtained for the rest of dispersions, more specifically differences of more than two decades with respect to ECO values, as well as an extended plateau region, with values of G' significantly higher than those found for G" in a wide frequency range, characteristic of gel-like dispersions such as traditional lubricating greases [54,55]. The relative elasticity of the different samples can also be inferred from the loss tangent vs. frequency plots (Figure 7b). This solid-like behavior can be mainly attributed to the ash content acting as

fillers in the matrix. However, in agreement with the values of the consistency index, dispersions of SD and BL fractions displayed the highest values of SAOS moduli within the whole frequency range studied, because of the already mentioned balance among the relevant characteristics of the different lignin fractions, i.e. ash content, MW, OH and PDI. In particular, from the comparison of SD and OD fractions with very similar total lignin and ash contents (see Table 3), the higher OH groups content in the former, as corroborated by the enhanced O:C ratio reported in the elemental analysis (Figure 2), proves to play a significant role in the establishment of chemical crosslinking, thus affecting their ensuing rheological behavior to some extent.

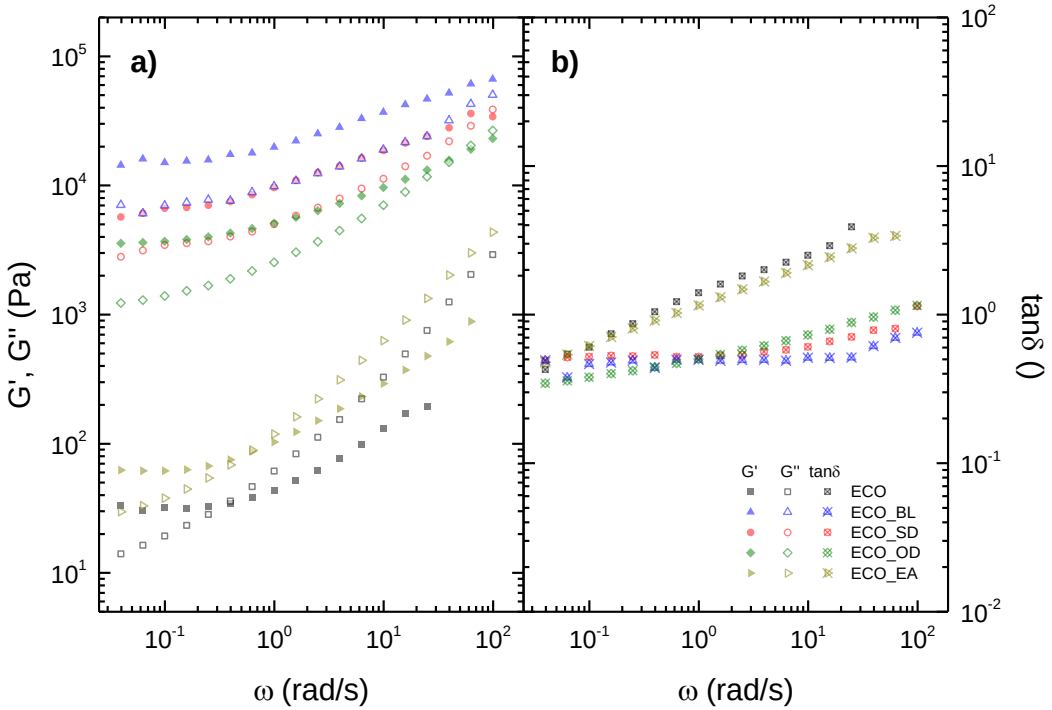

Figure 7. Evolution of the storage and loss moduli (a) and the loss tangent (b) with frequency for the dispersions of lignin fractions in epoxidized castor oil.

Finally, bearing in mind the potential application of these formulations as semi-solid bio-lubricants, a tribological characterization was carried out. Table 8 shows the stationary friction coefficient values within the mixed lubrication regime (20 N normal load and 10 rpm rotational speed, after 10 min) obtained when using the lignin-structured ECO formulations as lubricants in a tribological contact, in comparison with the neat epoxidized oil (ECO). As can be deduced the data collected in Table 8, similar and suitable friction coefficient values were obtained for all the formulations, displaying values only slightly higher than those shown by neat epoxidized castor oil (ECO), due to

the incorporation of lignin particles into the contact which provides a larger interface for friction, as previously observed for epoxidized lignins dispersed in castor oil [21].

Table 8. Values of the stationary friction coefficient and wear scar areas obtained on the steel plates when using the different lignin dispersions studied as lubricants in a ball-on-plates tribological contact.

Sample designation	μ (-)	Wear scar area (mm^2)
ECO	0.070 ± 0.005	0.41± 0.11
ECO_BL	0.089 ± 0.006	0.24± 0.04
ECO_SD	0.083 ± 0.006	0.34± 0.18
ECO_OD	0.080 ± 0.006	0.23± 0.02
ECO_EA	0.079 ± 0.005	0.19± 0.08

However, the main advantage of using these dispersions of lignin fractions as lubricants lies in a significant reduction of wear produced on the steel materials in contact. Thus, when analyzing wear scar dimensions on plates, as can be seen in Figure 8, enabled a noticeable reduction in the wear scar size, from 313 μm average diameter when using ECO as lubricants to, for instance, 160 μm in the case of ECO_EA samples. Although all lignin dispersions provide a significant improvement of wear, ECO_EA sample yielded the optimum results, probably due to the softer rheological characteristics that allow this sample to easily penetrate the contact area. These results may be explained on the basis of not only the reduced viscoelastic moduli and superior relative viscous character, but also taking into consideration the minimum ash content of only 2.3% (see Table 3), which may act as abrasive foreign particles [56,57], thus slightly increasing the ultimate wear scars, as depicted in Figure 8. Therefore, although the incorporation of lignin residues to structure epoxidized oils may slightly increase the friction in tribological contact, as otherwise found in all semi-solid lubricants respecting the base oil alone, their use led to a significant wear reduction, which may help to extend the service life of lubricated surfaces in tools and machinery.

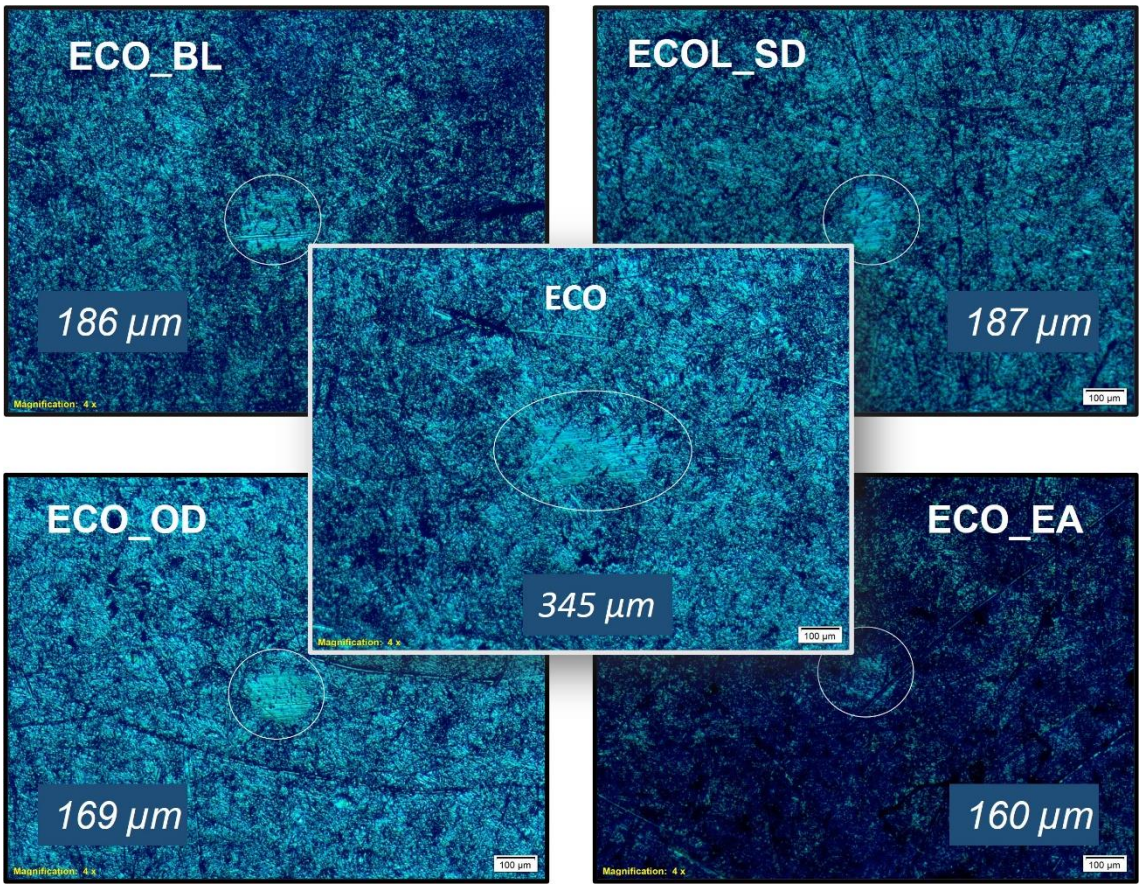

Figure 8. Microscopy images of wear scars obtained in the steel plates when using the lignin dispersions studied as lubricants in comparison to that generated by the neat epoxidized castor oil. Values of the average wear scar diameters are also inserted.

4. Conclusions

Supercritical water hydrolysis of weak black liquor yielded a series of depolymerized lignin fractions (spray-dried, oven-dried, and ethyl acetate extracted). Fast SCW hydrolysis prevents lignin repolymerization while promoting the depolymerization of lignin and the production of biopolyols. These lignin fractions, as well as the non-treated waste black liquor, have been successfully tested as feasible thickening agents for castor oil by implementing a chemical crosslinking route via epoxidation.

The castor oil-based formulations thickened with the different waste lignin fractions exhibit noteworthy physical stability, suitable appearance, characteristic shear-thinning and viscoelastic behaviors and adequate tribological response to be proposed as potential eco-friendly semi-solid lubricants.

The rheological behavior of these semi-solid lubricant formulations is the result of a delicate compromise among the filling effect of the ash content, average molecular weight and polydispersity index, and the likely chemical crosslinking ability of the lignin fractions, inherently related to the available OH groups content, among which molecular weight and PDI displayed the most significant contribution to the viscosity of lignin dispersions in the epoxidized castor oil.

The addition of the lignin fractions to epoxidized castor oil slightly increases the friction coefficient in a ball-on-plate steel-steel tribological contact, which is an expected result taking into account the internal friction contribution added by any thickener. However, the formulations thickened with the different lignin fractions significantly prevent wear in the contact elements as compared to the epoxidized castor oil. In particular, the ECO_EA system, with lower viscosity, may easily favour the replenishment of the tribological contact and combined with its minimum abrasive ash content, provides the highest wear protection.

In summary, this research not only highlights the feasibility of the SCW hydrolysis to treat pulp and paper biorefinery residues but also the tunability of the obtained lignin fractions to thicken castor oil to different extents and impart lubricating performance, depending on the depolymerization treatment and the subsequent separation stages.

REFERENCES

[1] S. Van Den Bosch, S.F. Koelewijn, T. Renders, G. Van den Bossche, T. Vangeel, W. Schutyser, B.F. Sels, Catalytic Strategies Towards Lignin - Derived Chemicals, Springer International Publishing, 2018. https://doi.org/10.1007/s41061-018-0214-3.

[2] J. Lappalainen, D. Baudouin, U. Hornung, J. Schuler, K. Melin, S. Bjelić, F. Vogel, J. Konttinen, T. Joronen, Sub- And supercritical water liquefaction of kraft lignin and black liquor derived lignin, Energies. 13 (2020) 3309. https://doi.org/10.3390/en13133309.

[3] Y.Y. Wang, X. Meng, Y. Pu, A.J. Ragauskas, Recent advances in the application of functionalized lignin in value-added polymeric materials, Polymers (Basel). 12 (2020) 1–24. https://doi.org/10.3390/polym12102277.

[4] E.C. Triviño, C. Valencia, M.A. Delgado, J.M. Franco, Modification of Alkali Lignin with Poly(Ethylene Glycol) Diglycidyl Ether to Be Used as a Thickener in Bio-Lubricant Formulations, Polymers (Basel). 10 (2018) 670. https://doi.org/10.3390/polym10060670.

[5] A.M. Borrero-López, C. Valencia, J.M. Franco, Lignocellulosic Materials for the Production of Biofuels , Biochemicals and Biomaterials and Applications of, Polymers (Basel). 14 (2022). https://doi.org/10.3390/polym14050881.

[6] F. Hernandez-Ramos, M.G. Alriols, T. Calvo-Correas, J. Labidi, E. Xabier, Renewable Biopolyols from Residual Aqueous Phase Resulting after Lignin Precipitation, ACS Sustain. Chem. Eng. 9 (2021) 3608–3615. https://doi.org/10.1021/acssuschemeng.0c09357.

[7] K.T. Barbosa, S.H. Fuentes Da Silva, W.L.E. Magalhães, S.C. Amico, R. de A. Delucis, Acid-catalyzed Kraft lignin liquefaction for producing polyols and polyurethane foams, J. Wood Chem. Technol. 44 (2024) 9–21. https://doi.org/10.1080/02773813.2024.2303036.

[8] L. Mu, Y. Shi, H. Wang, J. Zhu, Lignin in Ethylene Glycol and Poly(ethylene glycol): Fortified Lubricants with Internal Hydrogen Bonding, ACS Sustain. Chem. Eng. 4 (2016) 1840–1849. https://doi.org/10.1021/acssuschemeng.6b00049.

[9] M. Alinejad, S. Nikafshar, A. Gondaliya, S. Bagheri, N. Chen, S.K. Singh, D.B. Hodge, M. Nejad, Lignin-Based Polyurethanes: Opportunities for Bio-Based Foams, Elastomers, Coatings and Adhesives, Polymers (Basel). 11 (2019) 1202.

[10] N. Mahmood, Z. Yuan, J. Schmidt, C. Xu, Depolymerization of lignins and their applications for the preparation of polyols and rigid polyurethane foams: A review, Renew. Sustain. Energy Rev. 60 (2016) 317–329. https://doi.org/10.1016/j.rser.2016.01.037.

[11] J. Gharib, S. Pang, D. Holland, Synthesis and characterisation of polyurethane made from pyrolysis bio-oil of pine wood, Eur. Polym. J. 133 (2020) 109725. https://doi.org/10.1016/j.eurpolymj.2020.109725.

[12] K. Maniatis, Black Liquor Gasification, 2007. https://www.ieabioenergy.com/wp-content/uploads/2013/10/Black-Liquor-Gasification-summary-and-conclusions3.pdf.

[13] M.J. Cocero, Á. Cabeza, N. Abad, T. Adamovic, L. Vaquerizo, C.M. Martínez, M.V. Pazo-Cepeda, Understanding biomass fractionation in subcritical & supercritical water, J. Supercrit. Fluids. 133 (2018) 550–565. https://doi.org/10.1016/j.supflu.2017.08.012.

[14] N. Abad-Fernández, E. Pérez, M.J. Cocero, Aromatics from lignin through ultrafast reactions in water, Green Chem. 21 (2019) 1351–1360. https://doi.org/10.1039/c8gc03989e.

[15] C.M. Martínez, T. Adamovic, D.A. Cantero, M.J. Cocero, Scaling up the production of sugars from agricultural biomass by ultrafast hydrolysis in supercritical water, J. Supercrit. Fluids. 143 (2019) 242–250. https://doi.org/10.1016/j.supflu.2018.08.017.

[16] E.G. Mission, M.J. Cocero, Accessing suberin from cork via ultrafast supercritical hydrolysis, Green Chem. 24 (2022) 8393–8405. https://doi.org/10.1039/d2gc02498e.

[17] D.A. Cantero, M.D. Bermejo, M.J. Cocero, Reaction engineering for process intensification of supercritical water biomass refining, J. Supercrit. Fluids. 96 (2015) 21–35. https://doi.org/10.1016/j.supflu.2014.07.003.

[18] D.S. Bajwa, G. Pourhashem, A.H. Ullah, S.G. Bajwa, A concise review of current lignin production, applications, products and their environment impact, Ind. Crops Prod. 139 (2019) 111526. https://doi.org/10.1016/j.indcrop.2019.111526.

[19] F.H. Isikgor, C.R. Becer, Lignocellulosic biomass: a sustainable platform for the production of bio-based chemicals and polymers, Polym. Chem. 6 (2015) 4497–4559. https://doi.org/10.1039/c5py00263j.

[20] A.M. Borrero-López, F.J. Santiago-Medina, C. Valencia, M.E. Eugenio, R. Martin-Sampedro, J.M. Franco, Valorization of kraft lignin as thickener in castor oil for lubricant applications, J. Renew. Mater. 6 (2018) 347–361. https://doi.org/10.7569/JRM.2017.634160.

[21] M.A. Delgado, E. Cortés-Triviño, C. Valencia, J.M. Franco, Tribological study of epoxide-functionalized alkali lignin-based gel-like biogreases, Tribol. Int. 146 (2020). https://doi.org/10.1016/j.triboint.2020.106231.

[22] P. Figueiredo, K. Lintinen, J.T. Hirvonen, M.A. Kostiainen, H.A. Santos, Properties and chemical modifications of lignin: Towards lignin-based nanomaterials for biomedical applications, Prog. Mater. Sci. 93 (2018) 233–269. https://doi.org/10.1016/j.pmatsci.2017.12.001.

[23] A. Tenorio-Alfonso, M.C. Sánchez, J.M. Franco, Impact of the processing method on the properties of castor oil/cellulose acetate polyurethane adhesives for bonding wood, Int. J. Adhes. Adhes. 116 (2022). https://doi.org/10.1016/j.ijadhadh.2022.103153.

[24] P. Nagendramma, P. Kumar, Eco-friendly multipurpose lubricating greases from vegetable residual oils, Lubricants. 3 (2015) 628–636. https://doi.org/10.3390/lubricants3040628.

[25] T.M. Panchal, A. Patel, D.D. Chauhan, M. Thomas, J. V. Patel, A methodological review on bio-lubricants from vegetable oil based resources, Renew. Sustain. Energy Rev. 70 (2017) 65–70. https://doi.org/10.1016/j.rser.2016.11.105.

[26] H. Jahromi, S. Adhikari, P. Roy, M. Shelley, E. Hassani, T.S. Oh, Synthesis of Novel Biolubricants from Waste Cooking Oil and Cyclic Oxygenates through an Integrated Catalytic Process, ACS Sustain. Chem. Eng. 9 (2021) 13424–13437.

https://doi.org/10.1021/acssuschemeng.1c03523.

[27] C. Fajardo, A. Blánquez, G. Domínguez, A.M. Borrero-López, C. Valencia, M. Hernández, M.E. Arias, J. Rodríguez, Assessment of sustainability of bio treated lignocellulose-based oleogels, Polymers (Basel). 13 (2021) 1–12. https://doi.org/10.3390/polym13020267.

[28] R. Gallego, J.F. Arteaga, C. Valencia, M.J. Díaz, J.M. Franco, Gel-Like Dispersions of HMDI-Cross-Linked Lignocellulosic Materials in Castor Oil: Toward Completely Renewable Lubricating Grease Formulations, ACS Sustain. Chem. Eng. 3 (2015) 2130–2141. https://doi.org/10.1021/acssuschemeng.5b00389.

[29] E. Cortés-Triviño, C. Valencia, J.M. Franco, Thickening Castor Oil with a Lignin-Enriched Fraction from Sugarcane Bagasse Waste via Epoxidation: A Rheological and Hydrodynamic Approach, ACS Sustain. Chem. Eng. 9 (2021) 10503–10512. https://doi.org/10.1021/acssuschemeng.1c02166.

[30] T. Adamovic, X. Zhu, E. Perez, M. Balakshin, M.J. Cocero, Understanding sulfonated kraft lignin re-polymerization by ultrafast reactions in supercritical water, J. Supercrit. Fluids. 191 (2022). https://doi.org/10.1016/j.supflu.2022.105768.

[31] M. Ramos-Andrés, B. Aguilera-Torre, J. García-Serna, Biorefinery of discarded carrot juice to produce carotenoids and fermentation products, J. Clean. Prod. 323 (2021). https://doi.org/10.1016/j.jclepro.2021.129139.

[32] A. Sluiter, B. Hames, D. Hyman, C. Payne, R. Ruiz, C. Scarlata, J. Sluiter, D. Templeton, J.W. Nrel, Determination of total solids in biomass and total dissolved solids in liquid process samples, 2008.

[33] B. Hames, R. Ruiz, C. Scarlata, a Sluiter, J. Sluiter, D. Templeton, Preparation of Samples for Compositional Analysis Laboratory Analytical Procedure (LAP). Tech. Rep. NREL/TP-510-42620., Natl. Renew. Energy Lab. (2008) 1–9.

[34] A. Sluiter, B. Hames, R. Ruiz, C. Scarlata, J. Sluiter, D. Templeton, Determination of Sugars , Byproducts , and Degradation Products in Liquid Fraction Process Samples Laboratory Analytical Procedure (LAP) Issue Date : 12 / 08 / 2006 Determination of Sugars , Byproducts , and Degradation Products in Liquid

Fraction Proce, (2008).

[35] A. Sluiter, B. Hames, R. Ruiz, C. Scarlata, J. Sluiter, D. Templeton, Determination of ash in biomass. NREL Laboratory Analytical Procedure (LAP), Natl. Renew. Energy Lab. (2008) 18. http://www.nrel.gov/docs/gen/fy08/42622.pdf.

[36] ASTMD4274-99, Standard Test Methods for Testing Polyurethane Raw Materials: Determination of Hydroxyl Numbers of Polyols, Astm D 4274. 08 (2000) 1–9.

[37] P. Heyer, L. Jorg, Correlation between friction and flow of lubricating greases in a new tribometer device, Lubr. Sci. 21 (2009) 253–268. https://doi.org/10.1002/ls.88.

[38] M. Kienberger, S. Maitz, T. Pichler, P. Demmelmayer, Systematic review on isolation processes for technical lignin, Processes. 9 (2021). https://doi.org/10.3390/pr9050804.

[39] E. Pérez, N. Abad-Fernández, T. Lourençon, M. Balakshin, H. Sixta, M.J. Cocero, Base-catalysed depolymerization of lignins in supercritical water: Influence of lignin nature and valorisation of pulping and biorefinery by-products, Biomass and Bioenergy. 163 (2022). https://doi.org/10.1016/j.biombioe.2022.106536.

[40] R. Rinaldi, R. Jastrzebski, M.T. Clough, J. Ralph, M. Kennema, P.C.A.A. Bruijnincx, B.M. Weckhuysen, Paving the Way for Lignin Valorisation: Recent Advances in Bioengineering, Biorefining and Catalysis, Angew. Chemie - Int. Ed. 55 (2016) 8164–8215. https://doi.org/10.1002/anie.201510351.

[41] A. Wypych, Databook of Adhesion Promoters, 2nd Editio, ChemTec Publishing, 2023.

[42] M. Helander, H. Theliander, M. Lawoko, G. Henriksson, L. Zhang, M.E. Lindström, Fractionation of technical lignin: Molecular mass and pH effects, BioResources. 8 (2013) 2270–2282. https://doi.org/10.15376/biores.8.2.2270-2282.

[43] M.A. Hubbe, R. Alén, M. Paleologou, M. Kannangara, Lignin Recovery from Spent Alkaline Pulping Liquors Using Acidification, Membrane Separation, and Related Processing Steps: A Review, 14 (2019) 2300–2351. https://doi.org/10.15376/biores.8.2.2270-2282.

[44] G. Gea, M.B. Murillo, J. Arauzo, Thermal degradation of alkaline black liquor from straw. Thermogravimetric study, Ind. Eng. Chem. Res. 41 (2002) 4714–4721. https://doi.org/10.1021/ie020283z.

[45] J. D'Souza, R. Camargo, N. Yan, Biomass Liquefaction and Alkoxylation: A Review of Structural Characterization Methods for Bio-based Polyols, Polym. Rev. 57 (2017) 668–694. https://doi.org/10.1080/15583724.2017.1283328.

[46] M. Szycher, Szycher's handbook of Polyurethanes, 2nd Editio, CRC Press, Boca Raton, FL 33487-2742, 2013.

[47] R. Briones, L. Serrano, J. Labidi, Valorization of some lignocellulosic agro-industrial residues to obtain biopolyols, J. Chem. Technol. Biotechnol. 87 (2012) 244–249. https://doi.org/10.1002/jctb.2706.

[48] S.H.F. da Silva, I. Egüés, J. Labidi, Liquefaction of Kraft lignin using polyhydric alcohols and organic acids as catalysts for sustainable polyols production, Ind. Crops Prod. 137 (2019) 687–693. https://doi.org/10.1016/j.indcrop.2019.05.075.

[49] E.U.X. Péres, P.R.R. de Matos, F. Machado, P.A.Z. Suarez, Synthesis and characterization of a new biolubricant based on oligoesterification of ricinoleic acid, oxalic acid, and ethylene glycol, Brazilian J. Chem. Eng. (2023). https://doi.org/10.1007/s43153-023-00308-z.

[50] J.E. Martín-Alfonso, G. Moreno, C. Valencia, M.C. Sánchez, J.M. Franco, C. Gallegos, Influence of soap/polymer concentration ratio on the rheological properties of lithium lubricating greases modified with virgin LDPE, J. Ind. Eng. Chem. 15 (2009) 687–693. https://doi.org/10.1016/j.jiec.2009.09.046.

[51] S.H. Shafiai, A. Gohari, B.Y. Ying, Computational study of tsunami inundation using the LABSWETM—Sisko Model, Eur. J. Mech. B/Fluids. 88 (2021) 251–263. https://doi.org/10.1016/j.euromechflu.2021.04.010.

[52] M.A. Delgado, C. Valencia, M.C. Sánchez, J.M. Franco, C. Gallegos, Influence of soap concentration and oil viscosity on the rheology and microstructure of lubricating greases, Ind. Eng. Chem. Res. 45 (2006) 1902–1910. https://doi.org/10.1021/ie050826f.

[53] J.E. Martín-Alfonso, C. Valencia, M.C. Sánchez, J.M. Franco, C. Gallegos, Rheological modification of lubricating greases with recycled polymers from different plastics waste, Ind. Eng. Chem. Res. 48 (2009) 4136–4144. https://doi.org/10.1021/ie801359g.

[54] M.A. Delgado, S. Secouard, C. Valencia, J.M. Franco, On the steady-state flow and yielding behaviour of lubricating greases, Fluids. 4 (2019). https://doi.org/10.3390/fluids4010006.

[55] R. Sánchez, C. Valencia, J.M. Franco, Rheological and Tribological Characterization of a New Acylated Chitosan-Based Biodegradable Lubricating Grease: A Comparative Study with Traditional Lithium and Calcium Greases, Tribol. Trans. 57 (2014) 445–454. https://doi.org/10.1080/10402004.2014.880541.

[56] K. Nantha Gopal, R. Thundil Karuppa Raj, Effect of pongamia oil methyl ester-diesel blend on lubricating oil degradation of di compression ignition engine, Fuel. 165 (2016) 105–114. https://doi.org/10.1016/j.fuel.2015.10.031.

[57] A.K. Hasannuddin, J.Y. Wira, S. Sarah, W.M.N. Wan Syaidatul Aqma, A.R. Abdul Hadi, N. Hirofumi, S.A. Aizam, M.A.B. Aiman, S. Watanabe, M.I. Ahmad, M.A. Azrin, Performance, emissions and lubricant oil analysis of diesel engine running on emulsion fuel, Energy Convers. Manag. 117 (2016) 548–557. https://doi.org/10.1016/j.enconman.2016.03.057.

CHAPTER III

Process development:

Continuous black liquor and kraft lignin fractionation by supercritical water technology

Abstract

Black liquor and kraft lignin were depolymerized using supercritical water: no additional catalyst was used for black liquor, but NaOH served as the base catalyst for kraft lignin. This study represents the first rapid reaction screening of black liquor and precipitated kraft lignin, providing a comprehensive characterization of all fractions. The experiments were carried out at TRL4 in a continuous pilot plant with fast reaction times, at temperatures of 380°C and 390°C and a pressure of 26 MPa. Reaction times of 0.5, 1 and 1.5 seconds were investigated for both temperatures and feedstocks. The bio-oil fraction was separated using a specific fractionation method and its aromatic content was analyzed using several characterization techniques.

This study offers a viable approach to black liquor processing that uses intrinsic pulping chemicals as catalysts, eliminating the need for drying, lignin separation or additional logistics. It also utilizes lignin degradation compounds, making it an efficient, streamlined strategy.

This study shows that longer reaction times and higher temperatures during supercritical water (SCW) treatment of black liquor (BL) and kraft lignin (KL) significantly increase phenolic compound concentrations, resulting in lower pH and reduced total solids content. SCW treatment reduced the SSI fraction of BL from 24.96 wt% to only 1.25 wt% at 390°C, while the SSI fraction of KL decreased from 37.57 wt% to 5 wt% under similar conditions. The rapid depolymerization of BL indicates its high susceptibility to solubilization, making it a prime candidate for organic degradation processes.

BL's ethyl acetate extracted dissolved solids (DSEA) fraction (aromatic monomer rich oil) initially contained 9.32 wt% whereas KL started with only 5.74 wt%. BL achieved maximum DSEA yields of 21 wt% at 380°C and 24.64 wt% at 390°C compared to KL's peak yields of 13.36 wt% and 16.82 wt% respectively. Overall, the SCW process achieved maximum total oil yields of 79.45 wt% for BL and 68.54 wt% for KL at 390°C.

GPC analysis showed that the ethyl acetate extracted suspended solids (SSEA) fraction from KL had a higher molecular weight (Mw) than the raw material at 390°C and 0.5 seconds, but this Mw decreased significantly with longer reaction times of 1 and 1.5 seconds, confirming that KL benefits from longer processing.

It was found that the depolymerization and repolymerization reactions occurred simultaneously and that the onset of repolymerization didn't inhibit the production of lower molecular weight fragments. However, a more comprehensive experimental design with more data points is required to fully validate these observations.

1. Introduction

Biomass, particularly lignocellulosic materials from wood or inedible plant parts, has the advantage of being more readily available than other biomass sources. It can be used for energy production and as feedstock for the synthesis of chemicals, fuels, and materials [1]. Lignocellulose, comprising cellulose, hemicellulose, and lignin, along with minor components depending on the nature of the materials, such as pectin and triglycerides, presents conversion challenges due to its complex structure [2–4]. Despite the absence of a universal method for processing lignocellulosic materials, modern biorefineries developed strategies to simplify biomass into fractions, traditionally focusing on carbohydrates for paper/pulp or bioethanol production. Consequently, lignin is often underutilized, treated as a low-value by-product or used for energy [2,5]. Lignin is included inside the black liquor side stream of kraft pulping mills and is primarily used in recovery boilers to regenerate process chemicals and generate energy, often in excess quantities [6]. Burning lignin to close the energy requirements of the processes is the crucial part of the pulp mills in terms of its economy. However, lignin included black liquor has a high potential to be valued by tailoring this material according to the product distribution required by the industry using appropriate techniques [6,7].

Though it is hard to make clear distinction between the processes applied on lignin, classification of the lignin depolymerization studies can be done under four main groups, which are reductive [8–11], oxidative [12,13], solvolytic and thermal [14,15], and acid-base catalyzed depolymerization (BCD) [2,16–19]. Each process aims to produce a different type of product distribution in the organic fractions [2]. The pros and cons of these processes were discussed in the previous chapters and introduction. Nevertheless, generally these techniques were performed over 200°C, while some required elevated temperatures of more than 350°C [16]. Base catalyzed supercritical water depolymerization of the black liquor was one of the promising studies among the depolymerization strategies [7,20]. This technique, therefore, requires temperatures over critical temperature and pressure of water, that means high operating expenditures [1]. However, it is noteworthy that kraft recovery boilers produces more than 450°C [21]. Considering maximum kraft lignin price as 500$ per tonne [22], any process that will increases profits by producing value-added chemicals or an intermediate fraction that can be valorized represents a significant potential [23]. Additionally, since lignin or black liquor are soluble in a basic environment, a continuous processing can be applied to this

medium. This will help to improve reaction kinetics, heat and mass transfer, reduce capital expenditure and enable scale-up due to smaller reactor volumes [24–26].

Although scientific community is focused primarily on the lignin from the black liquor stream, black liquor stream as a whole includes water soluble lignin degradation compounds (monomers, dimers, oligomers, etc.) together with small amount of cellulose and hemicellulose decomposition products from pulping process [27]. In the literature only a few studies focused on black liquor processing [20]. Even though there are some studies that were focused on the gasification of black liquor to produce synthesis gas, there are only a few studies that focus on base catalyzed hydrothermal black liquor depolymerization [6]. A previous study by our group demonstrated total bio-oil yields of 72.6 wt% and 91.5 wt% from Sigma Kraft lignin and commercially extracted Kraft black liquor lignin, respectively [1,26,28], with optimal conditions of 0.3 seconds at 386°C and 26 MPa. Yong and Matsumura achieved complete lignin dissolution at rapid reaction times of 0.5 seconds under various supercritical water conditions, reaching a maximum bio-oil yield of 21 wt% at 390°C, and noted the possibility of repolymerization within only 0.5 seconds [29,30]. Investigation of Lee et al. with Sigma Kraft lignin yielded a maximum of 62 wt% bio-oil after 5 minutes of reaction at 350°C [31]. Nguyen and colleagues achieved 87.7 wt% bio-oil yield from LignoBoost lignin after 10-13 minutes at 310°C and 25 MPa [32]. Solantausta et al. reported 70 wt% bio-oil yield from the hydrothermal liquefaction of commercial softwood kraft black liquor at 350°C for 45 minutes [33]. Long reaction time experiments by Orebom et al. yielded 78 wt.% bio-oil yield from black liquor under 380°C and 34 MPa for 1 h [6]. Significantly, most of the referenced studies on base catalyzed depolymerization focused on increasing the yield of "oil", usually defined as the material extractable by organic solvents after acidification [7]. The primary aim of the strategy mentioned above is to ensure that materials that can be extracted using organic solvents are suitable for potential processes like catalytic hydrodeoxygenation, which will make the water-soluble fraction unsuitable for this goal due to the potential for catalyst poisoning and instability. Acidification can also aid in the precipitation of high molecular weight species. However, the goal of the depolymerization process depends on the downstream techniques chosen [7].

In this study, black liquor and kraft lignin were depolymerized using supercritical water with no additional catalyst for black liquor but using NaOH as a base catalyst for kraft lignin. To the best of our knowledge, this work represents the first screening of black liquor and its precipitated kraft lignin at rapid reaction times, accompanied by a

comprehensive characterization of all fractions. The experiments were carried out in a TRL4 level continuous pilot plant at rapid reaction times. The experiments were performed at two different temperatures of 380°C and 390°C. The pressure was set to 26 MPa for all experiments. Besides, three different reaction times of 0.5s, 1s, and 1.5s were studied for both temperature and raw material. The product was subjected to a fractionation method to separate the bio-oil fraction and determine the aromatics present in this fraction. Several characterization techniques were used to understand the products' characteristics. Regarding the black liquor this study presents a feasible processing strategy since it uses the intrinsic pulping chemicals as catalysts, there is no need for drying or separating lignin, skips logistics by directly using black liquor, and benefits from the degradation compounds from lignin in black liquor.

2. Materials and methods

2.1. Materials

Black liquor was provided by Ence Energía & Celulosa in Pontevedra, Spain. The following chemicals were purchased for analytical purposes: ethyl acetate (99%) and acetone (99%) from PanReac; sulfuric acid in concentrations of 72% and 96%; and sodium hydroxide pellets (98%). Calibration standards for gas chromatography including guaiacol (≥99%), syringol (98%), vanillin (99%), acetosyringone (97%), acetovanillone (98%) and syringaldehyde (97%) were all purchased from Sigma-Aldrich. In addition, N,O-bis(trimethylsilyl)trifluoroacetamide (BSTFA - 99%), and tetrahydrofuran (THF – 99.5%) were obtained from Merck. Milli-Q grade water was used for all analyses.

2.2. Kraft Lignin Production

Kraft lignin was produced using black liquor raw material. Black liquor pH was dropped using sulfuric acid until pH 2, and the solids were precipitated. After the precipitation, solids and liquids were separated using a centrifuge. Following the centrifuge, solids were washed three times with pH 2 water, and then solids were dried in a freeze drying. The precipitation step was carried out in 1L beakers, using around 400mL of black liquor in each batch. The separation of the solids in the centrifuge was performed using 4x750 mL containers in each set. The rpm and cfm of the centrifuge was around 3500. The centrifuge step was performed at 40°C, and each run of 1 hour. The ash content of the kraft lignin produced was found to be 8.1 ± 0.3 wt%.

2.3. Supercritical Water Depolymerization Process

The supercritical water depolymerization experiments performed in this chapter were conducted with a TRL4 level continuous pilot plant which is different from the first two chapters of this thesis. A detailed scheme of this TRL4 pilot can be found as reported elsewhere [28,34]. The experiments were carried out for both black liquor and precipitated kraft lignin from the black liquor. The initial total solids content of black liquor was found to be ~45 wt%. The biomass flow rate was set to 2 kg/h, and the water flow rate was 5 kg/h. The experiments were carried out at 380°C ± 2°C and 390°C ± 2°C, and both at 26 ± 0.5 MPa. Three different reaction times were carried out during this study which were 0.5s, 1s, and 1.5s. NaOH was used as a catalyst. Using BL as raw material did not require any NaOH addition since the medium is already at a high pH of over 13. Regarding the KL experiments, 0.3M of NaOH solution was prepared to reach over pH 13, and the required KL material was added to this solution. The concentration of the lignin inside the biomass tank was set around 3.5 wt% for both BL and KL. The lignin percentage in BL was approximately 14 wt%. The experiments were performed in triplicates, and the results are reported as a means. The process flow diagram of the equipment is given in Figure 1.

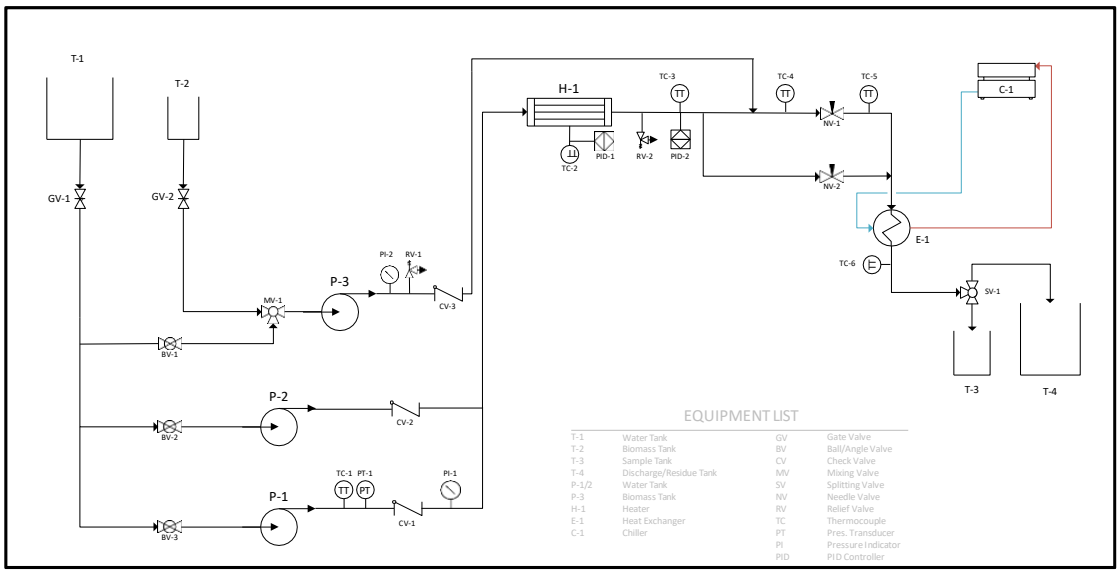

Figure 1. Process flow diagram of the TRL4 supercritical water depolymerization pilot plant.

2.4. Downstream Processing

2.4.1. Dissolved and Total Solids Analysis

The sample was first acidified using sulfuric acid until pH 2, then the phase separation between the liquid and the solid was performed using centrifuge at 10,000 rpm and cfm, at 40°C. Liquid and solid phases were separated and dried in an oven at 105°C overnight. The dried liquid phase formed dissolved solids, and the dried solids phase formed suspended solids fraction. The sum of these two fractions constituted the total solids after acidification. The added acid was removed from the calculations to correct the results. A simple illustration of the dissolved solids analysis can be found in Figure 2.

$$\%\boldsymbol{Dissolved\ Solids}(\boldsymbol{DS}) = \frac{\mathbf{Weight}_{dry\ pan\ plus\ dry\ liquor} - \mathbf{Weight}_{dry\ pan}}{\boldsymbol{Weight}_{liquor\ after\ filtration}}\ \boldsymbol{x}\ \mathbf{100} \qquad \text{Eq.1}$$

$$\boldsymbol{Total\ Solids}\ (\boldsymbol{TS}) = \boldsymbol{Dissolved\ Solids}\ (\boldsymbol{DS}) + \boldsymbol{Suspended\ Solids}\ (\boldsymbol{SS}) \qquad \text{Eq.2}$$

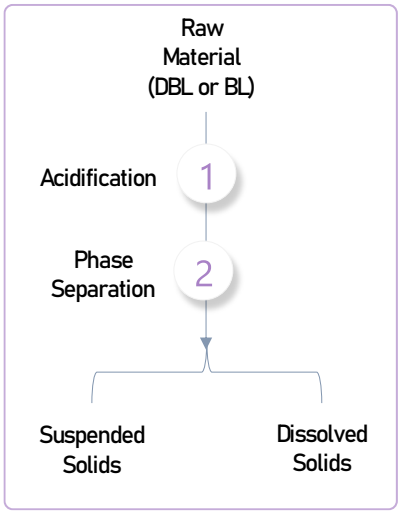

Figure 2. Illustration of dissolved solids analysis.

2.4.2. Fractionation Method

The fractionation method used in this work was a slightly modified version of the previous research [1]. The sample was first acidified using sulfuric acid until pH2, and then phase separation was performed using a centrifuge at 40°C, at 10.000 rpm and cfm. After the separation dissolved and suspended phases were placed into different tubes. The suspended phase was further washed with pH2 water three times, and the separation of the phases was carried out using centrifuge again. The liquid phase obtained after the washing steps was added into the dissolved phase obtained after the

first centrifuge. Further extraction was performed using ethyl acetate to extract the organic fractions into this solvent. Both dissolved and suspended fractions were extracted with ethyl acetate and separated using centrifuge again. At the end of the fractionation step four different fractions were obtained. From the dissolved phase, after ethyl acetate extraction two fractions were obtained which were dissolved solids water soluble fraction (DSW) and dissolved solids ethyl acetate extracted fraction (DSEA). From the suspended phase, after ethyl acetate extraction two fractions were obtained which were suspended solids insoluble (SSI) and suspended solids ethyl acetate extracted (SSEA). The suspended solids insoluble fraction was labeled since this fraction was not able to be dissolved in either water or ethyl acetate. However, it was possible to dissolve this fraction in THF. A simplified illustration of the fractionation method is given in Figure 3.

$$\%\ Fractionation\ Yield = \frac{\text{Weight}_{dry\ tube\ plus\ dry\ fraction} - \text{Weight}_{dry\ pan}}{Weight_{total\ solids}}\ x\ 100 \qquad \text{Eq.3}$$

$$\%\ Dry\ Mass\ Yield\ Sum = \sum_{i=1}^{n} c_i \qquad \text{Eq.4}$$

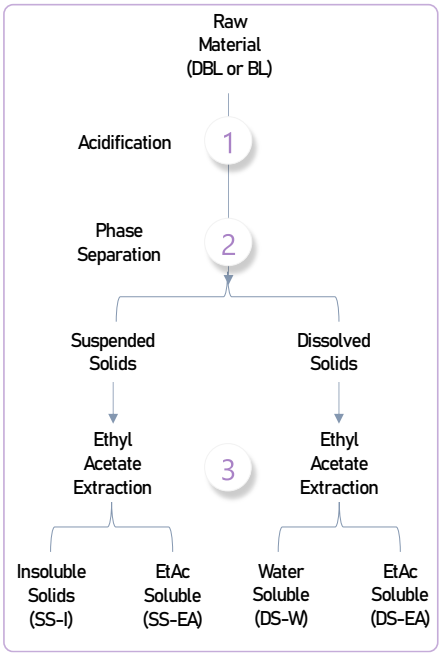

Figure 3. Illustration of fractionation method performed for raw materials and their depolymerized products.

The ash content of each raw material and their depolymerized products was determined using the NREL method [35]. Overnight conditioned crucibles at 550°C were weighed, tared and 1g of sample was placed inside the crucibles. The samples were maintained in the oven 24±4 h at 550°C to remove the organic content of the material. The residual sample inside the crucible was cooled down, the weight was recorded, and the ash content was calculated.

$$\%Ash = \frac{\text{Weight}_{crucible\ plus\ ash} - \text{Weight}_{crucible}}{\text{Weight}_{oven\ dried\ sample}}\ x\ 100 \qquad \text{Eq.5}$$

2.5. Characterization Techniques

The elemental Analysis of each fraction and raw material was performed using Leco CS-225 Elemental Analyzer to determine C, H, N, and S. After the analysis, the remaining was considered as inorganic and oxygen.

Attenuated total reflectance characterization of each fraction and raw material was carried out using Bruker Tensor 27 with internal diamond crystal lens. The range of the wavelength was between 400 to 4000 cm^{-1}. Each spectrum is characterized by a mean of 64 single scans.

Thermogravimetric analysis of BL raw material and its depolymerized products was conducted using Mettler Toledo TGA/SDTA RSI analyzer. Under nitrogen flow of 50 mL/min, 5 mg of sample was heated at a rate of 10°C/min. The set temperature was 900°C.

DSEA fraction of both raw material and their depolymerized products were analyzed and quantified using an Agilent 7820 GC gas chromatograph with a quadrupole mass spectrometer detector. Agilent HP-5ms column with the dimensions of 30m x 0.25mm x 0.25um was used. Helium was used as a carrier gas, and the injection was performed as splitless. To quantify the major monomers a modified version of the method that was used in our group's previous works [1,28]. The oven temperature program started at 32°C and held for 10 minutes; then increased to 52°C at a rate of 2°C/min and held for 2 minutes; then to 65°C at 2°C/min and held for 2 minutes; then to 93°C at 4°C/min and held for 2 minutes; then to 230°C at 2°C/min and held for 3 minutes; finally to 300°C at 15°C/min and held for 3 minutes. The solvent delay program was set to 4 minutes to prevent acetone from reaching the MS detector.

Each raw material and their depolymerized products were prepared for gel permeation chromatography to quantify their molecular weight distribution. A Hewlett Packard 1100 series autosampler equipped with Phenomenex Phenogel 5 µm GPC column was used for the analysis. THF concentration of 1 mg/mL was used to dissolve the dried samples. The column temperature was kept at 26 ºC, and THF was selected as the carrier solvent at a rate of 1 mL.min-1. UV-DAD detector at a wavelength of 220 nm with a reference wavelength of 360 nm and a slit width of 4 nm was used to analyze the samples. A calibration curve was established between molecular weight and residence time using PSS low molecular weight polystyrene ReadyCal set M(p) 266-66000. The UV response and residence time data were correlated with the calibration curve and used to calculate Mw, Mn and Mz.

Sugars and their derivatives analysis was performed using Waters high-performance liquid chromatography (HPLC). Shodex SH-1011 column was installed, and sulfuric acid (0.01 N) was used as the mobile phase at a flow rate of 0.8 mL/min. Waters RI detector (Waters 2414) was used for the detection of the components. The NREL Protocol for carbohydrate determination was followed for HPLC analysis [36].

Total organic carbon was used to determine the total carbon content of the liquid samples from the dissolved solids and total solids analysis. Shimadzu TOC-VCSH was used to perform the analysis. The sample concentration was kept between 400-500 ppm.

3. Results and Discussion

Dissolved solids (DS) and total solids (TS) dry basis yields of each condition after acidification of the samples were given in Table 1. As can be seen from the table, dissolved solids increase by temperature and reaction time for both black liquor and kraft lignin. For BL depolymerization products, at 380°C, DS% was increased from 50.06 wt% at 0.5 sec of reaction time to 63.88 wt% at 1.5 sec. At 390°C, the increment between 0.5 sec to 1.5 sec of reaction time was from 53.79 wt% to 70.37 wt%. Again, at 390°C, all the reaction time parameters studied corresponded to a higher yield of DS% compared to 380°C. When KL products were examined, at 380°C, DS% was increased from 27.03 wt% to 37.12 wt% between 0.5 and 1.5 sec of reaction time. Similarly, at 390°C, the DS% increased from 34.75 wt% to 45.68 wt%. For the case of black liquor, considering all the reaction time conditions, the largest gap between 380°C and 390°C was found at 1.5 sec. The DS% increased from 63.88 wt% to 70.37 wt%. For KL, the

largest gap between 380°C and 390°C was found at 1 second of reaction time, where the DS% increased from 31.39 wt% to 42.89 wt%.

For both BL and KL, TS% of the products were decreased by increasing the reaction time from 0.5 to 1.5 seconds. The difference between the raw materials (0th seconds of reaction time) and the products is reasonable due to the effect of the flow rate oscillations. The TS yield of BL raw material was calculated as 9.03 wt%, but this concentration belongs to the raw material inside the biomass tank, before the reaction. Due to the mixing inside the reactor between SCW and the biomass line, the biomass concentration decreases to 30 wt% ± 2wt% of the total flow rate. All the conditions lie between this flow rate oscillation, but KL 390°C, 1 and 1.5 sec experiments. At these conditions, having lower TS% could be attributed to the sign of producing a greater amount of low boiling point components or gas formation.

Table 1 also indicates another clear correlation between increasing DS% with decreasing pH and decreasing TS% with decreasing pH of the products by increasing reaction time. This relation between pH, DS% and TS% can be attributed to the increasing phenolic groups in the product composition compared to the raw material. A similar observation can be found in the literature [6]. The depolymerization of the organics in the BL or KL leads to a production of phenolics which causes the decrement of the pH. Increasing the reaction time for both temperature conditions also help to decrease the pH more. In comparison of each reaction time condition for 380°C and 390°C, for both BL and KL, it is obvious that any condition at 390°C always has a lower pH compared to the same reaction time used at 380°C.

Table 1. Yields of dissolved solids and total solids, and pH of each experiment condition of black liquor and kraft lignin.

Product	T (°C)	Time (s)	pH	TS%	TS% Error (±)	DS%	DS% Error (±)
BLACK LIQUOR	380°C	**0**	12.45	9.03	0.11	25.84	0.21
		0.5	10.65	2.94	0.02	50.06	0.07
		1	10.29	2.91	0.10	61.89	0.02
		1.5	9.96	2.71	0.07	63.88	0.06
BLACK LIQUOR	390°C	**0**	12.45	9.03	0.11	25.84	0.21
		0.5	10.53	2.73	0.02	53.79	0.03
		1	9.85	2.61	0.16	68.15	0.10
		1.5	9.76	2.38	0.09	70.37	0.01
KRAFT LIGNIN	380°C	**0**	12.14	4.07	0.19	17.30	1.32
		0.5	10.78	1.34	0.02	27.03	1.24
		1	9.87	1.29	0.11	31.39	1.98
		1.5	9.27	1.22	0.04	37.12	0.64
KRAFT LIGNIN	390°C	**0**	12.14	4.07	0.19	17.30	1.32
		0.5	10.20	1.18	0.12	34.75	1.73
		1	9.02	0.85	0.06	42.89	1.37
		1.5	8.87	0.81	0.02	45.68	1.53

This fundamental TS and DS analysis results were also compared with advanced fractionation techniques to separate the fractions into four different classes. In the fractionation of the downstream products, extra washing steps were carried out to separate all DS fraction from the suspended solids (SS) fraction. Also, this method enabled us to practice ethyl acetate extraction more precisely. The fractionation results and the mass balance data can be found in Table 2. As mentioned before in the experimental section, to remind the reader here, the fractions that were created after the fractionation method were labeled as Dissolved Solids Water Soluble (DSW), Dissolved Solids Ethyl Acetate Soluble (DSEA), Suspended Solids Insoluble (SSI), and Suspended Solids Ethyl Acetate Soluble (SSEA). Although the SSI fraction was soluble in other solvents such as THF, it was labeled at this point of the experiments as Suspended Solids Insoluble (SSI) since this fraction was not soluble in both water and ethyl acetate.

The fractions solid mass yields were given in bold (SSI %, etc.), and the carbon factor (C_SSI, etc.) of each fraction was given next to corresponding fraction given in bold. The carbon factors of the fractions were determined by analyzing the dried samples using the fractionation method. The solid mass yields of the fractions (SSI, etc.) were calculated according to each fraction TS% that was given in Table 1. Furthermore, the

C_SUM percentage column was created by multiplying each fraction percentage with carbon factor. These data were also accepted as the real carbon content in the fractions as the BL raw material carbon content was found around 31%, which is closed to the reported values [37,38].

As the 0th second of both BL and KL corresponds to the raw materials concentration in the tank, the CLOSURE column was created by dividing each product by the 0th sec raw material C_SUM percentage (vis. Eq.6). Table 2 includes the ash content of the samples as well. After acidification, due to the salt formation, the inorganic content of the fractions was migrated into the DSW fraction.

The mass balance for the solid fractions lay between 92.40% to 103.13%, whereas the carbon balance closure lay between 88.1% and 102.9%. As it can be seen from Table 2, both raw materials have a high amount of insoluble material. For BL raw material, the insoluble material percentage is 24.96 wt%, whereas for KL raw material, the insoluble material percentage was 37.57 wt%. The effect of the SCW treatment for the depolymerization of the BL and KL can be seen even at 0.5 sec, but as more effective for BL. The SSI fraction percentages for BL at 0.5 sec were found to be 7.59 wt% and 1.25wt% at 380°C and 390°C, respectively. Regarding the experiments with KL as the starting material, the SSI fraction percentages were recorded as 19.6 wt% and 5 wt% at 380°C and 390°C, respectively. At very short reaction times, SCW affects BL faster than KL in a positive way to solubilize or depolymerize the SSI fraction. However, compared to the raw material, solubilizing the SSI fraction in both BL and KL rapidly can be attributed to the unique properties of the supercritical water. Increasing the reaction time led to the decrement of the insoluble fraction and increment of all fractions, but more selectively total oil percentages.

Table 2. Black liquor and kraft lignin raw materials (inside the biomass tank) and their depolymerized products dry basis mass balance coupled with the carbon balance using the elemental analysis carbon percentage results of each fraction.

#	T	Time	SSI	C_SSI	DSW	C_DSW	DSEA	C_DSEA	SSEA	C_SSEA	SUM	SUM Error	C_SUM	CLOS.	CLOS. Error	DS	SS	OIL	OIL Error
	°C	s	%		%		%		%		%	±	%	%		%	%	%	%
BL	380	0	**24.96**	0.56	**53.64**	0.10	**4.66**	0.54	**16.62**	0.54	**99.86**	**1.82**	30.90	**100.0**	**0.67**	58.29	41.57	**21.27**	**0.66**
		0.5	**7.59**	0.59	**61.78**	0.06	**7.69**	0.55	**24.46**	0.64	**101.52**	**1.80**	28.37	**91.8**	**1.57**	69.47	32.05	**32.15**	**1.29**
		1	**0.96**	0.55	**60.17**	0.07	**10.83**	0.56	**31.18**	0.65	**103.13**	**0.87**	31.29	**101.3**	**0.37**	70.99	32.14	**42.00**	**0.34**
		1.5	**1.52**	0.56	**61.20**	0.06	**10.29**	0.55	**28.17**	0.65	**101.17**	**1.06**	28.49	**92.2**	**0.47**	71.48	29.69	**38.45**	**0.32**
BL	390	0	**24.96**	0.56	**53.64**	0.10	**4.66**	0.54	**16.62**	0.54	**99.86**	**1.82**	30.90	**100.0**	**0.67**	58.29	41.57	**21.27**	**0.66**
		0.5	**1.25**	0.59	**58.53**	0.06	**9.03**	0.56	**29.62**	0.64	**98.42**	**1.49**	28.10	**90.9**	**1.08**	67.56	30.87	**38.64**	**0.98**
		1	**2.55**	0.58	**60.14**	0.06	**11.64**	0.56	**25.75**	0.64	**100.07**	**2.06**	28.28	**91.5**	**0.53**	71.77	28.30	**37.39**	**0.35**
		1.5	**2.53**	0.56	**59.03**	0.08	**12.64**	0.56	**28.38**	0.65	**102.58**	**2.53**	31.61	**102.3**	**1.02**	71.67	30.91	**41.02**	**0.63**
KL	380	0	**37.57**	0.59	**31.71**	0.07	**5.21**	0.57	**26.24**	0.62	**100.71**	**1.82**	43.58	**100.0**	**1.44**	36.91	63.80	**31.44**	**1.28**
		0.5	**19.60**	0.58	**30.69**	0.07	**11.99**	0.60	**37.42**	0.64	**99.69**	**3.60**	44.82	**102.9**	**3.59**	42.67	57.02	**49.40**	**3.45**
		1	**6.61**	0.60	**37.56**	0.08	**8.25**	0.58	**44.70**	0.66	**97.11**	**4.38**	41.44	**95.1**	**1.77**	45.81	51.31	**52.95**	**1.28**
		1.5	**7.13**	0.59	**37.59**	0.08	**7.92**	0.60	**39.77**	0.66	**92.40**	**3.10**	38.37	**88.1**	**3.01**	45.51	46.89	**47.69**	**2.76**
KL	390	0	**37.57**	0.59	**31.71**	0.07	**5.21**	0.57	**26.24**	0.62	**100.71**	**1.82**	43.58	**100.0**	**1.44**	36.91	63.80	**31.44**	**1.28**
		0.5	**5.00**	0.58	**39.47**	0.07	**9.36**	0.59	**42.11**	0.66	**95.94**	**1.53**	39.08	**89.7**	**1.18**	48.83	47.11	**51.47**	**1.17**
		1	**0.45**	0.63	**34.02**	0.04	**14.46**	0.62	**46.59**	0.68	**95.51**	**1.90**	42.60	**97.8**	**1.89**	48.48	47.03	**61.05**	**1.78**
		1.5	**0.20**	0.60	**34.55**	0.07	**13.94**	0.62	**44.80**	0.67	**93.49**	**4.54**	41.19	**94.5**	**4.44**	48.49	45.00	**58.74**	**4.43**

C_SSI: Suspended solids insoluble fraction carbon factor; C_DSW: Dissolved solids water soluble fraction carbon factor; C_DSEA: Dissolved solids ethyl acetate soluble fraction carbon factor; C_SSEA: Suspended solids ethyl acetate soluble fraction carbon factor.

$$\%\ Closure = C_{SUM,i} / C_{SUM(raw\ material)} \qquad \text{Eq.6}$$

It is important to note that the washing step and the difference between the DS% of the unwashed (basic TS and DS analysis) and the washed (fractionation method) analytical methods. Using Table 2, DS% can be created by summing up DSW and DSEA fractions. The unwashed and washed fractions DS% were compared in Table 3. The washing step helped to recover more than double the DS% for the raw materials. Additionally, in all conditions washing step (fractionation method) assisted to increase the DS%.

Table 3. Comparison of washing steps effect on the dissolved solids yield. Unwashed DS% yields based on fundamental DS analysis, washed DS% yields based on fractionation method summation of dissolved solids products. The unwashed DS% error can be found in Table 2.

			unwashed	washed	washed
Product	**T (°C)**	**Time (s)**	**DS%**	**DS%**	**DS% Error (±)**
BLACK LIQUOR	**380°C**	**0**	25.84	58.29	1.73
		0.5	50.06	69.47	0.97
		1	61.89	70.99	0.81
		1.5	63.88	71.48	1.00
BLACK LIQUOR	**390°C**	**0**	25.84	58.29	1.73
		0.5	53.79	67.56	1.36
		1	68.15	71.77	2.02
		1.5	70.37	71.67	2.32
KRAFT LIGNIN	**380°C**	**0**	17.30	36.91	1.14
		0.5	27.03	42.67	3.07
		1	31.39	45.81	4.12
		1.5	37.12	45.51	1.65
KRAFT LIGNIN	**390°C**	**0**	17.30	36.91	1.14
		0.5	34.75	48.83	0.99
		1	42.89	48.48	1.45
		1.5	45.68	48.49	2.89

Total organic carbon (TOC), inorganic carbon (IC), and total carbon (TC) results of the samples were not correlated with the solids mass balance and carbon mass balance. The reason behind that is the effect of washing steps and wrong calculation/estimation of the carbon content by the equipment [39]. The TOC analysis was attempted to be implemented into the calculations as an easy step after TS and DS analyses. However, as can be seen also from the Table 3, effect of washing steps on the DS% to be recovered from the SS% affects the calculations negatively, and not correlates with the solids and carbon mass balance. Table 4 shows the TOC analysis results conducted before the acidification step, without any processing of the raw material or product. The purpose of this analysis was to examine if there was a trend change in the results due to gas or

volatile formation effects. It should be noted that the calculations were not representative of the solids mass balance.

As previously mentioned, the TOC analysis of black liquor products has a drawback which makes the numbers not reflect their real values. Nevertheless, it is useful to compare feedstocks and products to monitor changes in trend. In Table 4, raw materials accepted as reflecting the original values of the TC, and the products TC concentration at different reaction times were calculated concerning their raw material TC concentration. For example, at 380ºC, the TC concentrations were found between 29.27% and 33.38% between 0.5 and 1.5 sec of reaction time compared to the raw material TC concentration. As was mentioned in the discussion of Table 1, KL products TS% for 1 sec and 1.5 sec experiments at 390°C were the usual suspects for the potential gas or volatiles formation. The TOC analysis results of these conditions can also confirm that the difference compared to the raw material was less than the range of the flow rate oscillations of the pilot plant (30 wt% ± 2 wt%). This suggests that the formation of gases or volatiles was more prone in these conditions for KL material.

Table 4. Total carbon content of the raw materials and their depolymerized products at each condition. Change between the raw material and the product for each condition was given in the last column. This analysis was performed without any downstream processing to the raw materials and their products.

Product	T (°C)	Time (s)	TC (g/L)	Difference (%)
BLACK LIQUOR	**380°C**	**0**	**36.10**	**Basis**
		0.5	12.05	33.38
		1	11.78	32.62
		1.5	10.57	29.27
BLACK LIQUOR	**390°C**	**0**	**36.10**	**Basis**
		0.5	12.47	34.55
		1	10.90	30.19
		1.5	10.44	100.00
KRAFT LIGNIN	**380°C**	**0**	**20.90**	**Basis**
		0.5	6.66	31.88
		1	6.83	32.70
		1.5	6.29	30.11
KRAFT LIGNIN	**390°C**	**0**	**20.90**	**Basis**
		0.5	6.44	30.80
		1	5.37	26.51
		1.5	4.90	24.93

The presence of the inorganics in both BL and KL products affects the yield of each product compared to raw materials used. At the same time, it was important to analyze the ash percentages of the products to see if any inorganics were consumed during the reactions or not. This is strategically important to verify, because if the inorganics were not consumed during the reactions, then after the fractionation of the downstream products, inorganics including DSW fraction possibly can be sent directly to the pulp mill process cycle to recover the inorganics to be used. Confirming the inorganics after the reactions were not consumed or knowing the consumption of the inorganics after the reactions was essential to make corrections for the bio-oil or bio-polyol production yield.

There are a lot of sources that published the characteristics of black liquor in the literature. The presence of the inorganics, and their different forms were given in the study of Lappalainen and Niemelä [20,40]. Cooking chemicals of NaOH and Na_2S are the major ones that exist inside the black liquor. Also, the salts of sodium constitute a large fraction compared to the other metal salts. Na_2SO_4, Na_2SO_3, $Na_2S_2O_3$, and Na_2CO_3 are the main inorganic compounds that exist in the black liquor after cooking. Potassium salts of these anions that formed sodium salts also possibly exist as the second largest fraction in black liquor [20]. Other major metals that exist apart from sodium and potassium are aluminum, calcium, magnesium, phosphorus, and silica. The ash concentration found using ash analysis and the quantification of the metals together with the sulfur inside the DSW fraction using ICP-OES are given in Table 5.

Table 5. Ash content and the ICP-OES results of the metals together with the sulfur. Lowest and highest reaction time for both raw materials and temperatures were presented.

#	T	Time	Ash	Al	Ca	Mg	P	Si	K	Na	S	Total
	°C	s	%	ppm					ppt			%
BL	380	0	49.8	57.9	561	279	150	309	26.2	205	150	38.3
		0.5	50.7	22.2	143	130	101	229	27.4	213	152	39.3
		1.5	51.9	2	31.9	11.5	9.27	65.3	30.1	202	163	39.5
BL	390	0	49.8	57.9	561	279	150	309	26.2	205	150	38.3
		0.5	51.3	33.3	311	73.2	33.3	73.8	27.8	206	159	39.3
		1.5	49.9	27.6	116	86.8	20.6	159	28.5	209	167	40.5
KL	380	0	9.4	10.4	340	33.6	12	295	2.14	147	163	31.2
		0.5	8.8	11.9	266	53.2	2	643	2.28	142	164	30.9
		1.5	9.8	16	234	32	4	628	1.27	151	164	32.5
KL	390	0	9.4	10.4	340	33.6	12	295	2.14	147	163	31.2
		0.5	9.6	14.7	760	44.2	17.1	333	2.02	149	156	30.8
		1.5	9.6	48.7	285	29.8	8.93	302	1.99	134	144	28.1

The ash percentages of the samples were found to be ~50 wt% ± 2 wt% for the black liquor raw material and its products, whereas for the kraft lignin raw material and its products it was ~9 wt% ± 1 wt%. There was no clear ash concentration change regarding the BL products compared to the raw material of the BL. That means the inorganics were preserved during the SCW depolymerization. The same observations can be made for KL raw material and the products as well. The kraft lignin ash content was given in section 2.2, which was ~8 wt%. The NaOH concentration to arrange the pH over 13 of the kraft lignin biomass solution to be used in the experiments was 0.3M, which corresponds to ~1.3 wt% of solids. Therefore, the concentration of the ash for both KL raw material and its products confirms the range of ~9 wt% ± 1 wt%. Thus, calculated KL ash concentrations allow us to say the inorganics were not consumed in the SCW depolymerization process.

The inorganic metals concentrations in DSW fraction were found to be approx. 40 wt% ± 2 wt% for BL. Regarding the KL raw material and the products, identified inorganic metals concentration in the DSW fraction was found to be 30 wt% ± 2 wt%. There was no clear trend observed regarding the BL and KL raw material and the products. Although there are small changes in ppm levels of the metals, total concentrations of the metals are preserving well enough which enables this fraction to be recycled to the pulp mills process cycle (green liquor cycle) back to be used. The missing chemicals/metals in this

cycle are being replenished by adding the required chemicals/metals in this cycle after kraft recovery boiler process. In any traditional kraft pulp mills metals and salts concentrations are also being affected by recovery boilers, and make-up chemicals are being added in green liquor cycle [21].

Ash correction was employed to the raw data obtained after solids balance (using data from Table 5) to remove the inorganics from the mass balance calculations, and the corrections followed by the normalization of each fraction to sum of all fractions in each condition. These results were demonstrated in Table 6.

It is obvious that the insoluble material is converted to the soluble material after supercritical water treatment. SSI fraction counts around ~50 wt% of the organic fraction in BL, similarly KL material accounting for 41.44 wt% SSI fraction weight. After 0.5 sec of reaction time, at 380°C, ~15 wt% of the insoluble material is still present, whereas this value decreases to 2.55 wt% at 390°C in BL. Using KL as the raw material allowed less conversion of SSI into soluble material, at 380°C, 21.85 wt% of the sample was not depolymerized, but this number decreased to 5.79 wt% at 390°C. The reaction time of 1 and 1.5 sec at 380°C helped more for both BL and KL to convert the insoluble material into soluble material. This indicates that 380°C and 0.5 sec reaction conditions were not enough to convert SSI into soluble fractions completely. However, when we check the reactions at 390°C for BL, it can be seen that there is a slight increment in the SSI fraction from 2.55 wt% at 0.5 sec to 5.10 wt% and 4.93 wt% at 1 and 1.5 sec, respectively. This could be a signal of repolymerization reactions that took place at the longer reaction times. In depolymerization of kraft lignin, at 380°C, even for long reaction times of 1 sec and 1.5 sec, excess amount of SSI fraction did not go lower than ~8 wt%, while 390°C experiments showed almost complete conversion of SSI into dissolved phase.

Table 6. Black liquor and kraft lignin raw materials (inside the biomass tank) and their depolymerized products dry basis mass balance coupled with the carbon balance using the elemental analysis carbon percentage results of each fraction. Dissolved solids water soluble fraction was corrected by removing the ash content of each sample. After the correction the results were normalized to total organic fractions amount.

#	T	Time	SSI	C_SSI	DSW	C_DSW	DSEA	C_DSEA	SSEA	C_SSEA	SUM	C_SUM	CLOS.	DS	OIL	OIL Error
	(°C)	(s)	(%)		(%)		(%)		(%)		(%)	(%)	(%)	(%)	(%)	±
BL	380	0	49.98	0.56	7.42	0.10	9.32	0.54	33.28	0.54	100.0	51.86	100.0	16.74	42.60	1.32
		0.5	14.96	0.59	21.71	0.06	15.14	0.55	48.19	0.64	100.0	49.42	95.29	38.68	66.46	2.53
		1	1.87	0.55	16.68	0.07	20.99	0.56	60.46	0.65	100.0	53.57	103.3	36.47	78.86	0.67
		1.5	3.01	0.56	20.98	0.06	20.33	0.55	55.68	0.65	100.0	50.46	97.29	42.46	78.13	0.63
BL	390	0	49.98	0.56	7.42	0.10	9.32	0.54	33.28	0.54	100.0	51.86	100.0	16.74	42.60	1.32
		0.5	2.55	0.59	18.94	0.06	18.34	0.56	60.18	0.64	100.0	51.25	98.83	37.71	79.45	1.99
		1	5.10	0.58	20.18	0.06	23.25	0.56	51.46	0.64	100.0	50.36	97.10	44.73	76.94	0.69
		1.5	4.93	0.56	15.09	0.08	24.64	0.56	55.33	0.65	100.0	53.73	103.6	39.73	77.91	1.21
KL	380	0	41.44	0.59	23.87	0.07	5.74	0.57	28.94	0.62	100.0	47.28	100.0	29.61	34.69	1.41
		0.5	21.85	0.58	23.09	0.07	13.36	0.60	41.70	0.64	100.0	49.18	104.0	35.04	52.93	3.85
		1	7.56	0.60	31.86	0.08	9.43	0.58	51.14	0.66	100.0	46.52	98.40	41.97	61.57	1.47
		1.5	8.57	0.59	34.09	0.08	9.52	0.60	47.82	0.66	100.0	45.22	95.65	45.59	59.95	3.32
KL	390	0	41.44	0.59	23.87	0.07	5.74	0.57	28.94	0.62	100.0	47.28	100.0	29.61	34.69	1.41
		0.5	5.79	0.58	34.60	0.07	10.84	0.59	48.77	0.66	100.0	44.45	94.03	48.33	63.40	1.36
		1	0.52	0.63	28.47	0.04	16.82	0.62	54.19	0.68	100.0	49.07	103.8	43.63	68.42	2.07
		1.5	0.23	0.60	29.95	0.07	16.57	0.62	53.25	0.67	100.0	48.16	101.8	45.67	68.54	5.27

After removing the ash content from the DSW fraction, BL raw material had 7.42 wt% of DSW fraction. On the other hand, surprisingly, this value was three-fold more for the KL raw material. As was mentioned in the experimental section, KL was obtained after acidification and removal of the soluble fraction of the BL. Therefore, acidification could be responsible for creating a colloidal water soluble kraft lignin. Maitz et al. explain the effect of acidification and washing of kraft lignin to form a stable colloid in aqueous solution [41]. Though this solubilization was performed at higher pH around 8-9 in the cited study, and the kraft lignin used in this study was obtained after precipitating black liquor until pH 2. It is known that kraft lignin generally has a limited solubility once it is obtained using acidic pH range. Nevertheless, raw material downstream processing was performed after kraft lignin solubilized in NaOH solution. This could be the reason for observing higher DSW fraction for the KL raw material. Yet, this needs to be examined meticulously in the future by using more advanced techniques such as NMR.

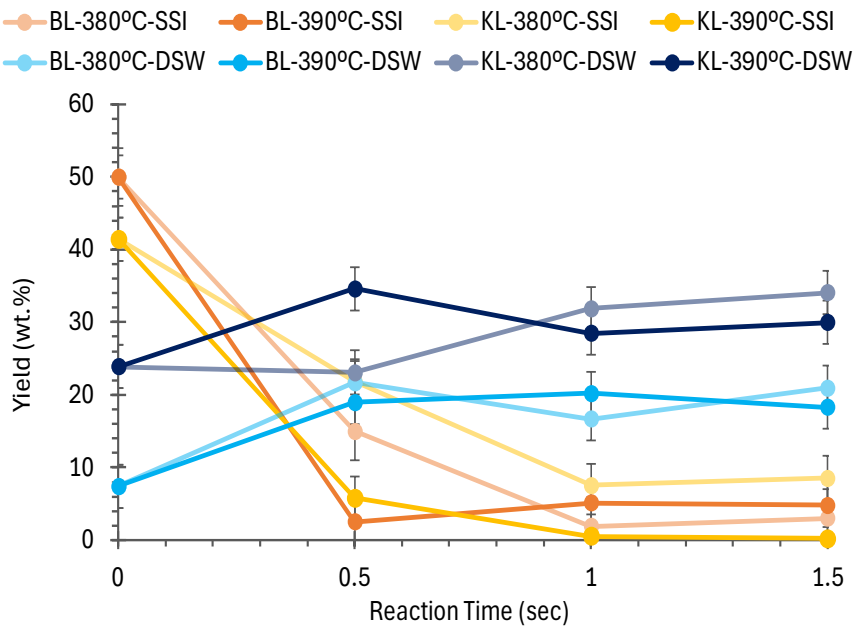

Figure 4. Comparison of black liquor and kraft lignin raw materials and their depolymerized products suspended solids insoluble fraction (SSI) and dissolved solids water soluble fraction (DSW) at each condition.

After the SCW depolymerization of BL and KL, it is apparent from Table 6 that DSW fractions increased for each reaction time. That means during depolymerization, the SSI fraction not only participates in depolymerization, but also partially becomes soluble in water, and contributes to the increment of the DSW fractions. Yields of SSI and DSW at each reaction time for BL and KL were demonstrated in Figure 4. As the SSI yield

decreases, DSW yield increases for both BL and KL. However, KL has higher yield of DSW fraction compared to BL at each reaction time except 0.5 sec and 380°C, which is within the margin of error.

Figure 5 illustrates the relationship between the yield of total bio-oil and the SSI fractions changes with respect to the reaction time of both BL and KL. The maximum oil yield obtained by the SCW depolymerization of BL was 79.45 wt% for 390°C and 0.5 sec. Nevertheless, this percentage was between the margin of the error for all BL experiments at 390°C. Although at 380°C, 0.5 sec experiment was not enough to obtain the highest bio-oil yield, by increasing reaction time, bio-oil yield of BL enhanced and reached 390°C yield levels at 1s and 1.5s reaction time. KL gave higher bio-oil yield at 390°C at each reaction time compared to 380°C. The maximum total bio-oil yield was observed as 68.54 wt% for 390°C, and 61.57 wt% for 380°C. Both SSI yield and total bio-oil yield for 1 and 1.5 sec reached the maximum for BL and KL at both temperatures.

As was mentioned throughout the thesis, while many studies have been conducted on lignin depolymerization with basic catalysts, only a few studies have employed direct black liquor depolymerization under supercritical water conditions with base catalysis. Making a comparison between each study is quite hard and indirect, due to the use of the terminology of “bio-oil” differently and subjectively by each author. Nevertheless, a summary and a comparison of the studies will be given here. It is worth starting with our previous group member’s study, Fernandez et al. indicated that it is possible to produce large amount of monomer rich light oil yield of 51.3 wt% for commercial hardwood black liquor. Optimum reaction conditions were found to be 386ºC and 26 MPa by 0.3 sec of reaction time. The same study claims that it is possible to obtain 60 wt% of monomer rich light oil using Sigma-Aldrich kraft lignin. Total bio-oil yield using hardwood kraft lignin and Sigma-Aldrich kraft lignin were found as 96.3 wt% and 72.6 wt%, respectively. Monomer yields found were reached around 20 wt% inside the light oil fraction [1]. Rodriguez studied in his thesis different biomass materials (almond shell, olive tree pruning, etc.), as well as kraft black liquor and kraft lignin depolymerization at high temperature and pressure (300ºC & 90 bar), with a long reaction time (80 min) using a batch reactor [23]. They used a meticulous downstream separation to be able to reach their four different classified fractions. They claimed that the maximum monomer rich light oil fraction lies between 20-25 wt% of the organic material. They evaluated suspended solid THF soluble fraction as residual lignin instead of classifying it as an oil fraction. As it was expected, the coke formation in the study of Rodriguez et al. was quite

high, which is a drawback of the batch reactors and long reaction times. Contrarily, in Fernandez's study, char formation was quite low since the reaction time was very low, and the advantage of instantaneous heating and cooling system [1]. However, both studies lack considering black liquor raw material organic fraction in their blank studies. Therefore, the bio-oil yield found in these studies does not reflect a real comparable value produced by their processes. Moreover, it can be said that this biased approach to determine bio-oil yield is not only limited to these two studies, but also could be seen in the rest of the literature.

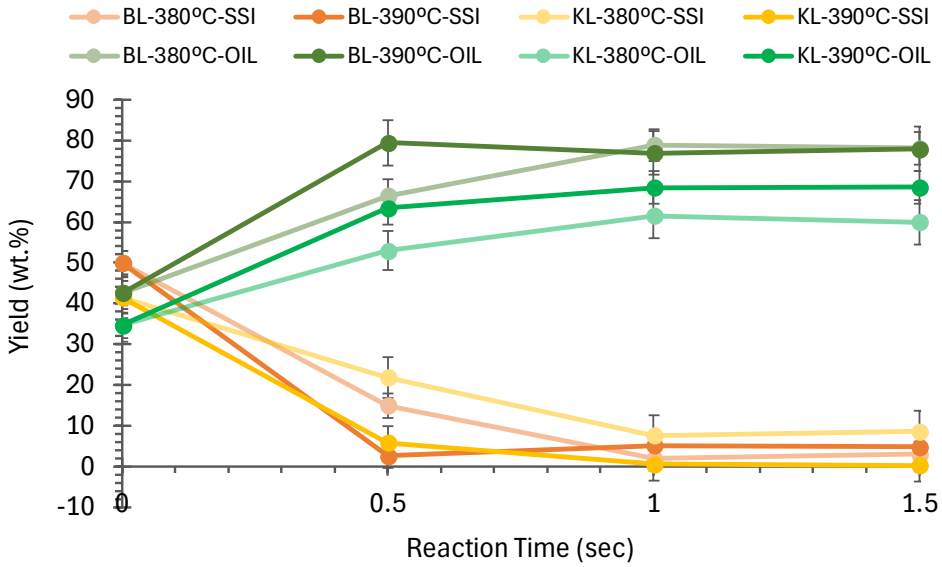

Figure 5. Comparison of black liquor and kraft lignin raw materials and their depolymerized products suspended solids insoluble fraction (SSI) and total bio-oil yield at each condition.

Orebom used black liquor directly at 380ºC, 34 MPa for 1 hour and found that bio-oil yield of ~78 wt.% based on the starting material of lignin [6]. In the study of Solantausta et al., hydrothermal liquefaction of softwood kraft black liquor yielded 70 wt.% of bio-oil under 350ºC, saturation pressure in 45 min [33]. These experiments were also conducted in a batch reactor. A summary of maximum bio-oil yields and their corresponding process conditions of the selected studies can be found in Table 7.

Table 7. Maximum bio-oil yields vs corresponding process conditions. Each process should be evaluated considering corresponding conditions.

Material	Reactor	Max_Yield	Conditions	Time	Ref.
Kraft Lignin	Continuous, Plug Flow	91.5 wt%	386°C, 26 MPa, with NaOH	0.3 sec	[1]
Sigma Kraft Lignin	Continuous, Plug Flow	72.6 wt%	386°C, 26 MPa, with NaOH	0.3 sec	[1]
Sigma Kraft Lignin	Continuous, Plug Flow	21 wt%	390°C	5 sec	[29,30]
Sigma Kraft Lignin	Batch	62 wt%	350°C	5 min	[31]
LignoBoost Lignin	Continuous, Fixed Bed	87.7 wt%	310°C, 25 MPa, ZrO2 catalyst	10-13 min	[32]
Black Liquor	Batch	70 wt%	350°C	45 min	[33]
Black Liquor	Batch	78 wt%	340-350°C, 34-41 MPa	1 h	[6]
Alkali Lignin	Batch	90 wt%	320°C, EtOH:H_2O 1:1 (v:v), 5 MPa H_2	2 h	[42]

In this work, different than the literature, the organic fraction effect of the initial raw material (inside the black liquor) was taken into account to create a proper and reliable mass balance data. The downstream separation fractions of BL and KL products created in this work have already been explained elsewhere before [1,43]. To remind the reader one more time in detail; ***SSI fraction*** supposedly includes the highest molecular weight components and includes larger size of the fragments which could be increased by the repolymerization reactions. If the repolymerization reactions took place after harsh processing conditions, then char or coke formation should be present in this fraction, which can be insoluble in any solvent. However, as this fraction does not possess affinity through water or ethyl acetate solvents, but can become soluble in other solvents, it is labeled in this work as a suspended solids insoluble fraction. ***SSEA fraction*** *(high molecular weight heavy oil)* contains high molecular weight fragments such as repolymerization products of oligomers and monomers between each other. It can also include unreacted lignin such as high molecular weight polyphenols which are not volatile. Depending on the nature of the process, this fraction could possess a huge value due to exhibiting biopolyol characteristics. Although SSEA fraction is insoluble in water, its affinity is close enough to be dissolved in ethyl acetate. ***DSEA fraction*** *(monomer rich aromatic light oil)* consists of mainly aromatic monomers, dimers, trimers and low boiling point oligomers. They have high functionality, and molecular weight generally under 400 Da which enables them to be analyzed by GC-MS. They are soluble in water, but their polarity makes them have higher affinity towards ethyl acetate. ***DSW fraction*** can consist of carbohydrates, and lignin fragments that are partially depolymerized and their

solubility enhanced in water. Aliphatic hydroxyl and carboxyl groups containing monomers can also exist in this fraction.

Figure 6 demonstrates the DSEA and SSEA yield for each reaction time for both BL and KL. Initially, without any treatment, BL raw material contained 9.32 wt% DSEA fraction (monomer rich aromatic oil), whereas for KL raw material DSEA yielded only 5.74 wt%. Maximum DSEA yield for BL was found to be around 21 wt% and 24.64 wt% at 380°C and 390°C, respectively. Regarding KL, strangely at 380°C and 0.5 sec, DSEA yields reach a maximum and then the yield decreases for longer reaction times. That means possibly during SCW depolymerization the monomers produced reacted with different fragments, and participated possibly in repolymerization reactions, which is quite likely as the SSEA fraction yield increases for both 1 and 1.5 sec reactions of KL at 380°C. At 390°C, KL DSEA yield increased until 1 sec, and then remained constant.

Considering a vast number of studies on base catalyzed depolymerization of lignin, and their average monomer yields, it is possible to say that the monomer yields of BCD are generally below 20 wt%, and the major distribution of the monomer yields accumulated around 10 wt% for this process [2]. It can be seen in the literature that there are a lot of experiments that reach higher oil yields but lower monomer yields using BCD for lignin, and only a few studies that focus on black liquor as a raw material [2,6,20,33].

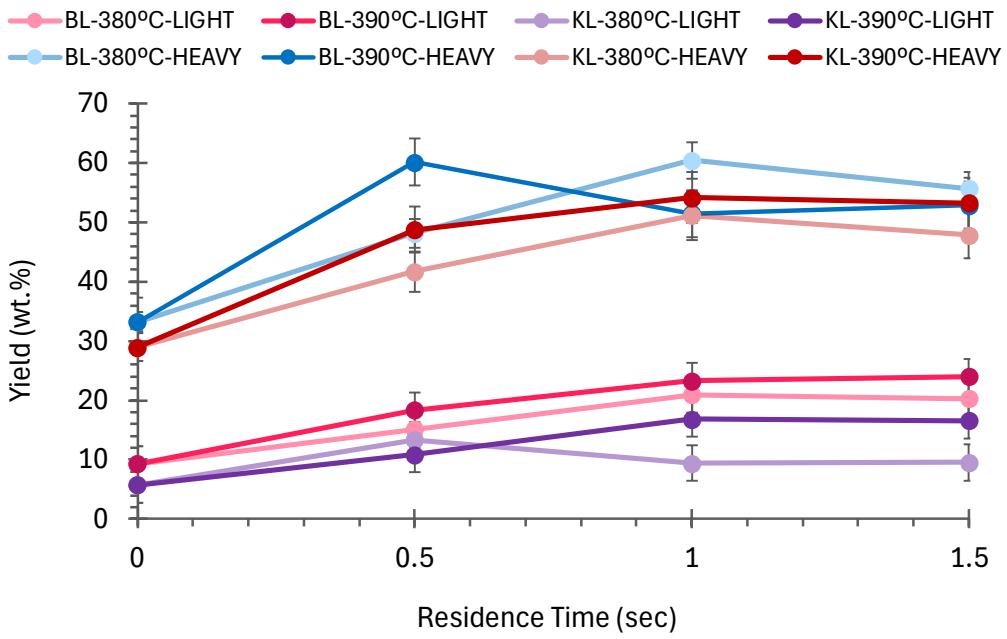

Figure 6. Comparison of black liquor and kraft lignin raw materials and their depolymerized products dissolved solids ethyl acetate extracted fraction (DSEA - light

oil) yield and suspended solids ethyl acetate extracted fraction (SSEA – heavy oil) yield at each condition.

The initial SSEA yield for BL raw material was found to be 33.28 wt%, while it was 28.94 wt% for KL raw material. After SCW depolymerization, these numbers increased for each reaction condition for both BL and KL products. Maximum SSEA yield was around 60 wt% for BL at 380°C and 1 sec, and 390°C and 1.5 sec conditions. Regarding KL, the maximum SSEA yield was around 54 wt% at 390°C, 1 sec and 1.5sec reaction times, while it was around 51.14 wt% at 380°C and 1 sec. Opposite to our previous group member's work [1,28], according to Table 6 and Figure 6, SSEA fraction was more favorable to produce compared to DSEA fraction by base catalyzed SCW depolymerization to convert insoluble lignin. However, it is worth noting that here, the concentration of the lignin at the inlet of the reactor was around 0.5 wt% in Fernandez's work, whereas in this work it was around 1.0 wt%.

Table 8. Dissolved solids ethyl acetate extracted fraction yield (DSEA – light oil) and the monomers identified and quantified in this fraction for both black liquor and kraft lignin raw materials and their depolymerized products at each process condition. Error percentage for any component was found lower than 12%.

			LIGHT OIL	MONOMERS							
	T	Time	DSEA	G	S	V	AVA	SA	ASY	Total in DSEA	Total In organics
#	°C	s	(%)	%	%	%	%	%	%	%	%
BL	380	0	9.32	0.38	1.03	0.61	0.55	1.57	2.29	6.43	0.60
		0.5	15.14	0.22	2.20	0.67	0.63	1.76	2.29	7.77	1.18
		1	20.99	0.30	4.91	1.16	1.26	2.47	3.65	13.75	2.89
		1.5	20.33	0.30	5.80	1.24	1.46	2.82	4.00	15.62	3.18
	390	0	9.32	0.38	1.03	0.61	0.55	1.57	2.29	6.43	0.60
		0.5	18.34	0.43	5.31	1.26	1.42	2.91	4.15	15.49	2.84
		1	23.25	0.36	6.33	1.50	1.48	2.23	3.35	15.25	3.55
		1.5	24.04	0.30	6.50	1.84	1.63	2.39	3.40	16.07	3.86
KL	380	0	5.74	-	-	0.27	0.42	0.64	2.22	3.55	0.20
		0.5	13.36	0.10	0.34	0.55	0.59	1.20	3.25	6.04	0.81
		1	9.43	0.11	2.82	0.60	0.92	1.46	4.04	9.96	0.94
		1.5	9.52	0.65	2.93	0.54	1.91	-	5.90	11.93	1.14
	390	0	5.74	-	-	0.27	0.42	0.64	2.22	3.55	0.20
		0.5	10.84	0.15	2.88	0.88	0.87	1.31	3.57	9.66	1.05
		1	16.82	0.43	5.31	-	1.86	-	4.23	11.83	1.99
		1.5	16.57	0.39	5.31	-	1.52	-	3.45	10.68	1.77

The yield of the aromatic monomers obtained during the reaction was quantified using GC-MS analysis. Guaiacol, syringol, vanillin, acetovanillone, syringaldehyde and

acetosyringone were the major monomers identified and quantified. These aromatic monomers were present inside the DSEA fraction of the SCW depolymerized black liquor product. The yield of the DSEA fraction was discussed before. One of the most important points of this study was to highlight the presence of the monomers inside the raw material. Black Liquor, as a raw material, accommodates approximately 6.43% of the aromatic monomers inside the DSEA fraction. Table 8 gives the yields of aromatic monomers in the DSEA fraction and yields of them in total organic fraction after eliminating the inorganics for each reaction condition.

Considering the black liquor as the raw material, the effect of temperature looks like has an effect at shorter reaction times of 0.5s and 1s. At 380°C and 0.5s the total aromatic monomers yield was found to be 7.77%, while at 390°C and 0.5s the yield was 15.49%. Increasing the reaction time by more than 0.5s at 390°C did not affect the total monomer yield significantly. However, at 380°C and 1s, it can be seen that total monomer yield is still 13.75% for black liquor, with a little gap to reach the maximum yield. After the reactions, monomers of syringol, syringaldehyde, and acetosyringone were the dominant ones compared to the other three monomers. By increasing the reaction time, a greater amount of aromatic monomers is produced at 380°C. At 390°C, this observation was also valid, except for the monomers of syringaldehyde and acetosyringone. These two monomers gave a maximum yield of 2.91% and 4.15%, respectively at 0.5s, and increasing the time resulted in less yield of these two. It could be possible that, at higher temperatures, these two monomers tend to be involved in (re)polymerization reactions, or they participated in depolymerization reactions to produce different kinds of compounds. Syringol, vanillin, and acetovanillone were found higher at 390°C, while syringaldehyde and acetosyringone were found higher at 380°C. Guaiacol yields were almost identical for both temperatures.

Regarding the aromatic monomers yields using KL as raw material, it was expected that there wouldn't be any aromatic monomers present after producing kraft lignin. Since kraft lignin production is carried out by precipitation of the solid material and the removal of the dissolved solids, not expecting any aromatic monomers inside the DSEA fraction would be reasonable. However, since the precipitation of kraft lignin was carried out in a large scale, only guaiacol and syringol were completely removed from the KL. The ash percentage of 7-8% of KL also includes the residual water-soluble components present inside the KL material. Though, except acetosyringone, other monomers were less than 1% inside the DSEA fraction of KL raw material. As can be seen in Table 8, increasing the

reaction time increases the monomer yields for both temperatures. However, at 390°C, between 1s and 1.5s reaction time, a decline in the monomer yields can be observed. Nevertheless, the monomer yields of KL, before and after the reaction, were obtained less than BL. The most interesting points of the KL experiments in monomer quantification were the disappearance of syringaldehyde at 380°C and 1.5s, and both vanillin and syringaldehyde at 390°C, 1s and 1.5s of reaction time.

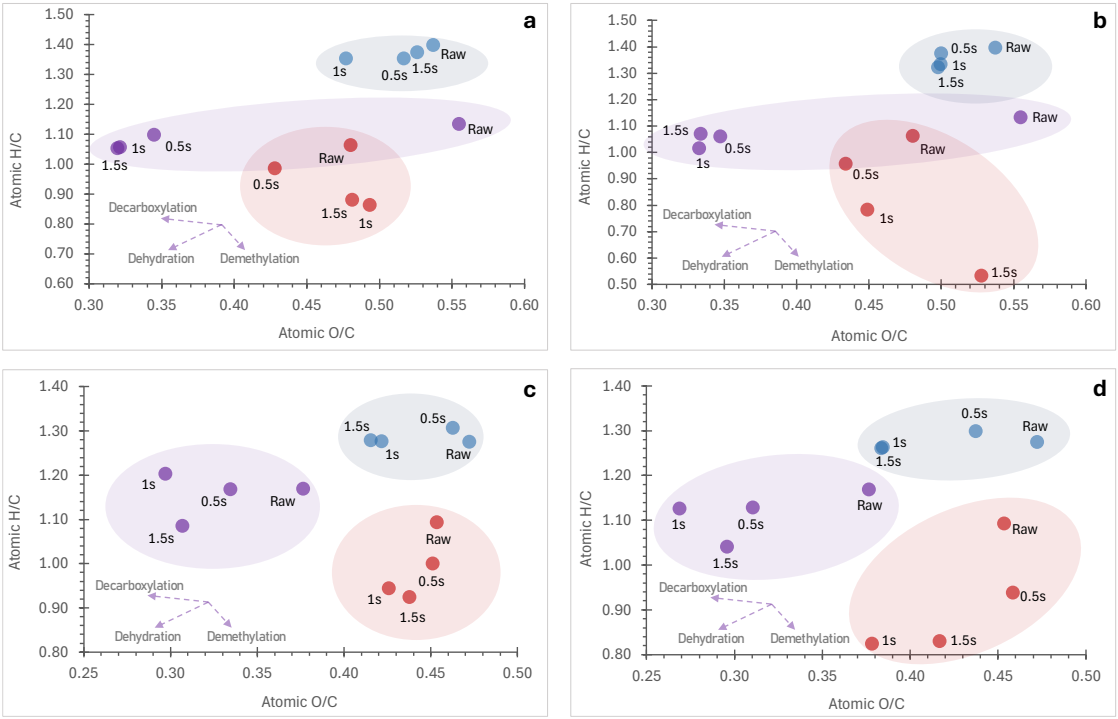

Figure 7. Illustration of the elemental analysis results using van Krevelen's diagram for the comparison of black liquor (BL) and kraft lignin (KL) raw materials and their depolymerized products fractions at different temperatures. Elemental analysis results of BL at 380°C **(a)**, BL at 390°C **(b)**, KL at 380°C **(c)**, and KL at 390°C **(d)**. ***Blue zone*** indicates *DSEA fraction*, ***purple zone*** indicates *SSEA fraction*, ***red zone*** indicates *SSI fraction*.

Van Krevelen's diagram of the elemental analysis results can be seen in Figure 7 as grouped for each temperature and raw material used in this study. These diagrams are used to understand which type of mechanisms were more dominant at each reaction time and each fraction. According to Figure 7a, it can be seen that at 380°C, the DSEA fraction first showed dehydration characteristics until 1s of reaction time, and then oxygenation. SSEA fraction, on the other hand, was under the influence of overall dehydration. The gap between the raw material and the products in terms of O/C ratio is quite striking. The O/C ratio decreased from 0.55 (BL raw material) to 0.32 (BL at 380°C

& 1.5s). The results of SSI fraction show that after having dehydration as the dominant mechanism at 0.5s, demethylation reactions became more prevailing between 0.5 to 1.5s. Similarly, the domination behavior of the reaction mechanisms at 390°C was almost the same as the ones at 380°C, except for small differences between subsequent reaction times. Nevertheless, overall, compared to the raw material, products were located in the dehydration zone.

Regarding the experiments with KL, the DSEA fraction underwent decarboxylation and dehydration route at both 380°C and 390°C. SSEA fraction at 380°C passed through decarboxylation and demethylation routes, while at 390°C dehydration followed by demethylation routes were more favorable. In terms of SSI fraction, after showing a dehydrogenation until 0.5s, the mechanism shifted through dehydration and demethylation at 380°C. SSI fraction of KL at 390°C experienced a higher ratio of dehydrogenation compared to 380°C, and then followed dehydration and oxygenation pathways.

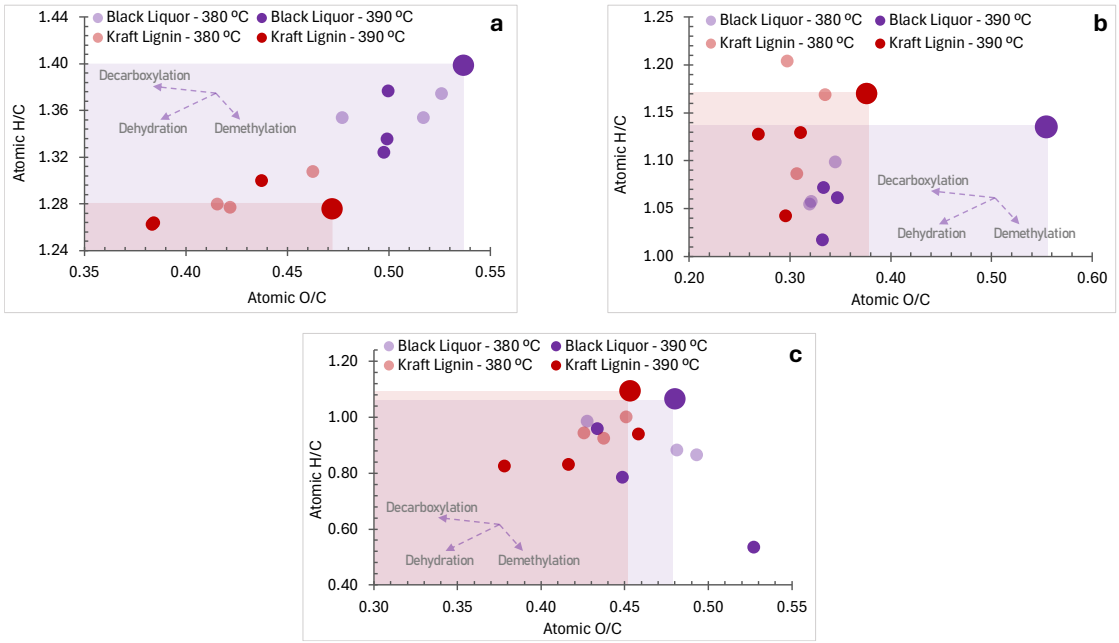

Figure 8. Illustration of the elemental analysis results using van Krevelen's diagram for all the conditions. Elemental analysis results were given as DSEA fraction **(a)**, SSEA fraction **(b)**, and SSI fraction **(c)** to compare each fraction. *Black liquor (BL)* results were indicated in ***purple***, and *kraft lignin (KL)* results were indicated in ***red***. The large data points indicate the raw material results of that fraction. The experimental errors of the

data points are inside the circle marker area. The dehydration zone was marked in ***purple rectangular zone for BL***, in ***red rectangular zone for KL*** to track the changes easily.
Figure 8 displays all experimental data points for both BL and KL, for both temperatures with respect to each fraction. It also allows us to make a comparison between BL and KL elemental analysis data points. Figure 8a demonstrates that using BL as a raw material leads all data points of DSEA fraction to be in the region of dehydration. Although only precipitation and washing processes were performed to obtain KL raw material, these two fundamental separation procedures led KL raw material to be in the dehydration zone of BL raw material. Compared to KL raw material, the products of KL had only 2 data points outside of the dehydration zone. Regarding the SSEA fraction of BL, as can be seen from Figure 8b, the products of BL are quite deoxygenated compared to the raw material, and all products hit the dehydration zone. This time SSEA fraction of KL shifts to the decarboxylation zone of raw BL just with the separation steps. The SSEA fraction of KL products indicates more decrement in the H/C ratio compared to the DSEA fraction of KL products. BL and KL raw materials position in the van Krevelen diagram in Figure 8c were very close to each other. KL products tend to stay inside the dehydration zone except for one case, while there are three data points of BL products inside the demethylation zone.

When it is looked at subsequently to the reaction times of each fraction, it is possible to see demethylation that comes after a dehydration or a decarboxylation step as more visible in Figure 7. However, Figure 8 demonstrated that, overall, only a few data points stayed outside of the dehydration zone compared to their corresponding raw material. 380°C 1 and 1.5s, and 390°C 1.5s SSI fraction of BL products followed demethylation compared to raw BL. Considering the complete reaction routes followed for both raw material and each experimental data point of elemental analysis results, a clear trend or correlation was not found. Although there were differences when the reaction time was considered subsequently for both BL and KL, overall, both had similar reaction routes with respect to the temperature for their corresponding raw material.

Gel permeation chromatography chromatogram results of BL and its depolymerized products are given in Figure 9. BL raw material DSEA fraction gave a multi-modal distribution of three clear and different molecular weight (Mw) sizes, while SSEA had a bimodal distribution with two clear peaks, and SSI presented one major peak and small shoulders. At 380°C, the higher intensity of bigger Mw sized components of the DSEA fraction of raw BL decreased by increasing the reaction time, and the medium Mw sized

components shifted to the right by increasing reaction time. Though raw material had a higher intensity of lowest Mw sized components (at 16.4 min), slight depolymerization was observed overall at this temperature by increasing the reaction time. At 390°C, the changes at each reaction time compared to the previous one were more dramatic. First, depolymerization at 0.5s can be seen clearly, which then led to repolymerization reactions of the DSEA components, at 1s of reaction time Mw sizes were larger than 0.5, and the largest Mw sized components were observed at 1.5 s of reaction time. Although the first peak at the highest Mw zone decreased significantly at 1.5s compared to the raw BL, the chromatogram shifted to the left clearly shows the increment of the Mw of the fraction.

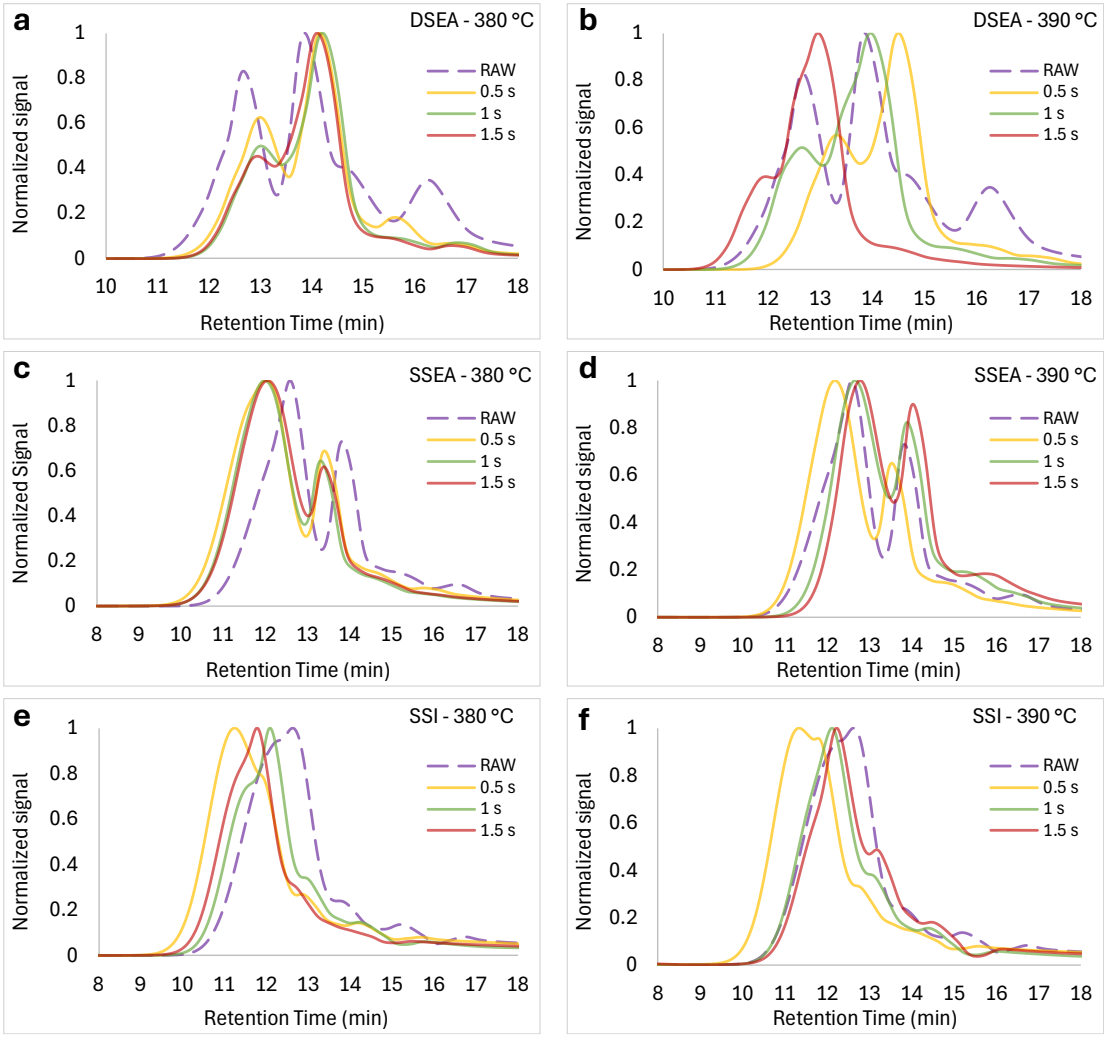

Figure 9. Illustration of the gel permeation chromatography results for the black liquor (BL) and its depolymerized products fractions after downstream processing. Molecular weight distribution of DSEA fraction at 380°C **(a)**, and at 390°C **(b)**; SSEA fraction at 380°C **(c)**, and at 390°C **(d)**; SSI fraction at 380°C **(e)**, and at 390°C **(f)**,

Regarding the SSEA fraction (Figure 9c and 9d), it is obvious that at 380°C, all the peaks shifted to the left, meaning that (re)polymerization occurred compared to the raw material. There is a very slight difference between the Mw of the products at each reaction time. At 390°C, on the other hand, the first polymerization occurred at 0.5s of reaction time, which was then followed by depolymerization reactions of the SSEA fraction. However, the products of BL at 390 for this fraction were found to have slightly higher Mw compared to the raw BL.

Comparing the results of the SSI fraction (Figure 9e and 9f) demonstrated that (re)polymerization reactions took place at each reaction time for both 380°C and 390°C. However, the level of these reactions at 380°C 0.5 was higher than 1s and 1.5s. Similar observations can be made for 390°C reactions as well. Mw of BL product at 0.5s had the highest Mw.

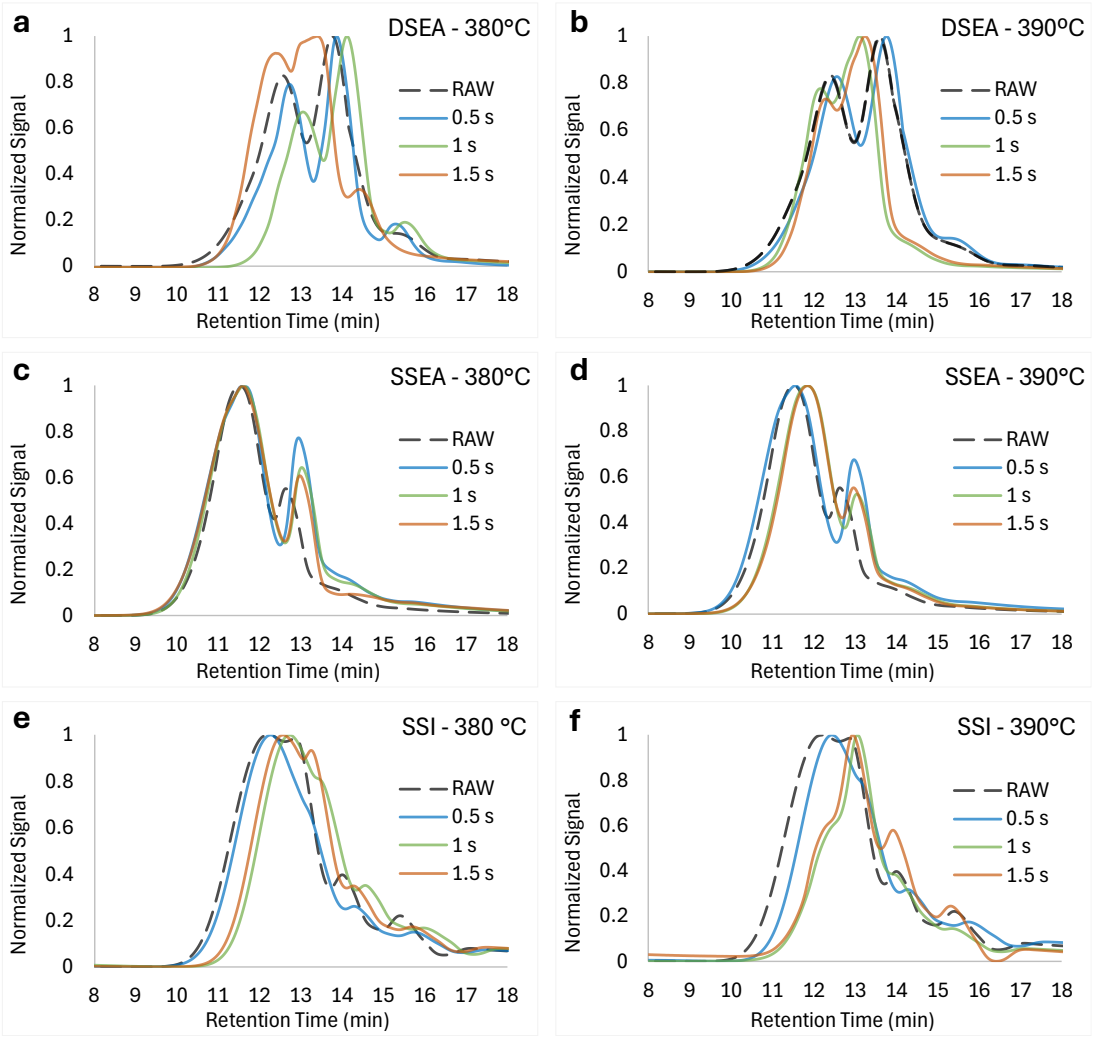

Figure 10. Illustration of the gel permeation chromatography results for the kraft lignin (KL) and its depolymerized products fractions after downstream processing. Molecular

weight distribution of DSEA fraction at 380°C **(a)**, and at 390°C **(b)**; SSEA fraction at 380°C **(c)**, and at 390°C **(d)**; SSI fraction at 380°C **(e)**, and at 390°C **(f)**,
GPC analysis results of KL and its depolymerized products are given in Figure 10. A similar multi-modal molecular weight distribution was observed for the KL raw material DSEA fraction (Figure 10a and 10b). The highest Mw peak was observed at a higher retention time at 380°C, however the smaller peak intensity at the lowest retention time was increased as the reaction time increased. That makes it obvious, repolymerization reactions took place for the DSEA fraction even at 380°C. The DSEA fraction of KL at 390°C had less dramatic changes interestingly. Although after 0.5s reaction molecular weight of the fraction decreased slightly, 1s and 1.5s reaction time results demonstrated a clear repolymerization tendency at these conditions. The reaction time of 1s yielded the highest Mw fraction at this temperature.

SSEA fraction at 380°C did not change with reaction time significantly (Figure 10c). This time the highest peak was at a lower retention time as a greater amount of high Mw fragments were expected to be in this fraction. At 0.5 seconds, lower Mw components gave the maximum, and then they showed a decrement at 1s and 1.5s experiments. The remarkable point of this fractions' analysis was that the SSEA fraction had higher Mw than the raw KL. From Table 9, it can be seen that the SSEA fraction of KL and its depolymerized products yield a higher Mw fraction compared to the SSI fraction, which supports the presence of the repolymerization reactions. At 390°C and 0.5s reaction conditions, had higher Mw compared to raw material, however, it is clear that depolymerization of the SSEA was performed at longer reaction times of 1s and 1.5s. This suggests that KL raw material requires a longer reaction time for the depolymerization of SSEA fraction.

Compared to the SSEA fraction, the SSI fraction at both temperatures yielded lower Mw, which was not expected. Possibly, the SSI fraction compounds participate in the depolymerization, but before depolymerizing more, these depolymerized fragments took part in the repolymerization reactions with higher functional group molecules which makes them soluble in ethyl acetate. This should be the reason why the SSEA fraction had higher Mw compared to the SSI fraction. This allows us to say that the reaction times applied in this study were not long enough to produce larger Mw sized fragments in the SSI fraction (char, coke, etc.) of KL products.

Table 9. Molecular weight (Mw) quantification results together with the polydispersity index (PDI) for both black liquor and kraft lignin raw materials and their depolymerized products at each process condition.

Product	T	Time	M_w			PDI		
#	°C	s	DSEA	SSEA	SSI	DSEA	SSEA	SSI
BL	380	Raw	251	415	589	2.782	3.027	3.139
		0.5	181	761	1261	2.191	3.668	4.677
		1	162	698	808	1.869	3.135	3.341
		1.5	169	665	1029	1.842	3.132	3.771
BL	390	Raw	251	415	589	2.782	3.027	3.139
		0.5	128	527	1134	1.830	3.065	4.200
		1	217	298	670	2.057	2.641	2.991
		1.5	417	253	568	2.064	2.489	2.856
KL	380	Raw	416	959	582	2.920	3.247	3.752
		0.5	326	1075	558	2.818	3.957	3.539
		1	383	1053	325	2.128	3.740	2.779
		1.5	385	1143	373	2.389	3.816	2.895
KL	390	Raw	416	959	582	2.920	3.247	3.752
		0.5	363	1090	441	2.865	3.838	3.252
		1	441	842	327	1.986	2.938	2.648
		1.5	383	838	366	2.000	2.849	3.243

GPC analysis quantification results are given in Table 9. The relationship between Mw and PDI also can be seen from this table. Regarding BL depolymerization experiments, the following order of the molecular weights and polydispersity index (PDI) were obtained DSEA<SSEA<SSI for both temperatures. KL raw material had higher Mw and PDI for both DSEA and SSEA fractions compared to BL raw material. That also proves after precipitation and removing the dissolved solids phase to obtain kraft lignin, smaller Mw compounds were removed from the medium, and caused higher Mw fraction KL raw material. A similar trend was observed for both BL and KL at 380°C regarding the SSEA fraction. At this temperature, the SSEA fraction molecular weight was increased using both raw materials. At 390°C, after an increase in SSEA fraction Mw at 0.5s of reaction time, increasing the time further helped to decrease the molecular weight of this fraction.

Differential thermograms of the thermogravimetric analyses are given in Figure 11. As the amount of the samples of KL was not enough, only BL and its depolymerized products were constructed this figure. As can be seen in the dotted regions of Figures 11a and 11b, the DSEA fraction had a higher weight loss rate at 390°C at lower evaporation temperatures compared to 380°C. Although at 390°C, the overall molecular weight of the DSEA fraction yields a higher molecular weight than in 380°C experiments,

this is because of the repolymerization reactions presence. Over 600°C of the TGA analysis, 1s and 1.5s products of BL showed weight loss, which corresponds to the presence of the repolymerization moieties. At 380°C depolymerization experiments, TGA analysis shows that over 600°C, the presence of repolymerization moieties is quite low. Nevertheless, Figures 11e and 11f demonstrate that, at 380°C, BL products SSI fraction does not completely lose high Mw fragments. This can be understood from Figure 11e due to the presence of the weight loss at any reaction time over 600°C of thermogram. Contrarily, at 390°C, there is no indication of the high Mw fragments of the BL raw material at any reaction time. Employing higher reaction times at the supercritical water conditions could have led to the presence of repolymerization moieties inside the SSI fraction. However, DTG data do not present any indication about that. Fernandez mentioned that in her thesis, this SSI fraction showed repolymerization peaks at 386°C and between 0.3s and 0.5s [1]. Their hypothesis was based on the production of a greater amount of monomers before repolymerization reactions take place. However, the experiments carried out in this work show that depolymerization and repolymerization reactions occur simultaneously and the starting of repolymerization reactions does not stop the production of lower molecular weight fragments by increasing reaction time. Though, by using larger experimental design data points this hypothesis should be challenged.

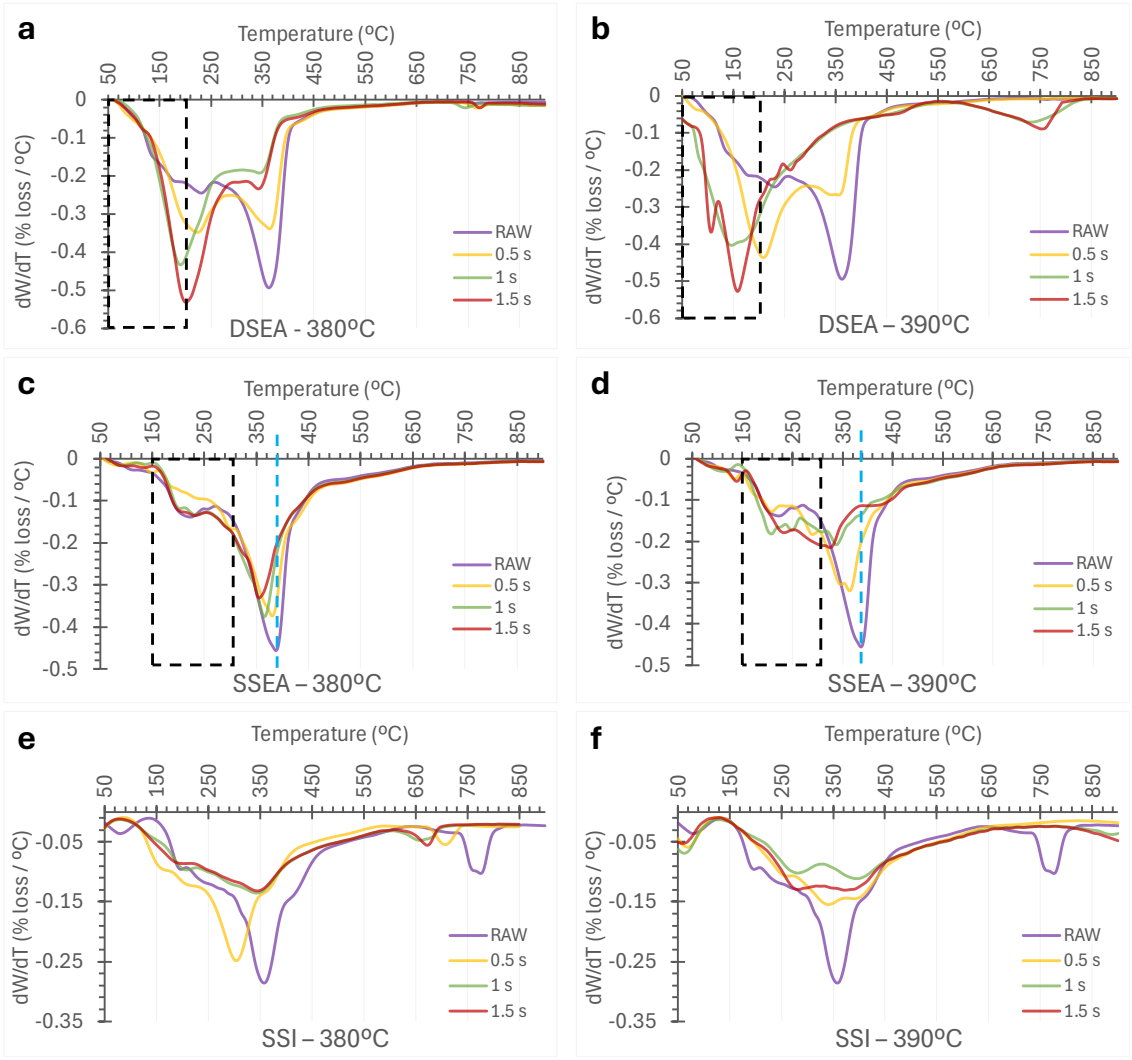

Figure 11. Illustration of the thermogravimetric analysis results for the black liquor (BL) and its depolymerized products fractions after downstream processing. Molecular weight distribution of DSEA fraction at 380°C **(a)**, and at 390°C **(b)**; SSEA fraction at 380°C **(c)**, and at 390°C **(d)**; SSI fraction at 380°C **(e)**, and at 390°C **(f)**,

The SSEA fraction of BL products did not show any weight loss peak over 600°C at both 380°C and 390°C temperatures. Still, the amount of weight loss rate was higher at 390°C, indicating the presence of depolymerized fragments or changes in composition. The depolymerized material may have a different chemical composition, with a higher proportion of less thermally stable components. This could be due to the selective breakdown of certain bonds or the presence of specific degradation products that were not significant or bonded differently in the raw material. This analysis can be easily understood visually from Figures 11c and 11d. Comparing the dotted zones of Figures 11c and 11d and taking into account the GPC results presented in Table 9, it can be

observed that low molecular weight fragments are present within the SSEA fraction at 390°C 1s and 1.5s BL products.

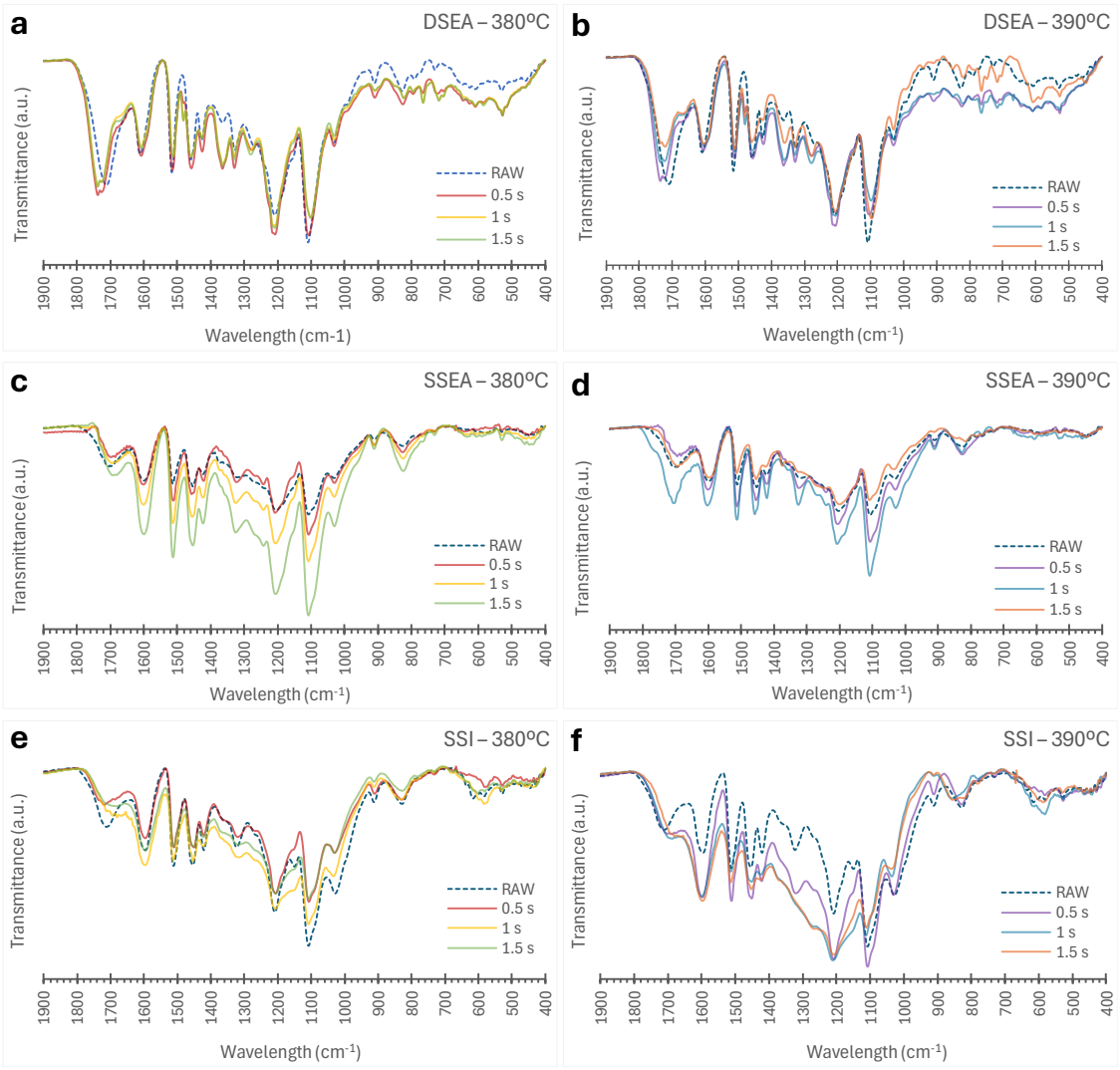

Figure 12. Illustration of the FTIR results for the black liquor (BL) and its depolymerized products fractions after downstream processing. Molecular weight distribution of DSEA fraction at 380°C **(a)**, and at 390°C **(b)**; SSEA fraction at 380°C **(c)**, and at 390°C **(d)**; SSI fraction at 380°C **(e)**, and at 390°C **(f)**,

Fingerprint region spectra of the BL and its depolymerized products analyzed using FTIR are given in Figure 12. As the amount of the samples of KL was not enough, only BL and its depolymerized products were constructed this figure. Although there were small differences between fingerprint zone FTIR signals of each fraction, a list of the wavelengths and their corresponding assignments with the origin of each band were given in Table 10. Comparing the DSEA fraction of both 380°C and 390°C experiments demonstrated the change of C=O unconjugated vibrations of the esters and ketones at

1730 cm^{-1}. At 380°C, at any reaction time the band at 1730 cm^{-1} still exists (Figure 12a), however, Figure 12b shows a decreasing intensity of this bond by increasing reaction time for 390°C. This peak was not observed in the fractions of SSEA and SSI. This is a clue of the presence of the hydrolysis reactions that took place during depolymerization.

Instead of the band at 1730 cm^{-1}, a band at 1710 cm^{-1} was observed which can be attributed to carboxylic acid C=O vibration. Another signal that was observed in the DSEA fraction, but not in SSEA nor in SSI C-H vibration at around 1360 cm^{-1} exists. The second highest decrement in the intensity of DSEA fractions was observed around 1110 cm^{-1} C-H in-plane deformation that belongs to S-units for both 380°C and 390°C BL products.

Table 10. FTIR spectrum assignments of the bonds to each band and the origin of the bands. Table created using references [1,23,44–46].

Wavelength (cm^{-1})	Assignment	Origin/Component
3300 – 3500	O–H stretching	All
2960 and 2840	C–H stretching for -CH_3 and CH_2 groups	All
1730	C=O unconjugated vibration	Ketones
1710 – 1680	C=O unconjugated vibration	Carboxylic acids
1670 – 1650	C=O stretch conjugated	*Aryl ketones*
1605 – 1590	C-C aromatic skeletal	S > G
1515 – 1500	C-C aromatic skeletal	G > S
1460 – 1420	C–H deformation for -CH_3 and CH_2 groups	Aromatics
1430	aromatic skeletal vibration C-H in plane deformation	Aromatics
1370	C-H vibration	All
1325	C-O stretch	S units
1270	C-O stretch	G units
1205	C-C and C-O stretch	G units
1140	C-H in plane deformation	G units
1110	C-H in plane deformation	S units
1030	C-H in plane deformation C-O deformation	G units > S units primary alcohols
909	C-H out of plane	Aromatics
825	C-H out of plane	G units

4. Conclusions

The study shows that longer reaction times and higher temperatures in the treatment of BL and KL significantly increase the concentration of phenolic compounds in the product, which consequently lowers the pH and reduces the total solids content, indicating the influence of temperature and time on the depolymerization process and the resulting chemical composition.

The SCW treatment of BL significantly reduced its SSI fraction from 24.96 wt% in the raw material to only 1.25 wt% at 390°C, compared to a reduction in KL where the SSI fraction decreased from 37.57 wt% to 5 wt% under similar conditions.

The greater responsiveness of BL to SCW treatment highlights its susceptibility to rapid solubilization and depolymerization, suggesting that BL may be a more suitable candidate for processes requiring efficient degradation of organic materials. In addition, the overall decrease in SSI fractions and increase in total oil percentages with longer reaction times confirms the efficacy of SCW in enhancing the degradation of complex materials, using the unique properties of supercritical water to facilitate significant chemical transformations.

BL raw material contained 9.32 wt% DSEA fraction (monomer rich aromatic oil), whereas for KL raw material DSEA yielded only 5.74 wt%. Maximum DSEA yield for BL was found to be around 21 wt% and 24.64 wt% at 380°C and 390°C, respectively. Regarding KL maximum DSEA yield was found 13.36 wt% and 16.82 wt% at 380°C and 390°C, respectively. The maximum oil yield obtained by the SCW depolymerization of BL was 79.45 wt%, and of KL was 68.54 wt% at 390°C.

Longer reaction times at 380°C result in greater production of aromatic monomers like guaiacol, syringol, vanillin, acetovanillone and syringaldehyde. However, at 390°C, yields of syringaldehyde and acetosyringone decline after 0.5 seconds, likely due to their involvement in repolymerization or alternative depolymerization pathways at higher temperatures. Furthermore, the experiments demonstrated that KL yielded significantly lower monomer amounts compared to BL. Notably, both vanillin and syringaldehyde disappeared at 390°C after 1 and 1.5 seconds of reaction time, indicating significant changes in monomer stability or reactivity under these conditions.

GPC analysis demonstrated that the SSEA fraction from KL had a higher molecular weight (Mw) than the raw material at 390°C and 0.5s. However, the SSEA fraction Mw decrement was observed at extended reaction times of 1 second and 1.5 seconds, indicating that KL raw material benefits from longer reaction times for depolymerization of this fraction.

The experiments conducted in this study demonstrate that depolymerization and repolymerization reactions occur simultaneously. Furthermore, the initiation of repolymerization does not inhibit the production of lower molecular weight fragments

as reaction time increases. However, to validate this hypothesis with absolute certainty, a broader experimental design with more data points is required.

REFERENCES

[1] N. Abad-Fernández, PhD Thesis: Lignin depolymerization by supercritical water ultrafast reactions, Universidad de Valladolid, 2019.

[2] W. Schutyser, T. Renders, S. Van Den Bosch, S.F. Koelewijn, G.T. Beckham, B.F. Sels, Chemicals from lignin: An interplay of lignocellulose fractionation, depolymerisation, and upgrading, Chem. Soc. Rev. 47 (2018) 852–908. https://doi.org/10.1039/c7cs00566k.

[3] M.B.G. Latarullo, E.Q.P. Tavares, G.P. Maldonado, D.C.C. Leite, M.S. Buckeridge, Pectins, endopolygalacturonases, and bioenergy, Front. Plant Sci. 7 (2016) 1–7. https://doi.org/10.3389/fpls.2016.01401.

[4] S. Xie, Q. Sun, Y. Pu, F. Lin, S. Sun, X. Wang, A.J. Ragauskas, J.S. Yuan, Advanced Chemical Design for Efficient Lignin Bioconversion, ACS Sustain. Chem. Eng. 5 (2017) 2215–2223. https://doi.org/10.1021/acssuschemeng.6b02401.

[5] R. Rinaldi, R. Jastrzebski, M.T. Clough, J. Ralph, M. Kennema, P.C.A.A. Bruijnincx, B.M. Weckhuysen, Paving the Way for Lignin Valorisation: Recent Advances in Bioengineering, Biorefining and Catalysis, Angew. Chemie - Int. Ed. 55 (2016) 8164–8215. https://doi.org/10.1002/anie.201510351.

[6] A. Orebom, J.J. Verendel, J.S.M. Samec, High Yields of Bio Oils from Hydrothermal Processing of Thin Black Liquor without the Use of Catalysts or Capping Agents, ACS Omega. 3 (2018) 6757–6763. https://doi.org/10.1021/acsomega.8b00854.

[7] R. Katahira, A. Mittal, K. McKinney, X. Chen, M.P. Tucker, D.K. Johnson, G.T. Beckham, Base-Catalyzed Depolymerization of Biorefinery Lignins, ACS Sustain. Chem. Eng. 4 (2016) 1474–1486. https://doi.org/10.1021/acssuschemeng.5b01451.

[8] P.J. Deuss, M. Scott, F. Tran, N.J. Westwood, J.G. De Vries, K. Barta, Aromatic Monomers by in Situ Conversion of Reactive Intermediates in the Acid-Catalyzed Depolymerization of Lignin, J. Am. Chem. Soc. 137 (2015) 7456–7467. https://doi.org/10.1021/jacs.5b03693.

[9] L. Shuai, M.T. Amiri, Y.M. Questell-Santiago, F. Heroguel, Y. Li, H. Kim, R. Meilan,

C. Chapple, J. Ralph, J.S. Luterbacher, Formaldehyde stabilization facilitates lignin monomer production during biomass depolymerization, Science (80-.). 354 (2016) 329–334.

[10] T. Renders, W. Schutyser, S. Van Den Bosch, S.F. Koelewijn, T. Vangeel, C.M. Courtin, B.F. Sels, Influence of Acidic (H3PO4) and Alkaline (NaOH) Additives on the Catalytic Reductive Fractionation of Lignocellulose, ACS Catal. 6 (2016) 2055–2066. https://doi.org/10.1021/acscatal.5b02906.

[11] H. Wang, H. Ruan, M. Feng, Y. Qin, H. Job, L. Luo, C. Wang, M.H. Engelhard, E. Kuhn, X. Chen, M.P. Tucker, B. Yang, One-Pot Process for Hydrodeoxygenation of Lignin to Alkanes Using Ru-Based Bimetallic and Bifunctional Catalysts Supported on Zeolite Y, ChemSusChem. 10 (2017) 1846–1856. https://doi.org/10.1002/cssc.201700160.

[12] M. Fache, B. Boutevin, S. Caillol, Vanillin Production from Lignin and Its Use as a Renewable Chemical, ACS Sustain. Chem. Eng. 4 (2016) 35–46. https://doi.org/10.1021/acssuschemeng.5b01344.

[13] T. Voitl, P.R. Von Rohr, Oxidation of lignin using aqueous polyoxometalates in the presence of alcohols, ChemSusChem. 1 (2008) 763–769. https://doi.org/10.1002/cssc.200800050.

[14] J.Y. Kim, J. Park, U.J. Kim, J.W. Choi, Conversion of Lignin to Phenol-Rich Oil Fraction under Supercritical Alcohols in the Presence of Metal Catalysts, Energy and Fuels. 29 (2015) 5154–5163. https://doi.org/10.1021/acs.energyfuels.5b01055.

[15] X. Huang, T.I. Korányi, M.D. Boot, E.J.M. Hensen, Catalytic depolymerization of lignin in supercritical ethanol, ChemSusChem. 7 (2014) 2276–2288. https://doi.org/10.1002/cssc.201402094.

[16] S. Van Den Bosch, S.F. Koelewijn, T. Renders, G. Van den Bossche, T. Vangeel, W. Schutyser, B.F. Sels, Catalytic Strategies Towards Lignin - Derived Chemicals, Springer International Publishing, 2018. https://doi.org/10.1007/s41061-018-0214-3.

[17] X. Erdocia, R. Prado, M.Á. Corcuera, J. Labidi, Base catalyzed depolymerization

of lignin: Influence of organosolv lignin nature, Biomass and Bioenergy. 66 (2014) 379–386. https://doi.org/10.1016/j.biombioe.2014.03.021.

[18] T. Yokoyama, Revisiting the mechanism of β-O-4 bond cleavage during acidolysis of lignin. Part 6: A review, J. Wood Chem. Technol. 35 (2014) 27–42. https://doi.org/10.1080/02773813.2014.881375.

[19] A.K. Deepa, P.L. Dhepe, Lignin Depolymerization into Aromatic Monomers over Solid Acid Catalysts, ACS Catal. 5 (2015) 365–379. https://doi.org/10.1021/cs501371q.

[20] J. Lappalainen, D. Baudouin, U. Hornung, J. Schuler, K. Melin, S. Bjelić, F. Vogel, J. Konttinen, T. Joronen, Sub- And supercritical water liquefaction of kraft lignin and black liquor derived lignin, Energies. 13 (2020) 3309. https://doi.org/10.3390/en13133309.

[21] E.K. Vakkilainen, Kraft Recovery Boilers - High Solids Firing, (2006) 5–254. https://www.researchgate.net/profile/Esa_Vakkilainen/publication/279871546_Kraft_recovery_boilers_-_Principles_and_practice/links/561a6dba08ae6d1730898b68/Kraft-recovery-boilers-Principles-and-practice.pdf.

[22] C. Abbati De Assis, L.G. Greca, M. Ago, M.Y. Balakshin, H. Jameel, R. Gonzalez, O.J. Rojas, Techno-Economic Assessment, Scalability, and Applications of Aerosol Lignin Micro- and Nanoparticles, ACS Sustain. Chem. Eng. 6 (2018) 11853–11868. https://doi.org/10.1021/acssuschemeng.8b02151.

[23] J. Fernández-Rodríguez, Lignin as a source of phenolic compounds: from lignin extraction to its transformation by different routes, University of Basque Country UPV/EHU, 2020.

[24] D.A. Cantero, M.D. Bermejo, M.J. Cocero, Reaction engineering for process intensification of supercritical water biomass refining, J. Supercrit. Fluids. 96 (2015) 21–35. https://doi.org/10.1016/j.supflu.2014.07.003.

[25] D.A. Cantero, M. Dolores Bermejo, M. José Cocero, High glucose selectivity in pressurized water hydrolysis of cellulose using ultra-fast reactors, Bioresour. Technol. 135 (2013) 697–703. https://doi.org/10.1016/j.biortech.2012.09.035.

[26] E. Pérez, N. Abad-Fernández, T. Lourençon, M. Balakshin, H. Sixta, M.J. Cocero, Base-catalysed depolymerization of lignins in supercritical water: Influence of lignin nature and valorisation of pulping and biorefinery by-products, Biomass and Bioenergy. 163 (2022). https://doi.org/10.1016/j.biombioe.2022.106536.

[27] F. Hernandez-Ramos, M.G. Alriols, T. Calvo-Correas, J. Labidi, E. Xabier, Renewable Biopolyols from Residual Aqueous Phase Resulting after Lignin Precipitation, ACS Sustain. Chem. Eng. 9 (2021) 3608–3615. https://doi.org/10.1021/acssuschemeng.0c09357.

[28] N. Abad-Fernández, E. Pérez, M.J. Cocero, Aromatics from lignin through ultrafast reactions in water, Green Chem. 21 (2019) 1351–1360. https://doi.org/10.1039/c8gc03989e.

[29] T.L.K. Yong, Y. Matsumura, Reaction kinetics of the lignin conversion in supercritical water, Ind. Eng. Chem. Res. 51 (2012) 11975–11988. https://doi.org/10.1021/ie300921d.

[30] T.L.K. Yong, M. Yukihiko, Kinetic analysis of guaiacol conversion in sub- and supercritical water, Ind. Eng. Chem. Res. 52 (2013) 9048–9059. https://doi.org/10.1021/ie4009748.

[31] H. shik Lee, J. Jae, J.M. Ha, D.J. Suh, Hydro- and solvothermolysis of kraft lignin for maximizing production of monomeric aromatic chemicals, Bioresour. Technol. 203 (2016) 142–149. https://doi.org/10.1016/j.biortech.2015.12.022.

[32] T.D.H. Nguyen, M. Maschietti, L.E. Åmand, L. Vamling, L. Olausson, S.I. Andersson, H. Theliander, The effect of temperature on the catalytic conversion of Kraft lignin using near-critical water, Bioresour. Technol. 170 (2014) 196–203. https://doi.org/10.1016/j.biortech.2014.06.051.

[33] Y. Solantausta, C. Anacker, U. Armbruster, D. Meier, J. Appelt, A. Martin, J.O. Strüven, P. Eidam, C. Mirodatos, Y. Schuurman, F. Chapon, A. Oasmaa, A. Välimäki, K. Melin, V. Passikallio, Liquid fuels from lignin by hydrothermal liquefaction and deoxygenation (LIGNOHTL), 1 (2018) 1–11. https://forestvalue.org/wp-content/uploads/2018/07/wwnet_jc4_final_reporting_lignoHTL.pdf.

[34] T. Adamovic, X. Zhu, E. Perez, M. Balakshin, M.J. Cocero, Understanding sulfonated kraft lignin re-polymerization by ultrafast reactions in supercritical water, J. Supercrit. Fluids. 191 (2022). https://doi.org/10.1016/j.supflu.2022.105768.

[35] A. Sluiter, B. Hames, R. Ruiz, C. Scarlata, J. Sluiter, D. Templeton, Determination of ash in biomass. NREL Laboratory Analytical Procedure (LAP), Natl. Renew. Energy Lab. (2008) 18. http://www.nrel.gov/docs/gen/fy08/42622.pdf.

[36] A. Sluiter, B. Hames, R. Ruiz, C. Scarlata, J. Sluiter, D. Templeton, Determination of Sugars , Byproducts , and Degradation Products in Liquid Fraction Process Samples Laboratory Analytical Procedure (LAP) Issue Date : 12 / 08 / 2006 Determination of Sugars , Byproducts , and Degradation Products in Liquid Fraction Proce, (2008).

[37] E. Furusjö, E. Pettersson, Mixing of Fast Pyrolysis Oil and Black Liquor: Preparing an Improved Gasification Feedstock, Energy and Fuels. 30 (2016) 10575–10582. https://doi.org/10.1021/acs.energyfuels.6b02383.

[38] V. Sricharoenchaikul, A.L. Hicks, W.J. Frederick, Carbon and char residue yields from rapid pyrolysis of kraft black liquor, Bioresour. Technol. 77 (2001) 131–138. https://doi.org/10.1016/S0960-8524(00)00155-3.

[39] N. Busayasakul, Total Organic Carbon As an Indicator of Wood Delignification, University of Maine, 1986.

[40] K.. Niemelä, R. Alén, Characterization of pulping liquors, in: S. Eero, R. Alén (Eds.), Anal. Methods Wood Chem. Pulping, Papermak., 1st ed., Springer, 1999: pp. 193–232. https://doi.org/10.1007/978-3-662-03898-7.

[41] S. Maitz, W. Schlemmer, M.A. Hobisch, J. Hobisch, M. Kienberger, Preparation and Characterization of a Water-Soluble Kraft Lignin, Adv. Sustain. Syst. 4 (2020). https://doi.org/10.1002/adsu.202000052.

[42] S. Cheng, C. Wilks, Z. Yuan, M. Leitch, C. Xu, Hydrothermal degradation of alkali lignin to bio-phenolic compounds in sub/supercritical ethanol and water-ethanol co-solvent, Polym. Degrad. Stab. 97 (2012) 839–848. https://doi.org/10.1016/j.polymdegradstab.2012.03.044.

[43] E. Pérez, C.O. Tuck, Quantitative analysis of products from lignin depolymerisation in high- temperature water, Eur. Polym. J. 99 (2018) 38–48. https://doi.org/10.1016/j.eurpolymj.2017.11.053.

[44] O. Faix, Methods in Lignin Chemistry, Springer Berlin Heidelberg, 1993. https://doi.org/10.1016/0305-0491(93)90261-3.

[45] C.M. Martinez, PhD Thesis: Demonstration of a Selective Process to Transform Biomass into Sugars by Ultrafast Hydrolysis in Supercritical Water, University of Valladolid, 2018.

[46] T. Adamovic, PhD Thesis: Lignin valorization using supercritical water technology, University of Valladolid, 2021.

CONCLUSION & FUTURE WORK

Valorization of Black Liquor using Hydrothermal Treatment

This thesis' major contribution is the feasibility of direct use of industrial black liquor without applying any pretreatment or separating lignin to produce aromatic monomer rich bio-oil. Black liquor successfully depolymerized using hydrothermal treatment using ultra-fast reaction times, and an end-user biomaterial is produced using the depolymerized fractions from this process. Higher concentrations of black liquor processing, revealing the presence of the biopolyols, investigating simple downstream processing, production of bio-lubricants and their detailed characterization, comprehensive characterization of each fraction from depolymerized black liquor and kraft lignin, and employing a consistent and comparable mass balance has been the key points that were achieved in this study.

Overall conclusions of this study were summarized as can be seen below:

The study successfully demonstrated the feasibility of continuous supercritical water depolymerization pilot plants built in PressTech laboratories which are capable of processing even high concentrations of black liquor up to 20 wt% total solids. Longer operation hours of up to 1 hour were also tested. Hydrothermal treatment of black liquor yielded ~77 wt% bio-oil yield in 0.4 sec of reaction time.

Downstream processing study to find a simple and effective method to minimize the cost and time revealed that fractionation method gives higher yield compared to the other simple separation processes. A derivatization method to the aromatic monomer rich bio-oil fraction was applied for gas chromatography analysis revealed the presence of biopolyols which can be utilized for different applications such as lubricants.

Selected depolymerized black liquor fractions obtained in chapter 1, further upgraded to produce bio-lubricants. These selected fractions were blended with the epoxidized castor oil and created original bio-lubricant formulations. These biomaterials exhibit notable physical stability, desirable appearance, characteristic shear-thinning and viscoelastic behaviors, and adequate tribological performance all of which makes them potential eco-friendly semi-solid lubricants.

Formulations thickened with different lignin fractions showed significant wear protection compared to epoxidized castor oil alone. Particularly, the system incorporating total bio-oil blended mixture of epoxidized castor oil (ECO_EA) fraction showed the highest wear protection due to its lower viscosity and minimal abrasive ash content. On the other hand, retaining the inorganic content within the depolymerized

black liquor fraction enhanced the thickening effect of the bio-lubricants, synergistically influenced by the molecular weight and polydispersity of the samples.

Application of the blank tests for the fractionation method to the black liquor raw material demonstrated that the organic and inorganic fractions are capable of producing four different fractions as in the case of depolymerized material downstream fractionation method. Therefore, a new mass balance and carbon balance was employed in this thesis to make a better comparison and understand the differences of the yields between the raw black liquor and depolymerized black liquor.

Longer reaction times and higher temperatures in the treatment of BL and KL significantly increase the concentration of phenolic compounds in the product, which consequently lowers the pH of the final product and reduces the total solids content, indicating the influence of temperature and time on the depolymerization process and the resulting chemical composition.

Considering the black liquor depolymerization, longer reaction times at elevated temperatures facilitated the production of aromatic monomers like guaiacol, syringol, vanillin, acetovanillone, and syringaldehyde. However, some monomers yield declined at higher temperature, likely due to their involvement in repolymerization or alternative depolymerization pathways. Conversely, kraft lignin demonstrated that vanillin and syringaldehyde completely disappeared at higher temperature and longer reaction time, which indicates they are decomposing and reacting at these conditions.

Black liquor exhibited higher aromatic monomer rich oil compared to kraft lignin which proves that the lignin separation is unnecessary step especially to produce chemicals using base-catalyzed hydrothermal processing. Using black liquor directly brings many advantages especially in terms of minimizing cost and time. Besides, the inorganics are separated after downstream processing can be reused inside the pulp-mill cycle (green liquor cycle) or can be evaluated for any other purposes or processes.

FUTURE WORK

Black liquor is a complex material that includes lignin, some carbohydrates, and possibly other types of organics that comes from the type of wood used during cooking in pulp mills, besides the inorganics that are used for the cooking process. Due to this reason, the nature of the material makes it hard to concretely talk about the conversion. Main

tendency in the literature to talk about the depolymerization rate was comparing the B-O-4 bonds between the raw material and the final sample. As the β-O-4 bonds are the ones that are easily breaking, it has been a good way to compare the conversion of the process. The next step of this study should be the implementation of a detailed NMR analysis and check the conversion rates and compare the advantages of the process to the ones in the literature.

Another important point will be the practicing P-NMR to check the functionality of the samples after the hydrothermal processing more precisely. The -OH groups presence and concentration plays a crucial role in determining the samples nature and relevance in which type of application (polyurethane, lubricants, adhesives, etc.) it can be used.

When it comes to molecular weight, gel permeation chromatography is being limited to enlighten the fractions molecular weight accurately. The limitation of the GPC comes from how it works, which is being dependent on the size of the fragments that are being soluble in the solvent. The difference between bowling ball and volleyball can be given as an example here. They are the same size, but different weights. Therefore, if we were able to analyze their molecular weight by using GPC, they would have the molecular weight, as GPC will analyze their differences in sizes, which is wrong in reality. Due to this reason, a time-of-flight spectrometer including instruments such as MALDI-TOF would give more accurate results than GPC. Carrying out this analysis will improve the reliability of the results.

Observing higher molecular weight for SSEA fraction of the supercritical water treated samples of the kraft lignin compared to its raw material should be examined deeper using MALDI-TOF and NMR, by employing larger data points in terms of the experimental design.

ANNEX I

Supercritical Water Depolymerization of Black Liquor, Refining and Comprehensive Analysis of Products Including Biopolyols

1. Equations used for the calculations.

Equation 1, determination of ash.

$$\%Ash = \frac{\text{Weight}_{crucible\ plus\ ash} - \text{Weight}_{crucible}}{\text{Oven Dried Weight of the sample}}\ x\ 100$$

Where "$\text{Weight}_{\text{crucible}}$" is the weight of the empty crucible; "$\text{Weight}_{\text{crucible plus ash}}$" is the weight of the crucible after calcination; and "Oven dried weight of the sample" is the dry mass of sample, dried in the oven.

Equation 2, determination of Total Solids.

$$\%Total\ Solids(TS) = \frac{\text{Weight}_{dry\ pan\ plus\ dry\ sample} - \text{Weight}_{dry\ pan}}{Weight_{sample\ as\ received}}\ x\ 100$$

Where "$\text{Weight}_{\text{dry pan}}$" is the weight of the empty pan; "$\text{Weight}_{\text{dry pan plus dry sample}}$" is the weight of the pan after oven drying; and "$\text{Weight}_{\text{sample as received}}$" is the mass of sample.

Equation 3, determination of Dissolved Solids.

$$\%Dissolved\ Solids(DS) = \frac{\text{Weight}_{dry\ pan\ plus\ dry\ liquor} - \text{Weight}_{dry\ pan}}{Weight_{liquor\ after\ filtration}}\ x\ 100$$

Where "$\text{Weight}_{\text{dry pan}}$" is the weight of the empty pan; "$\text{Weight}_{\text{dry pan plus dry liquor}}$" is the weight of the pan after oven drying; and "$\text{Weight}_{\text{liquor after filtration}}$" is the mass of sample after filtration through 0.22 microns syringe filter.

Equation 4, determination of Suspended Solids.

$$Total\ Solids\ (TS)\ =\ Dissolved\ Solids\ (DS)\ +\ Suspended\ Solids\ (SS)$$

Equation 5, determination of yield of extracted fraction.

$$\%Fraction\ Extracted = \frac{\text{Weight}_{dry\ pan\ plus\ dry\ extract} - \text{Weight}_{dry\ pan}}{Weight_{sample\ as\ received}\ \ x\ \ \%Total\ Solids}\ x\ 100$$

Where "$Weight_{dry\ pan}$" is the weight of the empty pan; "$Weight_{dry\ pan\ plus\ dry\ extract}$" is the weight of the pan after oven drying; and "$Weight_{sample\ as\ received}$" is the mass of sample.

Equation 6, determination of total solids free of ash.

$$\%Ash\ Free\ Total\ Solids(AFTS) = \frac{\%\text{Total Solids}\ x\ (100\ -\%Ash)}{100}$$

Equation 7, determination of yield of extractives free of ash.

$$\%Ash\ Free\ Fraction\ Extracted = \frac{\text{Weight}_{dry\ pan\ plus\ dry\ extract} - \text{Weight}_{dry\ pan}}{Weight_{sample\ as\ received}\ \ x\ \ \%AFTS}\ x\ 100$$

To calculate the yield of the fractionation product;

Equation 8, determination of yield of fractionation.

$$\%\ Fractionation\ Yield = \frac{\text{Weight}_{dry\ tube\ plus\ dry\ fraction} - \text{Weight}_{dry\ pan}}{Weight_{total\ solids}}\ x\ 100$$

2. Simplified Schemes of different refining methods

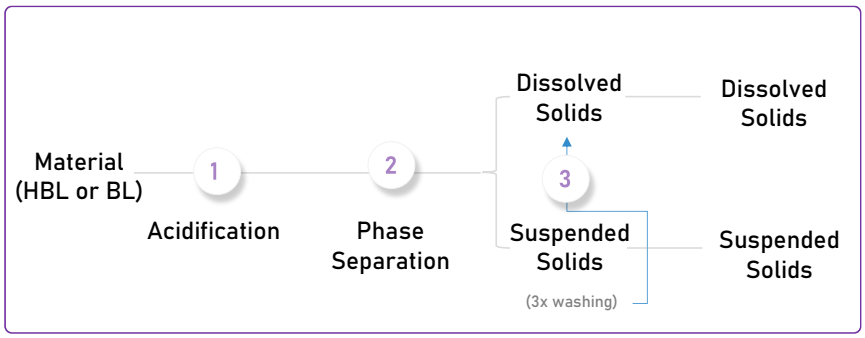

Figure S1. Samples solids split.

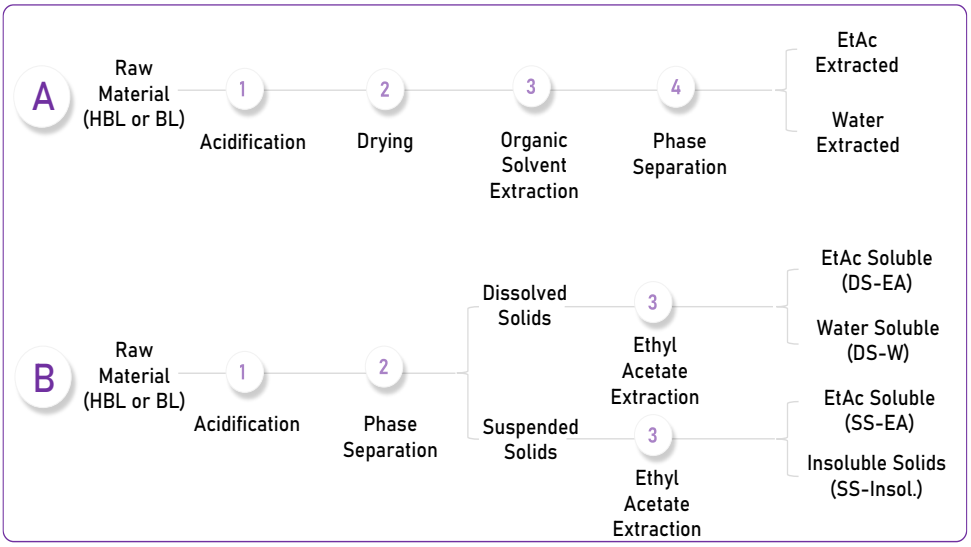

Figure S2. Different Refining Methods Simplified Scheme Procedure A (Direct Drying Methods – includes Oven Drying and Freeze Drying) and Procedure B (Indirect Drying Method – phase separation followed by drying which was named as Fractionation Method).

3. Calibration curves used for quantification of the main monomers by GC-MS

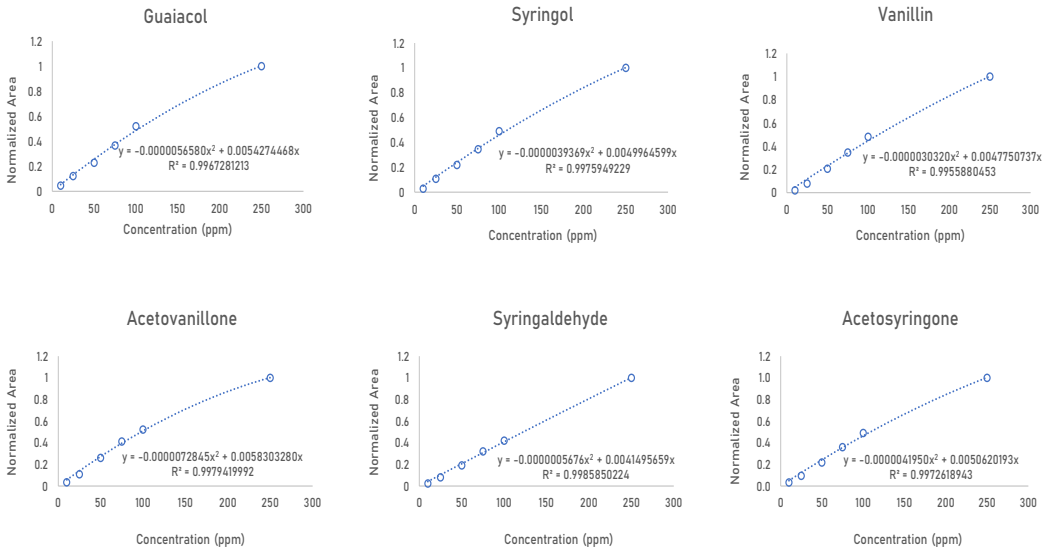

Figure S3. Calibration curves of aromatics used as standards for GC-MS.

4. Typical GC-MS chromatograms for BL and HBL according to monomer focused method

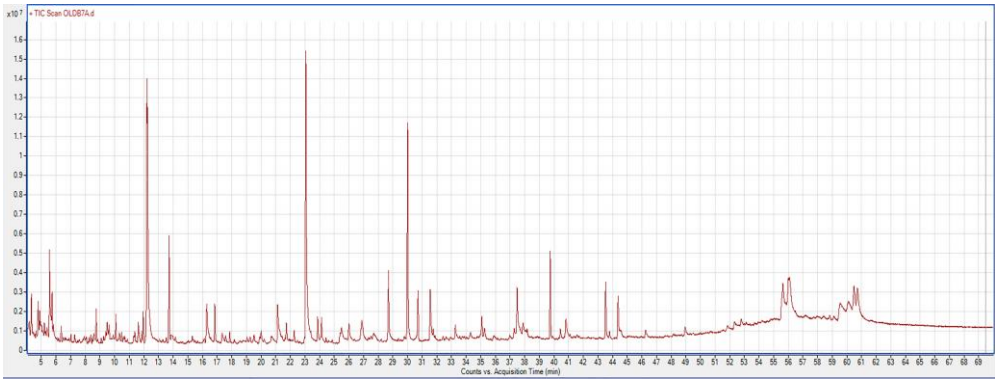

Figure S4a. Typical GC-MS chromatogram for black liquor monomer focused GC-MS method.

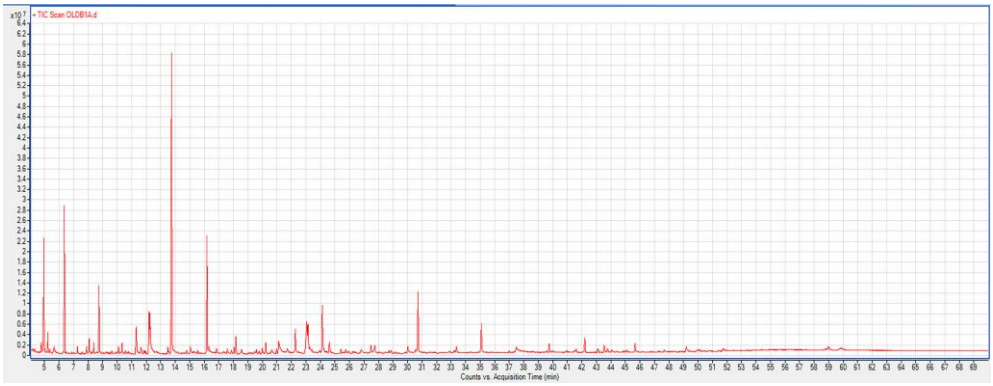

Figure S4b. Typical GC-MS chromatogram for hydrolyzed black liquor monomer focused GC-MS method.

5. Typical GC-MS chromatogram for HBL according to oligomer focused method

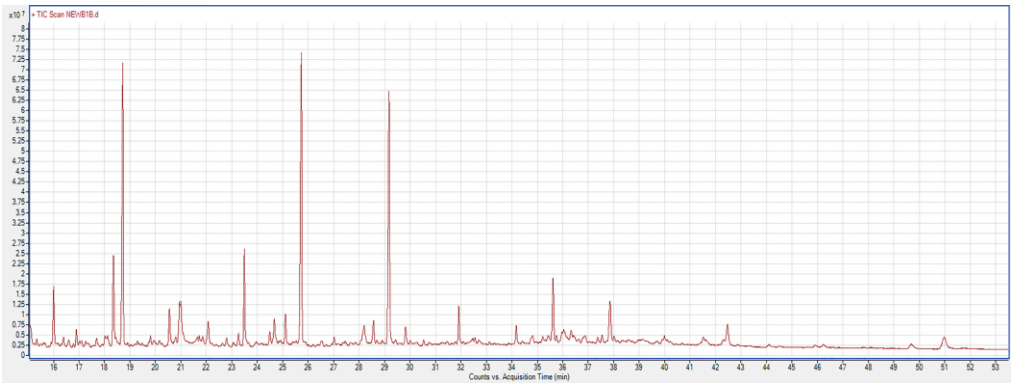

Figure S5. Typical GC-MS chromatogram for hydrolyzed black liquor oligomer focused GC-MS method.

6. Hydrolyzed black liquor products identified by using oligomer focused GC-MS method. (Including identified biopolyols)

Table S1. Hydrolyzed black liquor products identified by using oligomer focused GC-MS method.

RT (min)	COMPOUND
16.14	β-Hydroxypropiosyringone, O,O-bis-TMS
18.713	Stearic acid, TMS derivative
20.549	Stilbene Derivative
20.951	3',5'-Di(trimethylsilyl)oxyflavone
21.009	9-Octadecenamide, (Z)-
22.076	Oleamide, TMS derivative
22.793	D-Glucopyranosiduronic acid, 3-(5-ethylhexahydro-1,3-dimethyl-2,4,6-trioxo-5-pyrimidinyl)-1-methylbutyl 2,3,4-tris-O-(trimethylsilyl)-, methyl ester
23.51	4-Methylthio-N-phenyl-1,2-carbazoledicarboximide
25.107	2-Palmitoylglycerol, 2TMS derivative
25.73	1-Monopalmitin, 2TMS derivative
28.569	2-Monostearin, 2TMS derivative
29.169	Glycerol monostearate, 2TMS derivative
37.545	Plant hormone derivative
37.848	β-Sitosterol, TMS derivative
39.981	Medioresinol, 2-O-TMS
42.464	Syringaresinol, 2TMS

7. Van Krevelen diagram of the elemental analysis

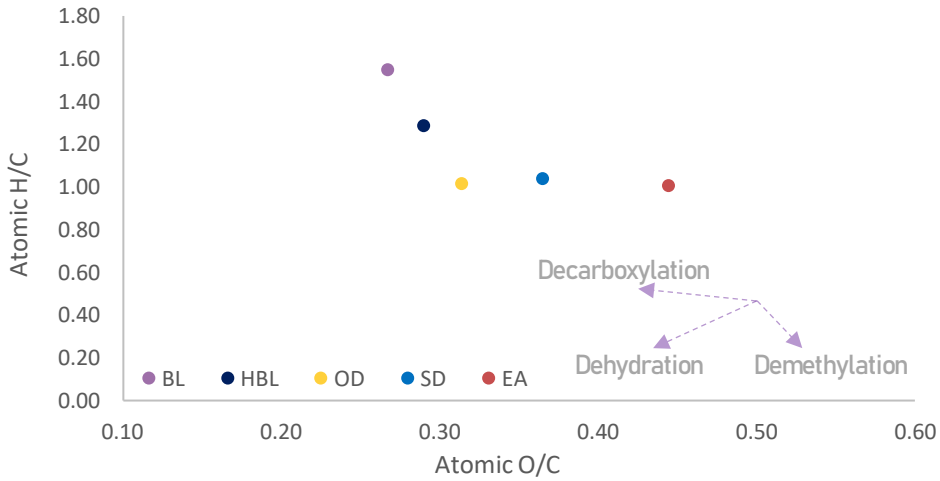

Figure S6. Van Krevelen diagram created using elemental analysis results of the designated samples.

Method A

Raw Material
(DBL or BL)

1 Acidification

2 Phase Separation

- Dissolved Solids
- Suspended Solids

*** Dissolved Solids, and Suspended Solids Analysis. Used to create Figure 3 in Chapter 1.

Method B

Raw Material
(DBL or BL)

1 Acidification

2 Drying (Freeze, Oven)

3 Ethyl Acetate Extraction

4 Phase Separation

- EtAc Extracted
- Water Extracted

*** Simple downstream processing methods, used together for comparison purposes with method C in Chapter 1. Helped to create figure 2.

Method C

Raw Material
(DBL or BL)

1 Acidification

2 Phase Separation

	Dissolved Solids	Suspended Solids
3	Ethyl Acetate Extraction	Ethyl Acetate Extraction
4	Phase Separation	Phase Separation
	-Water Soluble (DS-W) (Aq. Residue)	-Insoluble Solids (SS-I) (Char)
	-EtAc Soluble (DS-EA) (Light oil)	-EtAc Soluble (SS-EA) (Heavy oil)

*** Fractionation method, used together for comparison purposes with method B in Chapter 1. Helped to create figure 2. Used to create figures 4-7.

This method is used for GC-MS analysis both in chapter 1&2 as well.

Method D

Raw Material
(DBL or BL)

1 Acidification

2 Spray Drying / Oven Drying → Ethyl Acetate Extraction

*** Selected products for Chapter 1, characterization were done for section 3.4 and beyond.

Also, same materials produced in large amounts to be used for Chapter 2 biolubricant production.

ANNEX II

Product development:

Bio-lubricant production

using selected depolymerized

black liquor products

1. Commercial castor oil specifications obtained by the company technical sheet.

Table S1. Castor oil characteristics.

Characteristics	Units	Specifications
Acid Value	mg KOH/g	<2
Free Fatty Acids	%	<1
Moisture & Impurities	%	<0.375
Saponification Number	mg KOH/g	175-187
Iodine Value	g I2/100 g	80-90
Hydroxyl Value	mg KOH/g	143-170
Density	g/mL @ 20 °C	0.958-0.969
Solidifying Point	°C	<-10 °C

Table S2. Castor oil composition.

Carbon Number	Fatty Acid	Specification (%)
C-16	Palmitic	1-3
C-18	Stearic	1-3
C-18:1	Oleic	2-8
C-18:1 (OH)	Ricinoleic	82-95
C-18:2	Linoleic	2-6

2. Simplified Schemes of different refining methods

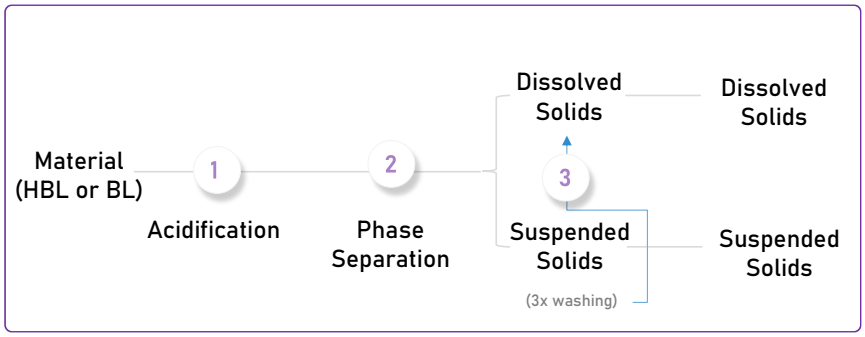

Figure S1. Samples solids split.

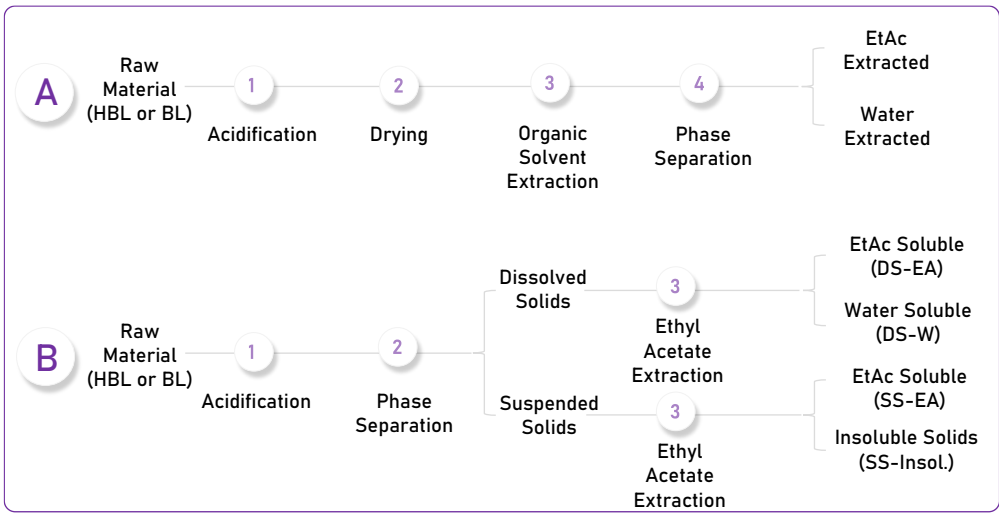

Figure S2. Different Refining Methods Simplified Scheme Procedure A (Direct Drying Methods – includes Oven Drying and Freeze Drying) and Procedure B (Indirect Drying Method – phase separation followed by drying which was named as Fractionation Method).

3. Elemental analysis results of the samples.

Table S3. Elemental analysis results of the samples in dry basis

	AVERAGES							
	C	***H***	***N***	***S***	***O + Inorg.***	***HHV (MJ/kg)***	***H:C***	***O:C***
BL	*33.36*	*4.34*	*1.51*	*0.00*	*48.9*	*14.47*	*1.55*	*0.27*
HBL	*33.02*	*3.56*	*1.69*	*0.49*	*48.5*	*13.40*	*1.29*	*0.29*
SD	*23.79*	*2.07*	*1.59*	*0.28*	*60.7*	*8.27*	*1.04*	*0.36*
OD	*24.41*	*2.08*	*1.54*	*1.96*	*59.8*	*8.83*	*1.01*	*0.31*
EA	*57.56*	*4.85*	*1.50*	*0.00*	*2*	*22.22*	*1.00*	*0.44*

4. DTG diagram and the decomposition percentages obtained by TGA.

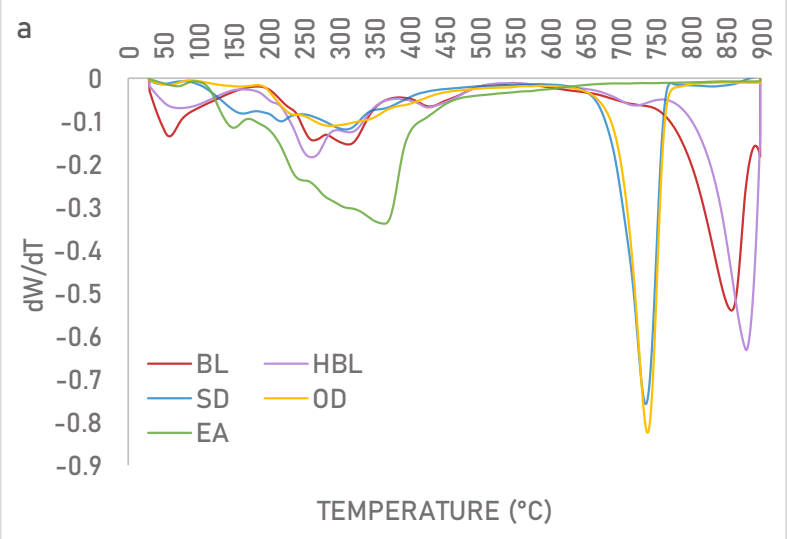

Figure S3. DTG diagram of the samples

Table S4. TGA degradation temperatures vs percentages.

	BL	**HBL**	**OD**	**SD**	**EA**
Moisture (<=100 °C)	7.45	4.81	0.74	0.92	0.94
Volatile organics (120-550 °C)	26.69	28.53	23.08	26.83	67.62
Metal-bonded organics (>600 °C)	44.56	41.11	37.16	37.08	1.70

5. Black Liquor identified compound and structures list obtained by monomer & oligomer focused GC-MS method.

Table S5. Black liquor identified structures by monomer & oligomer focused GC-MS method.

Row	RT (min)	Area	Area %	Compound Structure	Main Substructures
1	12.055	1.351E+08	6.47	lactic acid	COOH
2	12.544	3.205E+07	1.54	glycolic acid	COOH
3	14.45	2.896E+08	13.87	2-hydroxybutyric acid	COOH
4	16.566	4.284E+07	2.05	levulinic acid	COOH
5	17.551	1.702E+07	0.82	guaiacol	ArOR . ArOCH3
6	20.722	5.007E+07	2.40	catechol	ArOH .
7	21.124	4.030E+07	1.93	methylsuccinic acid	
8	23.368	7.731E+07	3.70	syringol	ArOR . ArOCH3
9	25.764	2.201E+07	1.05	3-methoxy-4-nitrobenzyl alcohol	
10	27.431	2.730E+07	1.31	vanillin	ArCHO . ArOR . PHCHO . ROH . ROR
11	29.91	2.596E+07	1.24	acetovanillone	ArCOR . ROH . ROR
12	32.251	8.585E+07	4.11	syringaldehyde	ArCHO . ArOR . PHCHO . ROH . ROR
13	33.953	4.353E+07	2.09	vanillic acid	ArCOOH . ArOR . PHCOH . ROH . ROR
14	34.151	1.402E+08	6.72	acetosyringone	ArCOR . ROH . ROR
15	37.473	1.271E+08	6.09	syringic acid	ArCOOH . ArOR . PHCOH . ROH . ROR
16	37.718	2.931E+07	1.40	pinosylvin	
17	39.992	2.408E+07	1.15	sinapinic acid	
18	40.516	4.449E+07	2.13	benzenepropanoic acid	ArCOOH . ArOR . PHCOH . ROH . ROR
19	40.673	1.651E+07	0.79	palmitic acid	
20	43.337	1.367E+08	6.55	gallic acid	ArCOOH . ArOR . PHCOH . ROH . ROR
21	45.773	1.725E+07	0.83	stilbene derivative	
22	50.961	3.521E+07	1.69	phytoestrogen structure	
23	51.334	1.729E+07	0.83	phytoestrogen structure	
24	53.053	1.826E+07	0.87	hydroxynaphtoquinone structure	β-5
25	53.52	2.679E+07	1.28	spirodienone	5-5, β-1
26	58.841	1.884E+07	0.90	naringenin type structure	
27	58.911	2.079E+07	1.00	plant hormone structure	
28	59.984	3.003E+07	1.44	gibberellin structure	
29	60.106	3.809E+07	1.82	tocopherol derivative	ArC . ArOH . ArOR
30	63.761	2.187E+07	1.05	plant hormone structure	ArCOR . ROH . ROR
31	65.498	1.763E+07	0.84	plant hormone structure	ArCOR . ROH . ROR
32	65.678	1.826E+07	0.88	plant hormone structure	ArCOR . ROH . ROR
33	65.993	3.749E+07	1.80	plant hormone structure	ArCOR . ROH . ROR
34	66.185	4.176E+07	2.00	phytoandrogen derivative	

35	67.468	5.387E+07	2.58	medioresinol	ArOH . ArOR . β-β
36	68.062	9.336E+07	4.47	phytosterol derivative	ArOH . ROH . ArCOOH
37	69.012	5.923E+07	2.84	syringaresinol	ArOH . ArOR . β-β

6. Hydrolyzed Black Liquor identified compound and structures list obtained by monomer & oligomer focused GC-MS method.

Table S6. Hydrolyzed black liquor products identified by using monomer & oligomer focused GC-MS method.

Row	RT (min)	Area	Area %	Compound Structure
1	12.043	6.581E+07	3.30	lactic acid
2	12.539	1.990E+07	1.00	glycolic acid
3	14.404	1.211E+08	6.08	2-hydroxybutyric acid
4	16.56	1.500E+07	0.75	levulinic acid
5	17.551	1.960E+07	0.98	guaiacol
6	20.661	5.197E+07	2.61	catechol
7	21.789	2.741E+07	1.38	fumaric acid
8	23.077	1.808E+07	0.91	4-methylcatechol
9	23.45	3.187E+08	16.00	syringol
10	26.009	1.601E+08	8.04	3-methoxy-4-nitrobenzyl alcohol
11	27.431	3.714E+07	1.86	vanillin
12	27.897	1.679E+07	0.84	vanillyl alcohol
13	28.043	4.135E+07	2.08	syringaldehyde, TMS derivative
14	29.914	4.738E+07	2.38	acetovanillone
15	32.274	1.200E+08	6.03	syringaldehyde
16	34.174	2.048E+08	10.28	acetosyringone
17	34.588	3.308E+07	1.66	methyl 4-methoxysalicylate
18	35.719	3.347E+07	1.68	homovanillic acid
19	37.438	1.917E+07	0.96	syringic acid
20	37.712	2.677E+07	1.34	pinosylvin
21	40.51	2.140E+07	1.07	benzenepropanoic acid
22	40.673	1.854E+07	0.93	palmitic acid
23	43.322	4.045E+07	2.03	gallic acid
24	61.697	2.027E+07	1.02	plant hormone structure

RESUMEN

Valorización del licor negro
mediante tratamiento hidrotérmico

A lo largo de la historia, la sociedad ha dependido en gran medida de los combustibles fósiles para obtener energía, pero su función ha ido cambiando con el paso del tiempo. Tras el auge de la Revolución Industrial y los años posteriores, surgió la preocupación por el posible agotamiento de estos recursos. Sin embargo, la revolución del petróleo de esquisto reforzó los combustibles fósiles como fuente de energía dominante. A pesar de este resurgimiento, existe un consenso cada vez mayor sobre el impacto medioambiental del consumo de combustibles fósiles, concretamente en lo que respecta a las emisiones de gases de efecto invernadero y el calentamiento global. Esta evidencia ha promovido un mayor interés por fuentes de energía alternativas como la solar, la eólica, la biomasa y la hidráulica. Aunque todas ellas pueden producir calor y electricidad, a la vez de reducir las emisiones netas de carbono, la biomasa destaca por su capacidad de proporcionar precursores de carbono esenciales para la síntesis de productos químicos, combustibles y materiales. En este contexto, el licor negro, un subproducto producido en cantidades significativas en las fábricas de pasta y las biorrefinerías, se perfila como un candidato prometedor para estos fines.

El objetivo principal de esta tesis es la valorización del licor negro mediante la tecnología de procesamiento hidrotermal (HTL). Se pretende crear un material de uso final (bio-lubricante) y evaluar diferentes condiciones para monitorizar los efectos de la HTL en esta investigación.

El primer capítulo de la investigación trató sobre la despolimerización en agua supercrítica del licor negro, el refinado y el análisis exhaustivo de los productos, incluidos los bio-polioles. En este estudio, se reveló la presencia de polioles en el licor negro despolimerizado (DBL) y se propuso un enfoque rápido y escalable para aumentar el rendimiento de esta fracción. El tratamiento hidrotérmico (HTL) del licor negro (385°C, 26 MPa) se llevó a cabo en una planta piloto de agua supercrítica (SCW) diseñada a medida con tiempos de reacción rápidos de unos 0,4 s. Como mejora, se utilizó una mayor concentración de licor negro como materia prima, con un 20% en peso de sólidos totales.

Se investigó un método simple de procesamiento posterior con el objetivo de reducir costos y tiempo para aplicaciones industriales. Se evaluaron el secado directo en estufa, la liofilización, el secado por atomización y un método de fraccionamiento completo. El secado por pulverización y la liofilización fueron superiores al secado en estufa en cuanto al rendimiento del bioaceite extraído. Asimismo, se caracterizó con mayor

profundidad el secado por pulverización, ya que es más fácil de escalar en comparación con la liofilización. El método de fraccionamiento proporcionó los mayores rendimientos de bioaceite en comparación con los otros procesos. El rendimiento total de bioaceite extraído de acetato de etilo sin cenizas fue de ~77 % en peso. Además de la contribución de los métodos de fraccionamiento detallados, este estudio destaca el funcionamiento continuo (>1 hora) y los tiempos de reacción cortos (~0,4 s) del licor negro crudo en SCW para producir bio-polioles y bioaceite aromático.

En el segundo capítulo de esta investigación se valorizó el licor negro mediante el tratamiento con agua supercrítica, abriendo una nueva línea de investigación para la producción de bio-lubricantes semisólidos. Para ello, se sometió el licor negro original a un proceso de despolimerización con agua supercrítica con un posterior procesamiento donde se obtuvieron tres fracciones diferentes (secado por pulverización, secado en horno y extracción con acetato de etilo). Posteriormente, estas fracciones se añadieron a aceites vegetales modificados con epoxi con el fin de desarrollar formulaciones de lubricantes sostenibles, seguido de la evaluación de sus propiedades reológicas y tribológicas. Los bio-lubricantes obtenidos no sólo presentaron una estabilidad y aspecto adecuados, sino que también exhibieron unas prestaciones reológicas y tribológicas destacables, lo que los convierte en potenciales lubricantes semisólidos ecológicos. Todas las muestras de lignina utilizadas para dispersiones en aceite de ricino epoxidado demostraron un comportamiento similar de adelgazamiento por cizallamiento, comparable al de las grasas convencionales espesadas con jabón de litio modificado con polímeros. Por otra parte, la retención del contenido inorgánico (contenido de cenizas) en la fracción de licor negro despolimerizado potenció el efecto espesante de los biolubricantes, influido sinérgicamente por el peso molecular y la polidispersidad de las muestras. Estas formulaciones espesadas con lignina reducen significativamente el desgaste de los elementos de contacto en comparación con el aceite de ricino epoxidado solo, siendo el sistema ECO_EA (bioaceite mezclado con formulación de aceite de ricino epoxidado), caracterizado por su menor viscosidad, el que proporciona la mayor protección contra el desgaste. Esto pone de manifiesto la viabilidad de la despolimerización para valorizar el licor negro, y que las fracciones de lignina resultantes mejoran la lubricidad de las formulaciones a base de aceite de ricino.

En el último capítulo, se llevó a cabo la despolimerización del licor negro y la lignina kraft utilizando agua supercrítica, sin utilizar ningún catalizador adicional para el licor negro, pero con el NaOH actuando como catalizador básico para la lignina kraft. Este estudio

representó el primer cribado rápido de reacción de licor negro y lignina kraft precipitada, proporcionando una caracterización exhaustiva de todas las fracciones. Los experimentos se llevaron a cabo en TRL4 en una planta piloto continua con tiempos de reacción rápidos, a temperaturas de 380°C y 390°C y una presión de 26 MPa. Se evaluaron tiempos de reacción de 0.5, 1 y 1.5 segundos para ambas temperaturas y materias primas. La fracción de bioaceite se separó mediante el método de fraccionamiento y su contenido aromático se analizó mediante técnicas detalladas de caracterización.

Este trabajo demostró que a tiempos de reacción más largos y temperaturas más altas durante el tratamiento con agua supercrítica (SCW) del licor negro (BL) y la lignina kraft (KL) las concentraciones de compuestos fenólicos aumentaron significativamente, lo que dio lugar a un pH más bajo y a una reducción del contenido total de sólidos. El tratamiento con SCW redujo la fracción SSI (solidos suspendidos insolubles) del BL del 24,96% en peso a sólo el 1,25% en peso a 390ºC, mientras que la fracción SSI de la KL disminuyó del 37,57% en peso al 5% en peso en condiciones similares. La rápida despolimerización del BL indicó su alta susceptibilidad a la solubilización, lo que lo convierte en un candidato idóneo para los procesos de degradación orgánica. La fracción de sólidos disueltos extraídos con acetato de etilo (DSEA) del BL, que es un aceite rico en monómeros aromáticos, presentó inicialmente un 9,32% en peso, mientras que KL comenzó con sólo un 5,74% en peso. BL alcanzó rendimientos máximos de DSEA del 21% en peso a 380°C y del 24,64% en peso a 390°C, en comparación con los rendimientos máximos de KL del 13,36% en peso y del 16,82% en peso, respectivamente. En general, el proceso SCW alcanzó rendimientos máximos de aceite total del 79,45 % en peso para BL y del 68,54 % en peso para KL a 390 °C.

Palabras Clave: Licor Negro, lignina, hidrotermal, agua supercrítica, poliol, despolimerización

ACKNOWLEDGEMENT

After all I reached the acknowledgement page of my PhD dissertation. It is an immense pleasure and relief to come this far in this journey. The whole journey has truly been a “blood, sweat and tears” experience in all aspects. Despite the challenges, it was undeniably worth every step, not only for the skills and perspectives that have enriched my professional growth but also for the invaluable experiences and maturity that shaped my personal and inner development.

The story of doing a PhD abroad goes back a long way when I was fully busy writing my MSc thesis in my teaching assistant office located at the Chemical Engineering Department of Izmir Institute of Technology. Although there was still lots of experience and wisdom that I could distill from my advisors, technical and project funding difficulties that I faced pushed me into taking this decision. Nor can I deny the indisputable charm of living abroad and experiencing new cultures all around the world. Long story short, once I got in touch with her, I received a quick reply from Prof. Maria Jose Cocero and stepped into this wild PhD adventure.

After a series of email exchanges, much to my delight, Prof. Maria Jose Cocero invited me to do my PhD at PressTech, where she would be my supervisor. And so, in the first quarter of 2019, I found myself in Spain, ready to take off on this new academic adventure.

Having told the short story of how I ended up doing a PhD in Spain, I would like to express my gratitude and thank to many people who supported me both scientifically and personally during this PhD journey.

In the first place, I would like to express my deepest gratitude to Prof. Maria Jose Cocero. Her encouragement, thoughtful insights, endless understanding, the freedom she provided and unwavering belief in my potential paved the way for this achievement. It was an honor to work under her guidance and I believe we will keep in touch and work together in the future.

I'm also grateful to my co-advisor Dr. Danilo Cantero for their fellowship, guidance, encouragement, and shared wisdom throughout this journey. His willingness to push me always and the time he dedicated to share his knowledge.

I would like to thank Prof. Jose Franco and his team in Pro2TecS group for their support, guidance and the time they dedicated to our collaboration for the second chapter of this thesis.

ACKNOWLEDGEMENT

It was a great pleasure to be a part of PressTech's multi-continental atmosphere. Many thanks to my colleagues and friends, for all the great time that we had and shared the same lab. I want to mention some of my colleagues with whom I had pleasure to work and interact: Andrea Casas, Constanza Maciel, Juan del Rio, Sergio Muñoz, Reinaldo Vallejo, Laura Quintana, Marta Ramos, Cristina Andres, Tijana Adamovic, Vesna Leontijevic, Luna Krstic, Mauricio de Souza Ribeiro, Maira Chinchilla, Silvia Gallego, Elaine Mission, Arancha Redondo, Manuela Castro, Enkeledo Menalla, Diego Pahino, Maria Anderez, and Ana Fernandez. I would like to thank all of you for your kind and friendly cooperation and interaction in various research activities/assignments.

A special thanks to Isabel Rodriguez, to our chief technical specialist, for the times that she dedicated to solving all kinds of difficulties that I faced, being a friend, listening to and sharing moments about my personal life. She was a big sister to me during my stay in Spain. She always believed in me and supported me during my difficult times.

I want to express my gratitude for the analytical specialists in our department as well. Many thanks to Enrique Marcos, Beatriz Muñoz, and PressTech IT specialist Daniel Fernandez. This work couldn't have been done without your assistance.

I'd like to thank my friends Gokalp Gozaydin, Seyma Bodur, Taylan Can Kose, Orkan Dal, Cem Karacasulu, and Ozgur Enes Taytas. Your support, presence, providing laughter, and a listening ear when the PhD road seemed particularly daunting were invaluable.

Another special heartfelt thank you to my beloved family for their unwavering support and understanding, even from miles away. Their encouragement, unconditional love, unlimited support, and endless motivation gave me strength and helped me overcome the many challenges along the way.

Lastly, I would like to express my deepest gratitude and pay tribute to the memory of my family members that I lost during my PhD, who played a crucial role in my academic journey and career. Their endless support, guidance, and encouragement continue to inspire me, even after their passing. May they rest in peace, and their legacy of kindness and wisdom will always hold a special place in my heart.